The Pricing of Uncertain Information:
From the Lab, to Derivatives Markets, to State-contingent Sovereign Debt

Dissertation
submitted to the
Faculty of Business, Economics and Informatics
of the University of Zurich

to obtain the degree of
Doktor der Wirtschaftswissenschaften, Dr. oec.
(corresponds to Doctor of Philosophy, PhD)

presented by

Felix Fattinger
from Arlesheim, BL

approved in October 2017 at the request of

Prof. Dr. Marc Chesney
Prof. Dr. Jean-Charles Rochet

The Faculty of Business, Economics and Informatics of the University of Zurich hereby authorizes the printing of this dissertation, without indicating an opinion of the views expressed in the work.

Zurich, 25.10.2017

Chairman of the Doctoral Board: Prof. Dr. Steven Ongena

Acknowledgements

First and foremost, I am indebted to my supervisor Marc Chesney. Without his continuous guidance and invaluable support during the many years of my PhD studies, the completion of this dissertation would not have been possible. Thank you, Marc, for the numerous stimulating discussions and the impeccable working environment you have provided me with at your chair. I also wish to express my deep gratitude to Jean-Charles Rochet for kindly accepting to serve on my PhD committee.

This dissertation is not solely my own work. I am very grateful to my coauthors Andrin Bögli and Alexandre Ziegler. Early on, Andrin and I have decided to work together on a problem whose full scope we probably both did not foresee. Thanks, Andrin, for being a tremendous coauthor and always a challenging intellectual sparring partner.

Not only during our collaboration, but throughout my dissertation, Alex's comments and suggestions have substantially improved my work. Thank you, Alex, and I am sorry that because of me our 3'15" Berlin Wall has not fallen yet.

My gratitude extends to the whole faculty at the Department of Banking and Finance at the University of Zurich. In particular, I wish to thank Michel Habib, Steven Ongena, Per Östberg, and Alexander Wagner. I have benefited greatly from their insight and encouraging advice.

During the last phase of my PhD studies, I was given the unique opportunity to spend one year as a visiting student at the Toulouse School of Economics. I am very grateful to Sébastien Pouget, Sophie Moinas, and Bruno Biais for being my hosts as well as for the many inspiring discussions and their invaluable comments on my work. Special thanks go to Sébastien, who has kindly accepted to attend my dissertation defense as an external expert.

I have always enjoyed working and teaching at Marc's chair and my thanks therefore extend to all current and former chair members: Anca Balietti, Delia Coculescu, Ruth Häfliger, Lena Hörnlein, Jonathan Krakow, Brigitte Maranghino-Singer, Lukas Münstermann, Tatjana Puhan, Kim Schartz, Bruno Troja, and Carlos Vargas.

I also thank my current and former fellow PhD students for having greatly enriched this long-lasting journey, to mention just a few: Konrad Adler, Amelie Brune, Kathrin de Greiff, Sebastian Dörr, Florian Eugster, René Hegglin, Ferdinand Langnickel, Felix Matthys, Magnus Nyboe, Diege Ostinelli, Marten Ovaere, Ivan Petzev, Thomas Richer, Jakub Rojcek, Cornelia Rösler, Adriano Tosi, Nikola Vasiljevic, Christoph Wenk, Jiri Woschitz, Ally Quan Zhang, and Jiakun Zheng.

Most importantly, I want to thank my family and friends for believing in me and being my source of inspiration. I am deeply grateful to my parents, who always have my back and encourage me in my endeavors. I thank my sister Sara and my brothers Nicolas and Stefan

for always standing by my side. With all my heart, I thank Corina for her love, patience, and unconditional support.

Thank you.

Felix Fattinger, Zurich, August 2017

Contents

Part I

Dissertation Overview

Dissertation Overview

Despite their increasing complexity, financial markets' fundamental purpose remains unchanged: the aggregation of decentralized information about uncertain prospects in order to enable optimal resource allocations and efficient risk sharing. As demonstrated by the financial crisis from 2007 to 2008, financial markets' well-functioning is more fragile than was generally believed. Moreover, from a European perspective, the subsequent and still ongoing sovereign debt crisis has called for unconventional monetary policy measures, whose unprecedented consequences on financial risks and real investments are currently unfolding. Overall, the recent past has reminded economists about the importance of a better understanding of how financial markets perform their economically important role and how sensitive they react to an increasingly complex environment.

The presented dissertation comprises four independent chapters. Each chapter represents one research paper written either in co-authorship or by myself over the course of my PhD at the University of Zurich. The four chapters span a wide vertical intersection of financial economics, ranging from a laboratory market experiment about trading complex risks, to derivatives markets' information processing role, to new sovereign debt instruments in response to persistently high sovereign debt levels. However, they all are centered on financial markets' evaluation and redistribution of uncertainty.

In Chapter 1, *Trading Complex Risks*, I experimentally study how heterogeneous investors price and share complex risks in a complete Walrasian market. I distinguish 'complex' from 'simple' risks in that the former refers to a situation in which agents only possess imperfect information about the underlying *objective* probabilities. Although this arguably corresponds to a specific notion of complexity, it naturally extends to financial markets' inherent uncertainty. Moreover, this probabilistic definition of complexity differs from what decision theorists usually refer to as 'ambiguity', where the underlying distribution is not objectively defined. A complete Walrasian market is chosen as it allows for the most simple benchmark comparison to the seminal asset pricing theory by Debreu (1959) and Arrow (1964): in the absence of complexity, risks should be perfectly shared among risk-averse agents and only aggregate risk is priced.

My experimental design consists of two components: (i) an experimental asset market, where subjects can trade either simple or complex risks, and (ii) a treatment which confronts subjects with the latter. Regarding (i), I closely follow Biais et al. (2017), whose asset market essentially corresponds to a Walrasian auction. Specifically, every buyer (seller) is provided with a predefined price vector, where, for every element of the vector, they are asked to specify the asset quantity they want to trade. The aggregated supply and demand curves are then crossed to determine market-clearing prices and quantities. By additionally introducing trading rounds

with random price draws, potential deviations due to the absence of perfect competition can be controlled for. Regarding (ii), I carefully design a two-sided complexity treatment that satisfies the following conditions: (a) it comprehensibly visualizes the asset's underlying payoff distribution, (b) it leaves no doubt about the problem's objective nature, and (c) it is complex enough to prevent (most) subjects from solving it analytically.

Before analyzing the experimental data, I develop a theoretical framework that allows for clear-cut predictions regarding individual trading behavior under both simple and complex risks. For simple risks, I generalize the predictions by Biais et al. (2017) with respect to the underlying probability distribution, however, this requires me to restrict my analysis to expected utility theory.[1] For complex risks, I analyze individual trading behavior in the presence of complexity-induced multiple priors, while allowing for both kinked and smooth preferences towards the fact that the true underlying payoff distribution is unknown.

In the absence of aggregate risk, for every agent there must exist a trading strategy such that she is perfectly hedged against future consumption risk. In brief, my theoretical analysis implies that, assuming agents dislike complexity, individual as well as aggregated supply and demand are less price sensitive for complex than simple risks, as agents become more reluctant to deviate from their perfect hedging strategy. Intuitively, if risks are complex, risk-averse agents not only want demand compensation for the risk they are bearing from not playing their perfect hedging strategy, but also for the uncertainty about the *actual riskiness* of not being perfectly hedged.

At the market level, the experimental data strongly conveys theory's prediction that complexity (locally) reduces supply and demand price sensitivity. In other words, subjects, on average, trade as theory predicts when presuming agents are complexity-averse. In equilibrium, complex risks are generally mispriced, but equally well shared as simple risks. At the individual level, complexity induces more mistakes in subjects' decision making, where mistakes are defined as actions that are strictly dominated according to the theory.

Comparing frequencies and distributions of dominated actions under simple and complex risks, I find that subjects' increasingly noisy trading behavior under the latter can be explained by random choice models. Strikingly, as the number of subjects is increased, this noise cancels out, generating theory-consistent risk allocations in equilibrium. Overall, markets' effectiveness in aggregating individual beliefs about complex risks is determined by the trade-off between reduced price sensitivity and increased noise levels in decision making. However, even under severe complexity-induced bounds to rationality, markets prove remarkably efficient in pricing complex risks. Beyond binding limits to rationality, this quality is eventually lost, while, strikingly, market's risk sharing qualities remain largely unimpaired.

Chapter 2, *Risk and Return around the Clock*, co-authored with Alexandre Ziegler, investigates around-the-clock price discovery for several benchmark assets from the main asset classes equities, bonds, currencies, and commodities. Based on high-frequency data, i.e., five-minute intervals, on futures contracts with recently extended trading hours, we study those assets' precise

[1] In contrast, the imposed symmetry in Biais et al.'s (2017) design allows for a more general model of individual behavior, i.e., by only imposing the absence of first order stochastically dominated actions.

risk and return distributions over the 24-hour trading day.[2]

Our sample consists of 13 very liquid contracts, i.e., the daily volume in the front-month contract alone generally exceeds 100,000 contracts. For equities, we focus on the S&P 500, EuroStoxx 50, and Nikkei futures; for bonds on the 10-year US Treasury Note, 10-year German Bund, and 10-year Japanese Bond futures; for currencies on the EUR/USD and JPY/USD futures; and for commodities on the West Texas Intermediate and Brent oil, as well as on the gold, silver, and high-grade copper futures. Besides longer trading hours relative to their underlying cash markets, futures contracts are particularly well-suited for analyzing price discovery due to their unified market organization and few regulatory restrictions, e.g., no short-selling constraints by construction.

We show that sizeable price discovery occurs around the clock. For a given asset, its risk-return distribution is fairly similar throughout the 24-hour trading day, indicating a broadly constant risk-return relationship. Although, the amount of price discovery varies significantly both during the day and across assets, relative price and variance contribution usually move hand in hand, suggesting an efficient information aggregation around the clock. In general, efficiency is higher during an asset's main (home) market hours. Nonetheless, we document short periods of inefficient price discovery, where relative price contribution leads relative variance contribution (JPY/USD) or vice versa (S&P 500).

For all assets, we document strong intraday volatility patterns, where the exact shapes of these patterns vary considerably across assets. Strikingly, US equities' well-known U-shaped intraday volatility pattern is absent for most assets. The release of US macroeconomic news not only strongly affects US equities, US treasuries, and USD related exchange rates, but the majority of other assets as well. Generally, assets' volatility is higher during US trading hours, but also strongly pronounced during different periods of the 24-hour trading day. When decomposing intraday volatility into its diffusion and jump components, we find that both risk types are crucial drivers of intraday volatility patterns. Moreover, jumps substantially contribute to total volatility levels: On average, jump risk accounts for approximately 5% to 13% of daily realized variance.

Furthermore, we observe that average volume-volatility relationships often break at jump times. This points to falling market depth in response to traders' anticipation of large price moves at times of scheduled news announcements. Overall, our results emphasize the importance of around-the-clock trading for modern financial markets' efficient price discovery.

Similar to Chapter 2, Chapter 3, *Multimarket Informed Trading and Risk Aversion*, also considers derivative contracts, but this time in a multimarket setting. Specifically, I study agents' trading behavior in the presence of asymmetric information, when the underlying risk can either be traded in the stock or in the options market. In general, the mechanism of how dispersed information is incorporated into prices of inherently linked assets that trade on different markets is crucial for the understanding of asset markets' information aggregation role.

[2]For most futures contracts, the extended trading hours range from 00:00 to 23:15 Central European Time.

In contrast to the literature, I assume informed traders to be heterogeneously risk-averse and only imperfectly informed about a future jump risk. Within a sequential trading model, I investigate the triangular trade-off between leverage, market depth, and risk in informed traders' choice of their preferred trading venue. In order to prevent no-trading equilibria, I adopt the literature's standard assumption of exogenously arriving liquidity traders.

In this setting, a rational expectation equilibrium needs to satisfy two conditions: (i) competitive market makers' price quotes have to leave them with zero profits in expectation, and (ii) given these quotes, informed traders' choice of trading venue must align with market makers' conjectures. A semi-separating equilibrium is reached whenever informed traders are separated between the two markets in such a way that both (i) and (ii) hold simultaneously. Due to their asymmetric payoff profile, trading options is more risky than trading the stock. Hence, in a semi-separating equilibrium, informed option traders are relatively more risk-averse than informed stock traders.

My numerical analysis demonstrates that, in the presence of heterogeneously risk-averse informed traders, a semi-separating equilibrium constitutes the robust outcome of the model. Moreover, as market makers' perception of adverse selection risk increases, so does the proportion of informed *stock* trading. However, the sensitivity of this relationship becomes smaller, as the probability of informed trading augments. In contrast to the risk-neutral benchmark, the relative amount of informed stock trading is always higher under a semi-separating equilibrium. Intuitively, risk-averse traders are less reluctant to forgo a given leverage advantage in return for a lower payoff risk. Unsurprisingly, if the stock market becomes more liquid, the amount of informed stock trading in equilibrium rises.

Since post-announcement returns of M&A target firms provide a nice fit with my model's underlying stock dynamics, I test its predictions by analyzing those firms' pre-deal announcement stock and options trading data. As predicted by the model, the relative amount of abnormal stock volume (vs. relative abnormal options volume) is increasing in the overall proportion of abnormal trading volume. Moreover, the data clearly rejects a linear in favor of a concave relationship. This is in line with the prediction that fewer informed traders switch from the options to the stock market as their relative presence increases.

Chapter 4, *Indebtedness, Interests, and Incentives: State-contingent Sovereign Debt Revisited*, co-authored with Andrin Bögli, has a somewhat different focus. By introducing new refinancing instruments for highly indebted sovereigns, it takes a macroeconomic perspective on financial markets. Compared to the variability of asset prices, macroeconomic risks can be considered rather small, i.e., with an average standard deviation of the growth rate lying around 3% per annum (see, e.g., Lucas (1987)). Due to these relatively low fluctuations in GDP, governments can accumulate substantial amounts of public debt during normal times. However, in the presence or rare growth disasters, such as the financial-crisis-induced 'Great Recession', such debt levels may become unsustainable.

This final chapter begins with the observation that, despite its most severe effects have abated, the preconditions for a recrudescence of the sovereign debt crisis still persist to date:

vast public debt-to-GDP levels in many European countries. In this context, we first refer to the European Central Bank (ECB)'s most effective crisis mitigation policy, i.e., its 'Outright Monetary Transactions' program (OMT). We argue that OMT's conditional guarantee, i.e., to buy unlimited amounts of distressed sovereign bonds in order to align their yields with fundamentals, can be interpreted as an implicit put option for highly indebted governments written by the ECB. However, soon after its announcement, concerns were raised that OMT's implicit put option fails to internalize risk sharing costs and could therefore lead to undesirable risk redistribution effects among Eurozone member states.[3] Based on these concerns, we propose two state-contingent refinancing alternatives to OMT, both temporary in nature and designed to provide indebted governments with more space for a feasible deleveraging.

First, motivated by OMT's inherent insurance mechanism, we consider puttable bonds, where investors have the right, upon default, to put their claims with a third party (e.g., an intergovernmental agency such as the European Stability Mechanism (ESM)) in return for the bonds principal plus accrued interests. This explicit insurance mechanism effectively turns puttable bonds into a risk-free investment, hence, paying investors only the risk-free rate. However, in sharp contrast to OMT, a government willing to issue puttable bonds has to *ex-ante* compensate the insurance-providing third party by paying the latter the premium of the bonds' embedded put option.

In the absence of default costs, we show that Merton's (1974) equivalence result holds: The risk-adjusted spread on standard sovereign debt equals puttable debt's embedded put premium. Hence, if a government does not face default specific costs, it is exactly indifferent between issuing standard or puttable bonds. However, under the issuance of puttable debt, sovereign default probabilities decrease due to its lower interest charges. Therefore, whenever default is costly, the attractiveness of puttable debt depends on the resulting reduction in *expected* default costs.

Second, based on the well-known proposal of GDP-linked bonds, we propose what we call 'GDR bonds', i.e., bonds whose interests are contingent on a country's current GDP-to-debt ratio (GDR) and hence *inversely* related to its relative indebtedness. Compared to puttable debt, GDR bonds allow for consumption smoothing, as their cyclical interest charges provide the issuing government with more fiscal leeway when growth, and therefore its tax income, declines. In contrast to standard GDP-linked bonds, a sustainable but credible deleveraging commitment allows for a competitive risk-return profile of GDR bonds, even in the face of pessimistic growth outlooks. This is a direct implication of GDP growth's low volatility.[4]

In order to compare state-contingent debt's welfare implications relative to standard sovereign debt, we conduct an empirical case study involving the five Eurozone countries most heavily affected by the debt crisis: Portugal, Ireland, Italy, Greece, and Spain. We ensure the validity of Merton's (1974) equivalence result by calibrating country-specific default costs. In the pres-

[3]The constitutional complaints of the Federal Constitutional Court of Germany against OMT's compliance with EU law were rejected by the European Court of Justice in 2015 (source: judgment of the court in case C-62/14, June 16, 2015, http://curia.europa.eu/jcms/jcms/j_6/).

[4]At this point, I refer to the discussion of GDR bonds' calibrated Sharpe ratios in Section 4.5 of Chapter 4.

ence of a risk-averse representative agent, we find the counter-cyclical fiscal leeway induced by GDR bonds to dominate puttable bonds' interest savings and (more pronounced) reduction in expected default costs. We conclude our analysis by discussing implied deleveraging incentives, limited commitment, and practical implementation issues for GDR bonds.

In summary, my dissertation adds to the understanding of financial markets' fundamental information aggregation and risk sharing mechanism in three particular contexts: (i) if risks are complex, i.e., if agents only possess imperfect information about the traded asset's objective payoff distribution, (ii) when asset markets' information processing role is extended to practically allow around the clock trading, and (iii) under the presence of asymmetric information in a multimarket setting involving a stock and an options market. Finally, the last chapter provides some novel insights regarding potential welfare improvements from making relatively lower macroeconomic risks tradeable via GDR bonds.

Probably the most characterizing feature of this dissertation is its combination of empirical and theoretical methods applied to experimental, high-frequency, as well as macroeconomic data in the study of financial markets. As every chapter presents one research paper, their accessibility via selective reading is ensured. Nevertheless, I hope readers will share my fascination for the manifoldness of financial economics, which I was allowed to discover during the challenging but very rewarding journey of my PhD. The structure of the dissertation is organized as follows. Part II comprises the herein previewed chapters. Part III contains the complete bibliography, and my curriculum vitae is provided in Part IV.

Part II

Research Papers

1 Trading Complex Risks

Complex risks differ from simple risks in that agents facing them only possess imperfect information about the underlying *objective* probabilities. This paper studies how complex risks are priced by and shared among heterogeneous investors in a Walrasian market. I apply decision theory under ambiguity to derive robust predictions regarding the trading of complex risks in the absence of aggregate uncertainty. I test these predictions in the laboratory. The experimental data provides strong evidence for theory's predicted reduction in subjects' price sensitivity under complex risks. While complexity induces more noise in individual trading decisions, market outcomes remain theory-consistent. This striking feature can be reconciled with a random choice model, where the bounds on rationality are reinforced by complexity. When moving from simple to complex risks, equilibrium prices become more whereas risk allocations become less sensitive to noise introduced by imperfectly rational subjects. Markets' effectiveness in aggregating beliefs about complex risks is determined by the trade-off between reduced price sensitivity and reinforced bounded rationality. Moreover, my results imply that complexity has similar but more pronounced effects on market outcomes than ambiguity induced by conventional Ellsberg urns.

1.1 Introduction

Financial markets have incurred a dramatic increase in complexity over the past decades. Successive market integration and ongoing financial innovation both have expanded and complicated the universe of tradable risks. The soaring levels of securitized contingent claims, a prominent example of the latter, are generally believed to have catalyzed what eventually turned into the Great Recession.[1] Meanwhile, the implications of this rising complexity in traded assets' inherited risk structure are still poorly understood.

Alongside information aggregation, financial markets' essential raison d'être is their efficiency in allocating tradable risks to those with the highest risk bearing capacities. Efficient risk sharing is, however, not prevailing unconditionally in such markets. Greenwald and Stiglitz

I am indebted to my advisor Marc Chesney for his support and guidance. I thank Peter Bossaerts, Markus Brunnermeier, Claire Célérier, Sylvain Chassang, Sebastian Dörr, Thierry Foucault, Andreas Fuster, Cars Hommes, Philipp Illeditsch, Chad Kendall, Carsten Murawski, Martin Schonger, Nicolas Treich, Roberto Weber, Alexandre Ziegler, and participants at the TSE Finance Workshop and the University of Zurich PhD seminar for helpful comments. I am especially grateful to Sébastien Pouget, Sophie Moinas, and Bruno Biais for countless discussions while visiting Toulouse School of Economics where part of this research was carried out. I also thank Kathrin De Greiff, Sara Fattinger, Sandra Gobat, René Hegglin, Jonathan Krakow, Ferdinand Langnickel, Patrick Meyer, Lukas Münstermann, and Carlos Vargas for participating in the first of two pilots. Last but not least, I am indebted to Cornelia Schnyder for her invaluable support in conducting the main sessions of the experiment. Financial support by the Swiss National Science Foundation is gratefully acknowledged.

[1] See, e.g., Ghent et al. (2014) for a complexity-controlled performance analysis of mortgage-backed securities.

(1986) show that when either information is imperfect or markets are incomplete, competitive market allocations are generally *not* constrained Pareto efficient.

In this paper I study how 'complex risks' are priced by and shared among heterogeneous agents. In contrast to simple risks, I regard a given asset's payoff distribution as complex, if agents only possess imperfect information about the underlying *objective* probabilities. Starting from a complete market, I focus on the role of imperfect information on the pricing and sharing of tradable risks when aggregate endowments are constant. I thus deliberately abstract from financial innovation's potential market completion effects in order to highlight complexity's informational role on market efficiency.[2]

My analysis rests on two integral parts: First, within a simple economy without aggregate uncertainty, I analyze competitive trading of both simple and complex risks via a complete Walrasian market. In order to account for complexity effects on agents' trading behavior, I apply decision theory under ambiguity, equivalently often referred to as Knightian uncertainty (Knight, 1921). Second, by conducting a laboratory experiment, I test the derived clear-cut predictions empirically.

Given market completeness, the absence of aggregate risk implies the existence of individual trading strategies that leave agents perfectly hedged against future consumption risk. Relying on ambiguity theory, I show that, for complexity-averse agents, competitive supply and demand become less price sensitive under complex risks, as agents become more reluctant to deviate from their perfect hedging strategy. This is intuitive: If risks are complex, the agents not only demand compensation for the risk they are bearing from not playing their perfect hedging strategy, but also for the uncertainty about the actual riskiness induced by such an action.

Experimental asset market equilibria corroborate complexity aversion-implied trading behavior, i.e., I find complexity to (locally) reduce supply and demand price elasticity. At the market level, complex risks are generally mispriced, but *equally well* shared relative to simple risks. At the individual level, complexity causes more mistakes in subjects' trading decisions, where mistakes are defined as adopting strictly dominated strategies as implied by theory.

A comparison of both frequencies and distributions of dominated actions under simple and complex risks confirms that subjects' trading strategies become increasingly noisy under the latter. Strikingly, as the number of subjects becomes larger, this noise cancels out in equilibrium and theory-consistent risk allocations prevail. This can be explained by a random choice model, where the relative likelihood of a given action is increasing in its ambiguity theory-based utility.

Overall, markets' effectiveness in aggregating individual beliefs about complex risks is determined by the trade-off between reduced price sensitivity and increased severity of bounded

[2]In reality, most markets, including those for financial assets, can hardly be characterized as being complete in a static sense, i.e., in the absence of retrading opportunities. Hence, the financial innovation industry's touted services towards market completion have to be evaluated against dynamic completeness as developed in Kreps (1982) and Duffie and Huang (1985). Assuming dynamic completeness, the existence of a Radner equilibrium (Radner, 1972) crucially depends on agents' ability of *perfect foresight*, i.e., to perfectly forecast today all future prices depending on information revealed tomorrow. Asparouhove et al. (2016) experimentally show how the inability of perfect foresight can cause considerable deviations from equilibrium prices. Thus, one reasonable concern implied by the increasing complexity of traded risks is that agents lacking the required resources to fully understand their complicated nature may fail to correctly forecast future price movements.

rationality (more dominated actions). Accounting for subjective beliefs, I find that, despite reinforced bounds to rational behavior, markets prove remarkably effective in pricing complex risks. Beyond binding limits to rationality, their information aggregation is impaired, while optimal risk sharing still prevails. Finally, my results indicate that complex risks have similar but more pronounced implications on market outcomes than ambiguity induced by conventional Ellsberg urns.

In contrast to a situation with known payoff distributions, complexity is introduced by providing subjects instead with the formal definition of the underlying process in addition to a dynamic visualization of its past trajectory. Thus, the presence of complex risks requires subjects to deductively determine traded assets' payoff distributions by processing complex information. The advantage of this implementation is the simple structure of the complicated but yet well-defined problem at heart. In fact, it requires solving a stochastic differential equation, which, although technically doable by hand, turns out to be infeasible for the vast majority of subjects.[3] However, the problem's simple formulation together with the visualized information of one random realization allows one to appraise—with more or less certainty—the apparently objective underlying risk.

In summary, the term complexity will henceforth refer to a complete Walrasian market for a risky asset whose true payoff distribution is not known with certainty, thereby imposing complex risks on utility maximizing traders. Although this notion of complexity is arguably specific, it naturally extends to real world financial markets' inherent purpose of multidimensional risk sharing.[4]

In the absence of perfect information, subjects possess a more or less precise estimate of the relevant payoff distribution, i.e., are faced with a smaller or wider set of possible priors. Considering the imperfection of the available information, "it would be irrational for an individual who has poor information about her environment to ignore this fact and behave as though she were much better informed" (Epstein and Schneider, 2010, p. 5). Trading decisions under complex risks are henceforth analyzed by applying two seminal ambiguity models in financial economics: a generalization of the multiple-priors model by Gilboa and Schmeidler (1989), and the smooth ambiguity model by Klibanoff et al. (2005). While the former implies kinked ambiguity preferences, the later allows for smooth ambiguity effects.

The intuition behind both models is simple. If agents are averse to perceived ambiguity, they, ceteris paribus, prefer to avoid being exposed to imperfectly understood risks. When starting

[3]This is not surprising given the means at hand and the limited time available during the experiment. Presenting subjects with an obviously solvable but complicated problem represents the design's integral treatment.

[4]There is a vast scientific literature on various notions of (financial) complexity. In computer science and machine learning one distinguishes, e.g., between computational complexity (required resources), sample complexity (minimum number of draws), and Kolmogorov complexity (minimum descriptive length) of problem solving. The herein considered form of complexity is somewhat different in that it directly relates to the analysis of pricing and risk sharing in a financial market. Interestingly enough, recent contributions in decision science provide evidence for commonalities between the human brain and computer algorithms solving and reacting to problems with varying levels of complexity (see, e.g., Bossaerts and Murawski (2016)).

from a zero ambiguity exposure, this leads to a no-trade interval.[5] For nonzero initial endowments in the risky asset, as pointed out by Dow and da Costa Werlang (1992), engaging in trade is generally still optimal. In my model economy, incentives to trade stem from nontradable but *hedgeable* consumption risk. In short, under both models, agents' price sensitivity of their perfect hedging strategy decreases in the presence of complex risks. Intuitively, being completely hedged insures agents not only against risk but also against potential complexity-induced ambiguity. The main difference between the two models lies in their implied conditions for mispricing. Within the smooth ambiguity model, incorrect beliefs immediately impact equilibrium prices, whereas this does not unconditionally hold for the multiple-priors model. Overall, my empirical evidence speaks in favor of kinked preferences as embedded in the latter.

The merits of taking the study of how individual decision making aggregates to market outcomes to the lab are manifold. First, by design, the lab easily allows for the construction of a complete market. Moreover, the experimenter can exercise full control over each market participants' information set and how their individual decisions interact towards equilibrium. Second, the laboratory environment offers the unique virtue of measuring subjects' beliefs, in particular their expectations, which most often constitutes an impossibility when confronted with real world data. Third, treatment effects under investigation can be analyzed in isolation, while controlling for any kind of endogeneity concerns. Thus, the lab enables a direct comparison between simple versus complex risks, while comparing the latter to the 'pure ambiguity' case usually associated with Ellsberg's (1961) urn experiment. Once the unobservability of expectations and the inability to monitor strategic uncertainty underlying field data are taken into serious account, the advantages of full laboratory control become evident.

My design directly builds on the experimental setup proposed by Biais et al. (2017). Relying on a two-state world with two nonredundant assets (a risk-free bond and a risky stock), it offers the simplest possible setting to test the seminal general equilibrium theory by Debreu (1959) and Arrow (1964). Controlling for subjects competitive behavior, Biais et al. (2017) find market outcomes to be consistent with the theory of complete and perfect markets: On average, (simple) risk is perfectly shared and only aggregate risk is priced. Therefore, Biais et al.'s (2017) parameter-free test of the most fundamental asset pricing theory constitutes the ideal benchmark upon which the trading of simple and complex risks can be compared.[6] Moreover, its simple market-clearing pricing scheme based on individual supply and demand functions can be controlled for any kind of strategic uncertainty. This constitutes an impracticality in the context of the continuous double auction that is normally used in experimental asset market studies.

This paper relates to three distinctive strands of the literature. First, a growing literature investigates the drivers and implications of financial complexity both from a theoretical as well

[5] For example, this phenomenon serves Dimmock et al. (2016) in explaining known household portfolio puzzles, e.g., the equity home bias.

[6] For their most general predictions, Biais et al. (2017) only rely on first order stochastic dominance. When allowing for deviations from their symmetric payoff distribution, my analysis assumes expected utility maximization instead.

as an empirical perspective. Ellison (2005) and Gabaix and Laibson (2006) demonstrate theoretically that inefficient levels of financial complexity can prevail in a competitive equilibrium. Carlin (2009) finds that financial complexity is an increasing function in the degree of competition among financial institutions. Carlin and Manso (2011) show how educational initiatives aiming to foster financial literacy may eventually cause welfare diminishing obfuscation, i.e., the strategic acceleration of complexity by financial service providers in order to preserve industry rents (see Ellison and Ellison (2009)). From an investor's view, Brunnermeier and Oehmke (2009) discuss three different ways to deal with complexity: (i) applying separation results, (ii) relying on models, or (iii) via standardization. Arora et al. (2011) illustrate how the usage of computationally complex derivatives may worsen asymmetric information costs.

Célérier and Vallée (2017) empirically test the implications of the Carlin (2009) model and indeed find complexity to be increasing in issuer competition. Furthermore, several studies analyze the steadily growing market for complex securities, in particular their pricing, historical performance, as well as the characteristics of the involved issuers and investors (Henderson and Pearson (2011), Ghent et al. (2014), Griffin et al. (2013), Sato (2014), and Amromin et al. (2011)). Relying on expected utility theory, Hens and Rieger (2008) moreover reject the often claimed market completing effect of structured products. In summary, there exists both theoretical and accumulating empirical evidence that financial institutions rely on a continuing increase in complexity to shield industry rents from competitors and learning by investors rather than to create higher quality products. My paper complements this literature by investigating rising complexity's implications on agents' trading behavior.

Second, the herein presented analysis naturally relates to experimental studies on trading ambiguous or complex assets. Implementing a continuous double auction of state-contingent claims based on an Ellsberg urn, Bossaerts et al. (2010) analyze how subjects' ambiguity aversion affects asset prices and final portfolio holdings. Similar to the no-trade result, they find that, for certain subsets of prices, ambiguity-averse agents prefer to hold nonambiguous portfolios. Furthermore, Bossaerts et al. (2010) show how, in the presence of aggregate risk, sufficiently ambiguity-averse investors indirectly impact asset prices by altering the per capita risk to be shared among marginal investors.

Carlin et al. (2013) study how computational complexity alters bidding behavior in a *deterministic* environment.[7] They find higher complexity to increase volatility, lower liquidity, and decrease trade efficiency, i.e., to reduce gains from trade. Moreover, Carlin et al. (2013) provide evidence that, additional to any noise arising from estimation errors, traders' bidding strategies are influenced by a complexity-induced adverse selection problem. Intuitively, given traders' private values of the tradable asset are affiliated, the fear of winner's curse, i.e., to systematically lose by trading against a better informed counterparty, leads traders to submit more conservative ask and bid quotes.

Asparouhove et al. (2015) show how ambiguity preferences can explain asset prices under

[7] In the experimental design by Carlin et al. (2013) participants trade different assets whose values have to be determined deductively by solving systems of linear equations, where the authors differentiate between simple and complex computational problems.

asymmetric reasoning. They consider a continuous double auction of arrow securities, where, midway through the auction, agents are confronted with an involved updating problem regarding the relative likelihood of the underlying states.[8] In line with Fox and Tversky's (1995) comparative ignorance proposition, Asparouhove et al. (2015) argue that agents perceive irreconcilable post-updating market prices as ambiguous. Hence, if ambiguity-averse, agents who apply incorrect reasoning become price-insensitive. Consistent with ambiguity aversion, the more price-sensitive agents there exist, the less severe is the experimentally documented mispricing.

Third, this paper also relates to an emerging literature comparing individuals' preferences towards pure Ellsberg-like ambiguity and complex risk(s), where, as in this paper, the latter is uniquely defined by an objective probabilistic structure. The findings in Halevy (2007) give support to a close relation between individuals' ability to correctly reduce compound lotteries and their attitudes to pure ambiguity. The vast majority of subjects (95%) who failed to disentangle compound objective lotteries, displayed nonambiguity-neutral behavior.

In their recent paper, Armantier and Treich (2016) provide strong empirical evidence for "a tight link between attitudes toward ambiguity and attitudes toward complex risk" (Armantier and Treich, 2016, p. 5). In their ambiguity treatment, subjects are confronted with lotteries whose outcomes depend on draws from an opaque Ellsberg urn, while complex risks are represented by lotteries that get settled by simultaneous draws from multiple transparent urns. Based on estimated certainty equivalents for both lottery types, Armantier and Treich (2016) elicit ambiguity as well as complex risk premiums. They find a strong positive correlation between the two premiums across subjects.

The remainder of the paper is organized as follows. Section 1.2 introduces the model economy and develops the necessary theory for generating predictions about trading both simple and complex risks. Section 1.3 describes the experimental design and confronts the theoretical predictions with the data. Section 1.4 concludes.

1.2 Theory

This section introduces the model economy for which I thereafter study individual trading behavior conditional on agents' information quality. If risks are simple, implications of varying risk-preferences are analyzed within the classical framework of expected utility. In contrast, if risks are complex, individual preferences are adjusted to account for their imperfect information. The first case provides a clear-cut benchmark to which complexity-induced implications can be compared to.

[8] The updating task in Asparouhove et al.'s (2015) experimental design is an adaptation of the famous 'Monty Hall problem'.

1.2.1 Model

I start from the simple economy of Biais et al. (2017). In the two-period interpretation of this trading economy, $t \in \{1, 2\}$, uncertainty gets resolved in the second period, where there are two possible states of the world, $\Omega = \{u, d\}$. The probability of reaching state u is denoted by π, i.e., $\mathbb{P}(\omega{=}u) = \pi$ and $\mathbb{P}(\omega{=}d) = 1 - \pi$, respectively. Contrary to Biais et al. (2017), I allow for any nontrivial binary payoff distribution $\pi \in (0, 1)$.[9] This generalization is crucial, given agents' subjective probability estimates in the context of complex risks.

The economy offers access to a complete asset market, where shares of a risky asset (stock) can be traded in exchange for units in the risk-free asset (numéraire). The stock pays a state-dependent dividend X per share in $t = 2$, but nothing beforehand. The dividend fully transfers the stock's final value to shareholders, i.e., after payments have been made, all shares expire worthless (no continuation value). Without loss of generality, it is assumed that $X(u) > X(d)$. The time difference between $t = 1$ and $t = 2$ is considered to be very short, allowing to abstract from any time discounting. Therefore, in-between periods, the risk-free asset simply serves as pure storage device (cash) that does not pay any interests.

There is an infinite number of agents populating the economy. I denote the unbounded set of agents by $\mathcal{I}$. Agent $i \in \mathcal{I}$ is endowed with nonnegative holdings in the risk-free asset B_i, S_i shares of the risky stock, and some state-contingent non-tradable income $I_i(\omega)$ paid out in $t = 2$ only. Moreover, every agent belongs to one of two types, i.e., either she is allowed to buy shares (potential buyer) or to sell them (potential seller). There exist as many buyers as sellers and their respective endowments are identical within each type. Every agent only cares about her utility of consumption $C_i(\omega)$ in $t = 2$, where consumption is given by the sum of the final holdings in the risk-free asset, dividend payments, and nontradable income. In the first period, potential buyers and sellers are able to trade shares via a call-market in order to maximize their increasing utility from consumption $U_i(C_i)$ in the second period.

Finally, agents' state-contingent income is set to exactly offset the aggregate consumption risk caused by the stock's dividend payments. If aggregate endowments are constant, I show that for risk-averse agents, the rational expectation equilibrium is independent from potentially heterogeneous attitudes towards simple consumption risks. In particular, under simple risks, the stock market-clearing price and quantity remain unaffected by the shape of agents' utility functions $(U_i)_{i\in\mathcal{I}}$. If, despite the income $I_i(\omega)$, aggregate risk prevailed, market equilibrium would necessarily reflect agents' (average) risk preferences.[10]

[9] Biais et al. (2017) only consider the symmetrical case, i.e., $\pi = 1/2$. Imposing symmetry has the advantage of delivering robust predictions even under the inapplicability of expected utility theory, i.e., by only assuming the absence of first order stochastically dominated actions.

[10] Constantinides (1982) shows that if agents with different risk attitudes all maximize expected utility subject to a common prior, equilibrium prices can always be rationalized in a representative agent framework. Hence, in the absence of complex risks, market equilibrium can be explained by the risk preferences of this representative agent.

1.2.2 Trading Simple Risks: Expected Utility

In the presence of simple risks, since the value of π is common knowledge, agents possess perfect information regarding the stock's payoff distribution. According to classical consumption-based asset pricing theory, the stochastic discount factor then corresponds to the representative agent's marginal rate of intertemporal substitution. In Biais et al.'s (2017) simple economy, with consumption restricted to $t = 2$, expected utility theory implies an equilibrium stock price P equal to the stock's normalized expected payoff weighted by her marginal utilities across states.[11] By choosing $(I_i(\omega))_{(i\in\mathcal{I})}$ such that aggregate consumption risk vanishes, the interconnectedness between P and marginal utilities disappears, allowing for predictions robust to any parameterization of any set of increasing utility functions $(U_i)_{i\in\mathcal{I}}$. The results in this subsection correspond to generalizations of Biais et al. (2017) to values of $\pi \neq 1/2$.

Recalling the two-state nature of the economy in $t = 2$, one can write agent i's expected utility from consumption as

$$\begin{aligned} E\big[U_i(C_i(\omega))\big] &= \pi\, U_i(C_i(u)) + (1-\pi)\, U_i(C_i(d)) \\ &= \pi\, U_i\left(\mu_i + \sqrt{\frac{1-\pi}{\pi}}\sigma_i\right) + (1-\pi)\, U_i\left(\mu_i - \sqrt{\frac{\pi}{1-\pi}}\sigma_i\right), \end{aligned} \tag{1.1}$$

where $\mu_i \equiv \pi C_i(u) + (1-\pi)C_i(d)$ and $\sigma_i^2 \equiv \pi(1-\pi)\left(C_i(u) - C_i(d)\right)^2$. Thus, any agent's expected utility can be rewritten as a function of her expected consumption, the standard deviation of consumption across states, and the probability π.

In the absence of aggregate risk, i.e., if aggregate endowment across $S_iX(\omega)$ and $I_i(\omega)$ is constant, there must exist a tradable quantity $\widehat{Q}$ at which every seller and buyer is perfectly hedged against any consumption risk in $t = 2$. If agents are risk-averse, i.e., whenever U_i is strictly concave for every agent i, there exists a unique equilibrium for the call-market in $t = 1$.

Proposition 1.1. *If U_i is differentiable and strictly concave $\forall i \in \mathcal{I}$, and there exists a tradable quantity $\widehat{Q}$ such that every seller and buyer is perfectly hedged, i.e., $\sigma_i = 0, \forall i \in \mathcal{I}$, then seller i's supply and buyer j's demand curve for the risky asset have the unique intersection point $(E[X], \widehat{Q}), \forall\{i, j\} \subset \mathcal{I}$.*

Proof. For proof see Appendix A1. □

[11] When deciding on her optimal trading strategy Q in $t = 1$, the representative agent solves the following problem (where $Q > 0$ implies buying)

$$\max_{Q} E[U_i(C_i(\omega))] \quad \text{s.t.} \quad C_i(\omega) = (S_i + Q)X(\omega) + (B_i - QP) + I_i(\omega),$$

maximizing her expected utility from consumption in $t = 2$ subject to her budget constraint (neglecting any borrowing constraints). Hence, the first order condition yields

$$P = E\left[\frac{U_i'(C_i(\omega))}{E[U_i'(C_i(\omega))]}X(\omega)\right].$$

The driving force behind Proposition 1.1 is the strict concavity of the utility functions, i.e., agents aversion to consumption risk. To see this, it is helpful to separately consider the shape of both seller i's supply and buyer j's demand curve for the risky stock.

First, note that for a price equal to one share's expected dividend, seller i's expected consumption in Eq. (1.1) is independent of the number of shares sold. Since seller i is risk-averse, for $P = E[X]$ she will therefore always decide to sell exactly $\widehat{Q}$ shares and thereby be perfectly hedged against future fluctuations in consumption. However, for $P < E[X]$ ($P > E[X]$) her expected consumption *only* increases, if she sells less (more) than $\widehat{Q}$ shares. Because she is only willing to incur risk, i.e., deviate from selling $\widehat{Q}$ shares, if appropriately compensated in return, her supply curve *must* lie somewhere in the lower left and upper right quadrant of the price-quantity space shown in Subfigure (a) of Figure 1.1.

Second, note that for $P = E[X]$, similarly buyer j's expected consumption in Eq. (1.1) is independent of the number of shares bought. Given her risk-aversion, she chooses to buy exactly $\widehat{Q}$ shares for $P = E[X]$, and more (less) than $\widehat{Q}$ shares if $P < E[X]$ ($P > E[X]$), as illustrated in Subfigure (b) of Figure 1.1. Thus, when there is no aggregate risk, seller i's supply and buyer j's demand curve exhibit the unique intersection point $(E[X], \widehat{Q})$ as depicted in Subfigure (c).

Interestingly enough, depending on the shape of U_i, a large opposite income effect can dominate the corresponding substitution effect of a given price change. Hence, seller i's supply or buyer j's demand curve can effectively be nonmonotonic within the respective dominating quadrants of the PQ-plane. The following remark provides an example of a nonmonotonic supply curve.

Remark 1.1. *Suppose, seller i's utility function is defined piecewise as follows*

$$U_i(C) = \begin{cases} c_1 \frac{C^{1-\epsilon}}{1-\epsilon}, & \text{for } 0 \leq C \leq \overline{C}, \\ c_2 - e^{-\alpha C}, & \text{for } \overline{C} \leq C, \end{cases}$$

where $\alpha > \epsilon > 0$ and ϵ small, $\alpha > 0$, and c_1 and c_2 are positive constants such that U_i is differentiable $\forall C \geq 0$. For certain parameter pairs (α, π), seller i's supply curve can be nonmonotonic over a nonempty subset of P.

Proof. For proof see Appendix A1. □

Figure D1.1 in the Appendix D1 shows an example of a nonmonotonic supply curve for similar parameter values as in the actual experiment. The intuition for this exemplary nonmonotonicity effect is simple. For every seller and any given Q, both $C(d)$ and $C(u)$ are strictly increasing in $P > 0$. If prices are high enough, seller i's higher CARA coefficient α, relevant for $C(\omega) > \overline{C}$, can dominate her lower CRRA coefficient ϵ. Thus, for even higher prices, she is willing to bear less and less risk, causing her supply curve to decrease until it eventually reaches $\widehat{Q}$, and thereby completely eliminating her consumption risk.

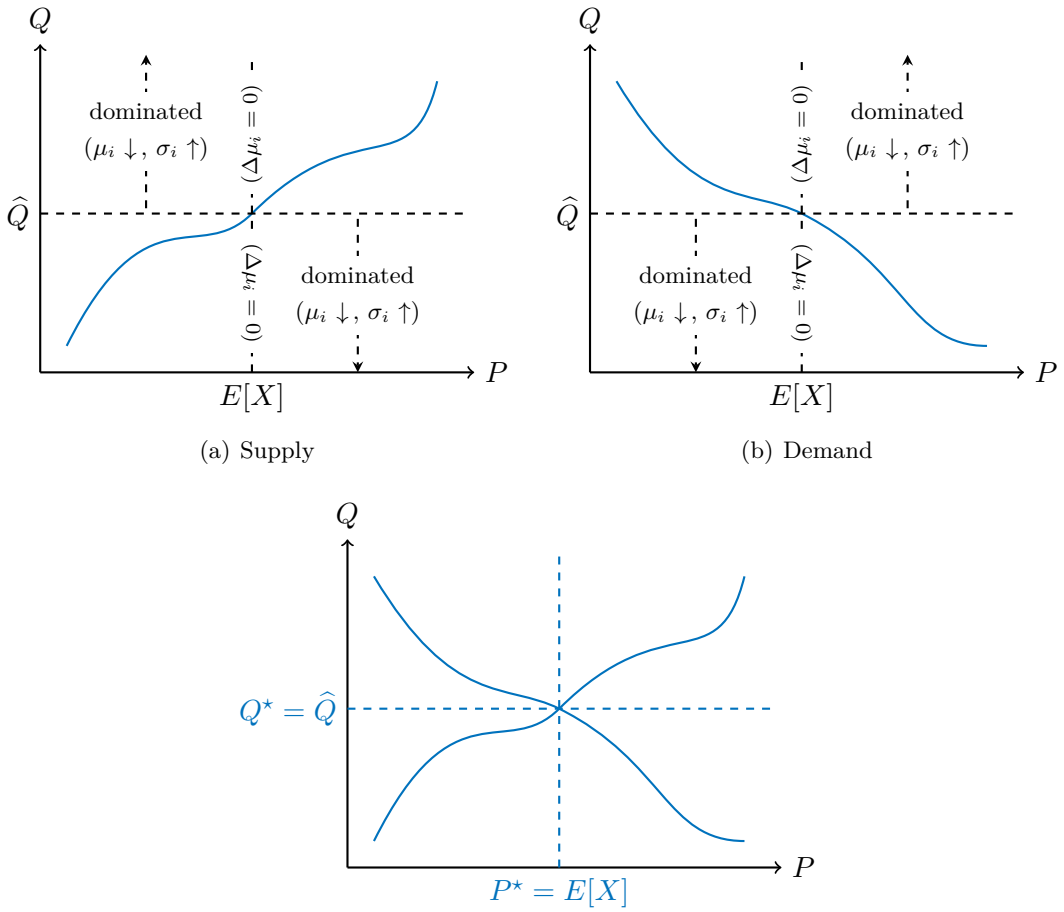

(a) Supply (b) Demand

(c) Equilibrium

FIGURE 1.1. TRADING EQUILIBRIUM FOR SIMPLE RISKS

Notes: This figure shows the unique equilibrium for risk-averse agents in the absence of aggregate consumption risk.

Absence of Risk Aversion

In case agents are *not* averse to consumption risk, for all $P \neq E[X]$, an even stricter separation between dominating and dominated strategies than shown in Figure 1.1 applies. From the proof of Proposition 1.1 it directly follows that whenever U_i is either linear or convex, seller i always strictly prefers to sell zero shares for $P < E[X]$. In contrast, for $P > E[X]$, her expected utility is maximized if and only if she sells her full initial endowment in shares. The symmetric behavior applies to risk-neutral and risk-loving buyers, respectively.

For $P = E[X]$, risk-neutral agents are indifferent between trading $\widehat{Q}$ shares or any other quantity, whereas risk-loving agents are indifferent between trading zero shares or the maximum number possible. In summary, as long as they do not consistently choose among their set of indifferent strategies in an *asymmetric* manner, the equilibrium in Figure 1.1 remains unaffected by a nonzero mass of nonrisk-averse agents.

1.2.3 Trading Complex Risks: Heterogeneous Complexity Preferences

When agents' information regarding the distribution of $X(\omega)$ is imperfect, I consider the associated consumption risk to be (more) complex. In the presence of such complex risks, rationality in decision making requires some form of acknowledgment regarding the information's inherent degree of (im)precision. The literature provides a vast number of models intended to account for individuals' degree of confidence in their relative likelihood estimates. In the following, I analyze individual trading of complex risks within two classes of seminal ambiguity models: multiple-priors utility and the 'smooth ambiguity' model proposed by Klibanoff et al. (2005). In the former, agents' information quality has a 'first order' effect on their trading decision (change in mean), whereas for the latter, lower information precision increases the total amount of perceived 'risk' (see Epstein and Schneider (2010)). For multiple-priors utility, there exists a direct mapping to rank-dependent expected utility, which I briefly discuss.

Multiple-priors Utility

Agents facing complex risks are unable to determine π with certainty, but rather consider several payoff distributions possible. Hence, intuitively, when making their trading decisions, they are guided by a set of potential probability laws. I denote agent i's subjective set of possible priors on the state space Ω by $\mathcal{C}_i$.

Based on this idea of multiple priors, Gilboa and Schmeidler (1989) axiomatize a multiple-priors maxmin decision rule that assumes infinite ambiguity-aversion. In order to allow for a full spectrum of ambiguity preferences, I employ the generalization proposed by Ghirardato et al. (2004), the so-called α-maxmin model, instead. Assuming the set $\mathcal{C}_i$ of subjective priors to be convex, agent i's utility from consumption in $t = 2$ is then given by

$$\mathcal{U}_i(C_i(\omega)) = \alpha_i \min_{\pi \in \mathcal{C}_i} \left(E\big[U_i(\pi)\big] \right) + (1 - \alpha_i) \max_{\pi \in \mathcal{C}_i} \left(E\big[U_i(\pi)\big] \right), \tag{1.2}$$

where, as before, $E\big[U_i(\pi)\big] \equiv \pi\, U_i(C_i(u)) + (1-\pi)\, U_i(C_i(d))$, U_i is a differentiable and strictly concave utility function, and $\alpha_i \in [0, 1]$. First, note the straightforward interpretation of Eq. (1.2). On the one hand, the cardinality or wideness of $\mathcal{C}_i$ measures agent i's ambiguity perception: The bigger her set of subjective priors, the more ambiguity she perceives. On the other hand, her preferences towards ambiguity are expressed by α_i: If $\alpha_i > 1/2$, she puts more weight on the minimal expected utility, implying ambiguity-aversion. In contrast, if $\alpha_i < 1/2$ ($\alpha_i = 1/2$), then she is ambiguity-loving (ambiguity-neutral). For their axiomatization, Gilboa and Schmeidler (1989) assume maximal ambiguity-aversion, i.e., $\alpha_i = 1$. Second, whenever $\mathcal{C}_i$ is a singleton, Eq. (1.2) reduces to Eq. (1.1) with subjective probability π_i, i.e., Eq. (1.2) converges to subjective expected utility as $\mathcal{C}_i \to \pi_i$. For ease of notation, I furthermore rely on the following definition:

$$E_i\big[X\big] := \alpha_i\, E_i\big[\underline{X}\big] + (1 - \alpha_i)\, E_i\big[\overline{X}\big], \tag{1.3}$$

where $E_i\big[\underline{X}\big] \equiv E^{\underline{\pi}_i}[X]$ with $\underline{\pi}_i := \arg\min_{\pi \in \mathcal{C}_i} \mu_i(\pi)$, and $E_i\big[\overline{X}\big] \equiv E^{\overline{\pi}_i}[X]$ with $\overline{\pi}_i := \arg\max_{\pi \in \mathcal{C}_i} \mu_i(\pi)$.

TABLE 1.1. AGENT TYPES WITH MULTIPLE-PIRORS UTILITY

		beliefs about π	
		correct ($\pi \in \mathcal{B}_i$)	incorrect ($\pi \notin \mathcal{B}_i$)
ambiguity-averse	yes ($\alpha_i > 1/2$)	Type AC	Type AI
	no ($\alpha_i \leq 1/2$)	Type NC	Type NI

Notes: In the presence of complexity-induced ambiguity, I distinguish between four different types of agents with multiple-priors utility. Agent i can either be ambiguity-averse or does not dislike ambiguity. Additionally, she can either apply correct or incorrect reasoning when processing her imperfect information about π.

When risks are complex, agents perceive ambiguity regarding the probability π. In order to analyze individual trading behavior within the α-maxmin model, a case-by-case analysis is required, whereby agent i can behave differently from agent j in two dimensions: First, agent i is either averse to ($\alpha_i > 1/2$) or not disliking ($\alpha_i \leq 1/2$) perceived ambiguity. Second, she can either have correct or incorrect beliefs about the true payoff probability π. More precisely, I classify agent i as having incorrect beliefs, if π is not sufficiently close to the midpoint of her set of priors, i.e., if $\pi \notin \mathcal{B}_i \subset \mathcal{C}_i$, where $\mathcal{B}_i$ itself depends on her ambiguity-aversion:

$$\mathcal{B}_i = \begin{cases} [\pi_M - \Delta(2\alpha_i - 1), \pi_M + \Delta(2\alpha_i - 1)], & \text{for } \alpha_i > \frac{1}{2}, \\ \pi_M & \text{for } \alpha_i \leq \frac{1}{2}, \end{cases} \tag{1.4}$$

where π_M denotes the midpoint of $\mathcal{C}_i$ with length (or maximum difference) 2Δ. We note that $\mathcal{B}_i \to \mathcal{C}_i$ as $\alpha_i \to 1$ and $\mathcal{B}_i \to \pi_M$ as $\alpha_i \to 1/2$. Table 1.1 summarizes the four possible combinations of types.

Price Sensitivity

In order to deduce the effect(s) of complexity-driven ambiguity on agents' trading behavior, the different types presented in Table 1.1 have to be considered separately. I start with the first row of Table 1.1. If aggregate endowments are constant, any risk-averse agent, as shown above, prefers to trade exactly $\widehat{Q}$ shares for $P = E[X]$. Now, given their distaste for the perceived ambiguity regarding π, agents of type AC and AI eventually both prefer to trade $\widehat{Q}$ for prices significantly different from $E[X]$. More precisely, for any given degree of risk-aversion, the subset of prices for which they wish to be perfectly hedged against consumption risk is increasing in both their ambiguity aversion and ambiguity perception.

Proposition 1.2. *In the presence of perceived ambiguity and if there exists a tradable quantity* $\widehat{Q}$ *such that* $\sigma_i = 0 \ \forall i \in \mathcal{I}$*, then agents of types AC and AI exhibit constant supply or demand curves over closed subsets of* P*. Their absolute price elasticity is a decreasing function in both* α_i *and the cardinality/length of* $\mathcal{C}_i$*.*

Proof. For proof see Appendix A1. □

In case of no aggregate risk, it holds for any *seller* i that $\underline{\pi}_i < \overline{\pi}_i$ for $Q < \widehat{Q}$ and $\underline{\pi}_i > \overline{\pi}_i$ for $Q > \widehat{Q}$, respectively. Intuitively, if seller i is hedged against varying consumption by selling exactly $\widehat{Q}$ shares, her expected consumption μ_i decreases in $1 - \pi_i$ (π_i) whenever she sells less (more) than $\widehat{Q}$ shares. Analogously, for any *buyer* j it holds that $\underline{\pi}_j > \overline{\pi}_j$ for $Q < \widehat{Q}$ and $\underline{\pi}_j < \overline{\pi}_j$ for $Q > \widehat{Q}$, respectively. These shifts in relative size of $\underline{\pi}_i$ and $\overline{\pi}_i$ around $\widehat{Q}$ in combination with ambiguity-aversion are the driving force behind Proposition 1.2.

To foster the reader's intuition, the result in Proposition 1.2 is illustrated in Figure 1.2 from the perspective of an ambiguity-averse seller—the analogous reasoning also applies to any ambiguity-averse buyer. First, due to seller i's risk-aversion, it can be shown (see proof of Proposition 1.2) that for $P = E_i[X]$, selling exactly $\widehat{Q}$ shares strictly dominates trading any other quantity of the risky asset. Moreover, given Eq. (1.2), she is only willing to sell less than $\widehat{Q}$ shares for prices strictly below $E_i[X]$ (see proof of Proposition 1.2). This is illustrated in Subfigure (a) of Figure 1.2. Analogously, seller i only agrees to sell more than $\widehat{Q}$ shares in return for $P > E_i[X]$ (see Subfigure (b)). Second, due to the above discussed order effect of $\underline{\pi}_i$ and $\overline{\pi}_i$, it follows that the lower price bound L in Subfigure (a) and the upper price bound U in Subfigure (b) do *not* coincide. Therefore, putting everything together, the piecewise constant supply curve depicted in Subfigure (c) prevails, where seller i's supply of the risky asset is constant over the closed subset $[L, U]$.

In comparison to the analysis under simple risks in Section 1.2.2, a nice and intuitive interpretation of Proposition 1.2 emerges. Since agents of types AC and AI are averse to ambiguity, selling or buying $\widehat{Q}$ shares becomes even more attractive compared to situations with objective payoff distributions. By trading exactly $\widehat{Q}$ units of the risky asset, agents are not only able to avoid risk, but additionally to dispose any exposure to perceived ambiguity. Trading $\widehat{Q}$ shares hence simultaneously corresponds to the perfect hedging strategy against both risk and ambiguity. In return for this dual insurance, agents are willing to forego potential gains from trade.

I now turn to the second row in Table 1.1. For nonambiguity-averse agents, there are two cases to be distinguished among. First, if α_i equals $1/2$, agent i is ambiguity-neutral. For a seller with $\alpha_i = 1/2$, L and U in Figure 1.2 coincide, i.e., under complex risks, she behaves as a *subjective* expected utility-maximizer. The analogous argument applies for an ambiguity-neutral buyer. Second, if $\alpha_i < 1/2$, agent i is ambiguity-loving. The same reasoning as in the proof of Proposition 1.2 implies that for an ambiguity-loving seller, it holds that $L > U$. Hence, when risks are complex, there exists a certain price between U and L for which she is indifferent between gaining exposure to ambiguity from selling less or more than $\widehat{Q}$ shares. At or precisely beyond this threshold, her supply curve therefore exhibits a discontinuity, i.e., jumping from strictly below to strictly above $\widehat{Q}$.[12] For prices below and above the threshold, her supply curve's price elasticity increases in comparison to simple risks. Again, the analogous argument can be made for an ambiguity-loving buyer.

[12] This can be interpreted as the natural counterpart of ambiguity-averse sellers' piecewise flat supply curves.

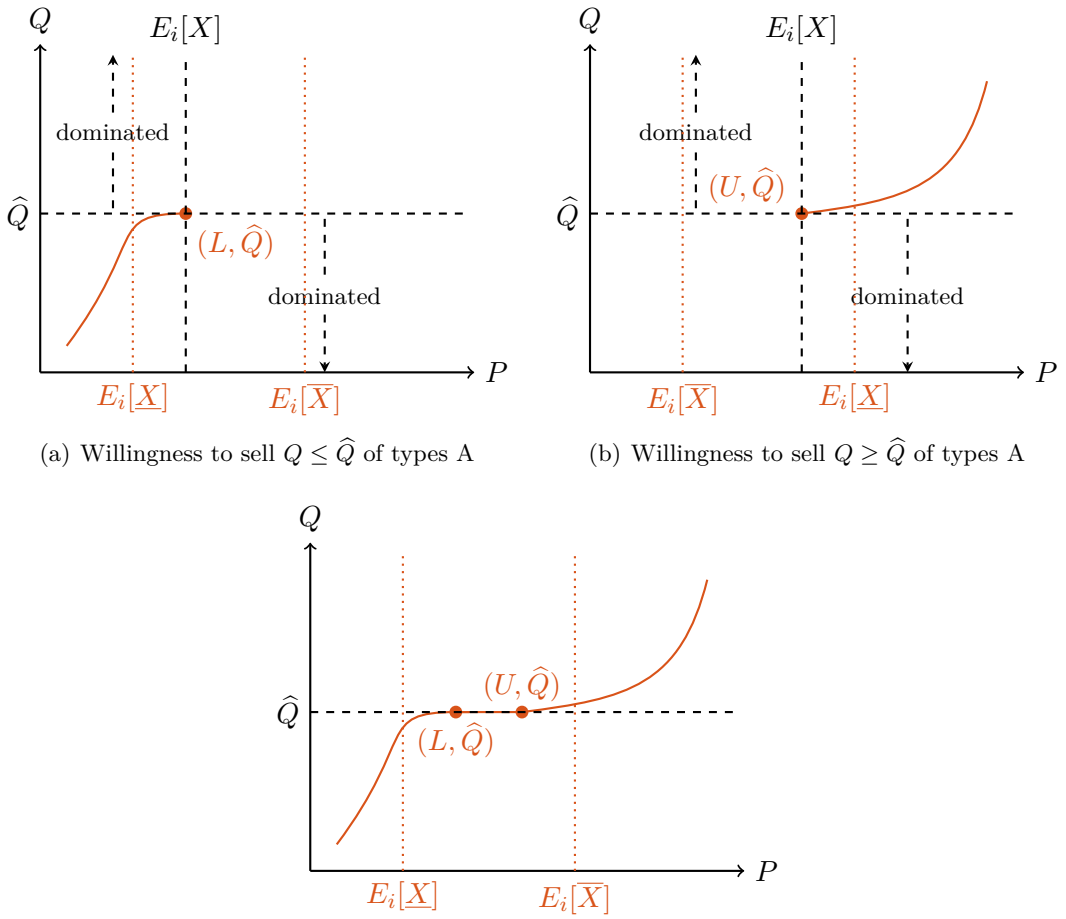

(a) Willingness to sell $Q \leq \widehat{Q}$ of types A

(b) Willingness to sell $Q \geq \widehat{Q}$ of types A

(c) Supply of types A

FIGURE 1.2. SUPPLY CURVE OF AMBIGUITY-AVERSE SELLER WITH MULTIPLE-PRIORS

Notes: This figure shows the piecewise flat supply curve for complex risks implied by the α-maxmin model (Eq. (1.2)) for a risk-averse and ambiguity-disliking seller i.

Mispricing and Suboptimal Risk Sharing

How complex risks are priced and shared in equilibrium, crucially depends on agents' beliefs regarding π. If aggregate endowments are constant, the risky asset is mispriced whenever the market-clearing price deviates from its expected dividend. Furthermore, the absence of aggregate risk in combination with a complete market allows for perfect risk sharing. Hence, whenever the market-clearing quantity (per capita) is different from $\widehat{Q}$, consumption risk is only suboptimally shared among risk-averse agents. I therefore subsequently refer to the market-clearing price and quantity for simple risks, i.e., $(E[X], \widehat{Q})$, as *benchmark equilibrium*.

Nonambiguity-loving agents ($\alpha_i \geq 1/2$) with correct beliefs ($\pi \in \mathcal{B}_i$) never cause any mispricing or incomplete risk sharing, simply because their supply or demand curves always go through (see above) the benchmark equilibrium. Due to the jump of their supply (demand) curve between U and L, an ambiguity-loving seller (buyer) almost surely never chooses to sell (buy) $\widehat{Q}$ shares at $P = E[X]$, independently of her beliefs regarding π. While it is clear why

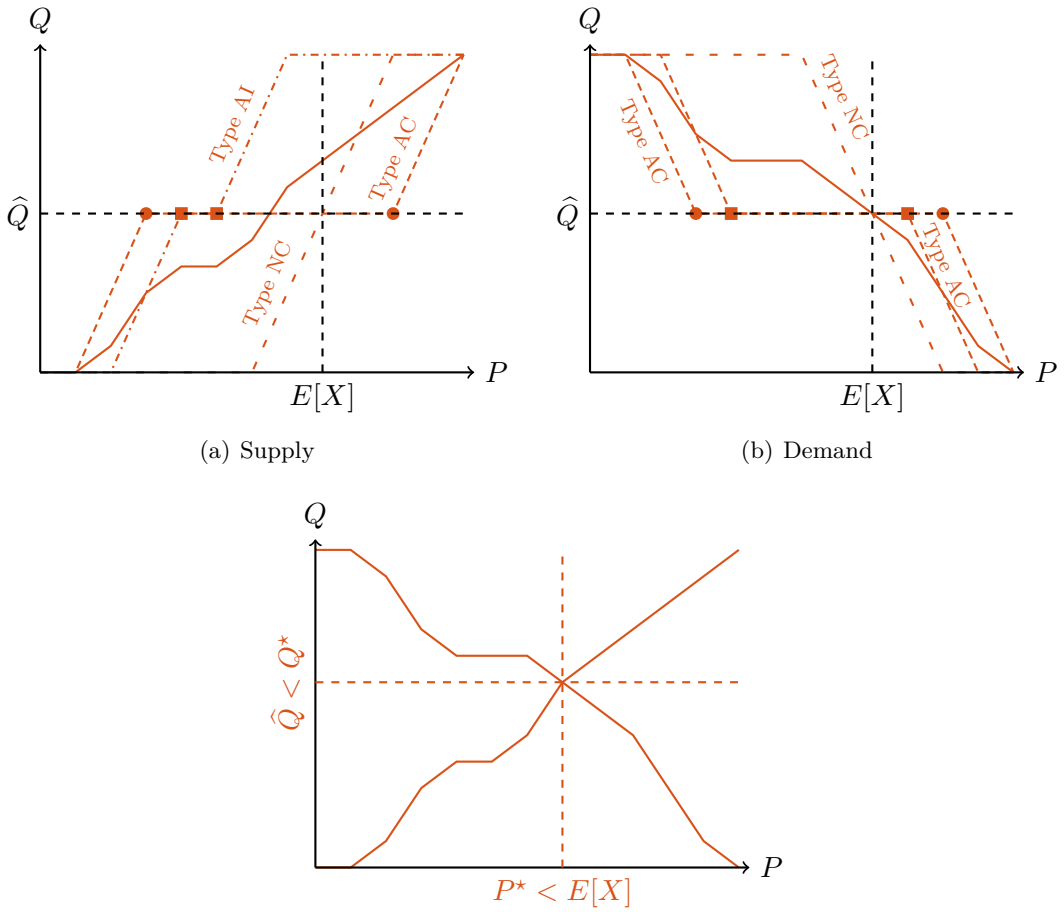

(a) Supply

(b) Demand

(c) Equilibrium

FIGURE 1.3. EQUILIBRIUM ANALYSIS FOR COMPLEX RISKS UNDER MULTIPLE-PRIORS UTILITY

Notes: For the α-maxmin model (Eq. (1.2)), this figure illustrates how ambiguity-averse agents with incorrect beliefs can cause mispricing and suboptimal risk sharing of complex risks in equilibrium (Proposition 1.3). Subfigure (a) shows three exemplary supply curves of one ambiguity-neutral (type NC) and two ambiguity-averse (type AC and AI) sellers. All exemplary buyers in Subfigure (b) are assumed to be nonambiguity-loving and to have correct beliefs. Subfigure (c) finally shows, how the incorrect beliefs of seller AI cause mispricing and incomplete risk sharing of complex risks in equilibrium. Due to the absence of aggregate consumption risk, both distortions are unambiguously defined and measurable.

ambiguity-neutral agents with incorrect beliefs provoke mispricing and suboptimal risk sharing, due to their piecewise constant supply and demand curves, this is, however, less clear for ambiguity-averse agents whose $\mathcal{B}_i$ does not contain π.

Proposition 1.3. *In the presence of perceived ambiguity and if there exists a tradable quantity $\widehat{Q}$ such that $\sigma_i = 0 \ \forall i \in \mathcal{I}$, then any nonzero mass of type AI sellers (buyers) moves aggregate supply (demand) away from the market equilibrium under simple risks.*

Proof. For proof see Appendix A1. □

Figure 1.3 illustrates the mechanics behind Proposition 1.3 for the simplified case of only three sellers and buyers, respectively. Subfigure (a) depicts the exemplary supply curves (for a given discrete price grid) from three different sellers. Assuming type NC to be ambiguity-neutral, she chooses—in line with her correct beliefs—to sell $\widehat{Q}$ shares for $P = E[X]$. Due to type AC's pronounced ambiguity-aversion, her supply curve is constant over a considerable subset of prices (delimited by circles). Importantly, since $\pi \in \mathcal{B}_{\text{AC}}$, its constant part still contains the benchmark equilibrium. In contrast, the constant piece of type AI's supply curve (delimited by squares) does *not* include the point $(E[X], \widehat{Q})$. Hence, neither the length of $\mathcal{C}_{\text{AI}}$ nor the degree of her ambiguity-aversion $\alpha_{\text{AI}} > 1/2$ are sufficient to prevent that $\pi \notin \mathcal{B}_{\text{AI}}$. Therefore, based on incorrect beliefs, her supply draws the *average* supply curve (solid line) away from the benchmark equilibrium.

For simplicity, all three buyers in Subfigure (b) are assumed to hold correct beliefs such that their demand curves all contain the benchmark equilibrium. This ensures that any mispricing and incomplete risk sharing in equilibrium is solely driven by the AI-type seller's supply curve in Subfigure (a). The solid line constitutes the resulting *average* demand curve. Finally, Subfigure (c) depicts the market-clearing price $P^\star$ and quantity $Q^\star$ (per capita) that corresponds to the intersection of the average supply and demand curves. Due to seller AI's underestimation of π, the market-clearing price is smaller than the stock's expected dividend, implying mispricing equal to $|P^\star - E[X]|$. Furthermore, the average market-clearing quantity of shares is greater than $\widehat{Q}$, i.e., in equilibrium, agents do not share complex risks perfectly.

Intuitively, Proposition 1.3 establishes a condition under which ambiguity-induced price insensitivity is sufficiently large in order to offset any equilibrium effects of incorrect beliefs about complex risks. Given the midpoint of agent i's set of priors $\mathcal{C}_i$, the more ambiguity-averse she is, i.e., the larger her α_i, the wider becomes the subset of payoff distributions $\mathcal{B}_i$ for which incorrect beliefs do not cause any deviations from the benchmark equilibrium. Note that for any $\alpha_i < 1$, the subset $\mathcal{B}_i$ in Eq. (1.4) is strictly smaller than $\mathcal{C}_i$. Thus, as long as agent i is not maximally ambiguity-averse, requiring the true payoff distribution π to be contained in $\mathcal{C}_i$ is not sufficient for precluding differences between simple and complex equilibria.

From Multiple-priors to Rank-dependent Expected Utility

Since the seminal work by Tversky and Kahneman (1992), cumulative prospect theory has become the most prominent alternative to expected utility for modeling decision making under uncertainty. Therefore, a reasonable question likely asked by the reader is the following: How do trading decisions under complex risks from agents with rank-dependent utility differ from the herein presented analysis? For binary acts, e.g., trading the above risky asset, Chateauneuf et al. (2007) show that their proposed 'neo-additive' decision weights allow for a one-to-one correspondence from α_i and $\mathcal{C}_i$ in Eq. (1.2) to (i) a likelihood sensitivity index and (ii) a pessimism (optimism) index as generally used in rank-dependent expected utility models.[13]

[13] In rank-dependent expected utility models, the likelihood sensitivity index measures the steepness of the probability weighting function and the optimism (pessimism) index its intersection point with the 45-degree line.

Smooth Ambiguity Preferences

Proposition 1.2's somehow extreme result of (local) perfect price inelasticity is arguably linked to the kinked preferences induced by the maxmin property of Eq. (1.2). In order to support the generalizability of the result's qualitative finding, I henceforth analyze individual trading behavior under the 'smooth ambiguity' model by Klibanoff et al. (2005). Adopting the above notation, agent i's utility from consumption in $t = 2$ can then be written as

$$\mathcal{U}_i(C_i(\omega)) = \int_{\Delta(\Omega)} \phi_i \left(E[U_i(\tilde{\pi})] \right) \mathrm{d}\mu_i(\tilde{\pi}), \tag{1.5}$$

where $\Delta(\Omega)$ is the simplex of all possible payoff distributions on Ω, μ_i is agent i's subjective probability measure on $\Delta(\Omega)$, and ϕ_i is a continuous, strictly increasing, real-valued function.

Eq. (1.5) has an intuitive interpretation: On the one hand, the more payoff distributions exhibit a nonzero probability mass under μ_i, the bigger agent i's set of possible priors. On the other hand, the curvature of $\phi_i(\cdot)$ expresses her ambiguity preferences: As for utility functions in the presence of risk, concavity of $\phi_i(\cdot)$ implies ambiguity-averse, linearity ambiguity-neutral, and convexity ambiguity-loving preferences. Hence, similar to the α-maxmin model in Eq. (1.2), the smooth ambiguity model allows for a separation between the level of ambiguity perceived by agent i as well as her general preferences towards ambiguity per se. For ease of notation and analog to Eq. (1.3), I rely on the following definition:

$$E_i[X] := \int_{\Delta(\Omega)} E_{\tilde{\pi}}[X] \mathrm{d}\mu_i(\tilde{\pi}), \tag{1.6}$$

where $E_{\tilde{\pi}}[X]$ denotes the expected payoff of the risky asset based on $\mathbb{P}(\omega{=}u) = \tilde{\pi}$ and $\mathbb{P}(\omega{=}d) = 1 - \tilde{\pi}$, respectively.

Proposition 1.4. *Let $\mu_i(\tilde{\pi})$ be the normalized Lebesgue measure on agent i's set of possible priors $[\underline{\pi}_i, \overline{\pi}_i] \subset [0, 1]$, i.e., $\mu_i(\tilde{\pi}) := {}^{1}/_{(\overline{\pi}_i - \underline{\pi}_i)} \mathrm{d}\tilde{\pi} \ \forall \tilde{\pi} \in [\underline{\pi}_i, \overline{\pi}_i]$. In the presence of perceived ambiguity and if there exists a tradable quantity $\widehat{Q}$ such that $\sigma_i = 0 \ \forall i \in \mathcal{I}$, then*

(i) agent i's price elasticity is an increasing function in the second order derivative of $\phi_i(\cdot)$.

(ii) any nonzero mass of sellers (buyers) for whom $\frac{\underline{\pi}_i + \overline{\pi}_i}{2} \neq \pi$ moves aggregate supply (demand) away from the benchmark equilibrium under simple risks.

Proof. For proof see Appendix A1. □

As implied by the proof of Proposition 1.4, with utility as in Eq. (1.5), any agent's supply (demand) curve goes through $(\widehat{Q}, E_i[X])$. Thus, independently of her ambiguity preferences, she always finds it optimal to sell (buy) $\widehat{Q}$ shares for a price P equal to her subjective expected payoff per share given her subset of priors.

For prices below and above $E_i[X]$, Figure 1.4 exemplary illustrates how imperfect information about π affects an ambiguity-averse seller's supply curve. The demand curve for any

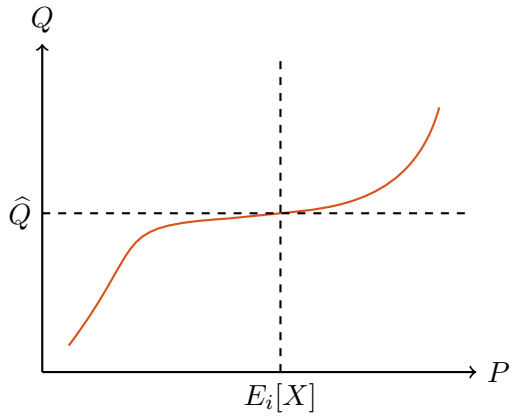

FIGURE 1.4. SUPPLY CURVE OF AMBIGUITY-AVERSE SELLER WITH SMOOTH PREFERENCES

Notes: This figure shows the decreased price elasticity of the supply curve for complex risks implied by the smooth ambiguity model (Eq. (1.5)) for a risk-averse and ambiguity-disliking seller i.

ambiguity-averse buyer behaves analogously. If, under complex risks, seller i dislikes any perceived ambiguity regarding π, selling $\widehat{Q}$ shares generally becomes more attractive than under simple risks. Due to her smooth distaste for ambiguity, i.e., the concavity of $\phi_i(\cdot)$, she smoothly decreases her supply's price elasticity for prices different from $E_i[X]$, as displayed in Figure 1.4. However, in contrast to Figure 1.2, her supply curve never becomes perfectly inelastic for any interior nonempty subset of prices.

In case seller i is ambiguity-loving, i.e., $\phi_i(\cdot)$ is convex, the slope of her supply curve amplifies when moving form simple to complex risks. Comparing Figure 1.4 to Subfigure (a) in Figure 1.1 moreover shows how increasing complexity under Eq. (1.5) manifests itself similarly as a shift in sellers' risk aversion under Eq. (1.1): If seller i is ambiguity-averse, she is always willing to accept a lower μ_i in return for a *gradual* reduction in σ_i.

For equally probable priors, the second part of Proposition 1.4 states that whenever there is a critical mass of agents for whom π is different from their respective midpoint of priors, they shift aggregate supply (demand) away from the benchmark equilibrium. Under the smooth ambiguity model, the pricing and allocation of complex risks is therefore more sensitive to agents' ex-ante beliefs than under kinked ambiguity-preferences. For smooth preferences, ambiguity-induced price insensitivity can never offset a critical mass' distorting equilibrium effects of incorrect beliefs, no matter how small the respective deviations relative to π are.

Summary

In contrast to the smooth ambiguity model, the pricing of complex risks by ambiguity-averse agents with multiple-priors utility is less sensitive to incorrect beliefs. Within the multiple-priors model, the necessary mispricing condition requires the exclusion from a set, i.e., $\pi \notin \mathcal{B}_i$, instead of a pointwise deviation from π. Another implication of its piecewise constant supply (demand) curve is the arising possibility of multiple equilibria. In an economy with three-dimensional

heterogeneous agents, i.e., with respect to their beliefs as well as their preferences towards risk and ambiguity, multiple equilibria are nevertheless unlikely to prevail. For instance, if the supply curve of a given mass of sellers equals $\widehat{Q}$ for a nonsingleton subset of prices, a nonzero mass of sellers whose supply is not constant over the same subset is sufficient for the average supply curve to be nonconstant.

In general, within both models, complex risks have similar implications for individual trading behavior and aggregate market outcomes:

1. If averse to complexity-induced ambiguity, the price sensitivity of agents with nonsingleton priors *decreases* under complex risks.

2. Agents with nonsingleton priors can cause *mispricing* and trade towards *suboptimal allocations* of complex risks.

These two implications are not independent. A decrease in price sensitivity around the perfect hedging quantity $\widehat{Q}$ reduces the potential for imperfectly shared idiosyncratic risks. This is intuitive, because, under complex risks, ambiguity-averse agents always prefer to trade (close to) $\widehat{Q}$ shares for a wider range of prices. However, for smooth ambiguity preferences, a reduction in price sensitivity does not attenuate the degree of mispricing induced by imperfect information (see above).

1.2.4 Price-taking Behavior, Asymmetric Information, and Strategic Uncertainty

Before turning to the experimental test of the above theory, three potentially interfering effects need to be addressed more carefully. First, my model economy assumes infinitely many agents. When implementing it in the laboratory, complying with this particular assumption constitutes an apparent impossibility. I meet this practical constraint by running all sessions with a relatively high number of at least 16 subjects.[14] Moreover, I alternate between two different pricing schemes: market-clearing—as persistently assumed above—and random price draws (see below). Comparing subjects' supply and demand functions between these two pricing schemes allows me to control for their price-taking behavior.

Second, and more importantly, depending on how agents self-assess their information processing capabilities relative to others, they might perceive considerable information asymmetries in the presence of complex risks. In a Grossman and Stiglitz (1980) rational-expectation equilibrium, market-clearing prices imperfectly reflect informed traders' costly information about the risky stock's expected payoff. Applied to my setting, there exists a dominant strategy for (completely) uninformed agents whose implications are in line with the ambiguity preference-based theory above: Agents who perceive themselves as uninformed (i.e., face too high information processing costs) and *simultaneously* believe markets to generate, at least partially, information efficient prices should always submit perfectly inelastic supply (demand) functions, i.e., $Q_i(P) = \widehat{Q} \ \forall P$.

[14] This minimum number is in line with the average number of 17.6 subjects per session in Biais et al. (2017).

Note, however, that in contrast to Grossman and Stiglitz (1980), I require some unobservable heterogeneity in agents' information processing abilities (costs) in order to prevent market-clearing prices to be fully informative.[15] Otherwise, given the *conditionality* of agents' supply (demand) functions on market-clearing prices, no one has an incentive to process the complex information in the first place. Thus, Grossman and Stiglitz's (1980) informational efficiency paradox would prevail.

Third, any further potential implications caused by strategic uncertainty must be accounted for. In a trading game such as the one considered herein, agent i generally faces strategic uncertainty about the behavior of the remaining $-i$ traders. Whenever agent i forms subjective beliefs about her opponents' actions, these beliefs—whether rationalizable or not—may affect her trading decisions ex-ante.

Alternating between market-clearing and random price draws not only allows for testing the price-taking hypothesis, but additionally enables me to control for any potential effects from either perceived asymmetric information or strategic uncertainty.

1.3 Experiment

In this section I first present the parameterization of the model economy, motivate and illustrate the chosen lab implementation of complex risks, and provide a detailed overview of the conducted sessions. The collected data is then analyzed on both the aggregate as well as on the individual level. For the latter, I construct two different measures of price sensitivity. The variant discrepancy between individual behavior and aggregate outcomes under simple versus complex risks can be reconciled with varying bounds on quasi-rational choice. Finally, markets' general effectiveness in aggregating traders' imperfect information about complex risks is evaluated.

1.3.1 Design and Sessions Overview

The selection process of the model parameters is twofold. On the one hand, the distribution of the stock's binary dividend needs to be fixed. In order to control for a natural focal point effect, I alternate between two values of π, i.e., $\pi \in \{1/3, 1/2\}$. Furthermore, to simplify calculations of expected payoffs, I set the stock's dividend $X(\omega)$ equal to ECU 150 (experimental currency units) in state u and ECU 0 in state d, respectively.

On the other hand, agents' endowments need to be as such that aggregate consumption is constant across states. Table 1.2 presents the endowments for both sellers and buyers that independently apply at the beginning of every trading round. Note, in the presence of equally many sellers as buyers, consumption risk is zero on the aggregate level. In particular, if any seller i and any buyer j agree to trade $\widehat{Q} = 2$ shares at a price per share of P, both are perfectly hedged with constant consumption equal to ECU $300 + 2P$ and ECU $600 - 2P$, respectively.

[15] Whenever agent i believes that there is a nonzero mass of agents submitting supply (demand) functions based on relatively less informative beliefs, she finds herself better off trading according to her more informative beliefs.

TABLE 1.2. ENDOWMENTS FOR SELLERS AND BUYERS

	Seller	Buyer
Stock	4	0
Bond	0	300
Cont. income $I(\omega)$		
State u: $I(u)$	0	0
State d: $I(d)$	300	300
Agg. endowment	constant	

Notes: This table shows the endowments for sellers and buyers, respectively, that apply at the beginning of every independent trading round. All figures except the number of shares are in experimental currency units (ECU).

The symmetry between sellers' and buyers' potential overall consumption is intentional. When comparing local sensitivities between their supply and demand, symmetric function arguments allow me to isolate and solely analyze preference driven differences.[16]

Complex versus Simple Risks in the Laboratory

When implemented in the laboratory, complex risks need to satisfy two necessary conditions in order to comply with the above definition:

(i) they have to follow an *objective* underlying probability distribution, and

(ii) subjects have to be aware of the problem's well-defined nature and the existence of its *unique* solution.

Moreover, when aiming for informative empirical data, the (imperfect) information about complex risks should

(iii) not be too complex, i.e., imposing at least some nontrivial restrictions on subjects' sets of priors, but

(iv) still be complex enough such that subjective priors neither are singletons.

I argue that the following implementation satisfies (i)–(iv). Consider the geometric Brownian motion shown in Subfigure (a) of Figure 1.5. In the 'complexity treatment', subjects were provided with both the *dynamic* visualization of a *reference* path between $t = 0$ and $t = 1$, as well as the *formal* specification of the stochastic differential equation governing its evolution. In order to map a continuous process S_t into the required binary payoff distribution,[17] a simple threshold approach was applied. More specifically, whenever the reference path in $t = 2$ was greater or equal than a predefined threshold L, i.e., if $S_2 \geq L$, the risky stock paid a dividend

[16] Despite the symmetry in total consumption, endowment effects and reference-dependent preferences (see, e.g., Kahneman et al. (1991)) could of course still be at play here. However, I find no such evidence in my experimental data.

[17] Not to be confused with seller i's share endowment S_i in Section 1.2.

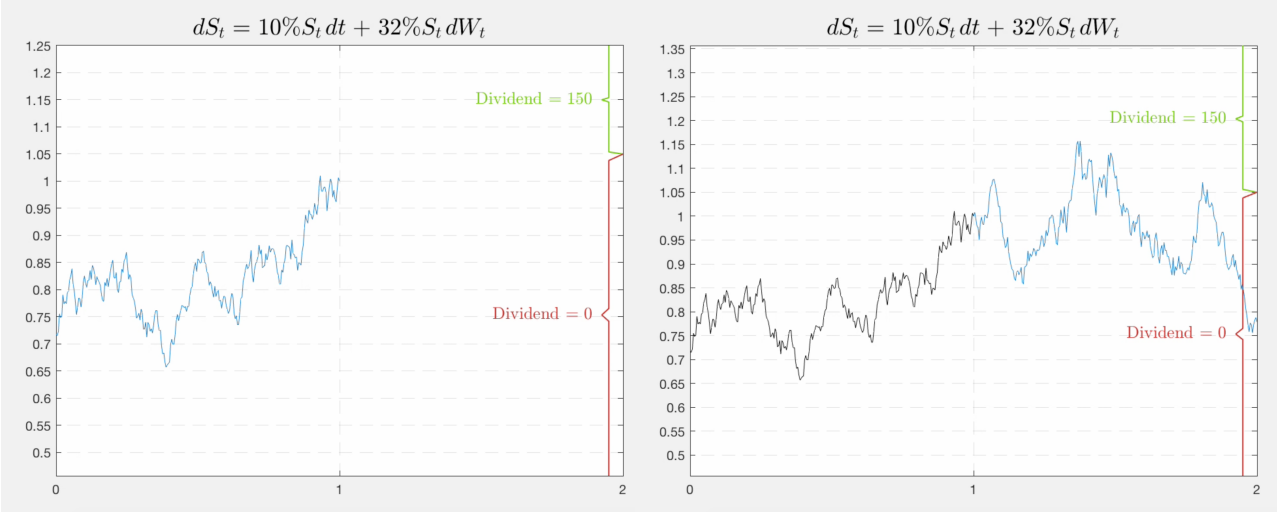

(a) Pre-trading screenshot (b) Post-trading screenshot

FIGURE 1.5. COMPLEX RISKS IN THE LABORATORY

Notes: This figure shows the information about complex risks subjects were provided with during the experiment. For the first stage, Subfigure (a) presents an example of the information displayed on subjects' screens when asked to enter their supply (demand) schedules. Whenever the blue reference path ends up in the green region, the stock pays a dividend per share equal to ECU 150 (experimental currency units) and zero otherwise. Given the here considered parameterization, Appendix B1 shows that the former probability equals $1/2$. For the second stage, Subfigure (b) presents a possible realization of the process and the stock's corresponding payoff per share.

$X(u)$ equal to 150 and zero otherwise. As demonstrated in Appendix B1, the problem of determining $\mathbb{P}(S_2 \geq L)$ as in Figure 1.5 can be solved with a back-of-the-envelope calculation applying Itō calculus.

When submitting their respective supply (demand) functions during the first stage of trading rounds with complex risks, subjects were presented the type of information as exemplary displayed in Subfigure (a) of Figure 1.5. While doing so, they were given the possibility to repeatedly observe the reference path's dynamic evolution between $t = 0$ and $t = 1$. Across complex trading rounds, two different parameterizations of S_t were used—one for $\pi = 1/3$ and one for $\pi = 1/2$, respectively—whereas the realized path was unique to every round. At the second stage, subjects were informed about their number of shares sold (bought) and were presented with the realization of S_2 as, e.g., shown in Subfigure (b).

For submitting their supply (demand) schedules, subjects faced—similar as in Biais et al. (2017)—a predefined price vector. The increment of the uniformly spaced price vector was set to five ECU, i.e., for every $P \in \{0, 5, 10, ..., 145, 150\}$, subjects were asked to choose the preferred number of shares to be sold (bought).[18] These quantities were entered with a precision of two decimal places.

[18]In order to minimize the number of necessary keyboard entries, the decision process was divided into two substages (see the experimental instructions in Appendix E1 for details).

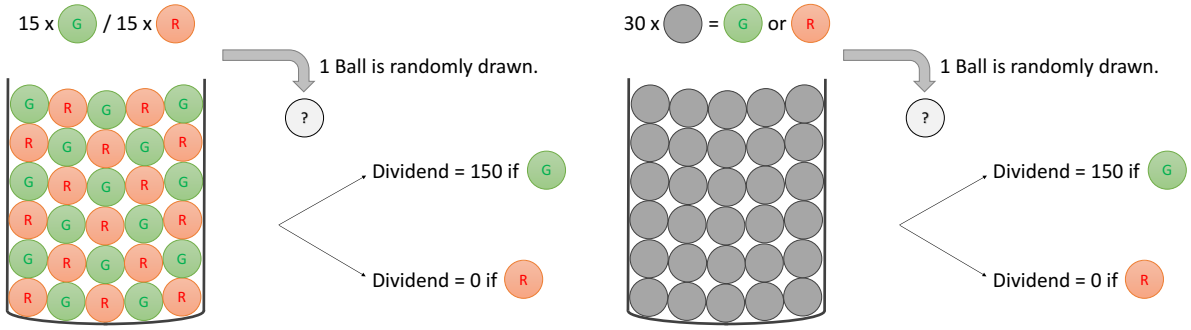

(a) Pre-trading screenshot for simple risks

(b) Pre-trading screenshot for ambiguous risks

FIGURE 1.6. SIMPLE AND AMBIGUOUS RISKS IN THE LABORATORY

Notes: This figure shows the information about simple and ambiguous risks subjects were provided with at the first stage during the respective trading rounds of the experiment. Whenever the randomly drawn ball is green, the stock pays a dividend per share equal to ECU 150 (experimental currency units) and zero otherwise. In contrast to simple risks in Subfigure (a), the distribution of green and red balls in Subfigure (b) is arbitrary.

In order to more precisely test the above theoretical predictions, it is helpful to control for subjects' beliefs about complex risks. This is achieved in the following way. During the first stage of complex trading rounds, subjects were additionally asked to provide their point estimate regarding the stock's expected payoff per share.[19] Independently of subjective preferences, the thereby elicited point estimates allow to anchor subjects' individual sets of priors.

In contrast, during the first stage of trading rounds with *simple* risks, subjects *knew* the exact probability of the stock paying a dividend equal to 150. For the case where $\pi = 1/2$, subjects were confronted with an urn containing 15 green and 15 red balls, as depicted in Subfigure (a) of Figure 1.6. At the second stage, the color of one randomly drawn ball was revealed. Whenever this ball happened to be green, the stock paid a dividend per share equal to ECU 150 and zero otherwise. Finally, as a control treatment, the tradable risks of the last trading round were purely ambiguous. Instead of a 'transparent urn', subjects were confronted with the Ellsberg (1961)-like urn shown in Subfigure (b), whose composition of green and red balls was unknown.

Sessions Structure, Incentivization, and Subject Summary Statistics

Table 1.3 provides an overview of the six sessions conducted in the 'Laboratory for Experimental and Behavioral Economics' at the University of Zurich during fall 2016. The number in parenthesis indicates the number of subjects in a given session. Each session consisted of ten independent trading rounds. All subjects only participated in one session. For every single trading round, Table 1.3 lists the actual payoff distribution, the nature of the underlying consumption risk—simple (S) versus complex (C), and the applied pricing scheme—market clearing (MC)

[19] Depending on subjects' respective preferences, the risky asset's expected payoff under complex risks is either defined by the mean of Eq. (1.3) for trading more or less than $\widehat{Q}$ shares, or by Eq. (1.6), respectively.

TABLE 1.3. SESSIONS OVERVIEW

	Session 1 (#16)			Session 2 (#18)			Session 3 (#16)		
Round	π	Type	Pricing	π	Type	Pricing	π	Type	Pricing
1	1	C (P)	MC	1	C (P)	MC	1	C (P)	MC
2	high	C (P)	random	high	C (P)	random	high	C (P)	random
3	low	C (P)	MC	low	C (P)	MC	low	C (P)	MC
4	1/2	C	MC	1/3	C	random	1/3	C	MC
5	1/3	C	MC	1/2	C	random	1/3	C	random
6	1/2	C	random	1/3	C	MC	1/2	C	MC
7	1/3	C	random	1/2	C	MC	1/2	C	random
8	1/2	S	MC	1/2	S	random	1/2	S	MC
9	1/3	S	random	1/3	S	MC	1/3	S	random
10	ambig	A	MC	ambig	A	random	ambig	A	MC
	Session 4 (#16)			**Session 5 (#16)**			**Session 6 (#16)**		
Round	π	Type	Pricing	π	Type	Pricing	π	Type	Pricing
1	1/2	S (P)	MC	1/2	S (P)	MC	1/2	S (P)	MC
2	9/10	S (P)	random	9/10	S (P)	random	9/10	S (P)	random
3	1/2	S	MC	1/2	S	random	1/2	S	MC
4	1/3	S	random	1/3	S	MC	1/3	S	random
5	high	C (P)	MC	high	C (P)	MC	high	C (P)	MC
6	1/2	C	MC	1/3	C	random	1/3	C	MC
7	1/3	C	MC	1/2	C	random	1/3	C	random
8	1/2	C	random	1/3	C	MC	1/2	C	MC
9	1/3	C	random	1/2	C	MC	1/2	C	random
10	ambig	A	MC	ambig	A	random	ambig	A	MC

Notes: This table provides an overview of the six conducted sessions. Each session consisted of ten independent trading rounds. The number in parenthesis indicates the number of subjects in a given session. For every session, the first column lists the actual payoff distribution, the second column the nature of the underlying consumption risk (simple (S) versus complex (C)), and the third column the applied pricing scheme (market clearing (MC) versus random price draw (random)). The 'high' ('low') π refers to an integer parameterization of the geometric Brownian motion that implies a 84.21% (15.89%) probability of a dividend per share equal to 150. Trading rounds with a 'P' in parenthesis are practice rounds.

versus random price draw (random). A 'high' ('low') π refers to an integer parameterization of the stochastic reference path S_t that results in a probability $\mathbb{P}(S_2 \geq L)$ of 84.21% (15.89%), and 'P' denotes a practice round. To control for potential 'comparative ignorance effects' (see Fox and Tversky (1995)), the sequential ordering of simple and complex risks is reversed between the first three and the last three sessions.

In each session, after the ten trading rounds shown in Table 1.3, subjects were additionally presented with two lotteries, each based on one of the two urns in Figure 1.6. For both lotteries, their certainty equivalents were elicited via Abdellaoui et al.'s (2011) computerized iterative choice list method. Importantly, the lotteries' payoffs were chosen such that they matched the range of possible consumption levels in each of the previous trading rounds (see Figure D1.2 in Appendix D1). Overall, one session lasted approximately 90 minutes.

Table 1.4. Summary statistics and randomization check

Variable	Total sample ($N = 98$)	Sellers ($N = 49$)	Buyers ($N = 49$)	p-value
Age	23.674	23.837	23.510	0.689
	(3.008)	(3.287)	(2.724)	
Gender	0.337	0.286	0.388	0.393
	(0.475)	(0.456)	(0.492)	
UZH (ETH)	0.582	0.653	0.510	0.219
	(0.496)	(0.481)	(0.505)	
# semesters	3.806	3.633	3.980	0.365
	(2.827)	(2.928)	(2.742)	
Knowledge BM	0.459	0.367	0.551	0.105
	(0.501)	(0.487)	(0.503)	
Risk aversion	0.060	0.087	0.035	0.328
	(0.265)	(0.294)	(0.232)	
CRRA-γ	0.684	1.045	0.323	0.335
	(3.358)	(4.415)	(1.740)	
Ambiguity aversion	0.101	0.067	0.133	0.133
	(0.245)	(0.225)	(0.262)	

Notes: This table reports means and standard deviations (in parenthesis) in the total sample and across sellers and buyers, respectively. p-values for the null hypothesis of perfect randomization are listed in the last column (Wilcoxon signed rank tests for interval variables and Yates (1934)' corrected χ^2 tests for binary variables). 'Age' is reported in years. 'Gender' and 'UZH' are dummy variables indicating female subjects and students from the University of Zurich (versus ETH). '# semesters' denotes the number of completed semesters. 'Knowledge BM' is a dummy variable equal to one for subjects who have heard about the mathematical object 'Brownian motion' before. Risk aversion is measured as the normalized difference ($\in [-1, 1]$) between the simple lottery's expected payoff and subjects' respective certainty equivalents. CRRA-γ denotes the corresponding constant relative risk aversion coefficient. Ambiguity aversion is measured as the individual differences in certainty equivalents between the simple and ambiguous lottery.

At the end of every session, one out of the seven nonpractice trading rounds *or* one of the two lottery outcomes was randomly chosen, each with equal probability. Subjects then were paid either their final wealth of the selected trading round or the outcome of the selected lottery, both divided by twelve. Additionally, if their point estimate regarding π was correct (within $\pm 3\%$), they earned an extra three Swiss francs, whenever the corresponding trading round was selected for payment. On average, participants received 38.40 Swiss francs, with a maximum of CHF 50 and a minimum of CHF 25.

Recruited subjects were students from either the University of Zurich or ETH Zurich, majoring in economics, business, mathematics, physics, engineering, or computer science, respectively. Their respective role of either a buyer or a seller was randomly assigned at the beginning of the experiment and thereafter retained throughout all trading rounds. The instructions provided to subjects acting as sellers are provided in Appendix E1.[20]

[20] Analogous instructions were provided to subjects acting as buyers and are available upon request.

Table 1.4 presents the average values (proportions) of certain socioeconomic variables collected via a short questionnaire following the main experiment. Risk aversion is measured as the normalized difference between the simple lottery's expected payoff and subjects' respective certainty equivalents. A value of one (minus one) denotes maximum (minimum) risk aversion,[21] a value of zero implies risk-neutrality. The total sample's average risk aversion of 0.060 corresponds to a constant relative risk aversion (CRRA) coefficient of 0.684.[22] Ambiguity aversion is defined as the individual differences in certainty equivalents for the simple and ambiguous lottery. Hence, a positive value indicates ambiguity aversion. A standard randomization check reveals no significant indications of an unbalanced sample.[23]

1.3.2 Aggregate Market Outcomes

Figure 1.7 shows average supply and demand curves across sessions with identical chronology of simple versus complex risks. For trading rounds with complex risks, the vertical solid (dotted) line indicates sellers' (buyers') average point estimate of the risky asset's expected payoff. In general, subjects overestimate the latter,[24] where in three of four cases, sellers' average estimate exceeds the one of buyers.[25] Focusing on average supply and demand curves around (average) expected payoffs, price sensitivities locally decrease for all four cases in Figure 1.7 when moving from simple to complex risks.

Table 1.5 reports average market clearing prices and quantities in concordance with Figure 1.7, i.e., across sessions with the same sequential order of simple and complex trading rounds. Moreover, column three and four of Table 1.5 list the degree of mispricing and suboptimal risk sharing according to the respective definitions in Section 1.2. As anticipated, mispricing is clearly less pronounced under simple than under complex risks. Notably, however, even under complex risks, the price of the risky stock seems relatively reasonable (average deviation from expected payoffs of approximately 14%). Both simple and complex risks are well shared. Strikingly, in three out of four cases, the degree of risk sharing is higher or equal for complex relative to simple trading rounds.

In order to better visualize local differences in price sensitivity, I adjust the average supply and demand curves under complex risks in Figure 1.7 to control for subjective beliefs. Essentially, the price grid, against which each individual curve gets plotted, is adapted such that average payoff estimates coincide with risky assets' true expected payoffs (see Appendix C1 for details).

---

[21] According to Abdellaoui et al.'s (2011) iterative choice list method.

[22] My estimate of average relative risk aversion is in line with the experimental literature: see Holt and Laury (2002) for binary lotteries, Goeree et al. (2002) for private value auctions, Goeree et al. (2003) for generalized matching pennies games, and Goeree and Holt (2004) for one-shot matrix games. Similarly, Biais et al. (2017) find the representative investor's CRRA coefficient to approximately equal 0.5.

[23] Throughout the entire paper, I report two-sided p-values.

[24] One possible explanation is that subjects fail to account for the second order effect due to the nonzero quadratic variation of the Brownian motion W_t.

[25] This could be due to an 'indirect' endowment effect.

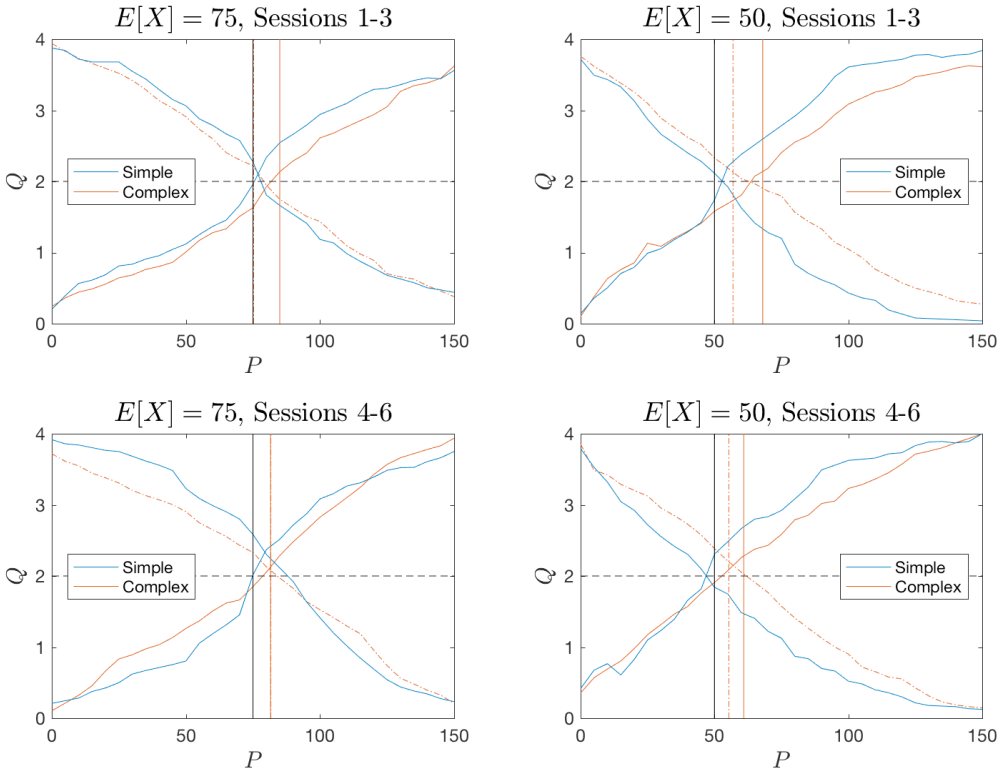

FIGURE 1.7. AVERAGE SUPPLY AND DEMAND

Notes: This figure shows the average supply and demand curves across subjects and trading rounds. In the top (bottom) row, averages are computed across sessions where complex (simple) trading rounds are followed by simple (complex) trading rounds. In the left (right) column, averages are computed across trading rounds where π is equal to $1/2$ ($1/3$). The black horizontal line (first from the left) corresponds to the risky asset's expected payoff. The solid horizontal line indicates sellers' average point estimate of the risky asset's expected payoff under complex risks, whereas the dotted horizontal line corresponds to the average of buyers' respective point estimates. In the lower left plot, the two exactly coincide.

Figure 1.8 presents the adjusted supply and demand curves under complex risks. In contrast to Figure 1.7, Figure 1.8 allows for a direct comparison of price sensitivities. For prices close to but below $E[X]$, all four supply curves for simple risks lie below the respective supply curves for complex risks, only to cross the latter for prices close to but (generally) higher than $E[X]$ (vertical lines in Figure 1.8). The opposite holds true for the two demand curves where π equals $1/2$ (left column of Figure 1.8). For π equal to $1/3$, demand curves coincide for very low prices, but are higher in the case of complex risks for prices around and above $E[X]$.

For a more systematic investigation of the empirical supply and demand functions depicted in Figure 1.8, I plot the respective averages across all sessions (to further reduce noise) together with their respective error bounds, indicating standard errors of the mean. The resulting supply and demand curves are shown in Figure 1.9. The above described pattern now manifests itself more clearly. For π equal to $1/2$ (left column of Figure 1.9), the average supply (demand) for simple risks crosses the respective supply (demand) for complex risks from below (above). For

TABLE 1.5. AVERAGE MARKET CLEARING PRICES AND QUANTITIES

	Market clearing		Mispricing	Suboptimal risk sharing
	$P^\star$	$Q^\star$	$\lvert P^\star - E[X]\rvert$	$\lvert Q^\star - \widehat{Q}\rvert$
Simple risks				
$\pi = 1/2$				
Sessions 1-3	76.87	2.10	1.87	0.10
Sessions 4-6	79.47	2.33	4.47	0.33
$\pi = 1/3$				
Sessions 1-3	52.82	2.01	2.82	0.01
Sessions 4-6	46.89	2.00	3.11	0.00
Complex risks				
$\pi = 1/2$				
Sessions 1-3	80.30	1.94	5.30	0.06
Sessions 4-6	80.98	2.10	5.98	0.10
$\pi = 1/3$				
Sessions 1-3	63.47	1.99	13.47	0.01
Sessions 4-6	56.98	2.15	6.98	0.15

Notes: This table reports average market clearing prices and quantities across sessions with the same sequential order of trading rounds involving simple and complex risks, respectively. Moreover, the measures of mispricing and suboptimal risk sharing as defined in Section 1.2 are listed in column three and four.

π equal to $1/3$, the same is true for sellers, whereas for buyers, average demands converge at a price close to the risky stock's expected payoff. Furthermore, in all four cases, there is a clear difference in price sensitivity around prices equal to expected values.

The statistical significance of the differences in Figure 1.9 is tested by conducting a Wilcoxon signed-rank test, where, in the case of complex risks, interpolated quantities are used. The results thereof are plotted in Figure D1.3 in Appendix D1. As conjectured, the average supply curves are statistically different for prices below and above expected payoffs. In case of π equal to $1/2$, the same statistically significant hump-shaped pattern around $E[X]$ is observed for average demand curves. For π equal to $1/3$, their p-values are close to 0.1 below $E[X]$, temporarily increase around $E[X]$, and decrease again sharply to values close to zero thereafter.

Naturally, an analogous analysis lends itself to contrast subjects' behavior between the two applied pricing mechanisms: market clearing and random price draws. Figure 1.10 presents the respective supply and demand curves averaged across complex trading rounds with equal pricing schemes. Overall, average supply and demand for complex risks look very similar between the two pricing mechanisms. The p-values of the corresponding Wilcoxon signed-rank test are plotted in Figure D1.4 in Appendix D1. The patterns in Figure D1.4 indicate that there exists no statistical evidence against the hypothesis of a globally (across pricing schemes) adopted price-taking behavior. Hence, neither the limited number of subjects, nor asymmetric information,

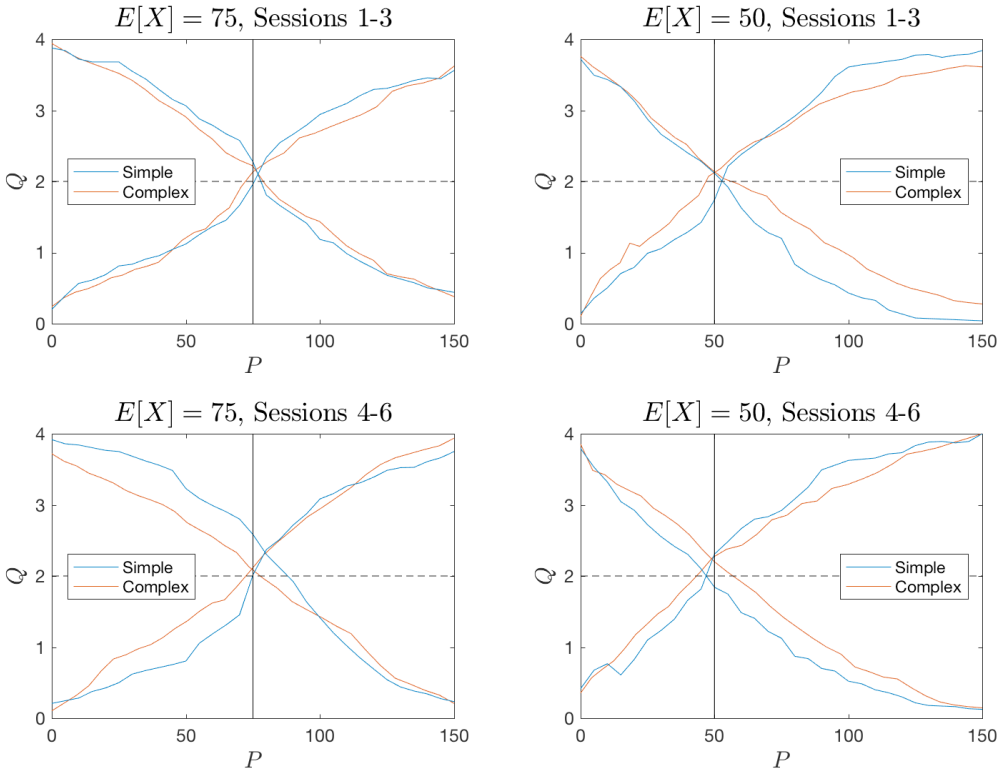

FIGURE 1.8. AVERAGE SUPPLY AND DEMAND ADJUSTED FOR SUBJECTIVE BELIEFS

Notes: This figure shows the average adjusted supply and demand curves across subjects and trading rounds. Average curves for complex risks are adjusted as described in Appendix C1 in order to account for deviations of average beliefs from the true underlying payoff distribution. In the top (bottom) row, averages are computed across sessions where complex (simple) trading rounds are followed by simple (complex) trading rounds. In the left (right) column, averages are computed across trading rounds where π is equal to $1/2$ ($1/3$). The black horizontal line corresponds to the risky asset's expected payoff.

nor strategic uncertainty has an effect on local price sensitivity under complex risks.

1.3.3 Individual Behavior

Aggregate market outcomes appear to corroborate the predictions from theory: Equilibrium quantities are less price-sensitive under complex than simple risks, thereby mitigating the suboptimality in the former's allocation. I subsequently turn to the analysis of individual trading behavior. Therefore, I propose two measures of local price sensitivity at the subject level.

First, from a quantity perspective, I count for each subject i the number of *consecutive* prices for which her submitted supply (demand) schedule equals $\widehat{Q}$ shares, i.e.,

$$\mathcal{M}_i^1 := |\{Q = \widehat{Q}\}_i|, \tag{1.7}$$

where the bars denote the cardinality of the considered set. When determining $\mathcal{M}_i^1$, I focus on subjects who adopt the perfect hedging strategy at least once. Note that this is a direct

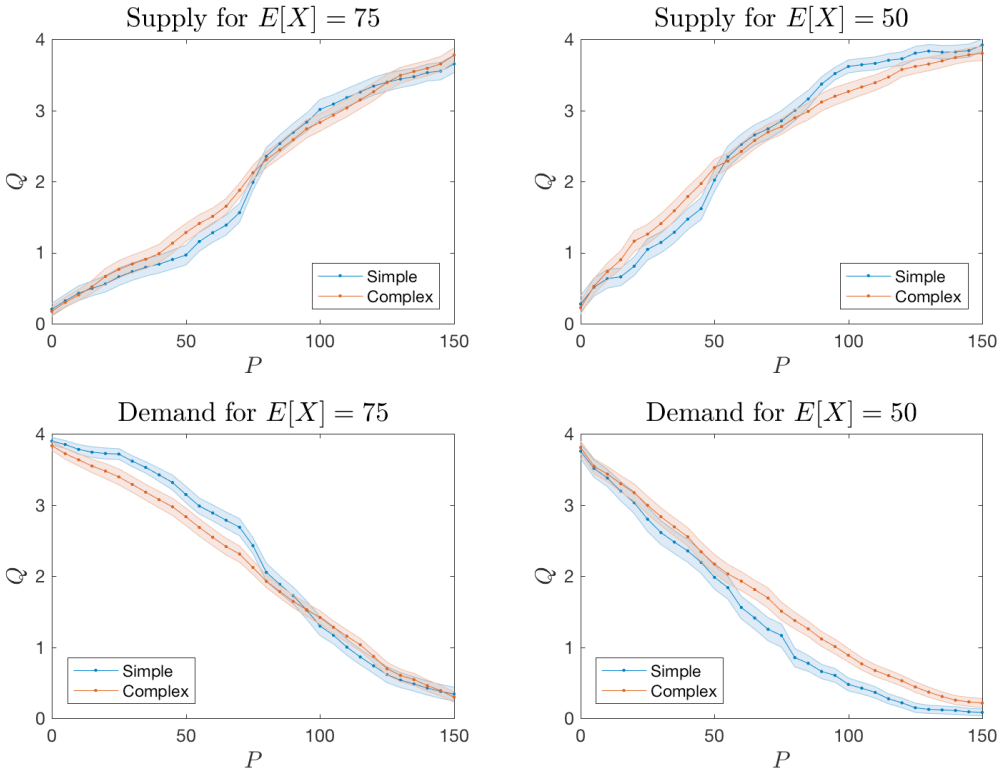

FIGURE 1.9. DIFFERENCES IN AVERAGE SUPPLY AND DEMAND FOR SIMPLE AND COMPLEX RISKS

Notes: This figure shows the average adjusted supply and demand curves across subjects and trading rounds. Average curves for complex risks are adjusted as described in Appendix C1 in order to account for deviations of average beliefs from the true underlying payoff distribution. In the top (bottom) row, average supply (demand) curves are computed across all sessions. In the left (right) column, averages are computed across trading rounds where π is equal to $1/2$ ($1/3$).

implication of risk- and ambiguity-aversion. Additionally, subjects who adopt the perfect hedging strategy more than once but for nonconsecutive prices, i.e., whose supply (demand) functions must be nonmonotonic, are excluded.[26]

Second, from a price sensitivity perspective, I compute the slope of each subject i's supply (demand) function at her individual point estimate $E_i[X]$, i.e.,

$$\mathcal{M}_i^2 := \Delta Q_i(E_i[X]), \tag{1.8}$$

where for sellers

$$\Delta Q_i(E_i[X]) \widehat{=} Q_i(P_{l+2}) - Q_i(P_l),$$

[26] As demonstrated in Figure D1.1 in Appendix D1, there exist strictly concave (piece-wise defined) utility functions that imply nonmonotonic supply (demand) curves. Therefore, I also compute $\mathcal{M}_i^1$ across *all* subjects, even allowing for zero values. None of the herein presented qualitative results are affected.

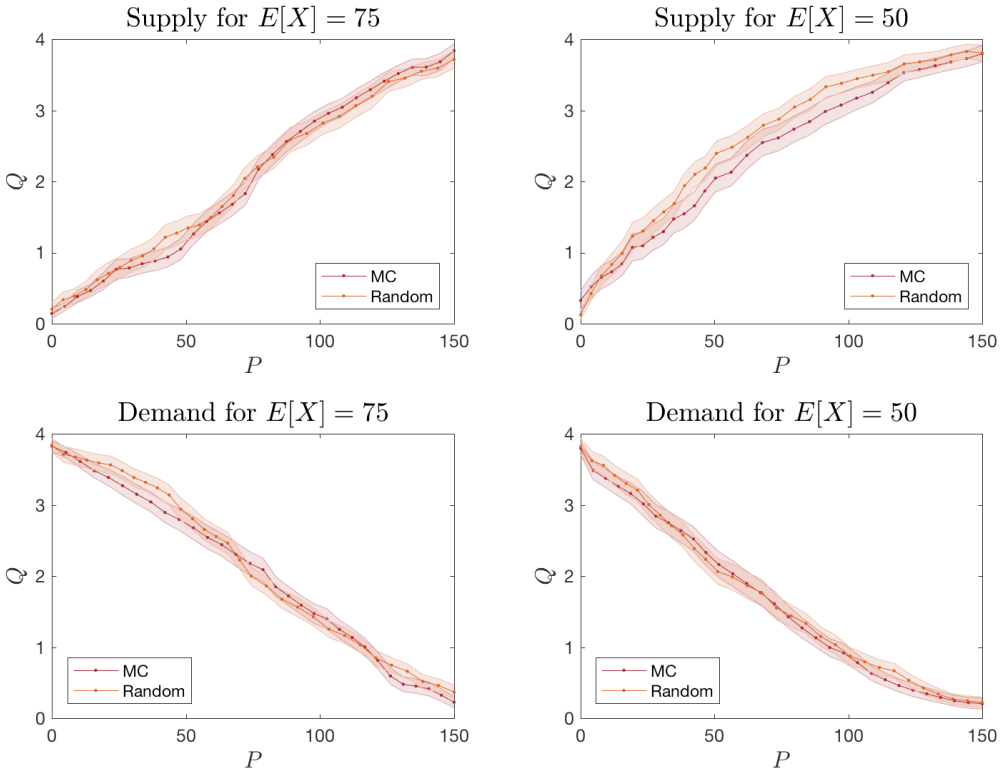

FIGURE 1.10. AVERAGE SUPPLY AND DEMAND ACROSS PRICING SCHEMES

Notes: This figure shows the average adjusted supply and demand curves for complex risks across subjects and the two different pricing schemes: market clearing (MC) and random price draws (random). Average curves are adjusted as described in Appendix C1 in order to account for deviations of average beliefs from the true underlying payoff distribution. In the top (bottom) row, average supply (demand) curves are computed across all sessions. In the left (right) column, averages are computed across complex trading rounds where π is equal to $1/2$ ($1/3$).

and for buyers

$$\Delta Q_i(E_i[X]) \mathrel{\widehat{=}} Q_i(P_{f-2}) - Q_i(P_f),$$

respectively, with P_l (P_f) denoting the last (first) price strictly below (above) seller (buyer) i's point estimate $E_i[X]$. The '± 2' in the index ensures that $P_l < E_i[X] < P_{l+2}$ for sellers and $P_{f-2} < E_i[X] < P_f$ for buyers, respectively. By construction, $\mathcal{M}_i^2$ can only be computed if P_{l+2} (P_f) is smaller or equal to $\max(P) = 150$. Under simple risks it holds of course that $E_i[X] = E[X]$ $\forall i \in \mathcal{I}$. Moreover, $\mathcal{M}^2$ can be interpreted as a less extreme measure of price sensitivity than $\mathcal{M}^1$, where the latter only accounts for perfect price inelasticity.

Figure 1.11 displays the between-treatment average values of $\mathcal{M}^1$ and $\mathcal{M}^2$ across all subjects. Subfigure (a) plots the average frequency with which the perfect hedging strategy is adopted. The average price range for which subjects choose to trade $\widehat{Q}$ shares increases by 0.225 under complex relative to simple risks (p-value = 0.726, t-test). Average slopes of pooled supply and demand curves as defined in Eq. (1.8) are plotted in Subfigure (b). Price sensitivity locally

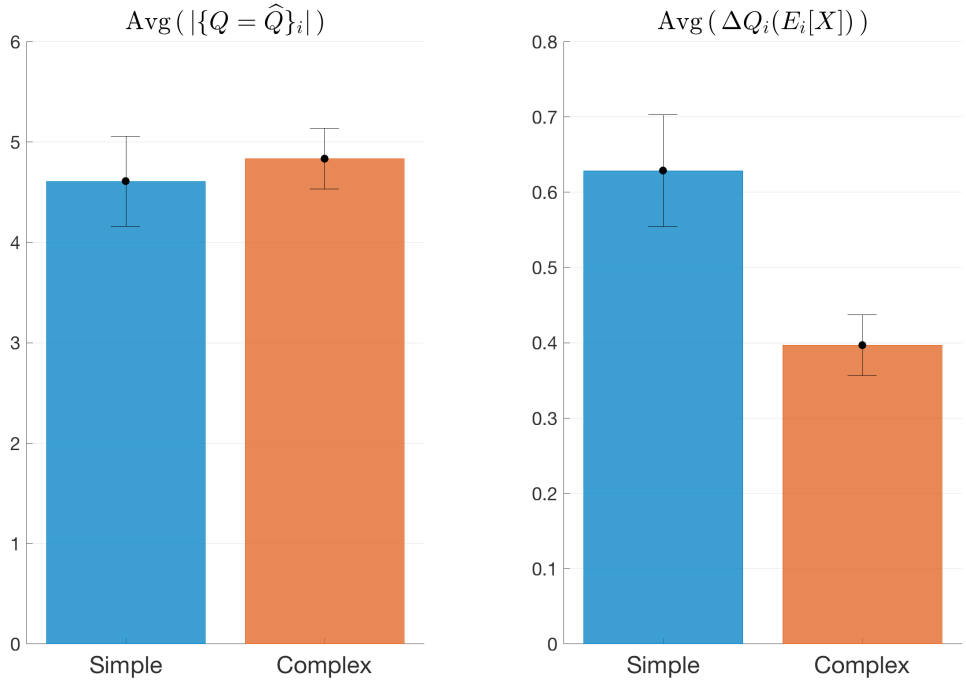

(a) Average frequency of perfect hedging strategy

(b) Average local slope

FIGURE 1.11. INDIVIDUAL MEASURES OF PRICE SENSITIVITY

Notes: This figure shows average individual trading behavior under simple and complex risks across all subjects. Subfigure (a) plots the average consecutive price range for which subjects adopt the perfect hedging strategy, i.e., aiming to trade $\widehat{Q}$ shares (see Eq. (1.7)). Subfigure (b) plots the average slope of subjects' supply and demand curves at their individual point estimates of the risky asset's expected payoff (see Eq. (1.8)). Error bars indicate standard errors of the mean.

decreases by 0.232 when moving from complex to simple risks (p-value = 0.003, t-test).

The results presented in Figure 1.11 are somewhat inconclusive. While, from a price sensitivity perspective, the empirical evidence conforms well to the theoretical predictions, from a pure quantity perspective, no significant increase in the average frequency of the perfect hedging strategy is observed. One can think of two possible reasons: (i) subjects exhibit smooth ambiguity preferences instead of multiple-priors utility, or (ii) subjects fail to trade in their best interest when risks are too complex.

The second argument requires some more elaboration. There exists no theory-consistent reason, why agents failing to trade $\widehat{Q}$ shares at a price equal to $E_i[X]$ should adopt the perfect hedging strategy more frequently under complex relative to simple risks. Put differently, increasing complexity of traded risks may tighten the bounds on traders' rationality as, thereby (partially) detracting the explanatory power of the proposed preference-based theory.

Complexity Bounds on Rationality

In order to control for varying bounds on rationality, I follow Biais et al. (2017) by contrasting individual trading data to a setting of bounded rationality in the spirit of McKelvey and Palfrey's (1995; 1998) quantal response models.[27] As proposed by Luce (1959), I hereafter assume that agent i's trading decisions follow a random choice model. Specifically, for a given price P, her probability density of trading Q_j shares under *simple* risks is given by

$$f_i(Q_j|P) = \frac{\overline{\psi}_i\left(E[U_i(Q_j|P)]\right)}{\int \overline{\psi}_i\left(E[U_i(Q|P)]\right) \mathrm{dQ}}, \tag{1.9}$$

where $\overline{\psi}_i(\cdot)$ denotes an increasing differentiable function and Q runs from zero to the maximum number of tradable shares.

Since $\overline{\psi}_i(\cdot)$ is increasing in $E[U_i(Q_j|P)]$, Eq. (1.9) implies that the likelihood with which agent i decides to sell (buy) Q_j shares is also increasing in $E[U_i(Q_j|P)]$. In other words, the higher the expected utility from trading Q_j shares for a price P, the greater the probability that agent i actually ends up doing so. Hence, the lower the slope of $\overline{\psi}_i(\cdot)$, the more frequently she deviates from her optimal strategy, i.e., the more severe are the bounds on her rationality.

As in Biais et al. (2017), applying bounded rational behavior as formalized in Eq. (1.9) to the above theory of trading simple risks imposes the following three implications:[28]

S1 For $P = E[X]$, the distribution of supplied and demanded shares has a unique mode at $\widehat{Q}$.

S2 For $P < E[X]$, the distribution of supplied and demanded shares is asymmetric around $\widehat{Q}$ and decreasing above (below) $\widehat{Q}$ for sellers (buyers).

S3 For $P > E[X]$, the distribution of supplied and demanded shares asymmetric around $\widehat{Q}$ and decreasing below (above) $\widehat{Q}$ for sellers (buyers).

According to Proposition 1.1, every risk-averse agent whose rationality is bounded as in Eq. (1.9) most likely aims to trade $\widehat{Q}$ shares for $P = E[X]$. Similarly, such risk-averse sellers and buyers more often adopt dominating instead of dominated strategies. Moreover, for a given price, the larger the distance between the chosen quantity and the corresponding set of dominating trades, the less frequently should they opt for the former. Because of the randomness implied by Eq. (1.9), all three implications are convergence results. Hence, if subjects' behavior is indeed governed by Eq. (1.9), whether the limited number of subjects in my sample suffices to yield according results remains an empirical question.

[27] A somewhat stricter caveat as in Biais et al. (2017) applies: In my competitive setting with sufficiently imperfect price informativeness (see above), agents solely trade according to their own beliefs. By differentiating between market-clearing and random pricing, I control for any deviations from such individual behavior.

[28] In contrast to Biais et al. (2017), risk-aversion, i.e., the accordance of agents' expected utilities with second order stochastic dominance, is a necessary condition for the decreasing quantity distributions for prices different than $E_i[X]$. If $\pi = 1/2$, which always holds in Biais et al. (2017), first order stochastic dominance is sufficient.

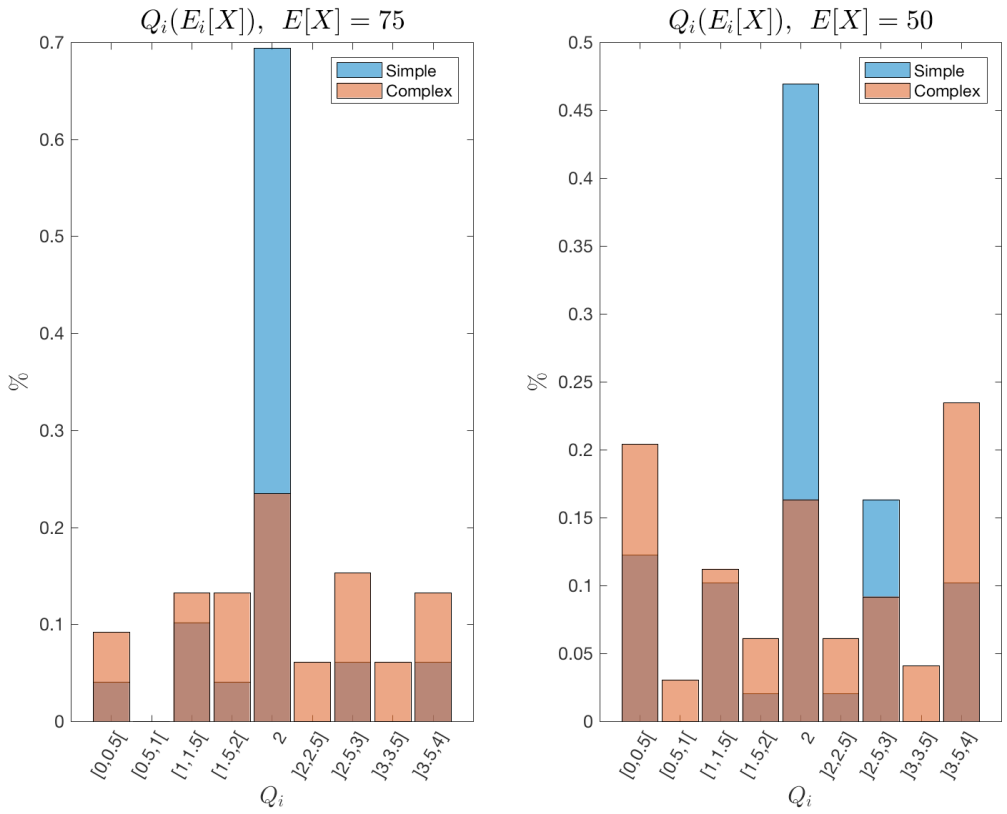

FIGURE 1.12. SUPPLY DISTRIBUTION FOR PRICES EQUAL TO EXPECTED PAYOFFS

Notes: This figure shows the number of shares supplied by sellers for prices equal to (estimated) expected payoffs. The empirical distributions are computed across subjects and sessions. The left (right) plot contrasts average distributions between simple and complex trading rounds with π equal to $1/2$ ($1/3$). If, under complex risks, sellers' point estimate $E_i[X]$ lies between two elements of the predefined price vector, linearly interpolated quantities are reported.

Similarly, under *complex* risks, agent i's decides to trade Q_j shares for a price P with probability

$$\underline{f}_i(Q_j|P) = \frac{\underline{\psi}_i\left(E_i[U_i(Q_j|P)]\right)}{\int \underline{\psi}_i\left(E_i[U_i(Q|P)]\right) \mathrm{dQ}}, \tag{1.10}$$

where, again, $\underline{\psi}_i(\cdot)$ denotes an increasing differentiable function. There are two differences between Eq. (1.9) and Eq. (1.10): On the one hand, given the complexity of traded risks under Eq. (1.10), agents rely on their individual expectation operator $E_i[\cdot]$. On the other hand, due to the different informational precision levels at hand, $\overline{\psi}_i(\cdot)$ and $\underline{\psi}_i(\cdot)$ most likely compose different functions. In particular, postulating more severe (global) bounds on agent i's rationality in the presence of complex risks is equivalent to

$$\overline{\psi}_i(x) > \underline{\psi}_i(x) \quad \text{and} \quad \overline{\psi}'_i(x) > \underline{\psi}'_i(x) \quad \forall x \in E_i[U_i(\cdot)], \tag{1.11}$$

which implies more frequent deviations from her optimal trading strategy. Eq. (1.11) translates to the following three implications regarding individual trading behavior under complex risks:

C1 For $P = E_i[X]$, the distribution of supplied and demanded shares still exhibits a unique mode at $\widehat{Q}$, but is more dispersed than under simple risks.

C2 For $P < E_i[X]$, the distribution of supplied and demanded shares is less asymmetric around $\widehat{Q}$ and decreases less above (below) $\widehat{Q}$ for sellers (buyers) than under simple risks.

C3 For $P > E_i[X]$, the distribution of supplied and demanded shares is less asymmetric around $\widehat{Q}$ and decreases less below (above) $\widehat{Q}$ for sellers (buyers) than under simple risks.

Analogously to S1–S3, the three distribution results C1–C3 hold if the number of agents behaving according to Eq. (1.10) goes to infinity.

Figure 1.12 presents the supply distribution for $P = E_i[X]$. While integer numbers are more frequently supplied than fractions of shares, both distributions are roughly symmetric around $\widehat{Q}$ = 2 shares, constituting the clear mode under simple risks and complex risks with $\pi = 1/2$ (left plot in Figure 1.12). When moving from simple to complex risks, the frequency of the perfect hedging strategy decreases sharply, i.e., from 0.694 to 0.235 for $\pi = 1/2$ and from 0.469 to 0.163 for $\pi = 1/3$ (p-values for differences = 0.000, t-test). In the case of $\pi = 1/3$, the frequencies of the most extreme deviations from $\widehat{Q}$ increase considerably under complex risks. These results are in line with both implications S1 and C1.

Figure 1.13 depicts the distribution of shares supplied for $P < E_i[X]$ and $P > E_i[X]$, respectively. Under both simple and complex risks, supplies of less (more) than $\widehat{Q}$ shares clearly occur most often for low (high) prices. Additionally, except for complex risks with $\pi = 1/3$ (upper right plot in Figure 1.13), the frequency of supplying more (less) than $\widehat{Q}$ shares is decreasing (increasing) in Q_i for $P < E_i[X]$ ($P > E_i[X]$), with generally lower frequency levels under simple risks. The supply distributions presented in Figure 1.13 reconcile well with the above proposed implications. First, subjects more often choose dominating instead of dominated actions, where the occurrence of the latter is decreasing in their inferiority (see implications C2–C3). Second, under complex risks, subjects deviate more frequently from utility-maximizing actions than under simple risks (S2–S3). The analogous analysis of the corresponding demand distributions (see Figure D1.5 and Figure D1.6 in Appendix D1) reveals similar evidence in support of S1–S3 and C1–C3 for buyers.

In summary, my empirical findings reconcile well with the random choice models postulated in Eq. (1.9) and Eq. (1.10): Complexity tightens the bounds on risk-averse agents' rational behavior, where, rationality under complex risks is defined in line with decision theory under ambiguity. A simple counting exercise further underpins this hypothesis. Figure 1.14 shows the distributions of dominated action frequencies between risk types. As expected, subjects more frequently fall for dominated trading strategies if risks are complex. Although, as can be deduced from Figure D1.7 in Appendix D1, some limited learning takes place while trading complex risks.

Once varying levels of rationality are controlled for, the inconclusiveness regarding the above two price sensitivity measures disappears. Figure 1.15 shows the between-treatment average

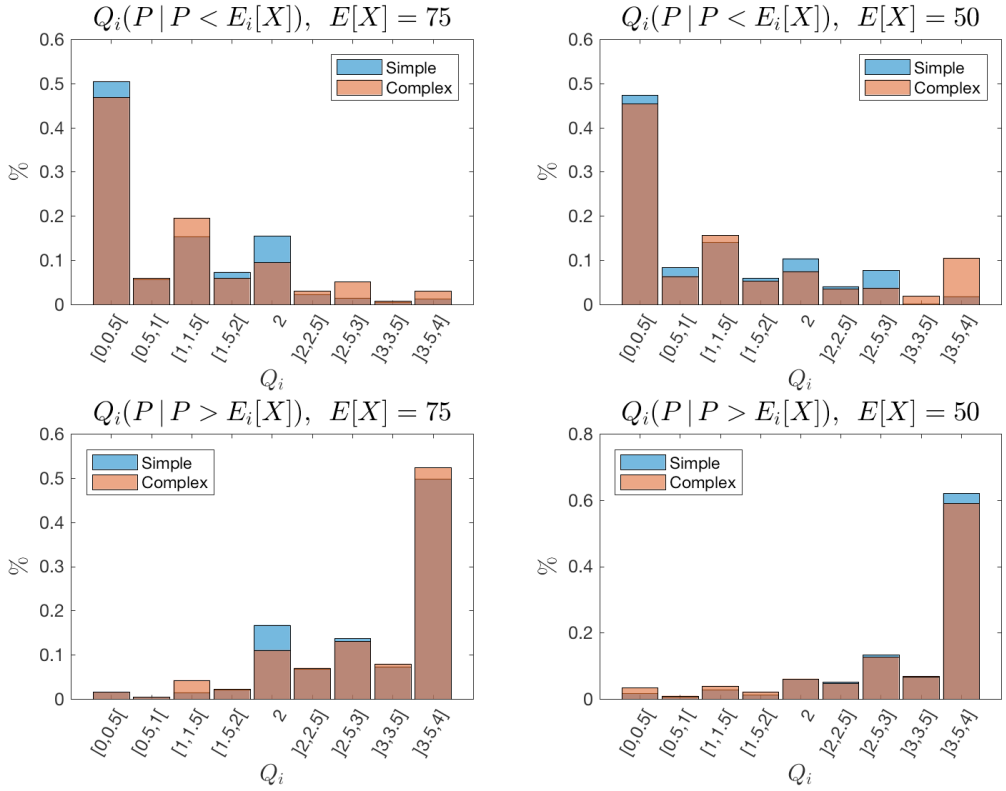

FIGURE 1.13. SUPPLY DISTRIBUTION FOR PRICES DIFFERENT FROM EXPECTED PAYOFFS

Notes: This figure shows the number of shares supplied by sellers for prices different from expected payoffs. The empirical distributions between simple and complex risks are computed across subjects and sessions. In the top (bottom) row, total supplies for prices below (above) $E_i[X]$ are reported. The left (right) column shows average supply distributions across trading rounds with π equal to $1/2$ ($1/3$).

values of $\mathcal{M}^1$, where two different rationality conditions are applied. In Subfigure (a), averages are only computed for subjects who prefer to be perfectly hedged for $P = E_i[X]$ under complex risks. For these subjects, the price range for which they supply (demand) $\widehat{Q}$ shares increases by 5.172 under complex relative to simple risks (p-value = 0.000, t-test).

In contrast, Subfigure (b) plots averages computed across potentially different subjects: Under simple risks, only nondominated supply and demand curves (as presented in Figure 1.14) are considered. Accordingly, the corresponding average for complex risks is solely based on nondominated supply and demand curves equal to $\widehat{Q}$ at $P = E_i[X]$. Relying on these conditions, the average cardinality of continuous prices for which the perfect hedging strategy is adopted increases by 3.853 under complex risks (p-value = 0.012, t-test). Hence, for both cases in Figure 1.15, the conditional $\mathcal{M}^1$ measure relates strikingly well with the theory's predictions, particularly so with those implied by kinked ambiguity preferences.

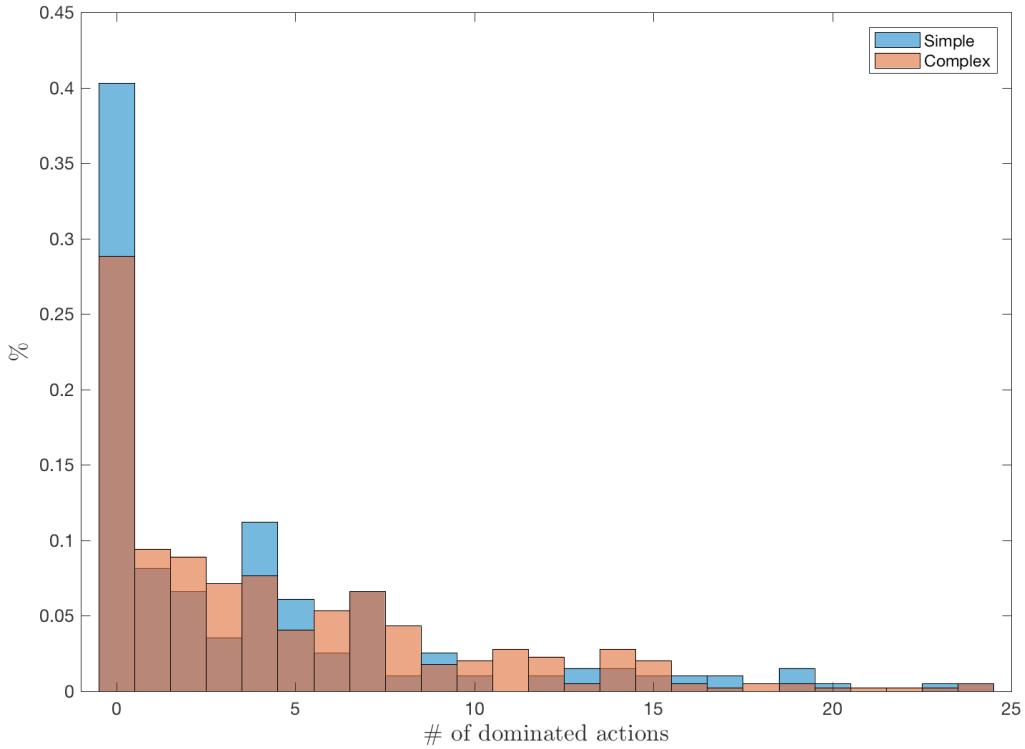

FIGURE 1.14. FREQUENCY OF DOMINATED TRADING STRATEGIES

Notes: This figure shows the distributions of dominated action frequencies across all subjects. Under simple risks, dominated actions correspond to offered (demanded) quantities above (below) $\widehat{Q}$ shares for $P < E[X]$ and vice versa for $P > E[X]$. Under complex risks, dominated actions correspond to offered (demanded) quantities above (below) $\widehat{Q}$ shares for $P < E_i[X]$ and vice versa for $P > E_i[X]$. Note that in the presence of complex risks, the price thresholds depend on subjects' individual point estimates.

Regression Analysis and Comparison to Ambiguity

For a full regression analysis, I additionally include the remaining data from each session's last trading round (see Table 1.3), where tradable risks are based on the draw from the nontransparent Ellsberg (1961)-like urn depicted in Figure 1.5. Since subjects' beliefs in these rounds are unknown, classifying individual trades involving ambiguous risks into dominated and non-dominated actions is no longer possible.

Table 1.6 reports OLS coefficient estimates of the following pooled regression model:

$$\begin{aligned}\mathcal{M}_{ir}^{1,2} = \beta_0 &+ \beta_1 Complexity_r + \beta_2 Ambiguity_r + \beta_3 RA_i \\ &+ \beta_4 \left(AA_i \times Complexity_r\right) + \beta_5 \left(AA_i \times Ambiguity_r\right) + \mathbf{b}\mathbf{X}_{ir} + \epsilon_{ir},\end{aligned} \tag{1.12}$$

where the dependent variable is either one of the above introduced sensitivity measures for subject i in trading round r. $Complexity_r$ and $Ambiguity_r$ are dummy variables indicating trading rounds with complex and ambiguous risks, respectively. RA_i and AA_i measure subject i's risk and ambiguity aversion (see Table 1.3). Finally, $\mathbf{X}_{ir}$ contains socio-economic and trading

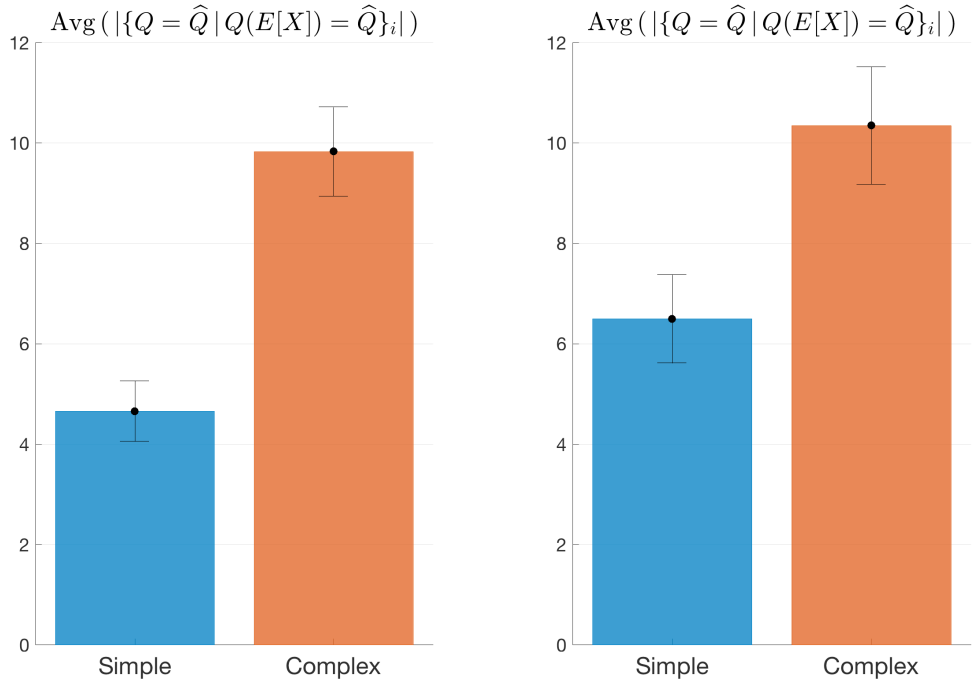

(a) Same subjects

(b) No dominated actions

FIGURE 1.15. CONDITIONAL FREQUENCY OF PERFECT HEDGING STRATEGY

Notes: This figure shows the average frequency of the perfect hedging strategy under simple and complex risks, conditional on rational trading behavior. Both subfigures plot conditional average cardinalities of the consecutive price ranges for which subjects supply (demand) $\widehat{Q}$ shares (see Eq. (1.7)). In Subfigure (a), averages are only based on subjects who, under complex risks, supply (demand) $\widehat{Q}$ shares at $P = E_i[X]$. In Subfigure (b), the average value for simple risks is computed across all nondominated (see Figure 1.14) supply (demand) curves. The corresponding average for complex risks is determined across all nondominated supply (demand) curves that additionally go through $\widehat{Q}$ at $P = E_i[X]$. Error bars indicate standard errors of the mean.

round specific control variables, and ϵ_{ir} denotes the idiosyncratic error term. Corrected standard errors clustered at the subject level are reported in parenthesis.

The reported coefficients in Table 1.6 affirm the findings from Figure 1.11. The second and fourth columns show that complex risks significantly decrease the slope of local supply (demand) by approximately 0.25 on average. As revealed by columns one and three, no such unconditional effect is observed on subjects' adopted frequency of the perfect hedging strategy. Nevertheless, as expected, the latter is higher in rounds with ambiguous risks and increases with subjects' risk aversion. When regressing local slopes on the ambiguity dummy and risk aversion, both coefficients exhibit the anticipated sign but lack statistical significance.

Controlling for a potential order effect, I find evidence for Fox and Tversky's (1995) comparative ignorance effect: If complex risks are proceeded by simple risks, the adopted perfect hedging frequency increases significantly. Furthermore, female subjects more often follow the

Table 1.6. Unconditional regression Analysis

	Dependent variable			
	$\mathcal{M}_1$	$\mathcal{M}_2$	$\mathcal{M}_1$	$\mathcal{M}_2$
Constant	3.974^a	0.661^a	3.413	0.685^b
	(0.511)	(0.096)	(2.373)	(0.335)
Complexity (dummy)	0.408	-0.240^a	-0.645	-0.249^a
	(0.646)	(0.065)	(0.709)	(0.085)
Ambiguity (dummy)	1.617^c	0.017	1.727^c	0.009
	(0.959)	(0.123)	(0.955)	(0.122)
RA (risk aversion)	5.389^b	-0.216	5.302^b	-0.263
	(2.111)	(0.252)	(2.137)	(0.229)
AA (ambig. aversion) × Complexity	1.935	-0.142	0.305	-0.061
	(1.978)	(0.156)	(1.817)	(0.150)
AA × Ambiguity	5.360	-0.299	4.573	-0.216
	(3.940)	(0.334)	(3.847)	(0.294)
Order × Complexity	-	-	2.269^b	0.005
	-	-	(0.959)	(0.087)
Gender	-	-	1.534^c	-0.294^a
	-	-	(0.830)	(0.098)
Controls	No	No	Yes	Yes
N	465	653	465	653

Notes: This table reports OLS coefficient estimates. The dependent variables are unconditional measures of local price sensitivity. $\mathcal{M}^1$ denotes the cardinality of consecutive prices for which subjects adopt the perfect hedging strategy, i.e., aiming to trade $\widehat{Q}$ shares. $\mathcal{M}^2$ measures the average slope of subjects' supply and demand curves at their individual point estimates of the risky asset's expected payoff. 'Complexity' and 'Ambiguity' are dummy variables indicating trading rounds with complex and ambiguous risks, respectively. 'Risk aversion' measures the normalized difference between the simple lottery's expected payoff and subjects' respective certainty equivalents. The first two interaction terms control for different effects of 'Ambiguity aversion' across trading rounds with simple and complex risks, where ambiguity aversion is measured as the difference between subjects' certainty equivalents for the simple and the ambiguous lottery. The term 'Order × Complexity' interacts the dummy variable 'Order', indicating sessions where complex risks were proceeded by simple risks, with complex trading rounds. 'Gender' is a dummy variable indicating female subjects. 'Controls' comprise subjects' age, their attended university, and number of completed semesters. Furthermore, 'Controls' contain subjects' self-evaluated understanding and difficulty level of the assigned task (measured by integers from one to five) and two additional dummy variables controlling for their familiarity and knowledge regarding the Brownian motion. Numbers in parenthesis denote robust standard errors clustered at the subject level. Superscripts ^{a}, ^{b}, and ^{c} indicate statistical significance at the 1%, 5%, and 10%-level, respectively.

perfect hedging strategy and submit significantly less (locally) sensitive supply (demand) functions. This contrasts the findings in Borghans et al. (2009) that men require higher compensation for the introduction of ambiguity than do women.

Despite having the expected sign in all eight cases, none of the estimates of β_4 and β_5 as defined in Eq. (1.12) are statistically significant. Under kinked ambiguity preferences, an affection for ambiguous risks potentially causes supply (demand) discontinuities. Although technically in line with the above predictions, such discontinuities likely augment the inherent

noise level of empirically observed supply (demand) functions. Therefore, I reestimate Eq. (1.12) for only nonambiguity-averse subjects. The corresponding coefficient estimates are reported in Table D1.1 in Appendix D1.

The results with respect to the complexity dummy as well as subjects' risk aversion remain qualitatively the same. Similar holds true for the above described order and gender effects. However, four of the eight coefficients interacted with ambiguity aversion become statistically significant (at least at the 5%-level). Strikingly, both magnitudes and statistical significance are clearly higher for the trading round with ambiguous risks relative to those with complex risks (despite the latter's fourfold larger sample size).

In summary, these findings point towards three important implications. First, ambiguity preferences appear to possess the highest explanatory power in the presence of purely ambiguous rather than complex risks. This comes as little surprise, but reassures the design's effectiveness in translating ambiguity preferences into measurable model-based trading predictions. Second, and more importantly, complex risks reduce local supply (demand) slopes more substantially than does pure ambiguity. In particular, this can be seen from comparing the coefficient estimates for the complexity and ambiguity dummies and recalling the small values of the applied ambiguity aversion measure. Third, in synthesis, while ambiguity preference-based theories explain individual behavior under complex risks reasonably well, the aversion to pure ambiguity underestimates the latter's impact on market outcomes.

Given the fundamental difference regarding the existence of a uniquely defined risk structure, it is not surprising that the magnitudes of subjects' reactions to complex and ambiguous risks are different. Even though their beliefs under pure ambiguity are unknown, a similar analysis as presented in Figure 1.12 lends itself as a simplified comparison of relative bounded rationality. For both simple and ambiguous risks, Figure D1.8 in Appendix D1 presents the joint distributions of supplied and demanded shares at a price of ECU 75. Assuming subjects adopt the natural reference point of a fifty-fifty chance under pure ambiguity, there is no evidence that pure ambiguity has any hampering effect on subjects' rationality.

1.3.4 Market's Effectiveness in Aggregating Complex Information

In light of the attained insights regarding individual trading behavior, I finally move back to an equilibrium perspective by returning to this paper's underlying elementary question: How well are financial markets suited to cope with complexity? In particular, are they capable of efficiently allocating complex risks at informative prices? I investigate this question by dissecting both the equilibration processes and their respective outcomes of the above asset markets.

Figure 1.16 displays bootstrapped distributions of aggregate market outcomes. All densities are based on ten thousand resamples of 49 individual supply and demand functions. For any given resample, average supply and demand are crossed and linearly interpolated market-clearing prices $P^\star$ and quantities $Q^\star$ deduced.

Comparing estimated densities between simple and complex risks unveils three striking characteristics of market equilibrium. First, and not surprisingly, both distributions of $P^\star$ under

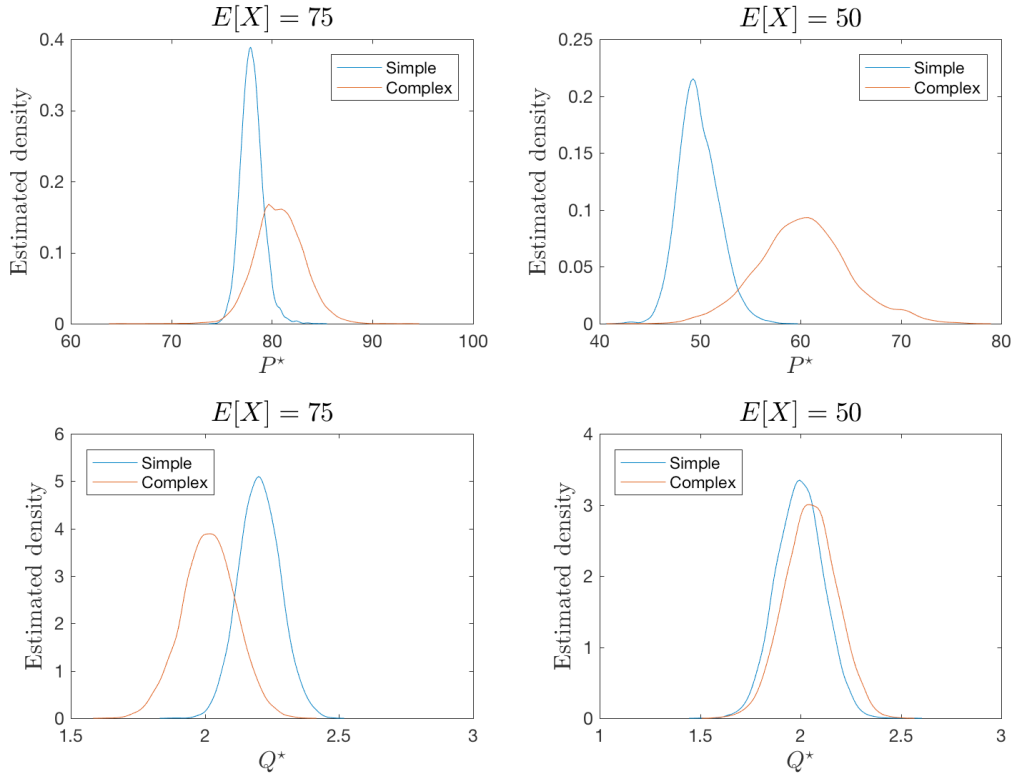

FIGURE 1.16. BOOTSTRAPPED EQUILIBRIUM DISTRIBUTIONS

Notes: This figure shows bootstrapped densities of market-clearing prices and quantities for simple and complex risks. Every average supply and demand curve is based on resampling 49 individual supply and demand schedules (same resampling size under simple and complex risks). For each pair of averaged supply and demand, the linearly interpolated market-clearing price and quantity are computed. Repeating this procedure ten thousand times yields the depicted estimated densities of equilibrium prices (top row) and quantities (bottom row). The left (right) column shows bootstrapped densities for trading rounds with π equal to $1/2$ ($1/3$).

simple risks are closer to and more centered around $E[X]$ than those under complex risks. Second, and contrary to market-clearing prices, the centers of both $Q^\star$ distributions under complex risks are remarkably close to $\widehat{Q} = 2$ shares, i.e., the perfect hedging strategy. In case of $\pi = 1/2$ (lower left plot in Figure 1.16), complex risks are even more efficiently shared than simple risks. Both observations are in line with actual market outcomes reported in Table 1.5.

Third but foremost, the relative variation between simple and complex risks is much larger for market-clearing prices than for market-clearing quantities. Given their predicted decrease in supply and demand sensitivity, this observation aligns well with the above ambiguity preference-based theories. Figure D1.9 in Appendix D1 furthermore illustrates how these relative variations in $P^\star$ and $Q^\star$ depend on the underlying resampling size. All variability ratios are considerably stable in the number of traders. At the maximum resampling size, both standard deviations of $P^\star$ under complex risks are still more than twice as high as under simple risks. In contrast, standard deviations of market clearing quantities are consistently much closer for simple and

complex risks. In the limit, the variation in $Q^\star$ under complex risks only exceeds the one under simple risks by approximately 30% for $\pi = 1/2$ and less than 10% for $\pi = 1/3$. Hence, throughout its equilibration path, the variation in markets' risk sharing ability are remarkably similar for simple and complex risks.

In order to conclusively evaluate markets' ability to (partially) aggregate agents' subjective information about complex risks, simply referring to the results shown in Figure 1.16 would not be fair. The above distributions of $P^\star$ under complex risks do not yet take into account the dispersion of subjects' beliefs regarding the risky asset's true expected payoff. Therefore, I propose to consider the following ratio of standard deviations instead:

$$Std(P^\star)\text{-Ratio} = \sqrt{\frac{Var(P_c^\star)}{Var\left(P_s^\star + E_c^\star[X]\right)}}, \tag{1.13}$$

where $P_s^\star$ ($P_c^\star$) denotes the market-clearing price for simple (complex) risks, and $E_c^\star[X]$ indicates subjects' average estimate of $E[X]$ under complex risks. When comparing variations in $P_c^\star$ to those in $P_s^\star$, Eq. (1.13) actually controls for the fluctuations of subjects' point estimates by adding $E_c^\star[X]$ to the variance in its denominator.

Whether the ratio in Eq. (1.13) is eventually greater or smaller than unity, i.e., whether markets efficiently aggregate complex risks or not, is again an empirical question. From a theoretical perspective, however, the answer is: *it depends*. The decisive factor is whichever of the following trade-off effects dominates: increased severity of bounded rationality versus reduced price sensitivity. In the absence of both effects, the ratio in Eq. (1.13) should equal one. Whenever risk-averse agents' behave fully rationally, $P_s^\star$ coincides with $E[X]$ and is thus deterministic. Moreover, if agents are neutral to complexity-induced ambiguity, $Var(P_c^\star)$ exactly corresponds to $Var(E_c^\star[X])$, since the market-clearing price always equals the average of agents' expected asset payoff.

In the presence of ambiguity aversion and a thereby implied decrease in local price sensitivity under complex risks, $Var(P_c^\star)$ may fall below $Var(E_c^\star[X])$, thereby pushing Eq. (1.13) downwards. To see this, consider two different agents: an ambiguity-neutral seller and an infinitely ambiguity-averse buyer. Facing complex risks, the seller shall belief that $E[X] \in [a, b]$ with uniform probability, while the buyer believes that $E[X]$ is uniformly distributed over $[\frac{a+b}{2}, b]$, where $a < b$. Hence, the seller's supply curve goes through $(\frac{a+b}{2}, \widehat{Q})$, whereas the buyer's demand curve is completely flat at $\widehat{Q}$ over the nonempty subset of prices $[\frac{a+b}{2}, b]$. Therefore, the unique trading equilibrium equals $(\frac{a+b}{2}, \widehat{Q})$ with $P_c^\star = \frac{a+b}{2}$ and $E_c^\star = \frac{3a+5b}{8}$. However, if instead the buyer believes that $E[X] \in [a, \frac{a+b}{2}]$, $P_c^\star$ would still equal $\frac{a+b}{2}$, but $E_c^\star$ would jump to $\frac{5a+3b}{8}$. In contrary, given more severe bounds on rationality under complex risks, i.e., in case Eq. (1.11) applies, the noise in $P_c^\star$ relative to $P_s^\star$ increases, which ultimately pushes Eq. (1.13) upwards.

Both cases are present in the experimental data. Figure 1.17 shows the respective values of Eq. (1.13), conditional on subjects' maximum number of dominated actions (see Figure 1.14). Unconditionally, the standard deviation ratio for $\pi = 1/2$ lies below one (0.813), whereas for $\pi = 1/3$ it exceeds one (1.170). This is in line with the observations from Figure 1.12 and

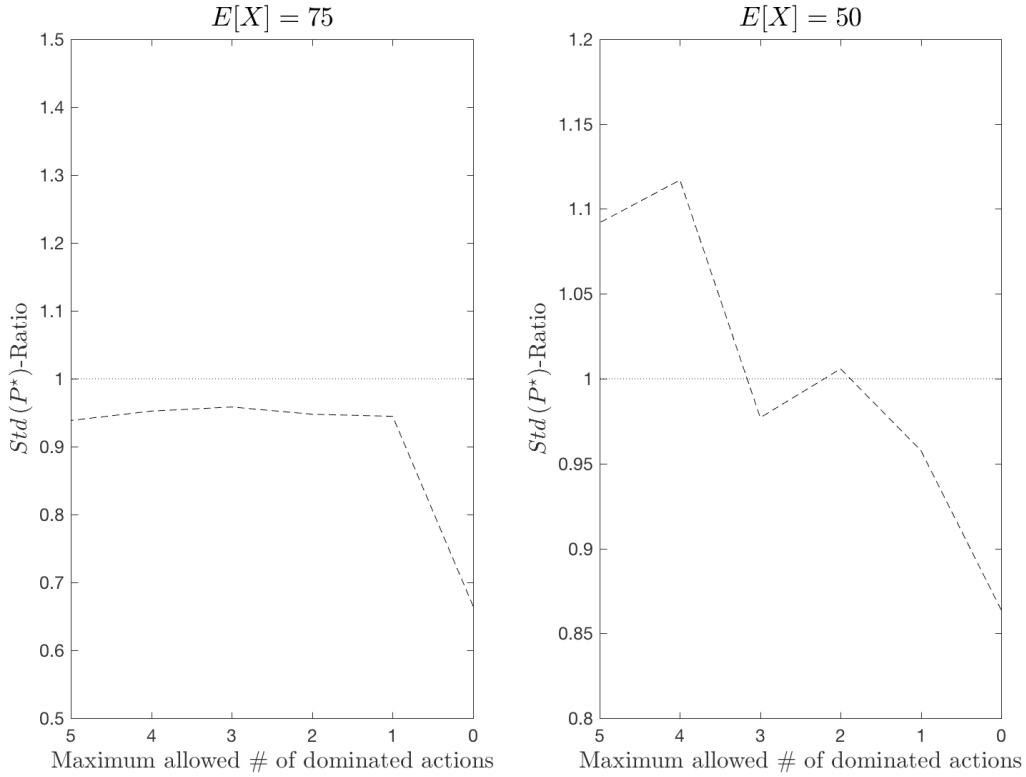

FIGURE 1.17. RELATIVE VARIABILITY OF MARKET-CLEARING PRICES

Notes: Conditioning on subjects' maximum number of dominated actions (see Figure 1.14), this figure shows the ratio

$$Std(P^\star)\text{-Ratio} = \sqrt{\frac{Var(P_c^\star)}{Var\left(P_s^\star + E_c^\star[X]\right)}},$$

where $P_s^\star$ ($P_c^\star$) denotes the market-clearing price for simple (complex) risks, and $E_c^\star[X]$ indicates subjects' average estimate of $E[X]$ under complex risks. Both estimates $P_s^\star$ and $P_c^\star$ are bootstrapped based on resampling and averaging individual supply and demand schedules. For each pair of averaged supply and demand, the linearly interpolated market-clearing price is computed. The respective resample size is set to the minimum number of sellers or buyers who satisfy the given rationality condition (maximum allowed number of dominated actions). This procedure is repeated ten thousand times. The left (right) plot shows standard deviation ratios for trading rounds with π equal to $1/2$ ($1/3$).

Figure 1.13: Relative to π equal to one half, the number of strongly dominated actions is substantially higher for π equal to one third, implying more severe bounds on subjects' rationality in the latter case. As shown in the right plot of Figure 1.17, the ratio for $\pi = 1/3$ is decreasing in the strictness of the applied rationality constraint. Focusing on subjects who completely abstain from any dominated actions, it eventually also falls below unity.

To sump up, markets' prove to be notably efficient in pricing and sharing complex risks, despite increased noise levels in individual trading behavior. Nevertheless, beyond binding limits to bounded rationality, their information aggregation is severely impaired, while their risk sharing ability yet prevails.

1.4 Concluding Remarks

In this paper, I study how complex but purely objective risks are traded in a competitive asset market. Relying on decision theory under ambiguity, the paper provides a novel perspective on agents' trading behavior in the presence of imperfectly understood uncertainty. In his seminal work, Ellsberg (1961) himself characterizes ambiguity as "a quality depending on the amount, type, and 'unanimity' of information, and giving rise to one's degree of 'confidence' in an estimate of relative likelihoods" (Ellsberg, 1961, p. 657)—an interpretation that advocates a bridging of ambiguity models and financial markets for increasingly complex assets.

In the absence of aggregate risk, the controlled setting of Biais et al. (2017) offers an ideal experimental framework to distinctively test for complexity's impact on individual trading decisions and aggregate market outcomes. Starting from Debreu (1959) and Arrow's (1964) seminal benchmark for simple risks, ambiguity preference-based predictions possess significant explanatory power regarding both adopted trading strategies and equilibrium allocations under complex risks. In general, I find asset markets to prove remarkably effective in pricing complex risks and even more robust in sharing them optimally across risk-averse investors. However, the former quality crucially depends on the severity by which complexity curtails agents' rationality under the perceived ambiguity of complex risks.

A1 Proofs

Proof of Proposition 1.1. Here I prove the case if agent i is a seller. In the case of a buyer, the analogous reasoning applies. Relying on the identities in Eq. (1.1), any agent i's expected utility from consumption can be rewritten as (neglecting the subscript i)

$$\begin{aligned} E[U(C(\omega))] &= \pi\, U\left(\mu + \sqrt{\frac{1-\pi}{\pi}}\sigma\right) + (1-\pi)\, U\left(\mu - \sqrt{\frac{\pi}{1-\pi}}\sigma\right) \\ &\triangleq f(\mu, \sigma, \pi), \end{aligned}$$

and since U is increasing it follows that

$$\begin{aligned} \frac{\partial f}{\partial \mu} &= \pi\, U'\left(\mu + \sqrt{\frac{1-\pi}{\pi}}\sigma\right) + (1-\pi)\, U'\left(\mu - \sqrt{\frac{\pi}{1-\pi}}\sigma\right) \\ &> 0, \end{aligned} \tag{A1.1}$$

and from decreasing marginal utility from consumption that

$$\begin{aligned} \frac{\partial f}{\partial \sigma} &= \pi\, U'\left(\mu + \sqrt{\frac{1-\pi}{\pi}}\sigma\right)\sqrt{\frac{1-\pi}{\pi}} \\ &\quad + (1-\pi)\, U'\left(\mu - \sqrt{\frac{\pi}{1-\pi}}\sigma\right)\left(-\sqrt{\frac{\pi}{1-\pi}}\right) \\ &= \sqrt{\pi(1-\pi)}\, U'\left(\mu + \sqrt{\frac{1-\pi}{\pi}}\sigma\right) - \sqrt{\pi(1-\pi)}\, U'\left(\mu - \sqrt{\frac{\pi}{1-\pi}}\sigma\right) \\ &< 0. \end{aligned} \tag{A1.2}$$

When selling Q shares for a price equal to P, the seller's consumption in $t = 2$ equals

$$C(u) = (S - Q)X(u) + (B + QP) + I(u) \tag{A1.3}$$

in state u, and

$$C(d) = (S - Q)X(d) + (B + QP) + I(d) \tag{A1.4}$$

in state d.

Let us now denote the expected asset payoff $E[X]$ by $P^\star$, i.e.,

$$P^\star := \pi X(u) + (1-\pi)X(d).$$

Furthermore, we define $\widehat{Q}$ as the quantity for which $\sigma^2 = 0$, i.e.,

$$\begin{aligned} \sigma^2 = 0 &\Leftrightarrow C(u) = C(d) \\ &\Leftrightarrow (S - Q)X(u) + I(u) = (S - Q)X(d) + I(d) \\ &\Leftrightarrow \widehat{Q} = S + \frac{I(u) - I(d)}{X(u) - X(d)}, \end{aligned} \tag{A1.5}$$

where we assume that $\widehat{Q} > 0$. From the definition of μ together with (Eq. (A1.3)) and (Eq. (A1.4)) we get

$$\frac{\partial \mu}{\partial Q} = \pi(P - X(u)) + (1-\pi)(P - X(d)),$$

and thus

$$\frac{\partial \mu}{\partial Q} \begin{cases} < 0 \text{ if } P < P^\star, \\ = 0 \text{ if } P = P^\star, \\ > 0 \text{ if } P > P^\star. \end{cases} \tag{A1.6}$$

First, strict concavity now implies

$$\begin{aligned} E[U(C(\omega))] &< U\left(\pi\mu + \sqrt{\pi(1-\pi)}\sigma + (1-\pi)\mu - \sqrt{(1-\pi)\pi}\sigma\right) \\ &= U(\mu), \end{aligned}$$

hence, from (Eq. (A1.5)) and (Eq. (A1.6)) it follows that, $\forall \pi \in (0,1)$, $(P^\star, \widehat{Q})$ *strictly dominates* all other points on the line $(P^\star, Q)$.

Second, (Eq. (A1.1)) & (Eq. (A1.6)) together with (Eq. (A1.2)) & (Eq. (A1.5)) imply that

(i) for any given price $P < P^\star$, any point in the upper left quadrant of Subfigure (a) of Figure 1.1 is *strictly dominated* by $(P, \widehat{Q})$;

(ii) for any given price $P > P^\star$, any point in the lower right quadrant of of Subfigure (a) of Figure 1.1 is *strictly dominated* by $(P, \widehat{Q})$.

Hence, $\forall \pi \in (0,1)$, the seller's supply curve has to lie somewhere in the lower left and upper right quadrant and has to go through the point $(P^\star, \widehat{Q})$. This completes the proof. □

Proof of Remark 1.1. Since ϵ can be arbitrarily small, I directly consider the limit $\epsilon \to 0$, i.e., $\lim_{\epsilon \to 0} U_i(C) = c_1 C$, for $0 \leq C \leq \overline{C}$. The corresponding first and second derivatives of $U_i(C)$ are

$$\lim_{\epsilon \to 0} U_i'(C) = c_1, \quad \text{and} \quad \lim_{\epsilon \to 0} U_i''(C) = 0.$$

For $C \geq \overline{C}$, the respective derivatives are

$$U_i'(C) = \alpha e^{-\alpha C}, \quad \text{and} \quad U_i''(C) = -\alpha^2 e^{-\alpha C}.$$

The following conditions ensure the differentiability of $U_i(C)$ at $\overline{C}$:

$$c_1 \overline{C} = c_2 - e^{-\alpha \overline{C}} \quad \Leftrightarrow \quad c_2 = c_1 \overline{C} + e^{-\alpha \overline{C}}, \tag{A1.7}$$

$$c_1 = \alpha e^{-\alpha \overline{C}}. \tag{A1.8}$$

Given Eq. (A1.3) and Eq. (A1.4), the FOC for $E[U(C(\omega))]$ with respect to Q implies

$$\pi U'(C(u))(P - X(u)) + (1-\pi)U'(C(d))(P - X(d)) = 0. \tag{A1.9}$$

Taking the first derivative of the LHS of Eq. (A1.9) with respect to P yields

$$\pi U'(C(u)) + (1-\pi)U'(C(d)) + \pi U''(C(u))Q(P - X(u)) + (1-\pi)U''(C(d))Q(P - X(d)).$$

Since $\frac{\delta}{\delta Q}$(LHS of Eq. (A1.9)) < 0 $\forall (P, Q) \in \mathbb{R}^2_{\geq 0}$, agent i's supply curve is decreasing in P if $\frac{\delta}{\delta P}$(LHS of Eq. (A1.9)) < 0. For the here considered utility function, this is the case whenever

$$c_1 < \frac{1-\pi}{\pi} \alpha e^{\alpha C(d)} \left(\alpha Q(P - X(d)) - 1\right).$$

Together with Eq. (A1.8), this implies that for high enough prices, i.e., if

$$P > X(d) + \frac{1 + \frac{\pi}{1-\pi} \alpha e^{-\alpha(\overline{C} - C(d))}}{\alpha Q},$$

seller i's supply curve can be *locally* decreasing in P. This completes the proof. □

Proof of Proposition 1.2. Here I prove the case if the ambiguity-averse agent i, i.e., $\alpha_i > 1/2$, is a seller. In the case of a buyer, the analogous reasoning applies. Relying on the identities in Eq. (1.1), any agent i's utility from consumption according to the α-maxmin in Eq. (1.2) can be rewritten as (neglecting the subscript i)

$$\begin{aligned}
\mathcal{U}(C(\omega)) &= \alpha \min_{\pi \in \mathcal{C}} \left(E[U(\pi)]\right) + (1-\alpha) \max_{\pi \in \mathcal{C}} \left(E[U(\pi)]\right) \\
&= \alpha \left(\underline{\pi}\, U\left(\underline{\mu} + \sqrt{\frac{1-\underline{\pi}}{\underline{\pi}}} \underline{\sigma} \right) + (1-\underline{\pi})\, U\left(\underline{\mu} - \sqrt{\frac{\underline{\pi}}{1-\underline{\pi}}} \underline{\sigma} \right) \right) \\
&\quad + (1-\alpha) \left(\overline{\pi}\, U\left(\overline{\mu} + \sqrt{\frac{1-\overline{\pi}}{\overline{\pi}}} \overline{\sigma} \right) + (1-\overline{\pi})\, U\left(\overline{\mu} - \sqrt{\frac{\overline{\pi}}{1-\overline{\pi}}} \overline{\sigma} \right) \right),
\end{aligned}$$

where $\underline{\pi} = \arg\min_{\pi \in \mathcal{C}} E[U(\pi)]$ ($\overline{\pi} = \arg\max_{\pi \in \mathcal{C}} E[U(\pi)]$) and $\underline{\mu}$ ($\overline{\mu}$) and $\underline{\sigma}$ ($\overline{\sigma}$) denote expected consumption and standard deviation of consumption according to $\underline{\pi}$ ($\overline{\pi}$). For $Q \neq \widehat{Q}$, i.e., for strictly positive $\underline{\sigma}$ and $\overline{\sigma}$, it directly follows from U's strict concavity that

$$\mathcal{U}(C(\omega)) < \alpha U(\underline{\mu}) + (1-\alpha) U(\overline{\mu}) < U(\alpha \underline{\mu} + (1-\alpha)\overline{\mu}).$$

Eq. (A1.3) and Eq. (A1.4) imply

$$\begin{aligned}
\alpha\underline{\mu} + (1-\alpha)\overline{\mu} &= \alpha \Big(\underline{\pi} \left((S-Q)X(u) + (B+QP) + I(u) \right) + \\
&\qquad (1-\underline{\pi}) \left((S-Q)X(d) + (B+QP) + I(d) \right) \Big) \\
&\quad + (1-\alpha) \Big(\overline{\pi} \left((S-Q)X(u) + (B+QP) + I(u) \right) + \\
&\qquad (1-\overline{\pi}) \left((S-Q)X(d) + (B+QP) + I(d) \right) \Big) \\
&= \text{... terms indep. from } Q \text{ ...} + Q \left(P - \left(\alpha E^{\underline{\pi}}[X] + (1-\alpha) E^{\overline{\pi}}[X] \right) \right).
\end{aligned}$$

Hence, if $P = \alpha E^{\underline{\pi}}[X] + (1-\alpha)E^{\overline{\pi}}[X]$, denoted by $\widetilde{P}$ hereafter, the linear combination of expected consumption (for constant $\underline{\pi}$ and $\overline{\pi}$) does not change for different quantities of shares sold. Therefore, for $\widetilde{P}$, it is optimal for the seller to exactly sell $\widehat{Q}$ share and get the constant utility $U(\alpha\underline{\mu} + (1-\alpha)\overline{\mu}) = U(\alpha\underline{\mu}) = U((1-\alpha)\overline{\mu})$.

In general, it holds that

$$\begin{aligned}\mathcal{U}(C(\omega)) &= \alpha\Big(\underline{\pi}U(C(u)) + (1-\underline{\pi})U(C(d))\Big) \\ &\quad + (1-\alpha)\Big(\overline{\pi}U(C(u)) + (1-\overline{\pi})U(C(d))\Big),\end{aligned}$$

and, for any given price, the corresponding FOC reads

$$\begin{aligned}\frac{\delta\mathcal{U}}{\delta Q} &= \alpha\Big(\underline{\pi}U'(C(u))(P-X(u)) + (1-\underline{\pi})U'(C(d))(P-X(d))\Big) \\ &\quad + (1-\alpha)\Big(\overline{\pi}U'(C(u))(P-X(u)) + (1-\overline{\pi})U'(C(d))(P-X(d))\Big) \;=\; 0, \qquad \text{(A1.10)}\end{aligned}$$

As shown, for $\widetilde{P}$, it is optimal to sell $\widehat{Q}$ shares. Hence, the question now is, for what prices it is optimal to sell less (more) than $\widehat{Q}$? Or, put differently, starting from $\widetilde{P}$ per share, below (above) which price does it become beneficial to sell less (more) than $\widehat{Q}$ shares?

Since when selling $\widehat{Q}$ shares $C(u) = C(d)$, Eq. (A1.10) yields

$$\frac{\delta\mathcal{U}}{\delta Q}\bigg|_{Q=\widehat{Q}} = 0 \quad \Leftrightarrow \quad P = \widetilde{P}.$$

I denote by $\widetilde{P}(\widehat{Q}\downarrow) = L$ ($\widetilde{P}(\widehat{Q}\uparrow) = U$) the lowest (highest) price for which the seller prefers to sell $\widehat{Q}$ shares. Because $\underline{\pi} < \overline{\pi}$ whenever the seller considers to sell less than $\widehat{Q}$, and $\underline{\pi} > \overline{\pi}$ whenever she thinks about selling more than $\widehat{Q}$, it follows that $L < U$.

Therefore, in summary, seller i's supply curve is constant over the closed subset $[L, U] \subset P$ and the difference $U - L$ becomes larger as her $\mathcal{C}$ becomes wider and/or as $\alpha \to 1$. This completes the proof. □

Proof of Proposition 1.3. Whenever there is a nonzero mass of ambiguity-averse agent whose supply (demand) curves do not go through the benchmark equilibrium $(E[X], \widehat{Q})$, they draw average supply (demand) away from the latter. Given the result in Proposition 1.2, this clearly occurs if either

$$L > E[X] \quad \text{or} \quad U < E[X]. \qquad \text{(A1.11)}$$

For ambiguity-averse agents, L is always strictly smaller than U, hence, the two cases in Eq. (A1.11) are mutually exclusive.

I begin with the first inequality in Eq. (A1.11). For any ambiguity-averse seller i it holds that (neglecting the subscript i)

$$L = \alpha E^{\underline{\pi}}[X] + (1-\alpha)E^{\overline{\pi}}[X],$$

where $\alpha > 1/2$ and $\underline{\pi} < \overline{\pi}$ since L denotes the lower price limit below which she prefers to sell *less* than $\widehat{Q}$ shares. Thus, denoting by π_M the midpoint and by 2Δ the length of the seller's set of priors,[29] the inequality $L > E[X]$ can be written as

$$\begin{aligned} E[X] &< L \\ E[X] &< \alpha\left((\pi_M - \Delta)X(u) + (1 - (\pi_M - \Delta))X(d)\right) \\ &\quad + (1-\alpha)\left((\pi_M + \Delta)X(u) + (1 - (\pi_M + \Delta))X(d)\right) \\ \pi X(u) + (1-\pi)X(d) &< \pi' X(u) + (1-\pi')X(d), \end{aligned} \tag{A1.12}$$

where $\pi' := \pi_M - \Delta(2\alpha - 1)$. By the analogous argument and relying on the same notation, it follows that the second inequality in Eq. (A1.11) is equivalent to

$$\begin{aligned} E[X] &> U \\ \pi X(u) + (1-\pi)X(d) &> \pi'' X(u) + (1-\pi'')X(d), \end{aligned} \tag{A1.13}$$

whereas now $\pi'' := \pi_M + \Delta(2\alpha - 1)$.

Together, Eq. (A1.12) and Eq. (A1.13) imply that

$$L < E[X] < U \quad \Leftrightarrow \quad \pi' < \pi < \pi'', \tag{A1.14}$$

where $\pi' < \pi''$ because $\alpha > 1/2$. Hence, whenever $\pi \notin \mathcal{B}$ as defined in Eq. (1.4), the seller's supply curve draws average supply away from the benchmark equilibrium. Because of perfect symmetry, the same condition simultaneously holds for any ambiguity-averse buyer. This completes the proof. □

Proof of Proposition 1.4. I first prove (ii). Eq. (1.5) can be written as (neglecting the subscript i)

$$\mathcal{U}(C(\omega)) = \frac{1}{\overline{\pi} - \underline{\pi}} \int_{\underline{\pi}}^{\overline{\pi}} \phi\left(E[U(\tilde{\pi})]\right) \mathrm{d}\tilde{\pi}.$$

For any given price, the FOC with respect to Q reads

$$\frac{\delta \mathcal{U}}{\delta Q} = \frac{1}{\overline{\pi} - \underline{\pi}} \int_{\underline{\pi}}^{\overline{\pi}} \phi'\left(E[U(\tilde{\pi})]\right) \left(\tilde{\pi} \frac{\partial}{\partial Q} U(C(u)) + (1-\tilde{\pi}) \frac{\partial}{\partial Q} U(C(d))\right) \mathrm{d}\tilde{\pi} = 0. \tag{A1.15}$$

Eq. (A1.3) and Eq. (A1.4) imply

$$\frac{1}{\overline{\pi} - \underline{\pi}} \int_{\underline{\pi}}^{\overline{\pi}} \phi'\left(E[U(\tilde{\pi})]\right) \Big(\tilde{\pi} U'(C(u))(P - X(u)) + (1-\tilde{\pi}) U'(C(d))(P - X(d))\Big) \mathrm{d}\tilde{\pi} = 0.$$

For $Q = \widehat{Q}$ the agent bears no consumption risk, i.e., $C(u) = C(d)\ \forall \tilde{\pi}$ and $E[U] \perp\!\!\!\perp \tilde{\pi}$. At

[29] Alternatively, for a discrete set of priors, 2Δ refers to the difference $\max(\mathcal{C}) - \min(\mathcal{C})$.

$Q = \widehat{Q}$, Eq. (A1.15) therefore becomes

$$\begin{aligned}
\frac{1}{\overline{\pi}-\underline{\pi}}\int_{\underline{\pi}}^{\overline{\pi}} \tilde{\pi}(P-X(u))+(1-\tilde{\pi})(P-X(d))\mathrm{d}\tilde{\pi} = 0 \quad &\Leftrightarrow \\
\frac{1}{\overline{\pi}-\underline{\pi}}\int_{\underline{\pi}}^{\overline{\pi}} P\mathrm{d}\tilde{\pi} = \frac{1}{\overline{\pi}-\underline{\pi}}\int_{\underline{\pi}}^{\overline{\pi}} \tilde{\pi}X(u)+(1-\tilde{\pi})X(d)\mathrm{d}\tilde{\pi} \quad &\Leftrightarrow \\
P = \frac{1}{2}\frac{\overline{\pi}^2-\underline{\pi}^2}{\overline{\pi}-\underline{\pi}}X(u)+\left(1-\frac{1}{2}\frac{\overline{\pi}^2-\underline{\pi}^2}{\overline{\pi}-\underline{\pi}}\right)X(d) \quad &\Leftrightarrow \\
P = \frac{\overline{\pi}-\underline{\pi}}{2}X(u)+\left(1-\frac{\overline{\pi}-\underline{\pi}}{2}\right)X(d). \quad &\text{(A1.16)}
\end{aligned}$$

Hence, any seller's (buyer's) supply (demand) curve only goes through the benchmark equilibrium $(\widehat{Q}, E[X])$, if the RHS of Eq. (A1.16) equals the stock's expected dividend, i.e.,

$$\frac{\overline{\pi}-\underline{\pi}}{2}X(u)+\left(1-\frac{\overline{\pi}-\underline{\pi}}{2}\right)X(d) = E[X] \quad \Leftrightarrow \quad \pi = \frac{\underline{\pi}+\overline{\pi}}{2}.$$

Thus, whenever π does not correspond to the midpoint of her set of priors $[\underline{\pi}, \overline{\pi}]$, she induces mispricing and suboptimal risk sharing of complex risks.

I hereafter prove (i) for the case where the considered nonzero mass of agents are sellers. In the case of buyers, the analogous reasoning applies. For a given seller i and price P per share, let $Q_i^\star(P)$ denote the number of shares satisfying Eq. (A1.15). Taking the first order derivative of the second integrand in Eq. (A1.15) with respect to $\tilde{\pi}$ yields (neglecting again the subscript i)

$$\begin{aligned}
&\frac{\partial}{\partial\tilde{\pi}}\Big(\tilde{\pi}U'(C(u))(P-X(u))+(1-\tilde{\pi})U'(C(d))(P-X(d))\Big) = \\
&\underbrace{U'(C(u))}_{>0}(P-X(u))-\underbrace{U'(C(d))}_{>0}(P-X(d)) < 0, \quad \text{(A1.17)}
\end{aligned}$$

i.e., is always strictly negative for $X(d) \leq P \leq X(u)$.

Regarding the first integrand in Eq. (A1.15), there are three different cases. First, if seller i is ambiguity-neutral, i.e., if $\phi'(\cdot)$ is a positive constant, only the second integrand is relevant for determining the optimal number of shares to be sold at P, hereafter denoted by $Q_N^\star(P)$. Second, if seller i is ambiguity-averse, i.e., if $\phi'(\cdot)$ is a decreasing function, then the first integrand becomes relevant for determining $Q_A^\star(P)$. Third, if she is ambiguity-loving, her increasing function $\phi'(\cdot)$ conversely affects $Q_L^\star(P)$.

Because Eq. (A1.17) strictly decreases at a constant rate over $[\underline{\pi}, \overline{\pi}]$, Eq. (A1.15) can only hold for $Q_N^\star(P)$, if the second integrand changes its sign between $\underline{\pi}$ and $\overline{\pi}$. For $Q < \widehat{Q}$, it holds that

$$\frac{\partial}{\partial\tilde{\pi}}E[U(\tilde{\pi})] = U(C(u)) - U(C(d)) > 0 \;\; \forall Q < \widehat{Q},$$

i.e., whenever seller i is ambiguity-averse, the first integrand in Eq. (A1.15) is a strictly decreasing function over $[\underline{\pi}, \overline{\pi}]$. Hence, for $Q_A^\star(P)$ the second integrand in Eq. (A1.15) needs to switch its sign for a smaller $\tilde{\pi} \in [\underline{\pi}, \overline{\pi}]$, relative to $Q_N^\star(P)$, in order to satisfy the first order condition.

Taking the first order derivative of the second integrand in Eq. (A1.15) with respect to Q yields

$$\frac{\partial}{\partial Q}\Big(\tilde{\pi}U'(C(u))(P-X(u))+(1-\tilde{\pi})U'(C(d))(P-X(d))\Big)=$$
$$\tilde{\pi}\underbrace{U''(C(u))}_{<0}(P-X(u))^2+(1-\tilde{\pi})\underbrace{U''(C(d))}_{<0}(P-X(d))^2<0,$$

i.e., is always strictly negative for any risk-averse seller. It therefore follows that $Q_A^\star(P) > Q_N^\star(P)$, i.e., that $Q_A^\star(P)$ is closer to $\widehat{Q}$ than $Q_N^\star(P)$. Since, for any ambiguity-loving seller, the first integrand in Eq. (A1.15) then is a strictly increasing function over $[\underline{\pi},\overline{\pi}]$, the analogous reasoning implies $Q_L^\star(P) < Q_N^\star(P)$. Thus, the distance between $\widehat{Q}$ and $Q_L^\star(P)$ is larger than between $Q_N^\star(P)$ and $\widehat{Q}$. Finally, the symmetric argument for $Q^\star(P) > \widehat{Q}$ yields $Q_A^\star(P) < Q_N^\star(P) < Q_L^\star(P)$. This completes the proof. □

B1 Determining π in the Presence of Complex Risks

Starting point is the SDE of the geometric Brownian motion in Figure 1.5, i.e.,

$$dS_t = 10\%S_t dt + 32\%S_t dW_t,$$

where W_t is a standard Brownian motion. Applying Itō to $f := \ln(S_t)$ yields

$$S_2 = \exp\left\{\left(10\% - \frac{32\%^2}{2}\right) + 32\%(W_2 - W_1)\right\}.$$

Hence,

$$\mathbb{P}(S_2 \geq 1.05) = \mathbb{P}\Bigg(W_2 - W_1 \leq \underbrace{\left(\ln(1.05) - 10\% + \frac{32\%^2}{2}\right)\frac{1}{32\%}}_{\approx 0}\Bigg).$$

Recalling that the increment $W_2 - W_1$ has a standard normal distribution,[30] it follows that $\mathbb{P}(S_2 \geq 1.05)$ corresponds to $1/2$.[31]

C1 Adjustment of average supply and demand curves according to subjective beliefs

For a given case, I denote by $\bar{E}_S[X]$ sellers' average point estimate of the risky asset's expected payoff under complex risks. In order to account for deviations of $\bar{E}_S[X]$ from $E[X]$, the following linear transformation is applied to the predefined price vector used to elicit sellers' supply

[30] This information was provided as part of the instructions.

[31] Strictly speaking, it holds that $\mathbb{P}(S_2 \geq 1.05) = 0.49999$. Linearly approximating $\ln(1.05)$ by 0.05 implies $\mathbb{P}(S_2 \geq 1.05) = 0.50150$.

functions:

$$adj(P) = \begin{cases} P - (\bar{E}_S[X] - E[X])\frac{P - X(d)}{\bar{E}_S[X] - X(d)}, & \text{for } X(d) \leq P < \bar{E}_S[X] \\ P - (\bar{E}_S[X] - E[X])\frac{X(u) - P}{X(u) - \bar{E}_S[X]}, & \text{for } \bar{E}_S[X] \leq P \leq X(u). \end{cases}$$

Furthermore, let $\bar{Q}_S$ denote the linearly interpolated average supply curve and $\bar{Q}_{S,adj}$ the corresponding curve plotted against $adj(P)$ instead of P. It then still holds that $\bar{Q}_{S,adj}$ spans from $X(d)$ to $X(u)$, but simultaneously that $\bar{Q}_{S,adj}(E[X]) = \bar{Q}_S(\bar{E}_S[X])$. The exact same linear transformation with $\bar{E}_B[X]$ instead of $\bar{E}_S[X]$, with B for buyers, is also used to adjust average demand curves under complex risks.

D1 Additional Tables and Figures

TABLE D1.1. REGRESSION ANALYSIS FOR NONNEGATIVE AMBIGUITY AVERSION

	Dependent variable			
	$\mathcal{M}_1$	$\mathcal{M}_2$	$\mathcal{M}_1$	$\mathcal{M}_2$
Constant	3.954^a	0.736^a	2.943	0.939^b
	(0.563)	(0.118)	(2.190)	(0.392)
Complexity (dummy)	0.238	-0.199^b	-0.452	-0.232^b
	(0.770)	(0.084)	(0.702)	(0.102)
Ambiguity (dummy)	0.517	0.213	0.926	0.181
	(1.208)	(0.185)	(1.225)	(0.196)
RA (risk aversion)	7.721^a	-0.091	6.931^a	-0.137
	(2.224)	(0.347)	(2.230)	(0.344)
AA (ambig. aversion) × Complexity	3.384	-0.542^b	0.096	-0.345
	(2.442)	(0.259)	(2.371)	(0.231)
AA × Ambiguity	9.792^b	-1.233^a	7.473	-1.041^b
	(4.669)	(0.472)	(4.729)	(0.522)
Order × Complexity	-	-	2.243^b	0.000
	-	-	(1.132)	(0.114)
Gender	-	-	1.187	-0.298^a
	-	-	(0.908)	(0.113)
Controls	No	No	Yes	Yes
N	373	518	373	518

Notes: This table reports OLS coefficient estimates for subjects with nonnegative ambiguity aversion (as indicated by the variable 'Ambiguity aversion'—see below). The dependent variables are unconditional measures of local price sensitivity. $\mathcal{M}^1$ denotes the cardinality of consecutive prices for which subjects adopt the perfect hedging strategy, i.e., aiming to trade $\widehat{Q}$ shares. $\mathcal{M}^2$ measures the average slope of subjects' supply and demand curves at their individual point estimates of the risky asset's expected payoff. 'Complexity' and 'Ambiguity' are dummy variables indicating trading rounds with complex and ambiguous risks, respectively. 'Risk aversion' measures the normalized difference between the simple lottery's expected payoff and subjects' respective certainty equivalents. The first two interaction terms control for different effects of 'Ambiguity aversion' across trading rounds with simple and complex risks, where ambiguity aversion is measured as the difference between subjects' certainty equivalents for the simple and the ambiguous lottery. The term 'Order × Complexity' interacts the dummy variable 'Order', indicating sessions where complex risks were proceeded by simple risks, with complex trading rounds. 'Gender' is a dummy variable indicating female subjects. 'Controls' comprise subjects' age, their attended university, and number of completed semesters. Furthermore, 'Controls' contain subjects' self-evaluated understanding and difficulty level of the assigned task (measured by integers from one to five) and two additional dummy variables controlling for their familiarity and knowledge regarding the Brownian motion. Numbers in parenthesis denote robust standard errors clustered at the subject level. Superscripts ^{a}, ^{b}, and ^{c} indicate statistical significance at the 1%, 5%, and 10%-level, respectively.

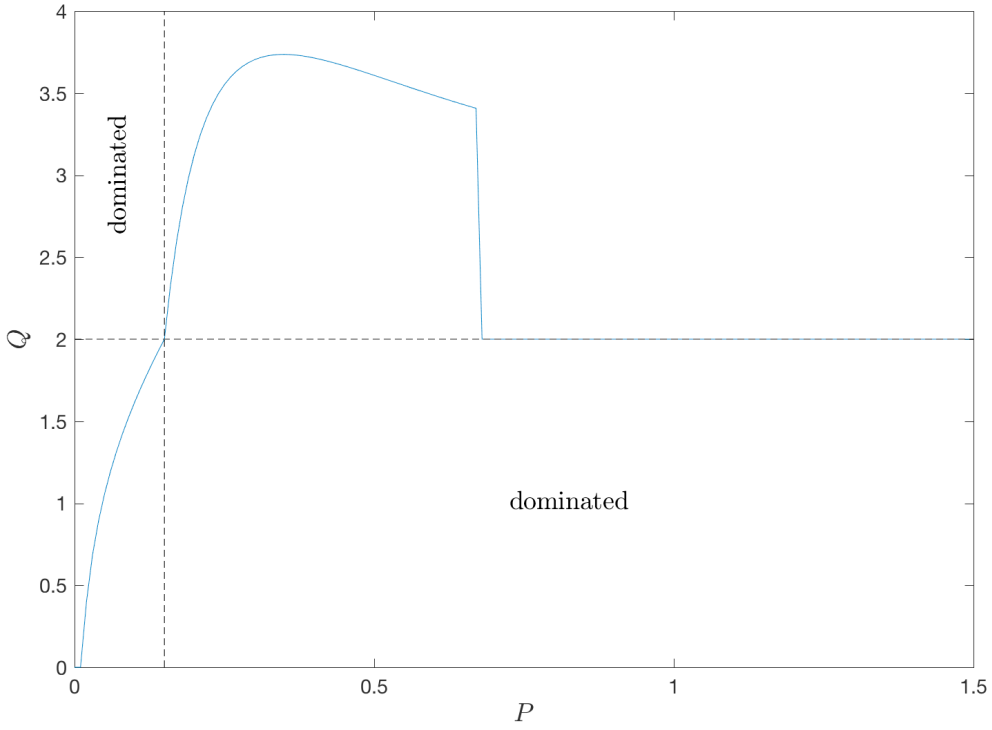

FIGURE D1.1. EXAMPLE OF NONMONOTONIC SUPPLY CURVE

Notes: Supply curve for seller i with utility function as defined in Remark 1.1. Parameters: $X(u) = 1.5$, $X(d) = 0$, $\pi = 1/10$, $\epsilon = 0$, $\alpha = 1$, $\overline{C} = 3+2\pi X(u)$, $E_i = 4$, $I_i(u) = 0$, $I_i(d) = 3$.

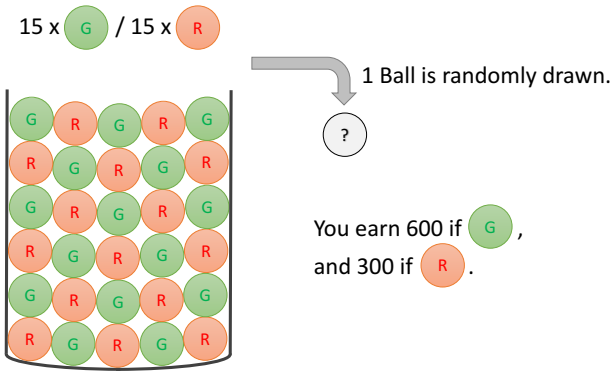

FIGURE D1.2. LOTTERY BASED ON URN WITH SIMPLE RISKS

Notes: This figure shows the lottery based on the urn with simple risks. Whenever the randomly drawn ball is green, the lottery pays ECU 600 (experimental currency units) and ECU 300 if it is red. Subjects' respective certainty equivalents were elicited via Abdellaoui et al.'s (2011) iterative choice list method.

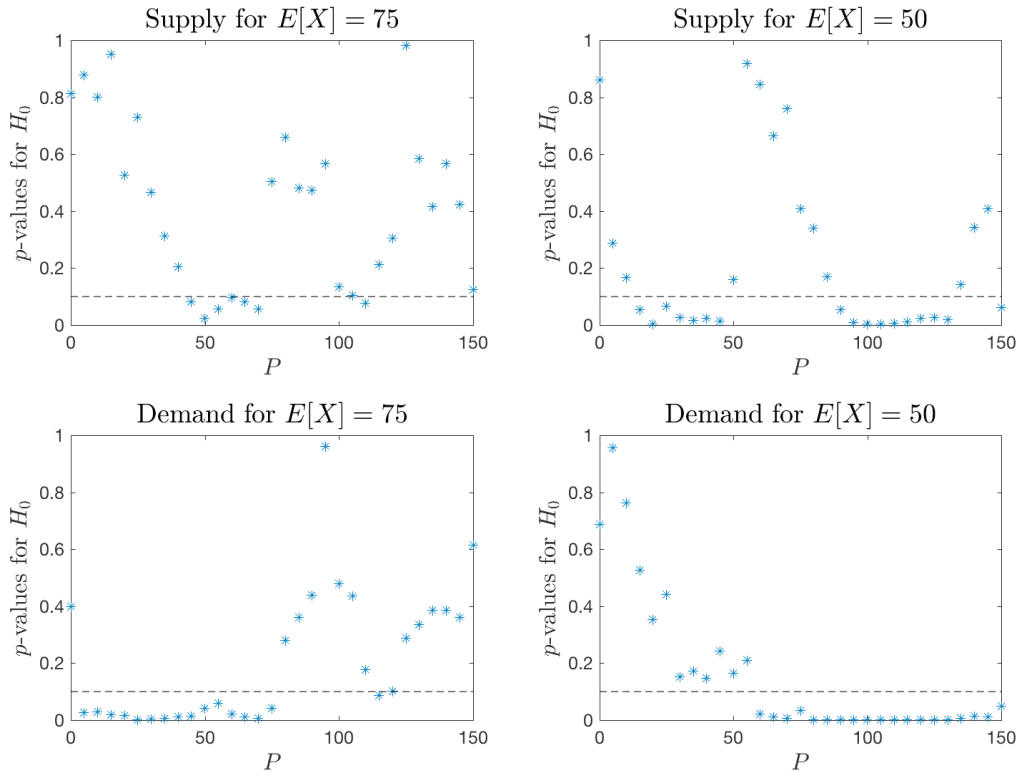

FIGURE D1.3. TESTING FOR DIFFERENCES IN PRICE SENSITIVITY

Notes: This figure reports the p-values of a Wilcoxon signed-rank test of the differences between average supply (demand) curves for simple and complex risks. Averages are computed across subjects and trading rounds. Average curves for complex risks are adjusted as described in Appendix C1 and linearly interpolated to allow for a direct comparison with simple risks. In the top (bottom) row, average supply (demand) curves are computed across all sessions. In the left (right) column, averages are computed across trading rounds where π is equal to $1/2$ ($1/3$). The dotted line indicates a p-value equal to 10%.

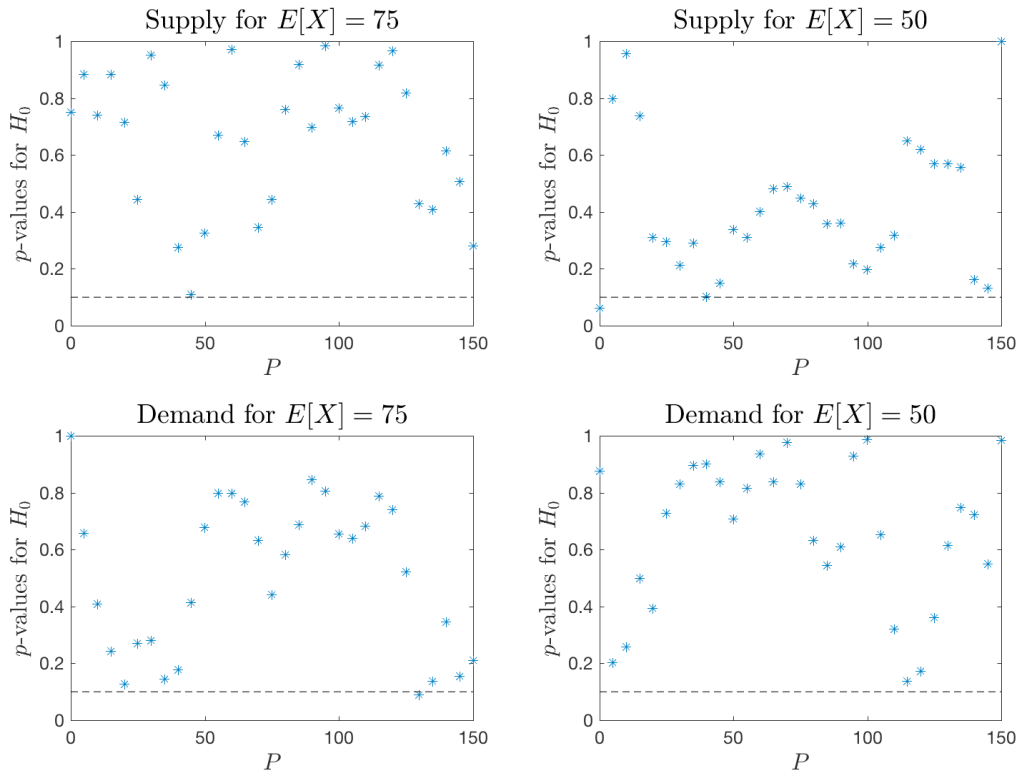

FIGURE D1.4. TESTING FOR PRICE-TAKING BEHAVIOR UNDER COMPLEX RISKS

Notes: This figure reports the p-values of a Wilcoxon signed-rank test of the differences between average supply (demand) curves for complex risks under market clearing and random price draws. Averages are computed across subjects and complex trading rounds. Average curves are adjusted as described in Appendix C1 and linearly interpolated to allow for a direct comparison with simple risks. In the top (bottom) row, average supply (demand) curves are computed across all sessions. In the left (right) column, averages are computed across complex trading rounds where π is equal to $1/2$ ($1/3$). The dotted line indicates a p-value equal to 10%.

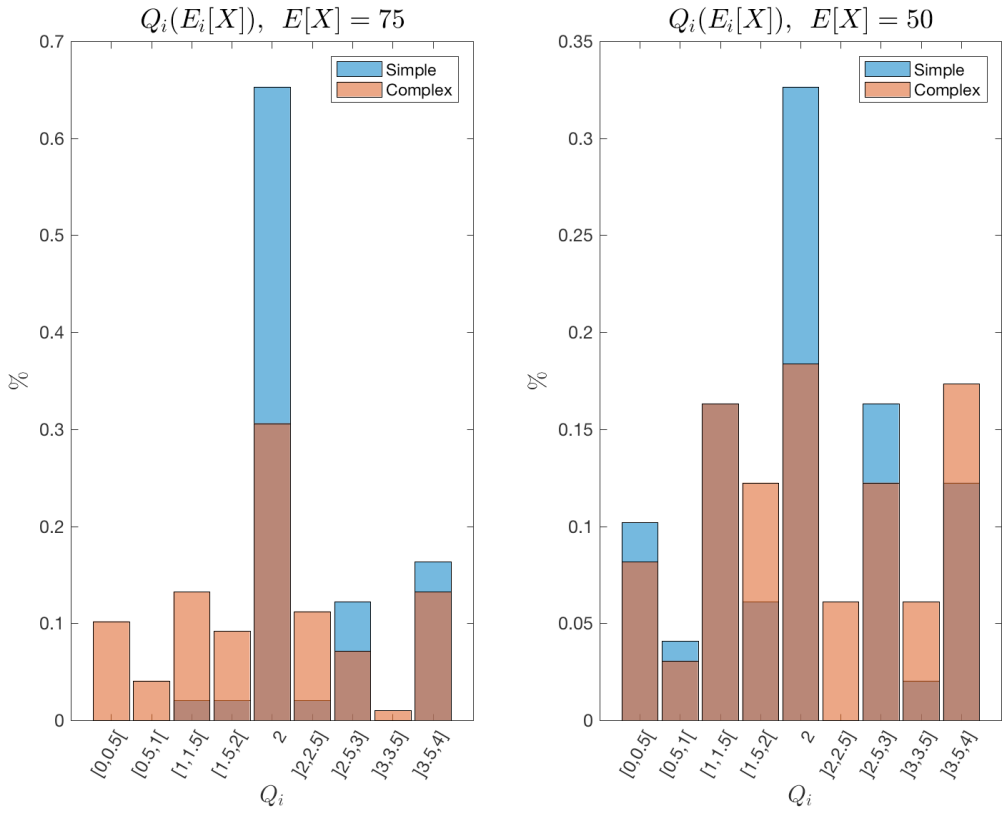

FIGURE D1.5. DEMAND DISTRIBUTION FOR PRICES EQUAL TO EXPECTED PAYOFFS

Notes: This figure shows the number of shares demanded by buyers for prices equal to (estimated) expected payoffs. The empirical distributions are computed across subjects and sessions. The left (right) plot contrasts average distributions between simple and complex trading rounds with π equal to $1/2$ ($1/3$). If, under complex risks, buyers' point estimate $E_i[X]$ lies between two elements of the predefined price vector, linearly interpolated quantities are reported.

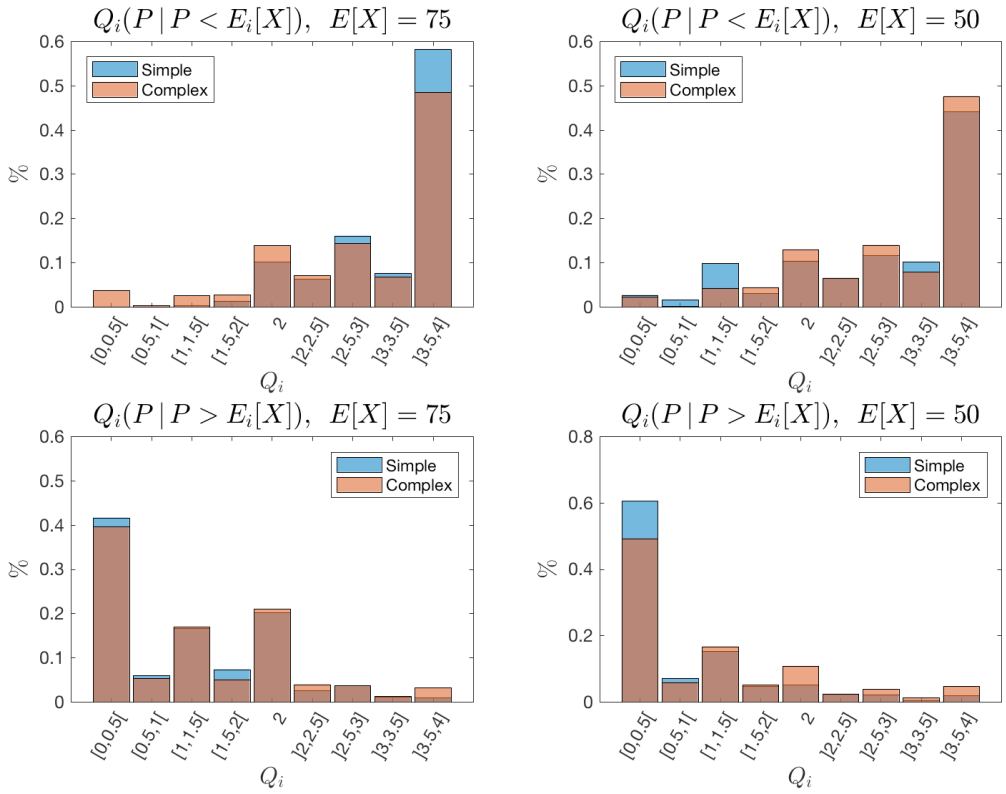

FIGURE D1.6. DEMAND DISTRIBUTION FOR PRICES DIFFERENT FROM EXPECTED PAYOFFS

Notes: This figure shows the number of shares demanded by buyers for prices different from expected payoffs. The empirical distributions between simple and complex risks are computed across subjects and sessions. In the top (bottom) row, total demands for pries below (above) $E_i[X]$ are reported. The left (right) column shows average demand distributions across trading rounds with π equal to $1/2$ ($1/3$).

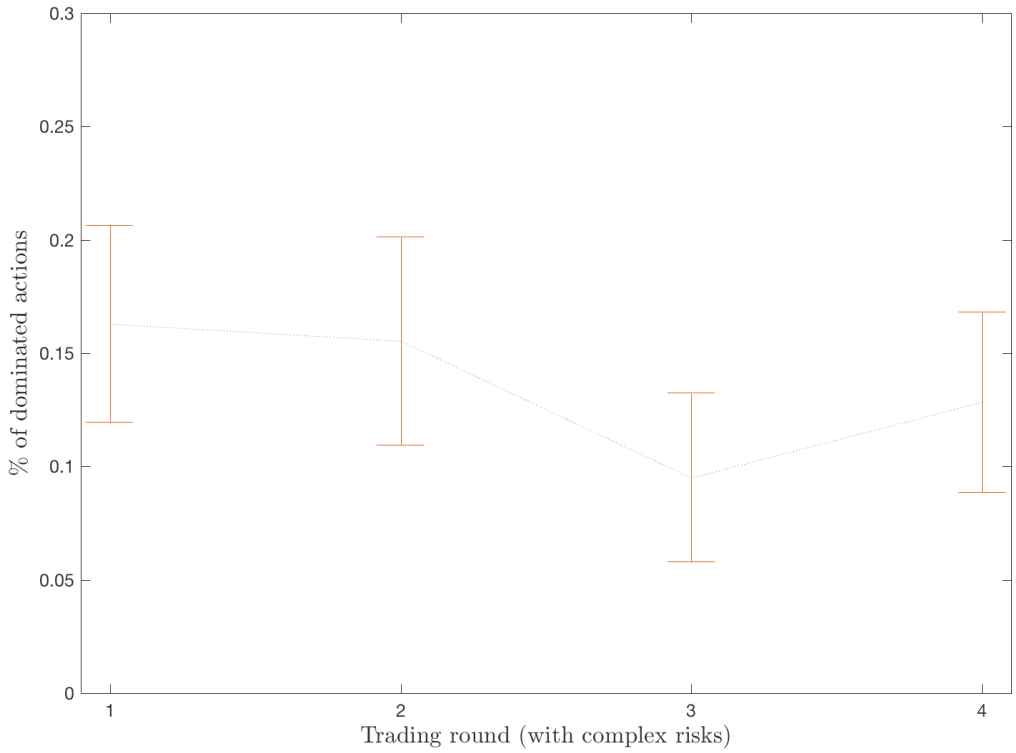

FIGURE D1.7. LEARNING UNDER COMPLEX RISKS

Notes: This figure shows the evolution of the average percentage of dominated trading strategies (see Figure 1.14) over the four trading rounds with complex risks (see Table 1.3). Error bars indicate standard errors of the mean.

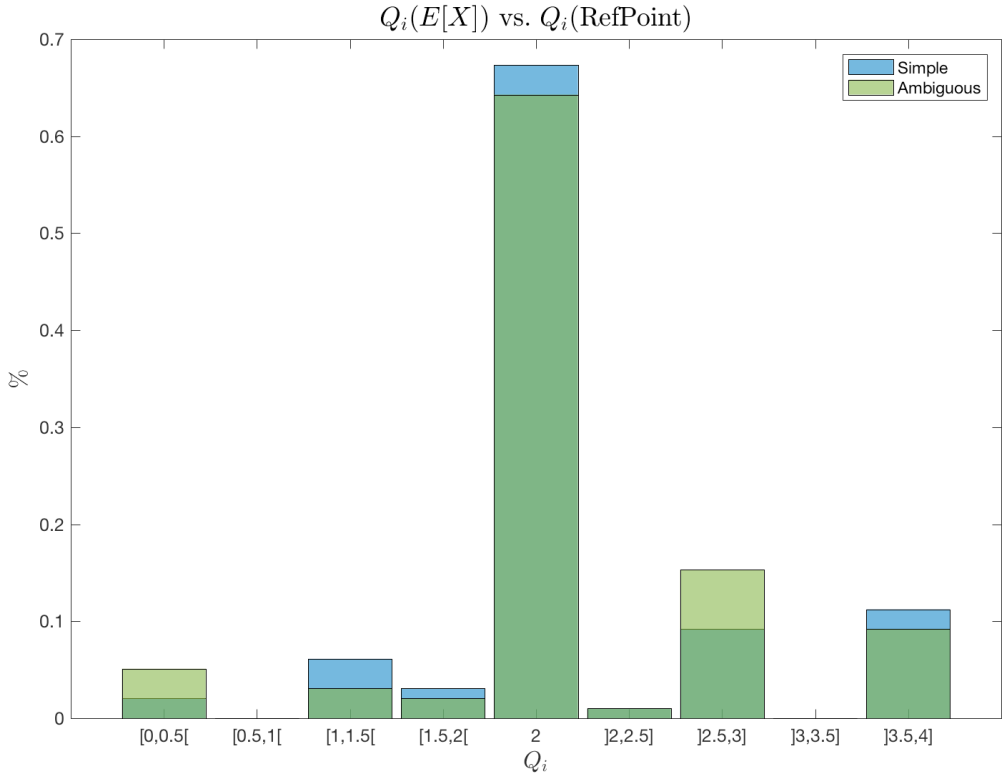

FIGURE D1.8. DISTRIBUTION FOR PRICES EQUAL TO EXPECTED PAYOFF (REFERENCE POINT)

Notes: This figure shows empirical distributions of supplied and demanded shares at a fixed price of ECU 75. Percentages are computed across subjects and sessions. For simple risks, only the trading round with π equal to $1/2$ is considered. For ambiguous risks, a price of ECU 75 corresponds to the natural reference point, assuming that subjects believe in a fifty-fifty likelihood under pure ambiguity.

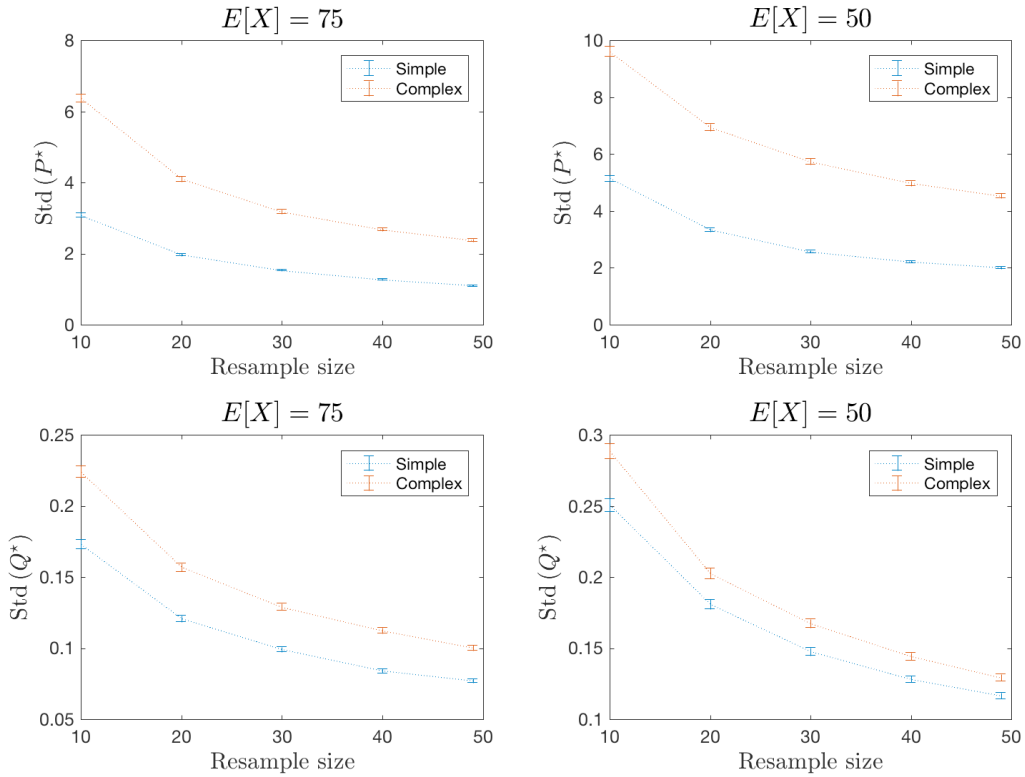

FIGURE D1.9. EQUILIBRATION VARIABILITY

Notes: This figure shows bootstrapped standard deviation estimates of market-clearing prices and quantities for simple and complex risks. Average supply and demand curves are determined for different resample sizes. For each pair of averaged supply and demand, linearly interpolated market-clearing prices and quantities are computed. Repeating this procedure ten thousand times yields the depicted standard deviation estimates of equilibrium prices (top row) and quantities (bottom row). The left (right) column shows bootstrapped moment estimates for trading rounds with π equal to $1/2$ ($1/3$). Error bars indicate 99%-confidence intervals.

E1 Experimental Instructions

The subsequent three pages present the experimental instructions for sellers. The analogous instructions for buyers are available upon request.

Instructions I/II

Welcome to this experiment at the Department of Banking and Finance, University of Zurich. This is the first out of 2 instruction sheets. Please read each sheet very carefully. Fully understanding the instructions will allow you to perform better on the task, thereby earning more money. Raise your hand if you have any questions or as soon as you have read everything and are ready to continue.

1 Situation

The experiment consists of a sequence of 7 trading rounds. In each trading round the same number of buyers and sellers are present. You are a **seller**. Your role will not change throughout the experiment.

At the beginning of every round, you will receive a fresh supply of 4 shares of a given security. During each round you can sell between 0 and 4 of these shares. The security either pays a dividend per share equal to 150 or 0. Besides this dividend per share, the security does not pay anything else (no capital gains). Additionally, you are provided with some non-tradable income: whenever the security happens to pay a dividend of 150 per share, you receive 0, and if it does not pay anything (dividend of 0), you receive 300. This additional income **does not depend** on how many shares you are selling. The following graph summarizes your holdings at the beginning of every round:

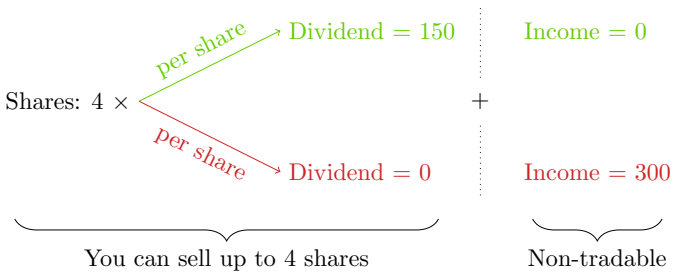

Your wealth at the end of each round is the sum of received proceeds from trading, collected dividends, and additional income. It is not carried over to the subsequent round, this means you always start out with 4 shares. At the end of every round, the trading outcome, realized dividends, and your respective wealth are displayed.

2 Trading

Trading happens in 2 phases. First, you have to select how many shares you want to sell in case the price equals 0, 25, 50, 75, 100, 125, or 150. The computer then linearly fills up your selling quantities for the remaining 5-unit steps between 0 and 150 (5, 10, 15, ...). Second, you are asked to make **further adjustments** until you end up with the **exact** quantities you want to sell for any given price. Note, quantities can be entered with up to 2 decimal places of precision.

The price determination method of the current round is always displayed in the upper right corner of your screen. There are two ways how prices are determined. If there is **market clearing**, the computer sets the price such that the number of traded shares is maximized. Alternatively, the computer will choose the price randomly (**random price**) with equal probabilities across the full list of given prices.

****

You will now go through a first practice round. This practice round will not impact your payment.

Instructions II/II

Please read this sheet very carefully. Raise your hand if you have any questions or as soon as you have read everything and answered the comprehension questions at the end.

3 How Dividends Are Determined

The computer randomly determines whether the security is going to pay a dividend or not. However, the information about the structure that governs the computer's random choices varies between trading rounds. There are 2 different cases:

1. Urn.—The computer draws 1 ball out of an urn with 30 balls. The balls are either green or red, the respective composition is revealed at the beginning of the trading round. Whenever the color of the drawn ball is green, the security pays a dividend equal to 150 per share (and 0 if red).

2. Simulated reference path.—The computer simulates the evolution of a reference path over 2 time periods, but only the first period will be displayed. Whenever the path ends up above a certain limit, the security pays a dividend equal to 150 per share (and 0 if the path ends up below this limit). The **only purpose** of this path is to determine whether the security pays a dividend or not.

What you will see.—You are provided with a **formal description** of the reference path S_t, where the random component is denoted by W_t. W_t follows a normal distribution with mean equal to 0 and variance equal to the corresponding change in time. For example, the full description of the path S_t could look like this

$$dS_t = 5\%S_t\,dt + 10\%S_t\,dW_t,$$

where dS_t denotes the change of S_t over the very small (infinitesimal) time change of length dt. Additionally, you will see a **video** of the path S_t between time 0 and the end of period 1:

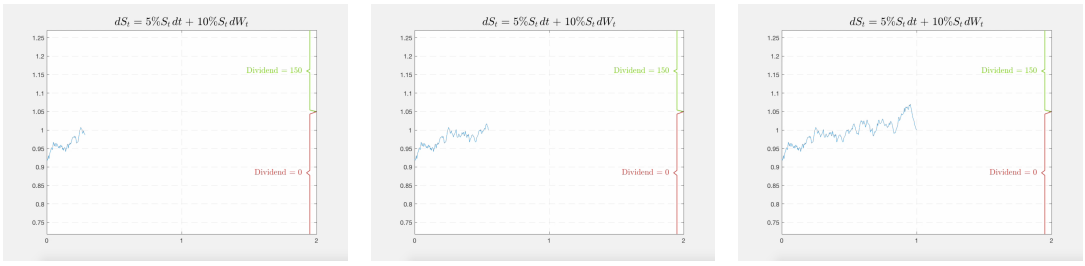

(a) Beginning of period 1 (b) Middle of period 1 (c) End of period 1

The difference of the random component W_t between the ends of period 1 and 2, $W_2 - W_1$, follows a normal distribution with mean 0 and variance 1. For simplicity, every path is scaled such that $S_1 = 1$.

Based on this information you can assess the probability of the dividend being equal to 150 ($\rightarrow$ path ends up in the green region at time 2).

4 List of Lotteries, Questionnaire, and Payment

After the 7 trading rounds, you have to repeatedly choose 1 out of 2 options for 2 lists of lotteries. For both lists, the computer randomly selects and plays 1 of your chosen options. Finally, you will be asked

to fill-in a short questionnaire.

Your final payment will be determined as follows:

1. The computer randomly picks 1 out of the 7 trading rounds or 1 of the 2 lottery outcomes with equal probability ($\frac{1}{9}$ for each). It is therefore critical that you concentrate on **every round**. You will be paid either your wealth at the end of the selected trading round or the outcome of the selected lottery, both in CHF divided by 12.

2. In all rounds with simulated reference paths, you are asked to submit your best guess regarding the probability of the dividend being equal to 150. If your guess is correct (within +/- 3%), you earn an additional 3 CHF whenever this round is selected for payment.

5 Comprehension Questions

(1) Assume you have sold **4** shares at a price of **50** per share, what is your wealth in the 2 scenarios?

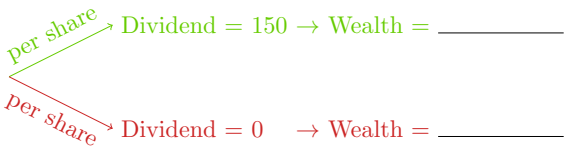

(2) Assume you have sold **4** shares at a price of **150** per share, what is your wealth in the 2 scenarios?

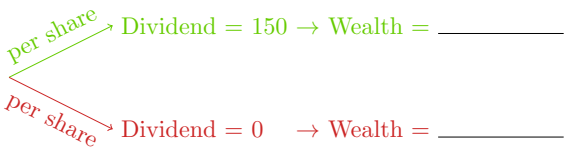

(3) Assume you have sold **2** shares at a price of **50** per share, what is your wealth in the 2 scenarios?

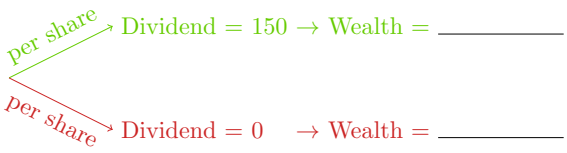

(4) Does the **difference** between your wealth in the green and the red scenario depend on...?

☐ The paid price ☐ The number of sold shares

(5) What is the difference between your wealth in the 2 scenarios, if you exactly sell **2** shares?

Difference = _____

****

Raise your hand after you have answered the comprehension questions. After double-checking, you will go through 2 last practice rounds. These practice rounds will not impact your payment.

2 Risk and Return around the Clock

Joint with Alexandre Ziegler

We investigate price discovery over the 24-hour trading day for equities, currencies, bonds, and commodities. Sizable price discovery occurs around the clock for most assets. For a given asset, intraday risk and return distributions are fairly similar, indicating a broadly constant risk-return-relationship during the day. Although the amount of price discovery varies significantly during the day and differs across assets, price discovery is generally efficient around the clock. Most assets do not exhibit the U-shaped intraday volatility pattern that has been documented for US equities, even if only main trading hours are considered. Intraday spikes in volatility are driven by the open or close of the market for the respective asset or other assets and by macroeconomic announcements. Both diffusion and jump risk are important drivers of intraday volatility patterns, and US macroeconomic news account for a sizable fraction of jump-driven volatility. For some – but not all – assets, the relationship between volume and volatility that can generally be observed during the trading day does not hold at the time of jumps, suggesting that traders anticipate large price moves at the time of scheduled announcements and market depth falls accordingly.

2.1 Introduction

How important are news coming from different parts of the world for asset prices, and how is this reflected in the distribution of risk and return during the trading day? While intuition allows making qualitative statements about these issues for some assets, actual figures are unknown. For example, one would expect US equity prices at large to be driven mostly by US macroeconomic news, but to also react – probably to a lesser extent – to macroeconomic news coming out of Europe and Asia. What share of equities' returns and volatility can be attributed to these different sources? Turning to a less intuitive case, what intraday return and volatility patterns should we expect for oil, which is consumed around the world and largely produced in the Middle East and Russia, where political risk can be sizable? How about gold, whose two largest producers are China and Australia, but which is used globally both in industrial applications and as a monetary asset? In this paper we investigate price discovery around the clock for a number of benchmark assets from the main asset classes equities, currencies, bonds, and commodities.

While price discovery has been studied extensively in the literature, around-the-clock analyses have not been possible for most assets (with the exception of currencies) because of limited

We thank Ramo Gençay and Michel Habib for valuable suggestions.

trading hours. During the last couple of years, however, the trading hours of futures contracts on a number of global benchmark assets have been progressively extended, with some contracts now trading almost 24 hours a day. This recent development offers an unique opportunity to investigate price discovery around the clock. In addition to trading hours that are longer than those of the underlying cash market for most instruments, the use of futures contracts has a number of advantages. First, it allows performing a comprehensive analysis using a unified methodology, thus ensuring that differences in price behavior across assets are not driven by differences in the way the market is organized. Second, trading on futures markets is subject to relatively few institutional or regulatory restrictions; in particular, taking long and short positions is equally easy and short-selling bans cannot be imposed by construction. To our knowledge, this paper is the first comprehensive analysis of price discovery across time zones and asset classes.

Our analysis considers 13 contracts from the asset classes equities, bonds, currencies, and commodities; for the latter we focus on oil and metals. Specifically, we consider the S&P 500, EuroStoxx 50, and Nikkei equity index futures; the 10-year US Treasury Note, 10-year German Bund, and 10-year Japanese Bond futures; the EUR/USD and JPY/USD currency futures; West Texas Intermediate and Brent oil futures; as well as gold, silver, and high-grade copper futures. These contracts are widely regarded as global benchmarks and are all very liquid. By contrast with individual stocks, where after-hours trading volume is typically a small fraction of total volume, most of these contracts have sizable trading volume outside of the underlying cash market's trading hours.

The main findings of our analysis can be summarized as follows. First, sizable price discovery takes place around the clock for almost all assets, but its distribution during the day is considerably different across assets. While the amount of price discovery per unit time is larger when underlying cash markets are open, a large amount of price discovery nonetheless takes place when they are closed. Indeed, adjusted for trading volume, price discovery is higher outside of main trading hours. Generally, the distribution of price discovery during the day is similar for equities and bonds from the same region. Moreover, for a given instrument and even within some asset classes (currencies, oil, and metals), the distribution of risk and return during the day is fairly similar, indicating a broadly constant risk-return-relationship during the trading day. Put differently, it is not the case that returns accrue in the morning and risk in the afternoon or vice versa.

Second, although the amount of price discovery varies significantly during the day and across assets, price discovery is quite efficient around the clock for most assets. Nevertheless, efficiency tends to be higher during an asset's main market hours, and there exist short periods where price discovery is inefficient. For most instruments, inefficiency is concentrated before the open of Asian markets and during the first few hours of trading on Asian markets.

Third, while all assets exhibit strong intraday volatility patterns, the precise shapes of these patterns vary substantially. Strikingly, most assets do not exhibit the U-shaped intraday volatility pattern that has been widely documented for US equities, even if only the trading hours of the underlying or pit market are considered. Generally, intraday spikes in volatility occur at four sets of times: (i) at the open or close of the market for the respective asset, (ii) at the

open or close of the futures pit for the respective asset, (iii) at the open or close of other markets (both the underlying cash market and markets for other assets), and (iv) at the time of macroeconomic news releases. Most assets react strongly to US macroeconomic news releases and have higher volatility during US trading hours, but also exhibit strong volatility outside of US trading hours. This is in particular the case for metals and currencies. The S&P 500 is the only asset in our sample that exhibits a clear-cut U-shaped volatility pattern, and that pattern only holds during hours when the underlying cash market is open. This observation calls for new theories to explain intraday volatility patterns for around-the-clock markets.

Fourth, when decomposing intraday volatility into its diffusion and jump components, we find both diffusion and jump volatility to be important drivers of overall intraday volatility patterns. The contribution of jumps to overall volatility is substantial, accounting for approximately 5% to 13% of total daily return variance. A sizable fraction of jump-driven volatility occurs around US macroeconomic news announcements, affecting all assets in our sample.

Finally, while there is strong comovement between trading volume and volatility during the trading day, the relationship is far from perfect. Volume generally significantly exceeds volatility during US trading hours. Interestingly, the relationship between volume and volatility that can generally be observed during the trading day often does not hold at jump times. Specifically, while both volume and volatility spike at the time of jumps, the difference between the two sometimes does and sometimes does not. This suggests that in some – but not all – markets, traders anticipate large price moves at the time of scheduled announcements and market depth falls accordingly. Furthermore, the opening and closing of stock markets or futures pits tend to be associated with spikes in trading volume that are much larger than the contemporaneous spikes in volatility. Moreover, these spikes in volume are often substantially larger than those associated with price jumps.

The remainder of the paper is organized as follows. Section 2.2 provides a concise review of the related literature. Section 2.3 describes the assets that we consider in the study and our dataset. Section 2.4 analyzes the distribution of returns during the trading day. Section 2.5 investigates the rate and efficiency of price discovery during the trading day. Section 2.6 describes intraday volatility patterns, and Section 2.7 performs a decomposition of intraday volatility into its diffusion and jump components. Section 2.8 investigates the intraday relationship between trading volume and volatility with particular emphasis on the behavior at jump times. Section 2.9 concludes.

2.2 Literature Review

A large literature investigates return and volatility patterns across weekdays and during the trading day. As mentioned above, however, most of this literature only describes intraday risk and return patterns for limited hours – usually between seven and nine depending on the country – during which exchanges are typically open, with price discovery between the close and the open reflected in highly variable overnight returns.

Wood et al. (1985) find unusually high returns and volatilities at the beginning and the end of the trading day for NYSE stocks. Similar U-shaped volatility patterns have been documented in several markets (see, for example, Jordan et al. (1988) for soybean futures and Ekman (1992) as well as Lee and Linn (1994) for S&P 500 futures). Daigler (1997) takes advantage of the fact that futures market trading hours are longer than those of cash markets to investigate the Admati and Pfleiderer (1988) and Brock and Kleidon (1992) intraday volatility pattern theories using S&P 500, Eurodollar, and Treasury Bond Futures. However, at the time his study was conducted, futures trading hours were not much longer than those of the cash market.[1] He finds that the U-shaped volatility pattern is present in the data, but that for S&P 500 and Eurodollar futures, volatility decreases before the close of the cash market. Cyree and Winters (2001) document the presence of a U-shaped pattern in the Fed Funds (cash) market. Batten and Lucey (2010) also observe such a U-shaped intraday volatility pattern in the gold futures market; however, their analysis is restricted to trading hours between 8:20 and 15:30 US Eastern time.[2] Zwergel and Heiden (2012) analyze intraday volatility patterns for DAX futures that are traded from 8:00 to 22:00 central European time, i.e., covering both European and US main market hours. They find a W-shaped volatility pattern, with a first burst of volatility at the open of European stock markets, a second one at the open of US stock markets, and a third one at the close of US markets. Their results also reveal short volatility spikes at the open of futures trading and at the time of US macroeconomic announcements.

Studies seeking to investigate price discovery around the clock have generally had to use cross-listed securities or currencies. Papers using cross-listed securities include Neumark et al. (1991), Craig et al. (1995) as well as Werner and Kleidon (1996). Andersen and Bollerslev (1998) is one of the few studies providing a characterization of intraday volatility patterns around the clock. Analyzing Deutsche Mark-Dollar foreign exchange quotes, they document pronounced intraday volatility patterns. Volatility is subdued during Pacific hours, picks up at the time of the Tokyo market open, increases again during European trading hours until about 16:00 central European time, then declines monotonically towards the level associated with Pacific hours. Interestingly, they find no signs of elevated volatility when trading closes in New York. Barclay and Hendershott (2003) use the extension of trading hours brought by the emergence of electronic communications networks to investigate price discovery for Nasdaq stocks during the preopen (8:00 to 9:30 US Eastern time) and the postclose (16:00 to 18:30). They find that although after-hours trading volume is relatively low, it generates significant price discovery, but that prices after hours are noisier, implying that price discovery is less efficient. Breedon and Ranaldo (2013) analyze aggregated hourly trading data on the most important currency crosses and document a significant tendency of both a depreciation as well as more seller- than buyer-initiated trades of the base currency during local trading hours. They conclude that local

[1] In 1988 and 1989, the S&P 500 futures opened at the same time as the cash market but closed 15 minutes later, the Eurodollar futures opened 15 minutes before the cash market and closed at the same time as the S&P 500 futures, while the Treasury Bond futures traded from 8:20 to 15:00 US Eastern time and then reopened for a night session lasting from 18:00 to 21:30.

[2] At the time of their study, 8:20 to 13:30 were main market hours and available extended hours were from 13:30 to 15:30.

market participants tend to be net purchasers of foreign currencies.

A large literature relates interday and intraday volatility patterns to macroeconomic announcements. Harvey and Huang (1991) find no U-shaped pattern in foreign exchange futures volatilities during US trading hours (which were from about 7:30 to 13:30 US Central time in their sample). Intraday volatility is hump-shaped on Mondays through Wednesdays, while on Thursdays and Fridays, volatility is highest during the first hour of trading. The authors explain this by the fact that the most important macroeconomic announcements take place during the opening hour of trading on Thursdays and Fridays. Ederington and Lee (1993) specifically investigate the impact of macroeconomic announcements and find that they are responsible for most of the time-of-day and day-of-the-week volatility patterns for the Treasury Bond, Eurodollar, and Deutsche Mark futures. Moreover, after controlling for these announcements, volatility is basically flat both across the trading day and across the trading week.[3] Christie-David et al. (2000) consider the responses of 15-minute prices of gold and silver futures to monthly US macroeconomic news. While macroeconomic news overall affect metal prices less than interest rates, gold and silver futures both respond strongly to Capacity Utilization and Unemployment Rate news releases. Almeida et al. (1998) investigate the reaction of the DEM/USD exchange rate to both US and German macroeconomic news at the five-minute frequency. They provide evidence that the exchange rate quickly and significantly reacts to unexpected news and that its reaction generally reflects anticipated policy responses by monetary authorities. They also find German announcements to have a smaller impact on the exchange rate and to be incorporated more slowly into prices than US ones. Evans and Lyons (2008) consider DEM/USD returns both at the five-minute and daily frequency and find the arrival of broad macroeconomic news to account for over 30% of total daily price variance. Importantly, they show that the indirect order flow effect – the effect attributable to an increase in the order flow subsequent to the news release – turns out to be about twice as large as the direct news effect.

Another strand of the literature is concerned with cross-market information transmission, both across countries and across different markets within the same country. Lin et al. (1994) investigate the transmission of stock returns and volatility across country indices (specifically the S&P 500 and the Nikkei), while Engle et al. (1990) consider the transmission of volatility in the Yen/Dollar exchange rate across markets. Booth et al. (1997) investigate the transmission of intraday volatility between the S&P 500, FTSE 100, and Nikkei 225 futures. They find evidence that volatilities of S&P 500 and FTSE 100 futures significantly react to information from other markets, whereas the volatility shocks of Nikkei 225 futures are mainly country-specific. Fleming et al. (1998) estimate correlation coefficients of bivariate AR(1) volatility processes of daily returns on S&P 500 index futures, T-bond futures, and T-bill futures and find strong volatility linkages, which they partially attribute to cross-hedging spillovers. Booth and So (2003) investigate intraday information transmission between the German DAX index, futures, and options and document volatility spillover effects for all three markets. Analyzing the VIX and five European implied volatility indices at a daily frequency, Jiang et al. (2012)

[3] At the time their study was conducted, however, trading hours for the futures contracts they investigate were only from 8:20 to 15:00.

provide evidence of mutual volatility spillovers and find implied volatilities to drop (rise) on days with scheduled (unscheduled) news events.

A number of papers relate return and volatility linkages across markets to macroeconomic announcements. Becker et al. (1995) analyze 30-minute returns of both S&P 500 and FTSE 100 futures during main market hours.[4] Focusing on the most important macroeconomic announcements in both countries, both markets appear to respond similarly but independently to US news. However, while FTSE prices react to UK news, the S&P 500 ignores them. Their finding that international stock markets respond to US information but US markets ignore foreign news suggests that US returns lead foreign prices. Andersen et al. (2007) analyze five-minute returns on futures across different countries and asset classes (S&P 500, FTSE 100, Euro Stoxx 50, 30-Year-Treasury Bond, British Long Gilt, German Euro Bobl, USD/GBP, USD/JPY, and USD/EUR) around essentially all US macroeconomic news announcements. However, their analysis focuses on open auction regular trading hours and does not include after hours trading. In general, they observe very quick price discovery, i.e., the price response to macroeconomic news occurs within the first five minutes after the actual announcement. Furthermore, many of the US macroeconomic fundamentals also significantly impact foreign bond markets, and in the same direction. Finally, using return spillover regressions, they provide empirical evidence of international stock market cross-correlations (not only from the US to Europe but also vice versa) even when controlling for the effect of US macroeconomic news releases.

2.3 Sample and Data

Since futures contracts exist on a wide range of assets, the number of contracts that could be investigated is very large. Our analysis focuses on 13 contracts from the main asset classes, namely equities, bonds, currencies, and commodities; for the latter we focus on oil and metals. Specifically, we consider the E-Mini S&P 500 (ES), Nikkei (NK), and EuroStoxx 50 (XX) equity index futures; the 10-year US Treasury Note (TY), 10-year German Bund (BN), and 10-year Japanese Bond (JB) futures; the EUR/USD (EC) and JPY/USD (JY) currency futures; West Texas Intermediate (CL) and Brent (CO) oil futures; as well as gold (GC), silver (SV), and high-grade copper (HG) futures. All these contracts are widely regarded as global benchmarks and are very liquid, with the daily volume in the front-month contract alone generally exceeding 100,000 contracts.

We obtain five-minute data on these contracts from TickData for the period from April 10, 2010 (the beginning of around-the-clock trading for the Nikkei futures) to August 30, 2013. Our choice of a five-minute frequency balances our aim of obtaining a precise picture of price behavior around specific times such as the opening of trading on the cash market and the time of scheduled news releases, while avoiding distortions caused by microstructure noise.

For each instrument, we use the front-month contract as it is generally the most liquid. We rollover to the first back-month contract when the latter becomes more liquid. This usually

[4] At the time of their study, main market hours were from 9:30 to 16:15 US Eastern time for the S&P 500 and from 09:35 to 17:10 central European time for the FTSE 100.

occurs about a week before the front-month contract's last trading date, with the exception of metals, which exhibit a number of peculiarities. For gold, although contracts exist for each calendar month, only the February, April, June, August, October, and December contracts (G, J, M, Q, V, and Z) are liquid at some point during their lifetime. Moreover, trading volume in the front-month contract declines sharply before the first notice date, which is about one month before the last trade date. Therefore, we only make use of data for these six expiration months and perform the contract rollover 35 calendar days prior to expiration. Similarly, for copper and silver, only the March, May, July, September, and December contracts (H, K, N, U, and Z) are liquid at some point during their lifetime, and volume also declines sharply before the first notice date, which is again about one month before the last trade date. Hence, we only consider data for these five expiration months and perform the contract rollover 35 calendar days prior to expiration. For equity index, bond, and currency futures, contracts mature on the March quarterly cycle (H, M, U, and Z), while oil contracts mature each calendar month.

Trading hours for the different instruments and their trading volume are summarized in Table 2.1.[5] For those contracts that have trading pits, we also report pit trading hours since they will turn out to be important when interpreting our results. For comparability, we convert all times to central European time (CET). As is apparent in Table 2.1, CET is the most natural time zone to use in our setting since when expressed in CET, trading in all contracts ends before midnight and reopens either at midnight or in early morning hours. Moreover, cash markets for most instruments are closed at midnight CET, i.e., when we switch from one day to the next. Using US Eastern time, for example, would cause us to switch from one trading day to the next when Japanese cash bond and equity markets are open, while using Japanese time would mean switching trade dates while cash markets in Europe and the US are open. Some care must be used in order to deal with daylight savings time (DST). While both the US and Europe have DST, Japan does not. Furthermore, the DST switch dates in Europe and the US often differ, with US DST generally starting earlier and finishing later in the year. In order not to introduce additional noise in our results, we delete days where the US has DST but Europe does not from the sample, which eliminates about four weeks of data each year. We adjust for DST when converting Japanese trade times and dates to CET.

As can be seen in Table 2.1, most contracts in our sample are traded almost around the clock, with nine of the 13 contracts (namely ES, NK, TY, EC, JY, CL, GC, SV, and HG) trading 23 hours a day or more. Brent Oil (CO) is traded 22 hours a day, while the EuroStoxx (XX) and Bund (BN) futures are traded 14 hours per day. Accounting for two trading halts of 28 minutes each, Japanese Bond futures (JB) have the shortest trading hours; nevertheless, this contract trades 13 hours and 44 minutes per day. Trading volume in the different contracts is quite large, and ranges from about 10'000 contracts for the Nikkei futures to almost two million contracts for the S&P 500 E-Mini future (ES). Average volume per five-minute interval ranges from 35 contracts for the Nikkei to almost 7'000 contracts for ES. Moreover, with the exception of the Nikkei and Japanese Bond futures, trading occurs throughout the day, with the share of

[5] In this chapter, due to their large size, all tables and figures are provided at the end of the paper.

five-minute intervals with zero trading volume at most a couple of percentage points.

Table 2.2 reports the distribution of daily volume during the trading day. We divide the trading day into eight periods constructed based on cash market trading hours and the timing of macroeconomic announcements in the different regions as follows (all times are in CET):

1. 00:00-01:00, when all cash markets except currencies are closed but several futures contracts are trading and most Japanese macroeconomic news announcements are released;

2. 01:00-08:00, corresponding to Japanese main market hours;

3. 08:00-09:00, corresponding to European pre-market trading, where Eurex futures are trading but European cash markets are closed;

4. 09:00-13:00, when European cash markets are open, most European macroeconomic announcements are made, but no US macroeconomic news announcements occur;

5. 13:00-15:30, when European cash markets are open, US cash markets are closed, and most US macroeconomic news announcements take place;[6]

6. 15:30-17:30, when both European and US cash markets are open and a few US macroeconomic news announcements are released;[7]

7. 17:30-22:00, when European cash markets are closed, US cash markets are open, and US Federal Reserve announcements occur;

8. 22:00-00:00, when all cash markets except currencies are closed but several futures contracts are trading.

The results in Table 2.2 reveal sizable trading volume outside of the trading hours of the instruments' main cash markets. For example, about 25% of S&P 500 futures trading volume is transacted outside of the periods when US stock exchanges are open. Similarly, over 30% of Brent trading volume is observed after the close of European markets. The lowest share of volume outside of main market hours is observed for Japanese government bonds, for which over 85% of volume is transacted between 01:00 and 08:00 CET. While the share of volume transacted during Asian hours is quite small for oil, it is sizable for metals.

Throughout our analysis, we use log-returns to ensure time additivity. At the beginning of each trading day and following each trading halt, we compute the return from the previous close to the open and record it as the return for the previous five-minute interval (whose endpoint matches the time of the opening of trading).[8] The return for the first five-minute interval of the trading day and following each trading halt is computed as the open-to-close return during that

[6]The pre-market period for the US starts at 13.00 CET, which is the time of the first US macroeconomic news announcements (i.e., MBA Mortgage Applications).

[7]For example, ISM, leading indicators and consumer confidence are released at 16:00; see Table 2.6 for details.

[8]Two contracts in our sample have intraday trading halts: the S&P 500 E-Mini futures (from 22:15 to 22:30 CET) and Japanese government bond futures (from 3.02/4.02 to 4.30/5.30 CET and from 7.02/8.02 to 7.30/8.30 CET in winter/summer).

interval. Finally, the returns for all subsequent five-minute intervals until the close or the next trading halt are computed as the logarithm of the ratio of the closing price in that interval to the closing price in the previous interval in which the instrument traded. Using this approach guarantees a complete set of returns – one for each period in which the instrument traded – whose sum over our sample period equals the return of a long position in the front-month futures that was systematically rolled over before maturity.

2.4 Price and Variance Contribution during the Day

As is custom in the literature, we use price contribution to measure the amount of information incorporated into prices during a given time period. Price contribution reflects the fraction of the daily return that has occurred during a given period, i.e.,

$$PC_i = \frac{r_i}{r} \ , \tag{2.1}$$

where r_i denotes the return during period i and r the total return for the day (from the close of after hours trading on the previous day to the close of after hours trading on the current day). Since we use log-returns, price contribution sums to unity on each day. As recommended in Barclay and Hendershott (2003), we calculate the mean price contribution of each interval across days and use its time-series standard error for statistical inference.

Table 2.3 reports price contribution for the different assets during the eight periods defined in Section 2.3; periods where an instrument is not traded are marked with dashes. The results in Table 2.3 reveal sizable price discovery for most instruments outside of their cash market trading hours. For example, over half of both S&P 500 and EuroStoxx 50 and almost half of Nikkei returns accrue while their respective cash markets are closed. Although price discovery outside of main hours is somewhat smaller for bonds, it remains sizable perhaps with the exception of Japanese bonds. Interestingly, WTI oil exhibits significant price discovery during European trading hours, and Brent oil significant price discovery during US trading hours.

We know from Table 2.2 and Table 2.3 that both volume and price contribution are sizable outside of main market hours. This raises the natural question of how much price discovery is achieved relative to volume during the different periods of the trading day. To answer this question, we compute the ratio of price contribution relative to the share of daily volume transacted in each period; we call this measure the volume-weighted price contribution

$$VWPC_i = \frac{r_i/r}{V_i/V} \ , \tag{2.2}$$

where V_i denotes trading volume during period i and V total daily volume. As was the case for price contribution, volume-weighted price contribution is calculated for each day and then averaged across days.[9] Barclay and Hendershott (2003) perform a similar analysis on their data,

[9]Note that since r_i can be both positive and negative, differences in weighting between price contribution and volume-weighted price contribution can result in sample averages with opposite signs.

but scaling price contribution by the number of trades instead of volume. If trading volume were equally informative at different times of the day, the volume-weighted price contribution would be unity for all periods.

The results in Table 2.4 reveal that this is by far not the case. While consistent patterns are difficult to identify, it is clearly apparent that many instruments have sizable price contribution per unit of volume outside of their main trading hours. For example, the S&P 500 has large price contribution during European hours, the EuroStoxx during European pre-market trading, and the Nikkei during Japanese pre-market hours. US and Japanese bonds have high price contribution during the US pre-market period. The Euro has large price contribution during Asian and European pre-market trading. Brent oil has high price contribution during Japanese main hours and the US pre-market period, while WTI oil has high price contribution during European main hours.

An analysis similar to that of price contribution can be performed for variance. For each day, we compute the variance contribution as the sum of the squared returns across all five-minute intervals falling in a given period (plus the squared open return if the market opened at the beginning or during the period in question) divided by the sum of all squared returns for the day. In a second step, we calculate the mean variance contribution of each period across days. As was the case for price contribution, this definition ensures that the sum of the variance contributions of the different periods sum to unity. The results are reported in Table 2.5. They once again reveal substantial return variation outside of most instruments' main trading hours. To take a few extreme examples, almost 50% of S&P 500 return variance and about 60% of Nikkei return variance occur outside of the trading hours of their respective cash markets. Although they are somewhat more variable when both European and US markets are open, metal prices exhibit sizable variability throughout the day.

Figure 2.1 reports cumulative price and variance contribution during the day for all instruments grouped by market segment. Four key observations can be made. First, sizable price discovery takes place around the clock for almost all assets. Second, the patterns of price and variance contribution are quite different across assets. Third, price discovery patterns for equities and bonds from the same region are very similar. Finally, for most assets, price and variance contribution appear to move broadly in line. Put differently, it is not the case that risk and return mainly accrue at different times during the trading day.

Taking a closer look at the price contributions for the different assets reveals some intuitive patterns and some surprising ones. As one would expect, a large part of price contribution for the Nikkei and Japanese government bonds and, to a lesser extent, for the Yen are realized during Japanese trading hours. Also consistent with intuition, price discovery happens earlier in the day for the Yen than for the Euro; for both currencies, however, price discovery is essentially complete by the close of European markets. Interestingly, price discovery also happens earlier for Brent oil than for WTI oil, in spite of the fact that the two are close substitutes. It is noteworthy that price contribution for Brent oil is virtually zero and that for WTI oil is negative but insignificant until European markets open. Here again, price discovery is essentially completed by the close of European markets. More surprisingly, price contribution for the S&P 500 is virtually zero until

European markets open. The same holds for gold and copper, although China and India are the two largest consumers of gold and the former is the largest consumer of copper. Strikingly, price contribution is sizable for silver during Asian market hours, even though the distribution of consumption across continents is quite similar to that for gold, with India, China, and Japan together accounting for over 35% of world consumption.

As mentioned above, price and variance contribution appear to move broadly in line during the day for most instruments. To substantiate this observation, Figure 2.2 reports the difference between price and variance contribution for the asset in each category for which this difference is largest, as well as 90% confidence bounds computed from the empirical distribution of the difference in the sample. It is apparent that the difference between price and variance contribution is generally not statistically different from zero. However, interestingly enough, Figure 2.2 does provide evidence of some persistent deviations between the two. For both the S&P 500 (during most of US main hours) and WTI Oil (almost until US pre-market hours) variance contribution appears to lead price contribution, while the opposite holds for the Yen (during most of European main hours) and silver (until US pre-market hours).

2.5 Efficiency of Price Discovery

In order to assess the efficiency of price discovery, we estimate so-called unbiasedness regressions for each time period i during the day,

$$r = \alpha_i + \beta_i r_{ci} + \epsilon_i \ , \tag{2.3}$$

where r is the total return for the day (from the close of after-hours trading on the previous day to the close of after-hours trading on the current day) and r_{ci} the return from the close of after-hours trading on the previous day to the end of period i on the current day. Such regressions have previously been used by Biais et al. (1999) as well as Barclay and Hendershott (2003), who show that if the true return process is serially uncorrelated, the slope coefficient from the unbiasedness regression is equal to the ratio of signal to signal plus noise in the return process. Accordingly, estimates of β_i around one indicate efficient price discovery, while estimates below one indicate noisy price discovery.

In order to measure how the rate of price discovery changes during the day, we also consider the behavior of the regression R^2 over time. If the amount of price discovery were constant throughout the day, R^2 would lie on a straight line starting at zero at the time corresponding to the close of the previous day and reaching one at the time of the close of after-hours trading.[10] Price discovery is stronger (weaker) than average whenever R^2 is steeper (flatter) than that benchmark straight line.

Two factors will cause the rate of price discovery to vary during the day: (i) variation in the rate at which new information is released, and (ii) variation in the efficiency with which

[10]For example, for an instrument closing at 23:15, the line would start at zero at a time of -0.75 and reach one at a time of 23.25.

new information is processed. In order to assess the extent to which these two effects drive the intraday R^2 patterns, we compute the difference between the regression R^2 for period i and the share of overall daily price variance that accrues up to the end of period i, i.e.,

$$\psi_i = R_i^2 - \frac{\text{var}(r_{ci})}{\text{var}(r)} \ . \tag{2.4}$$

Positive values imply that price discovery between the previous close and the end of period i exceeds price variability, indicating that price discovery up to that time is relatively efficient. Conversely, negative values indicate lower price discovery than price variability, implying inefficient price discovery. If price discovery were equally efficient throughout the day, the slope of R^2 plotted against time would vary according to the rate at which new information is released, but ψ_i would be zero throughout. Summarizing, plotting β_i against time informs us about the average ratio of signal to signal plus noise from the previous close to the end of period i, plotting R_i^2 against time reveals what share of overall daily price discovery occurs up to the end of period i, and plotting ψ_i against time indicates whether the share of accrued price discovery taking place up to the end of period i is higher or lower than could be expected based on the corresponding share of accrued daily price variability.

Figure 2.3 reports the results of this analysis for each of the 13 assets. The upper panels show the slope estimates β_i from the unbiasedness regressions, their 95% confidence bounds, and the regression R^2s, while the lower panels report the differences between R^2 and the share of accrued variance, ψ_i. Almost all slope coefficients are statistically different from zero and most are not statistically different from unity, indicating that price discovery takes place and is quite efficient around the clock. There are a few noteworthy exceptions, most of which lie during Asian market hours. For example, Japanese government bond price discovery (Panel (d)) is noisy around 2:00, as is Yen price discovery (Panel (g)) until the beginning of Japanese main market hours. Price discovery is also noisy for US Treasuries, the Euro, gold, silver, and WTI oil (Panels (f), (h), (i), (j), and (l)) during the first two to five hours of trading. Thus, while there is evidence of some inefficiency at specific times, price discovery appears fairly efficient around the clock.

Considering the R^2 patterns shown in the upper panel for each instrument reveals a number of interesting facts. First, most R^2 curves are far from linear. Second, the curves are increasing almost everywhere, confirming that price discovery occurs around the clock. There are a couple of essentially flat segments indicating a low rate of price discovery at some times. Most of these segments appear during Asian pre-market hours, the first few hours of Asian trading or after US main market hours. Third, as one would expect, the R^2 curves are generally steeper during an instrument's main market hours. For example, R^2 is steeper during Japanese market hours for the Nikkei (Panel (a)), during European hours for the EuroStoxx (Panel (b)), and during US exchange hours for the S&P 500 (Panel (c)). A similar picture emerges for the three bond markets (Panels (d)-(f)). Fourth, for European assets (EuroStoxx, Bund, and the Euro, see Panels (b), (e), and (h)), the rate of price discovery is highest when both European and US main markets are open. Fifth, the distribution of price discovery during the day differs across metals

(Panels (i)-(k)): while silver price discovery is very low during Asian hours, price discovery for copper is quite high, with gold lying somewhere in-between. Finally, there is very little price discovery for both oil contracts (Panels (l) and (m)) until the open of European markets, at which point price discovery accelerates. The rate of price discovery then increases again once US markets open, but the increase is more pronounced for WTI than for Brent. Here again, the rate of price discovery is highest when both European and US markets are open.

The lower panels of Figure 2.3 reveal large differences across assets in the efficiency of price discovery during the day. Overall, efficiency tends to be largest during an instrument's main market hours. For example, for the Nikkei, efficiency is high during Japanese hours, fair during European hours, but low during US hours. For the EuroStoxx, efficiency is highest when both European and US markets are open. By contrast, for the S&P 500, efficiency is low in early Asian hours, increases during European hours, and is highest during US main market hours. For Japanese bonds, efficiency is low during the first couple of hours of trading, then fair, and then drops sharply at the close of Japanese main markets. For the German Bund, efficiency is high during main market hours and declines around the close of European markets. For US Treasuries, efficiency is low until the release of US macroeconomic news at 14:30 and increases substantially afterwards, before dropping sharply at the close of pit trading at 21:00. Efficiency is quite erratic during the day for the Yen, but exhibits a clear pattern for the Euro: low efficiency until the early afternoon, high efficiency after the release of US macroeconomic news, decreasing efficiency towards the close of European markets, and increasing efficiency during afternoon US trading. All three metals have low efficiency for the first three to four hours of trading. Gold and silver have high efficiency mostly during US hours, but copper also exhibits a period of high efficiency during late Asian hours. For all metals, efficiency drops sharply between the close of Asian markets and the open of European ones. Finally, both oil contracts have low efficiency until about 11:00 and high efficiency afterwards, while for Brent it declines earlier in the evening than for WTI.

Summarizing, the results in this section reveal that there is substantial price discovery around the clock for most assets and that it is quite efficient most of the time. Nevertheless, efficiency tends to be larger during an instrument's main market hours. For most instruments, inefficiency is concentrated before the open of Asian markets or during the first few hours of trading on Asian markets.

2.6 Intraday Volatility Patterns

Figure 2.4 shows the average return volatility of the different instruments for each five-minute interval during the trading day, computed as the square root of the average squared return during each interval. While all instruments exhibit strong intraday volatility patterns, the precise shapes of these patterns vary substantially. Strikingly, most assets do not exhibit the U-shaped intraday volatility pattern that has been widely documented for US equities, even if only the trading hours of the underlying or pit market are considered. Generally, intraday spikes in volatility occur at four sets of times: (i) at the open or close of the market for the

respective instrument, (ii) at the open or close of the pit for the respective instrument, (iii) at the open or close of other markets (both the cash market for the contract's underlying and markets for other assets), and (iv) at the time of macroeconomic news releases. The remainder of this section describes these effects for the different instruments. The role of US macroeconomic announcements will be investigated in detail in Section 2.7; for the current discussion, it suffices to note that the main news releases occur in three waves, one at 14:30, one at 16:00, and the last one between 20:00 and 20:45 (details will be provided in Table 2.6).

Considering equities first (see Panel (a)), S&P 500 volatility is very low during Asian market hours. This is followed by a short rise in volatility at the start of European pre-market trading at 8:00 and a substantial increase at the open of European stock markets at 9:00. Afterwards, a U-shaped pattern similar to that documented in the literature during US cash market hours is clearly visible. At the release of US macroeconomic news at 14:30, volatility spikes and declines quickly thereafter. Volatility spikes again at the open of US stock markets at 15:30. During US cash market hours, the above mentioned U-shaped pattern is visible; however, two short spikes in volatility occur at the time of the second and third waves of US macroeconomic releases (16:00 and 20:00-20:45). S&P 500 volatility then falls sharply around the time of the close of the cash market. For the EuroStoxx, volatility is very high at the open of pre-market trading at 8:00, as the information accumulated during the night gets incorporated into prices. Afterwards volatility is rather low during the rest of pre-market trading and increases sharply at the open of European cash markets at 9:00. It thereafter exhibits a U-shaped pattern before spiking at the time of US macroeconomic news releases at 14:30. While that pattern is quite similar to that for the S&P 500 during the same period, EuroStoxx volatility is much higher, even at the exact time of US macroeconomic news releases. Volatility then decreases slowly before rising substantially at the open of US stock markets at 15:30. It remains elevated and much higher than S&P 500 volatility until the close of European stock markets at 17:30, and is thereafter virtually equal to S&P 500 volatility for the rest of the day. Finally, the Nikkei has elevated volatility during Japanese market hours, but no U-shape pattern is apparent during that time. Its volatility declines sharply at the close of Japanese cash markets and, after a brief increase at the beginning of European cash market trading, decreases progressively towards the level of S&P 500 volatility during European hours. Nikkei volatility then spikes twice, at the time of US macroeconomic news announcements and at the open of US stock markets. During US stock market hours, it is very similar to S&P 500 volatility, increases substantially towards the close of US stock markets, before declining somewhat towards the close of after-hours trading.

Turning to bonds (see Panel (b)), after initial spikes at the open and at the release of Japanese macroeconomic news shortly thereafter, US Treasury volatility is quite low during Asian trading hours, increases at the open of European pre-market and main market trading, afterwards rises progressively before spiking at the time of US macroeconomic news releases at 14:30. No major increase in volatility occurs at the open of US stock markets at 15:30, but there is a large spike in volatility at the time of the second wave of US macroeconomic news releases at 16:00, followed by one at 19:00 and one at the time of Federal Reserve policy announcements at 20:00. Interestingly, no U-shaped pattern is visible. For German Bunds, the early part of the day exhibits a pattern

similar to the EuroStoxx: volatility is very high at the open of pre-market trading when the information accumulated during the night gets incorporated into prices, then falls during the rest of pre-market trading and increases sharply at the open of cash markets at 9:00. It declines thereafter with short increases at 10:00, 10:30, and 11:00, when some European macroeconomic news are released. During this period Bund volatility is much larger than US Treasury volatility. At 14:30, volatility spikes as it does for US Treasuries. Bund volatility exceeds US Treasury volatility until the close of European cash markets and thereafter decreases. The three volatility spikes at 16:00, 19:00, and 20:00 that were observed for Treasuries are also clearly visible for Bunds, but are somewhat smaller. Finally, Japanese bond volatility is largest at the open of Japanese markets, fairly large during Japanese main market hours, especially in the afternoon (4:00-7:00 CET), declines during European hours and spikes at the time of the 14:30 and 16:00 US macroeconomic news releases.

As can be seen in Panel (c), volatility patterns for currencies are much less smooth than for bonds and equities. Overall, the patterns for the Euro and the Yen are quite similar; the main difference between the two is that – as one could expect – Yen volatility exceeds Euro volatility during Asian hours and Euro volatility exceeds Yen volatility during European hours. Put differently, Yen volatility is similar during Asian and European hours, while Euro volatility is much higher during European hours than during Asian hours. Both Euro and Yen volatility spike at the time of the 14:30 and 16:00 US macroeconomic news releases. After the close of European markets, Yen and Euro volatility remain pretty similar.

Turning to oil (see Panel (d)), Brent volatility exceeds WTI volatility in early trading; there is a spike in Brent volatility at 2:00, corresponding to the open of Brent futures trading on weekdays. Afterwards, the volatility of both contracts is quite similar until US markets open, hovering at low levels during Asian hours, increasing sharply when European markets open, and spiking at the time of the 14:30 macroeconomic announcements. Once US markets open, WTI volatility exceeds Brent volatility. There are numerous spikes during US trading hours: one at the open of the WTI futures pit at 15:00, one at the open of US stock markets at 15:30, one at the time of the second wave of macroeconomic releases at 16:00, one at the time of the release of US oil inventory data at 16:30, and one at the close of the WTI futures pit at 20:30. After 20:30, oil volatility declines substantially and remains rather low until the end of the day.

Panel (e) reveals that metals exhibit the most erratic intraday volatility patterns across all asset classes. Out of the three metals, gold is the least and silver the most volatile. The volatility patterns for both are quite similar: large volatility at the open, spikes at the open of Japanese cash markets, an increase in the volatility level until the open of European markets, and large spikes at the time of the 14:30 and 16:00 US macroeconomic news releases. There are also substantial volatility spikes at 19:25 for silver and 19:30 for gold, which correspond to the close of pit trading for these two metals. Volatility then declines before increasing at the time of the Federal Reserve announcements at 20:00; thereafter it decreases before spiking again at the close of US stock markets at 22:00 and drops sharply afterwards. Finally, copper volatility spikes at the open, decreases thereafter before spiking again at the open of Japanese cash markets, then declines until the open of European cash markets. It spikes at the time of

US macroeconomic announcements, remains fairly elevated until the close of European markets, falls thereafter before spiking twice – once at 19:00, the close of pit trading for copper, and once at 20:00, the time of Federal Reserve announcements. Overall, copper volatility differs somewhat less between the main trading hours of the different regions than gold and silver volatility.

2.7 Diffusion and Jump Risk During the Trading Day

The sharp spikes in intraday volatility documented in Section 2.6 are consistent with the strong empirical evidence for the presence of both diffusion and jump components in asset returns (see, e.g., Chernov et al. (2003), Eraker (2004), Broadie et al. (2007), Aït-Sahalia and Jacod (2009), Lahaye et al. (2011), and the references therein). In this section, we aim to disentangle the two for every five-minute interval of the trading day. This is a non-trivial task since when considering individual high frequency returns, there is no guarantee that standard measures of diffusion risk are actually bounded by total return variance. We propose the following procedure in order to mitigate this issue.

Our starting point is the fact that the total variance TV of any given five-minute return r_i is the sum of its diffusion component DV and jump component JV, i.e.,

$$TV_i = DV_i + JV_i \,. \tag{2.5}$$

To estimate the diffusion component, we use the jump-robust integrated variance estimator $MedRV$ proposed by Andersen et al. (2012). Formally, our estimator of the diffusion component of total variance during interval i is

$$DV_i = \frac{\pi}{6 - 4\sqrt{3} + \pi} \operatorname{med}\left(|r_{i-1}|, |r_i|, |r_{i+1}|\right)^2 , \tag{2.6}$$

where "med" denotes the median and the scaling factor ensures the unbiasedness of DV as an estimator of spot variance if returns are i.i.d. Gaussian.

Each day, for each five-minute interval i, we use Lee and Lee and Mykland (2008) jump detection test to assess the likelihood that a jump in the return process has occurred during that interval. The test statistic proposed by Lee and Mykland (2008) is given by

$$\mathcal{L}_i \equiv \frac{r_i}{\widehat{\sigma}_i} \,, \tag{2.7}$$

where $\widehat{\sigma}_i$ denotes the estimate of the underlying price process' instantaneous volatility. Intuitively, the larger the absolute value of $\mathcal{L}_i$ (i.e., the absolute size of the return r_i relative to the current volatility estimate) during interval i on a given trading day, the higher the probability that a jump occurred during that interval. To be consistent with our definition of DV, we again rely on the jump-robust $MedRV$ to estimate instantaneous volatility in Eq. (2.7), i.e., we

estimate $\widehat{\sigma}_i$ using

$$\widehat{\sigma}_i = \frac{1}{K-2} \sum_{j=i-K+1}^{i-2} \frac{\pi}{6-4\sqrt{3}+\pi} \operatorname{med}\left(|r_{j-1}|, |r_j|, |r_{j+1}|\right)^2, \tag{2.8}$$

where K denotes the window size.

Following Lee and Mykland (2008), we then compute the centered test statistic

$$\frac{|\mathcal{L}_i| - C_n}{S_n}, \tag{2.9}$$

where

$$C_n = \frac{\sqrt{2\ln n}}{c} - \frac{\ln\pi + \ln(\ln n)}{2c\sqrt{2\ln n}}, \quad S_n = \frac{1}{c\sqrt{2\ln n}}, \quad c = \sqrt{\frac{2}{\pi}}, \tag{2.10}$$

and n denotes the number of observations per day. The null hypothesis of no jump during interval i is rejected whenever the centered test statistic exceeds the critical value $q_\alpha = -\ln(-\ln(\alpha))$, where α corresponds to the test's confidence level. Consistent with Lee and Mykland's (2008) proposed implementation, we choose the window size K equal to 288 (the number of five-minute intervals per day) and set the confidence level to 99.9% ($\alpha = 0.999$).

Finally, we compute the diffusion and jump components DV_i and JV_i using the following decomposition algorithm:

1. For each five-minute return r_i, compute the corresponding centered test statistic $\frac{|\mathcal{L}_i|-C_n}{S_n}$ in order to determine whether a jump has occurred during interval i.
2. If *no* jump has occurred during interval i, then $JV_i = 0$ and $TV_i = DV_i$.
3. If a jump *has* occurred during interval i, then $JV_i = \max\{r_i^2 - DV_i, 0\}$ and $TV_i = DV_i + JV_i$.

Although this procedure imposes the non-negativity of JV, the constraint will only be binding if $\frac{|\mathcal{L}_i|-C_n}{S_n} > q_{0.999}$ *and* either (i) $|r_i|$ is the median or the smallest absolute return in Eq. (2.6) or (ii) $|r_i|$ is the largest absolute return in Eq. (2.6) but at least one of $|r_{i-1}|$ and $|r_{i+1}|$ is greater than $|r_i|$ divided by the scaling factor in Eq. (2.6). Essentially, a binding non-negativity constraint requires the presence of at least one additional jump in the immediately adjacent intervals.[11] When we relax the above non-negativity constraint, only six average jump components are below -0.0005 across all intervals and contracts (of which there are over 3,000 in total).[12] The results presented below are not affected by the non-negativity restriction on JV.

Figure 2.5 presents the average total variance TV and its diffusion and jump components DV and JV during the trading day for all 13 contracts. For three contracts (EuroStoxx, Bund, and Brent oil) we report the value for the opening interval instead of its corresponding data point in order to enhance visibility. The results in Figure 2.5 clearly demonstrate that both diffusion and jump variance components are important drivers of overall intraday variance patterns.

[11] For case (i) to occur, there must be at least one additional, larger jump in an adjacent interval. For case (ii) to occur, the size of the return in at least one of the adjacent intervals must be over $\frac{6-4\sqrt{3}+\pi}{\pi} = 70.45\%$ of the size of the return in interval i, implying a second jump or extremely high diffusion volatility in an adjacent interval.

[12] There are three for NK, one for SV and one each at the open of CO and XX.

Considering first the diffusion component, intraday variance patterns for the three equity indices are rather different (see Panels (a)-(c)). In general, most diffusive price fluctuations occur during the main trading hours of the respective underlying asset, but Nikkei volatility increases when US stock markets are open. The well-documented U-shape of S&P 500 intraday volatility during US main market hours is strikingly clear once the jump component is removed from total variance. The U-shapes for the EuroStoxx, however, are much less pronounced. Confirming the findings in Section 2.6, none of the other assets has a U-shaped intraday volatility pattern, even when only considering diffusive risk. The results in Figure 2.5 also reveal that once the effect of jumps is removed, gold and silver variances appear strikingly similar, as do those of WTI and Brent oil (see Panels (i)-(j) and (l)-(m), respectively).

Turning to the jump component, the three main release times of US macroeconomic news (14:30, 16:00, and 20:00-20:45) are strikingly visible for all three equity indices. For the Bund, US Treasury bonds, the Yen, and gold, the 14:30 macroeconomic announcements account for the bulk of jump risk. By contrast, both oil contracts, copper, and to a lesser extent silver exhibit sizable jumps at numerous times during the day. Both oil contracts have strikingly similar jump variance patterns.

Finally, we provide a quantitative assessment of the variance contribution of jumps associated with US macroeconomic announcements. In contrast to most previous studies, our aim is not to quantify the variance impact of individual announcement types, but to assess their overall relevance for intraday variance patterns. Accordingly, we group the announcements in three groups based on their scheduled release times (14:30, 16:00, and 20:00-20:45). Table 2.6 provides an overview of all announcements considered in each group, their frequency, source, and scheduled release time in CET. Since the release time of Federal Reserve announcements varies somewhat by announcement type and changed slightly during our sample period, we include all such announcements in the third group; their release times all lie between 20:00 and 20:45 CET.

For each announcement group, Table 2.7 provides the size rank and contribution to total daily return variance of the jump component for the five-minute interval immediately following the release time. Because of the slight changes in the time of Federal Reserve announcements discussed above, for the third announcement group we report the values for the largest jump between 20:00 and 20:45 as well as the time at which it occurs. The results in Table 2.7 clearly indicate that for almost all assets, the largest jump occurs right after the first announcements at 14:30 CET, the only exceptions being the Nikkei and both oil contracts. For both oil contracts, the largest jump (not reported in the table) happens at the release of US oil inventory data at 16:30 CET. The largest contributions of the 14:30 announcement jump to total daily variance are observed for US Treasuries (4.77%), the S&P 500 (1.69%), the Bund (1.54%), and gold (1.22%). The size of these contributions is remarkable since they represent averages across all trading days and the announcements listed in Table 2.6 are released monthly or weekly at most. For equities, the second most important announcements are the FOMC press conferences. By contrast, for metals and perhaps surprisingly bonds, the second group of announcements appears to be more likely to cause large jumps.

The right-most column in Table 2.7 reports the total contribution of jumps to overall daily

return variance. The contribution of jumps is important, accounting for approximately 5% to 13% of total daily return variance even though most days do not have any announcements. The contribution of jumps is largest for the Yen, US, and Japanese government bonds, as well as for gold and silver.

Summarizing, the results in this section show that the contribution of jumps to overall daily volatility is substantial, that both diffusion and jump components are significant drivers of observed intraday volatility patterns, and that a sizable fraction of jump-driven volatility occurs around US macroeconomic news announcements, which strongly affect all assets classes.

2.8 The Volume-Volatility Relationship during the Day

Previous research documents that volatility and trading volume are strongly positively correlated, and a number of theoretical results suggest that one should expect a linear relationship between the two Huberman and Stanzl (2004) and the references therein). The standard explanation for the existence of a relationship between volume and volatility is that asymmetric information gets incorporated into prices through trading. As shown in Section 2.7, however, jumps are mostly associated with the public release of information. This suggests that the relationship between volume and volatility could be very different at the time of jumps.

Figure 2.6 reports the share of overall trading volume and of price volatility for each five-minute interval during the day, as well as the difference between the two. While there is clearly strong comovement between volume and volatility, the relationship is far from perfect. Three main observations can be made. First, with the exception of Japanese government bonds, volume is generally significantly higher than volatility during US trading hours. Second, the relationship between volume and volatility that can be observed during most of the day often does not hold at the time of jumps. Specifically, while both volume and volatility spike at the time of jumps, the difference between the two sometimes does and sometimes does not. This suggests that in some – but not all – markets, traders anticipate large moves in the price at the time of scheduled announcements and market depth falls accordingly. Third, the opening and closing of stock markets or futures pits tend to be associated with spikes in trading volume that are much larger than the contemporaneous spikes in volatility. Moreover, these spikes in volume are often substantially greater than those associated with price jumps. We now discuss these effects for the different instruments.

Considering first equities, for the Nikkei (Panel (a)), volume is much smaller than volatility during Japanese main market hours, somewhat greater during European hours, and sizably larger than volatility during US hours.[13] Volume spikes more strongly than volatility at the time of the 14:30 and 16:00 US macroeconomic releases, at the close of European stock markets at 17:30, and at the close of US stock markets at 22:00. For the EuroStoxx (see Panel (b)), volume is

[13]To some extent, the fact that volume is smaller than volatility during Japanese hours could be caused by the fact that a competing contract with essentially the same specifications is traded on the Osaka stock exchange and is likely to be preferred by Japanese investors. We have chosen to use the CME contract as its trading hours are much longer.

considerably lower than volatility during European pre-market trading but exceeds volatility during the first hour after the open of European stock markets. Both volume and volatility are about the same until the open of US stock markets, at which point volume increases more strongly than volatility. Interestingly, the spikes in volume and volatility at the time of the 14:30 US macroeconomic news releases are equally large. Volume spikes at the time of the close of European stock markets at 17:30, but volatility increases only slightly. After the close of European markets, volatility is much higher than volume. No sizable change in volume is apparent at the time of the price jump associated with Federal Reserve announcements around 20:00. For the S&P 500 (see Panel (c)), volume is lower than volatility until the open of US stock markets, after which it is substantially larger. Volume spikes slightly less than volatility at the time of the jumps associated with 14:30 US macroeconomic news releases and the Federal reserve announcements at 20:00. The opposite is true for the second wave of US macroeconomic announcements at 16:00.

Turning to bonds, the relationship between volume and volatility is quite erratic at the open for Japanese government bonds (see Panel (d)). Overall, volume is much larger than volatility during Japanese main market hours and lower afterwards. There is a large increase in volume at the close of the main market at 7:00/8:00 (winter/summer), but it is not associated with a commensurate spike in volatility. For the German Bund (see Panel (e)), volume exceeds volatility during European morning hours and from the 14:30 US macroeconomic news releases until the close of European markets at 17:30. Volume spikes more sharply than volatility at the time of the 14:30 price jump. For US Treasuries (see Panel (f)), volume is notably lower than volatility outside of US trading hours. There are two spikes in volume that are larger than those in volatility, one at the open of the pit market at 14:20, and a second at the time of the 14:30 US macroeconomic news releases. The open of US stock markets at 15:30 is associated with a sharp rise in volume but very little movement in volatility. Volume spikes more strongly than volatility when the second wave of US macroeconomic releases is issued at 16:00. Both volume and volatility spike about equally strongly at the time of Federal Reserve announcements at 20:00. Finally, there is a very large spike in volume, but a much smaller increase in volatility right before the close of the pit market at 21:00.

For currencies, the relationship between volume and volatility is quite similar for the Yen and the Euro (Panels (g) and (h)): volume is lower than volatility during Asian trading hours, about the same during European hours, and much larger between the time of the 14:30 US macroeconomic releases and the close of European stock markets. After the close of the futures pit at 21:00, volume is considerably lower than volatility. Volume spikes more strongly than volatility at the time of the price jumps associated with US macroeconomic announcements, 14:30 and 16:00. The same can be observed before the close of European markets at 17:30. There are also two spikes in volume that are stronger than those in volatility at the open and close of the futures pits, 14:20 and 21:00.

Considering metals (Panels (i)-(k)), trading volume is lower than volatility outside of pit trading hours and higher than volatility during pit trading hours. Volume spikes more strongly than volatility at the open and close of the pits (14:20 and 19:30 for gold, 14:25 and 19:25 for

silver, and 14:10 and 19:00 for copper), at the time of the price jumps associated with the 14:30 and 16:00 US macroeconomic releases, and at the open of US stock markets at 15:30.

For WTI oil (see Panel (l)), volume is lower than volatility outside of pit hours (15:00-20:30) and exceeds it during pit hours. At the open and close of the pit, volume spikes much more strongly than volatility. The same holds at the open of US stock markets, at the time of the 16:00 macroeconomic announcements, and when oil inventory data is released at 16:30. For Brent oil (see Panel (m)), volume is lower than volatility during Asian hours, about the same during European hours, and higher when both European and US markets are open. The largest spikes in volume occur at the close of European stock markets and of the WTI pit. The spikes in volume at the times of the main price jumps – the 14:30 macroeconomic releases, the 16:30 oil inventory releases, and the 20:00 Federal reserve releases – are somewhat, but not much, larger than the associated spikes in volatility.

Overall, two facts about intraday volume-volatility relationships are especially striking. First, the behavior at jump times differs significantly across instruments. To illustrate, at 14:30, the spikes in volume are much larger than those in volatility for some assets – the Nikkei, the Bund, US Treasuries, both currencies and all metals – while they are of about the same magnitude for others – the EuroStoxx, the S&P 500, and oil. This suggests differences across markets in traders' anticipation of large price moves at the time of scheduled announcements. Second, a number of assets have very large spikes in volume that are not associated with commensurate spikes in volatility not just at times when the underlying cash market or futures pit opens or closes, but also when markets for other assets open or close. The most striking examples are the rise in Nikkei volume at the open of US stock markets and that in Brent volume at the close of European stock markets.

2.9 Conclusion

We investigate price discovery around the clock for 13 global benchmark assets from the main asset classes equities, currencies, bonds, and commodities. We document that sizable price discovery occurs around the clock for almost all assets. For a given asset, the distribution of risk and return during the day is fairly similar, indicating a broadly constant risk-return-relationship during the trading day.

Although the amount of price discovery varies significantly during the day and across assets, price discovery generally is quite efficient around the clock for most assets. Nevertheless, efficiency tends to be higher during an asset's main market hours, and there exist short periods where price discovery is inefficient. For most instruments, inefficiency is concentrated before the open of Asian markets or during the first few hours of trading on Asian markets.

All assets show strong intraday volatility patterns, but the precise shapes of these patterns vary substantially across assets. Strikingly, most assets do not exhibit the U-shaped intraday volatility pattern that has been widely documented for US equities, even if only the trading hours of the underlying or pit market are considered. Intraday spikes in volatility occur at four sets of times: (i) at the open or close of the market for the respective asset, (ii) at the open or

close of the futures pit for the respective asset, (iii) at the open or close of other markets (both the underlying cash market and markets for other assets), and (iv) at the time of macroeconomic news releases. Most assets react strongly to US macroeconomic news releases and have higher volatility during US trading hours, but also exhibit strong volatility outside of US trading hours.

The decomposition of intraday volatility into its diffusion and jump components reveals that both diffusion and jump volatility are important drivers of overall intraday volatility patterns. The contribution of jumps to overall volatility is substantial, accounting for approximately 5% to 13% of total daily return variance. A sizable fraction of jump-driven volatility occurs around US macroeconomic news announcements, which affect all assets in our sample.

In general, volume significantly exceeds volatility during US trading hours. The relationship between volume and volatility that can be observed during most of the day often does not hold at jump times. Both volume and volatility spike at the time of jumps, but the difference between the two sometimes does and sometimes does not. This suggests that in some – but not all – markets, traders anticipate large price moves at the time of scheduled announcements and market depth falls accordingly. The opening and closing of stock markets or futures pits tend to be associated with spikes in trading volume that are much larger than the contemporaneous spikes in volatility. Strikingly, these spikes in volume are often considerably greater than those associated with price jumps. For some assets, such spikes even occur at the open or close of markets for other assets.

Overall, our results highlight the importance of around-the-clock trading for price discovery. Explaining the observed differences in intraday volume and volatility patterns across assets that are traded around the clock is a promising avenue for future research.

Table 2.1. Trading Hours and Summary Statistics

Futures Contract	Exchange	Trading Hours (CET)		Average Trading Volume		% of empty 5-Min. Intervals
		Electronic	Pit	Per Trading Day	Per 5-Min. Interval	
Equities						
S&P 500 (ES)	CME	00:00-23:15	–	1'927'540	6'884	2.3 %
EuroStoxx 50 (XX)	Eurex	08:00-22:00	–	1'062'657	6'325	0.2 %
Nikkei (NK)	CME	00:00-23:15	–	9'772	35	29.9 %
Bonds						
10y US T-Note (TY)	CBOT	00:00-23:00	14:20-21:00	1'024'050	3'710	2.5 %
10y German Bund (BN)	Eurex	08:00-22:00	–	732'713	4'361	0.2 %
10y Japanese Bond (JB)	OSE	00:45-15:25	00:45-07:02	30'938	200	24.9%
Currencies						
EUR/USD (EC)	CME	00:00-23:15	14:20-21:00	280'630	1'017	0.9 %
JPY/USD (JY)	CME	00:00-23:15	14:20-21:00	112'325	407	0.9 %
Oil						
WTI Oil (CL)	NYMEX	00:00-23:15	15:00-20:30	207'072	742	0.6 %
Brent Oil (CO)	ICE	02:00-00:00	–	100'599	388	6.1 %
Metals						
Gold (GC)	NYMEX	00:00-23:15	14:20-19:30	101'728	365	3.9 %
Copper (HG)	NYMEX	00:00-23:15	14:10-19:00	36'097	129	2.1 %
Silver (SV)	NYMEX	00:00-23:15	14:25-19:25	39'142	140	2.1 %

This table provides the total available and pit trading hours (CET) as well as the respective exchanges for all futures contracts in our sample. The sample period is from April 10, 2010 to August 30, 2013. Trading hours for Japanese bond futures (JB) expressed in CET vary between winter and summer since Europe has daylight savings time (DST) but Japan does not. The time entries in the table refer to winter time; during the part of the year where DST is used in Europe, all times for JB expressed in CET are one hour later. For the E-Mini S&P 500 equity index futures (ES) there exists one trading halt (from 22:15 to 22:30 CET) and for JB there exist two trading halts (from 3:02/4:02 to 4:30/5:30 CET and from 7:02/8:02 to 7:30/8:30 CET in winter/summer, respectively) during our sample period. Trading for Brent oil futures (CO) starts at 02:00 on weekdays; however, on Sundays trading already opens at midnight. The fifth and sixth columns report the average daily trading volume and the average trading volume per five-minute interval (considering only five-minute intervals that fall within trading hours), respectively. The last column reports the percentage of five-minute intervals during trading hours with zero trading volume.

Table 2.2. Distribution of Volume during the Trading Day

Futures Contract	Japan		Europe		Europe & US		US	
	Pre-Market	Main Hours	Pre-Market	Main Hours	Main Hours Europe Pre-Market US	Main Hours	Main Hours	After Hours
	00:00-01:00	01:00-08:00	08:00-09:00	09:00-13:00	13:00-15:30	15:30-17:30	17:30-22:00	22:00-00:00
Equities								
S&P 500 (ES)	0.83 %	2.49 %	0.69 %	6.21 %	7.55 %	34.77 %	39.28 %	8.66 %
EuroStoxx 50 (XX)	–	–	2.46 %	34.84 %	16.71 %	28.68 %	17.03 %	0.28 %
Nikkei (NK)	0.71 %	8.30 %	2.80 %	18.43 %	12.55 %	27.20 %	26.09 %	4.40 %
Bonds								
10y US T-Note (TY)	0.80 %	3.80 %	1.77 %	11.81 %	22.02 %	27.76 %	30.89 %	1.60 %
10y German Bund (BN)	–	–	5.36 %	39.27 %	23.76 %	24.58 %	6.98 %	0.07 %
10y Japanese Bond (JB)	1.67 %	86.37 %	4.65 %	6.64 %	0.72 %	0.19 %	–	–
Currencies								
EUR/USD (EC)	0.99 %	7.04 %	3.22 %	22.76 %	20.75 %	25.65 %	19.18 %	0.89 %
JPY/USD (JY)	1.35 %	16.07 %	3.44 %	18.23 %	18.68 %	22.39 %	19.39 %	0.96 %
Oil								
WTI Oil (CL)	0.84 %	3.32 %	0.82 %	7.37 %	15.78 %	32.26 %	39.09 %	0.92 %
Brent Oil (CO)	0.42 %	1.84 %	1.01 %	22.67 %	16.58 %	25.79 %	31.64 %	0.43 %
Metals								
Gold (GC)	1.33 %	10.23 %	2.59 %	13.77 %	19.89 %	27.35 %	24.14 %	1.15 %
Copper (HG)	1.05 %	15.08 %	3.57 %	13.95 %	20.21 %	24.93 %	21.04 %	0.64 %
Silver (SV)	1.30 %	8.37 %	2.25 %	11.99 %	20.69 %	28.46 %	26.37 %	0.99 %

This table reports the share of overall volume transacted during different periods of the day. The periods were defined to capture the pre-market and main hours of the three global financial centers Japan, Europe, and the US (see Section 2.3 for details). All listed time periods are left-closed and right-open time intervals in CET.

Table 2.3. Price Contribution during the Trading Day

Futures Contract	Japan		Europe		Europe & US		US	
					Main Hours Europe			
	Pre-Market	Main Hours	Pre-Market	Main Hours	Pre-Market US	Main Hours	Main Hours	After Hours
	00:00-01:00	01:00-08:00	08:00-09:00	09:00-13:00	13:00-15:30	15:30-17:30	17:30-22:00	22:00-00:00
Equities								
S&P 500 (ES)	−2.02 %	3.70 %	2.69 %	35.87 % ^{c}	5.16 %	−11.54 %	47.52 % ^{c}	19.04 % ^{c}
EuroStoxx 50 (XX)	–	–	18.18 % ^{b}	26.14 % ^{c}	18.01 % ^{b}	9.50 %	27.15 % ^{c}	1.09 %
Nikkei (NK)	7.41 % ^{b}	45.42 % ^{c}	1.35 %	10.19 % ^{b}	4.75 %	17.19 % ^{c}	19.35 % ^{c}	−5.09 %
Bonds								
10y US T-Note (TY)	10.20 % ^{c}	6.84 % ^{a}	2.54 %	7.78 %	35.15 % ^{c}	7.00 % ^{c}	21.33 % ^{c}	−0.32 %
10y German Bund (BN)	–	–	8.05 %	41.38 % ^{c}	22.59 % ^{c}	18.17 % ^{c}	10.00 % ^{b}	−0.16 %
10y Japanese Bond (JB)	4.55 % ^{c}	76.60 % ^{c}	6.35 % ^{c}	7.18 % ^{b}	3.63 % ^{b}	1.83 % ^{a}	–	–
Currencies								
EUR/USD (EC)	6.24 %	10.08 % ^{a}	8.08 % ^{a}	22.45 % ^{b}	20.13 % ^{c}	24.67 % ^{c}	8.92 %	−0.43 %
JPY/USD (JY)	5.95 %	29.65 % ^{c}	7.01 % ^{a}	37.38 % ^{c}	14.69 % ^{b}	4.35 %	6.96 %	−5.38 %
Oil								
WTI Oil (CL)	−25.70 %	−11.41 %	8.75 %	32.21 % ^{a}	23.46 % ^{b}	47.25 % ^{b}	16.12 %	9.52 % ^{b}
Brent Oil (CO)	−1.02 %	6.85 %	−5.05 %	28.00 % ^{b}	42.95 % ^{b}	18.49 %	8.87 %	1.15 %
Metals								
Gold (GC)	2.29 %	6.73 %	5.49 % ^{a}	16.24 % ^{c}	23.75 % ^{c}	28.89 % ^{c}	17.07 % ^{b}	−0.21 %
Copper (HG)	−4.99 %	20.22 %	16.06 % ^{b}	30.61 % ^{b}	−20.10 %	39.02 % ^{c}	32.39 % ^{a}	−12.70 %
Silver (SV)	3.52 %	30.01 % ^{c}	2.43 %	9.91 %	20.77 % ^{b}	19.01 %	9.17 %	5.72 % ^{a}

This table reports the relative price contribution during different periods of the day. The periods were defined to capture the pre-market and main hours of the three global financial centers Japan, Europe, and the US (see Section 2.3 for details). All listed time periods are left-closed and right-open time intervals in CET. For each period i during the trading day, the price contribution is computed as $PC_i = \frac{r_i}{r}$, where r_i denotes the return during period i and r the total return for the day. Price contribution is calculated for each day and then averaged across days. ^{a}, ^{b}, and ^{c} denote statistical significance (difference from zero) at the 10%, 5% and 1%-level, respectively.

Table 2.4. Volume-Weighted Price Contribution during the Trading Day

Futures Contract	Japan		Europe		Europe & US		US	
	Pre-Market	Main Hours	Pre-Market	Main Hours	Main Hours Europe / Pre-Market US	Main Hours	Main Hours	After Hours
	00:00-01:00	01:00-08:00	08:00-09:00	09:00-13:00	13:00-15:30	15:30-17:30	17:30-22:00	22:00-00:00
Equities								
S&P 500 (ES)	0.11	2.99	7.45	5.27 ^{c}	0.11	−0.44	1.19 ^{b}	2.19 ^{c}
EuroStoxx 50 (XX)	–	–	5.67 ^{b}	0.75 ^{c}	0.89 ^{b}	0.26	1.67 ^{c}	5.11
Nikkei (NK)	170.90 ^{b}	25.46 ^{b}	8.30	0.45	0.18	0.65 ^{c}	0.20	−2.13
Bonds								
10y US T-Note (TY)	12.26	1.70	1.60	0.84 ^{a}	1.44 ^{c}	0.46 ^{b}	−0.23	0.60
10y German Bund (BN)	–	–	1.05	1.01 ^{c}	0.83 ^{c}	0.77 ^{c}	0.86	−3.23
10y Japanese Bond (JB)	0.36 ^{a}	0.88 ^{c}	1.15 ^{b}	0.79 ^{a}	2.96 ^{a}	3.23	–	–
Currencies								
EUR/USD (EC)	7.86 ^{a}	0.83	2.67 ^{b}	0.97 ^{c}	0.84 ^{b}	0.80 ^{c}	1.26 ^{b}	1.48
JPY/USD (JY)	0.33	1.84 ^{c}	1.76 ^{a}	1.89 ^{c}	0.37	−0.10	1.60	−6.86
Oil								
WTI Oil (CL)	−22.38	−3.24	2.02	3.77 ^{a}	1.32 ^{a}	1.22 ^{a}	0.58 ^{a}	11.00 ^{a}
Brent Oil (CO)	−2.91	6.83 ^{a}	−10.26	1.11 ^{b}	2.36 ^{b}	0.31	0.29	11.57
Metals								
Gold (GC)	3.42	0.22	0.73	1.04 ^{b}	0.94 ^{b}	0.93 ^{c}	0.85 ^{b}	1.30
Copper (HG)	−0.21	1.44	4.17 ^{a}	1.88 ^{b}	−0.62	1.42 ^{b}	1.15	−17.35
Silver (SV)	4.41	3.08 ^{b}	−0.42	1.00	0.67 ^{a}	0.49	0.49	6.13 ^{a}

This table reports volume-weighted relative price contribution during different periods of the day. The periods were defined to capture the pre-market and main hours of the three global financial centers Japan, Europe, and the US (see Section 2.3 for details). All listed time periods are left-closed and right-open time intervals in CET. For each period i during the trading day, the volume-weighted price contribution is computed as $VWPC_i = \frac{r_i/r}{V_i/V}$, where r_i denotes the return during period i, r the total return for the day, V_i trading volume during period i and V total daily volume. Volume-weighted price contribution is calculated for each day and then averaged across days. ^{a}, ^{b}, and ^{c} denote statistical significance (difference from zero) at the 10%, 5% and 1%-level, respectively.

Table 2.5. Variance Contribution during the Trading Day

Futures Contract	Japan		Europe		Europe & US		US	
	Pre-Market	Main Hours	Pre-Market	Main Hours	Main Hours Europe Pre-Market US	Main Hours	Main Hours	After Hours
	00:00-01:00	01:00-08:00	08:00-09:00	09:00-13:00	13:00-15:30	15:30-17:30	17:30-22:00	22:00-00:00
Equities								
S&P 500 (ES)	2.64 %	11.59 %	2.38 %	14.55 %	11.91 %	23.82 %	28.96 %	4.66 %
EuroStoxx 50 (XX)	–	–	14.03 %	32.50 %	15.81 %	20.68 %	16.49 %	0.55 %
Nikkei (NK)	5.76 %	38.29 %	4.48 %	13.32 %	7.43 %	11.26 %	16.02 %	3.98 %
Bonds								
10y US T-Note (TY)	3.54 %	12.01 %	3.48 %	16.10 %	21.91 %	17.01 %	24.69 %	1.78 %
10y German Bund (BN)	–	–	15.21 %	32.84 %	20.48 %	18.67 %	12.56 %	0.30 %
10y Japanese Bond (JB)	3.40 %	71.45 %	4.78 %	12.34 %	5.98 %	2.18 %	–	–
Currencies								
EUR/USD (EC)	4.11 %	15.01 %	5.01 %	23.93 %	17.62 %	17.12 %	16.36 %	1.37 %
JPY/USD (JY)	5.75 %	24.18 %	4.07 %	17.75 %	16.47 %	14.90 %	15.20 %	2.26 %
Oil								
WTI Oil (CL)	3.12 %	9.39 %	2.05 %	13.98 %	18.06 %	23.45 %	28.85 %	1.54 %
Brent Oil (CO)	1.88 %	11.18 %	2.39 %	18.46 %	15.78 %	20.98 %	27.80 %	1.85 %
Metals								
Gold (GC)	3.98 %	14.42 %	2.71 %	14.23 %	20.32 %	21.90 %	21.29 %	1.63 %
Copper (HG)	4.87 %	25.22 %	3.75 %	16.38 %	16.20 %	16.99 %	15.35 %	1.77 %
Silver (SV)	4.43 %	16.20 %	3.03 %	14.00 %	19.23 %	20.30 %	21.60 %	1.70 %

This table reports the relative variance contribution during different periods of the day. The periods were defined to capture the pre-market and main hours of the three global financial centers Japan, Europe, and the US (see Section 2.3 for details). All listed time periods are left-closed and right-open time intervals in CET. For each period during the trading day, the variance contribution is computed as the sum of the squared returns across all five-minute intervals falling in a given period (plus the squared open return if the market opened at the beginning or during the period in question) divided by the sum of all squared returns for the day. The variance contribution is calculated for each day and then averaged across days.

Table 2.6. Scheduled US News Announcements

Announcements	Frequency	Source	Time (CET)
1st Announcements			
Consumer Price Index	Monthly	Bureau of Labor Statistics	14:30
Durable Goods Orders	Monthly	US Census Bureau	14:30
Gross Domestic Product	Monthly	Bureau of Economic Analysis	14:30
Initial Jobless Claims	Weekly	Department of Labor	14:30
Non-Farm Payroll Employment	Monthly	Bureau of Labor Statistics	14:30
Producer Price Index	Monthly	Bureau of Labor Statistics	14:30
Retails Sales Less Automotive	Monthly	US Census Bureau	14:30
2nd Announcements			
Consumer Confidence Index	Monthly	Conference Board	16:00
ISM Manufacturing Index	Monthly	Inst. for Supply Management	16:00
ISM Non-Manuf. Index	Monthly	Inst. for Supply Management	16:00
Leading Indicators	Monthly	Conference Board	16:00
New Home Sales	Monthly	US Census Bureau	16:00
3rd Announcement			
Federal Reserve Beige Book	Eight times per year	Federal Reserve Bank	20:00
FOMC Rate Decision		Federal Reserve Bank	20:00/20:15
FOMC Meeting Minutes		Federal Reserve Bank	20:00
FOMC Meeting Press Conference		Federal Reserve Bank	20:30-45

This table reports the most important scheduled US news announcements (divided into three chronologically ordered groups). The time of FOMC Rate Decision announcements changed during our sample period (20:15 CET until March 2013 and 20:00 CET afterwards). The beginning of the chairman/chairwoman's press conference is scheduled at approximately 20:30 CET.

Table 2.7. Jumps at Times of Scheduled US News Announcements

Futures Contract	1st Announcements		2nd Announcements		3rd Announcement			Var. Contr. Jumps (total)
	Rank	Var. Contr.	Rank	Var. Contr.	Rank	Var. Contr.	Time (CET)	
Equities								
S&P 500 (ES)	1	1.69 %	3	0.76 %	2	0.89 %	20.40-45	6.89 %
EuroStoxx 50 (XX)	1	0.78 %	3	0.39 %	2	0.50 %	20.40-45	6.20 %
Nikkei (NK)	3	0.29 %	21	0.05 %	4	0.26 %	20.40-45	4.31 %
Bonds								
10y US T-Note (TY)	1	4.77 %	3	0.68 %	4	0.49 %	20.00-05	11.00 %
10y German Bund (BN)	1	1.54 %	3	0.18 %	6	0.10 %	20.00-05	5.43 %
10y Japanese Bond (JB)	–	0.23 %	–	–	–	–	–	11.00 %
Currencies								
EUR/USD (EC)	1	0.69 %	5	0.19 %	4	0.20 %	20.15-20	7.29 %
JPY/USD (JY)	1	2.89 %	2	0.48 %	4	0.31 %	20.15-20	12.59 %
Oil								
WTI Oil (CL)	2	0.48 %	4	0.23 %	6	0.23 %	20.25-30	5.87 %
Brent Oil (CO)	3	0.21 %	5	0.11 %	4	0.19 %	20.25-30	5.00 %
Metals								
Gold (GC)	1	1.22 %	4	0.36 %	7	0.24 %	20.00-05	10.34 %
Copper (HG)	1	0.38 %	6	0.14 %	20	0.05 %	20.00-05	4.98%
Silver (SV)	1	0.61 %	9	0.20 %	31	0.08 %	20.00-05	9.57 %

This table provides both the rank (in terms of size) and the average variance contribution (relative to average total daily return variance) of jumps occurring at the times corresponding to scheduled US news announcements listed in Table 2.6. Jumps associated with the opening of the market are ignored when determining the ranking. Since the times of announcements in the third group in Table 2.6 (FOMC Rate Decision, FOMC Meeting Minutes, Federal Reserve Beige Book and FOMC press conferences) changed during our sample period, the table only reports the variance of the largest jump over all possible five-minute intervals between 20:00-20:45 CET together with the time at which it occurs. The last column provides the total contribution of all jumps (including market opening jumps) to daily variance. For Japanese bond futures (JB) the 1st announcements occur simultaneously with the reopening of the market (after an intraday trading halt) and the corresponding jump is therefore not ranked. Moreover, the market for JB is closed at the time of the 2nd and 3rd announcements.

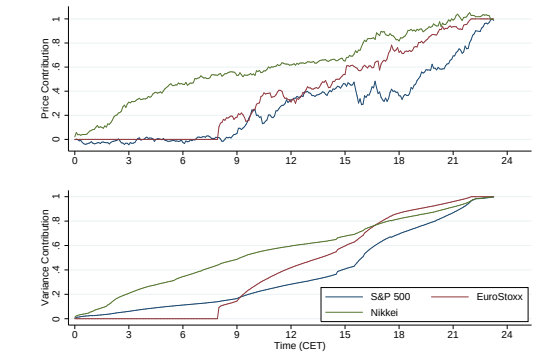

(a) Equities

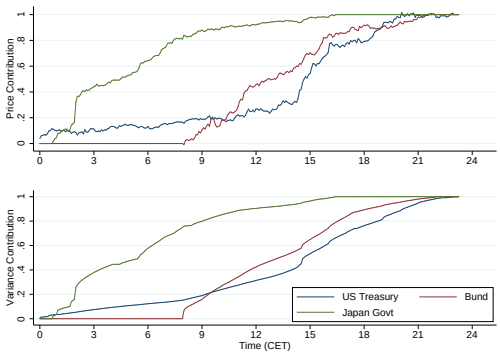

(b) Bonds

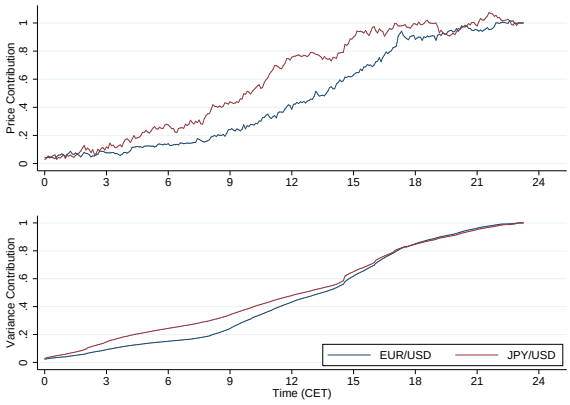

(c) Currencies

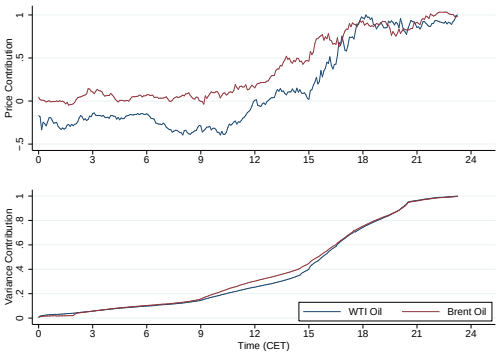

(d) Oil

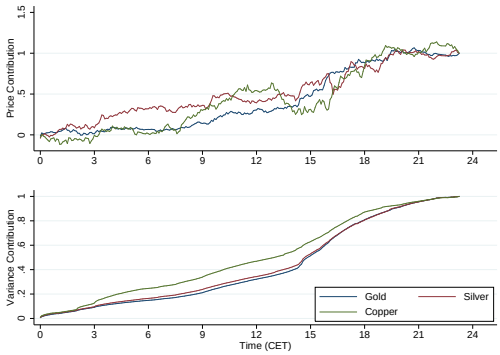

(e) Metals

FIGURE 2.1. CUMULATIVE PRICE AND VARIANCE CONTRIBUTION.

This figure shows the cumulative price and variance contributions for each asset during the trading day. For each five-minute interval i during the trading day, the price contribution is computed as $PC_i = \frac{r_i}{r}$, where r_i denotes the return during interval i and r the total return for the day. The variance contribution is computed as the squared return for each interval i divided by the sum of all squared returns for the day. Price and variance contribution are calculated for each day and then averaged across days.

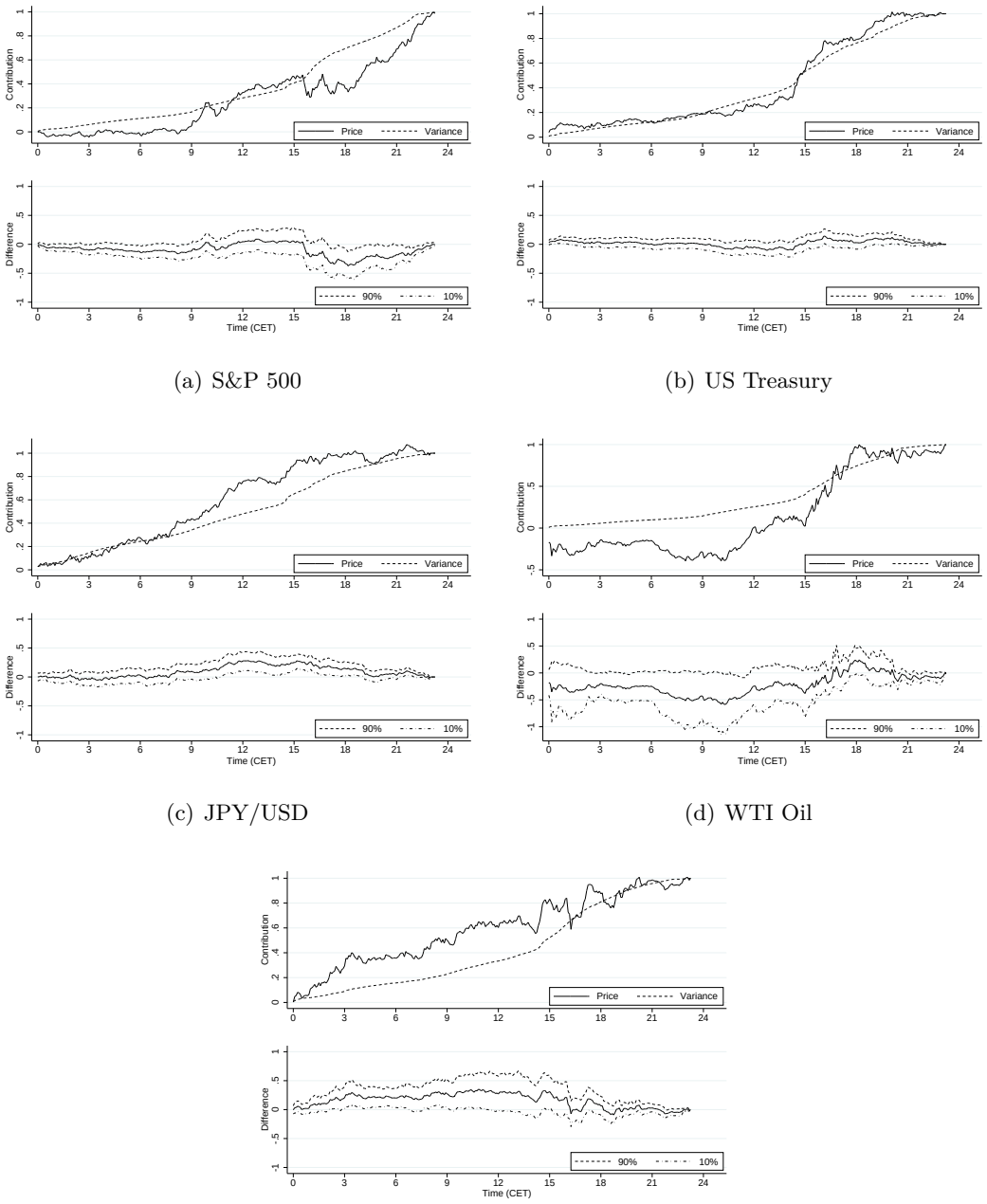

(a) S&P 500

(b) US Treasury

(c) JPY/USD

(d) WTI Oil

(e) Silver

FIGURE 2.2. DIFFERENCE BETWEEN PRICE AND VARIANCE CONTRIBUTION FOR SELECTED ASSETS.

This figure shows the cumulative price and variance contributions during the day, the difference between the two, as well as 90% confidence bounds for this difference. In each category, we select the asset for which the difference is largest. Price and variance contribution are computed for each day as described in Figure 2.1 and then averaged across days. The confidence intervals for the difference are obtained using its empirical distribution in the sample.

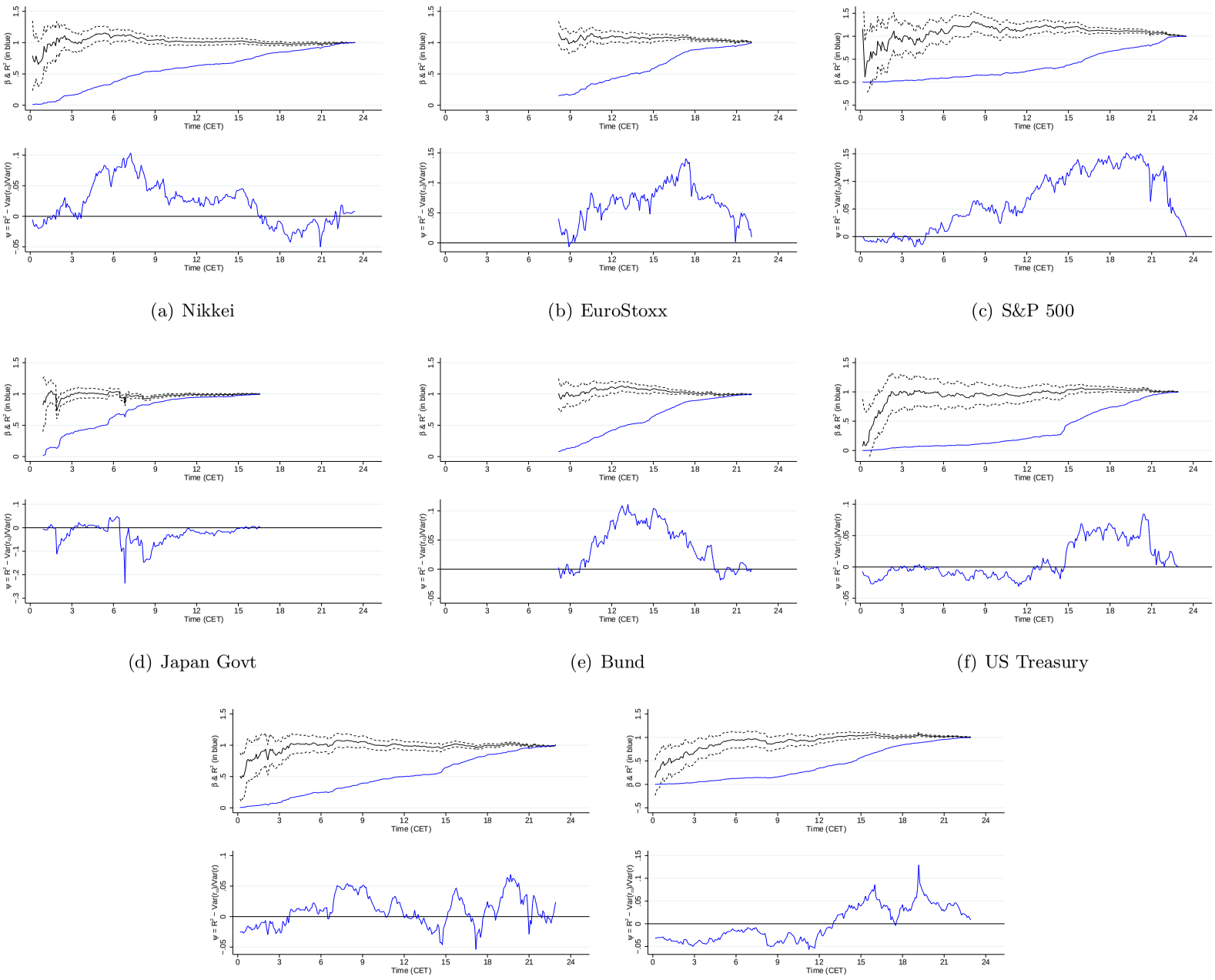

(a) Nikkei (b) EuroStoxx (c) S&P 500

(d) Japan Govt (e) Bund (f) US Treasury

(g) JPY/USD (h) EUR/USD

FIGURE 2.3

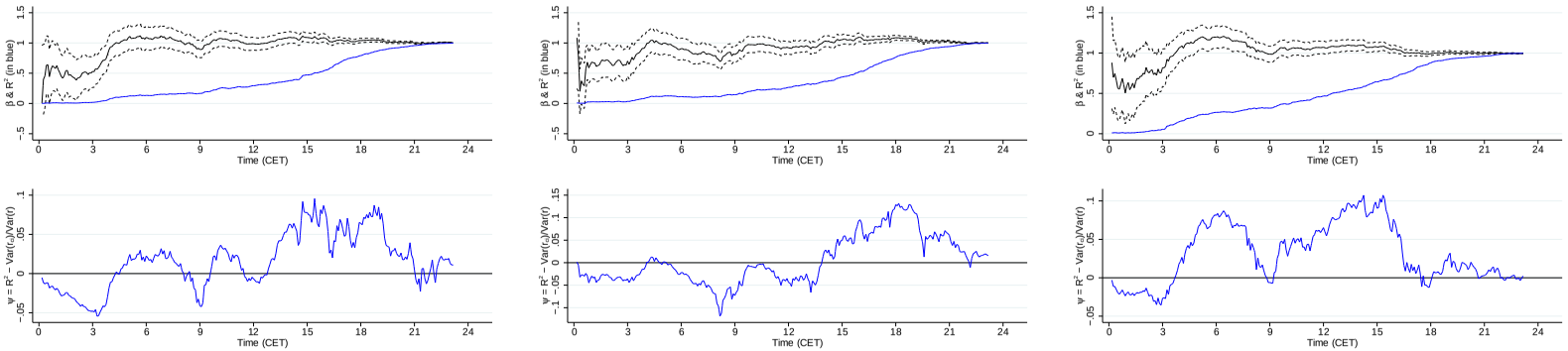

(i) Gold (j) Silver (k) Copper

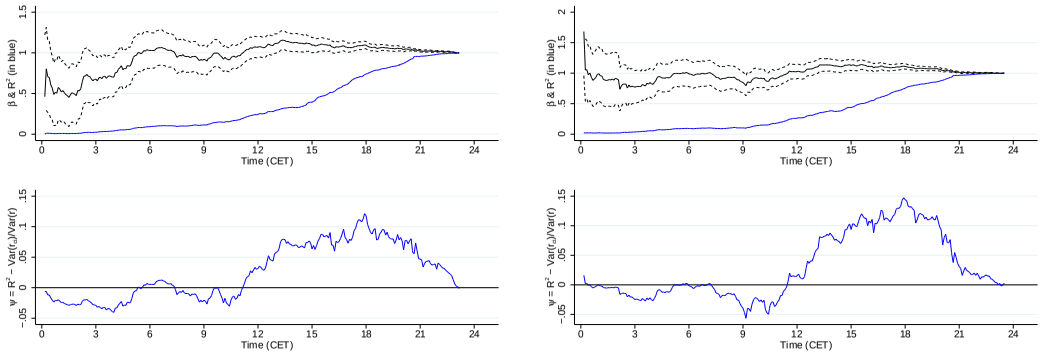

(l) WTI Oil (m) Brent Oil

FIGURE 2.3. UNBIASEDNESS REGRESSIONS.

For each asset, the upper panels in this figure report the coefficient estimates β_i, their confidence intervals and the R^2 from unbiasedness regressions estimated for each time period i during the day,

$$r = \alpha_i + \beta_i r_{ci} + \epsilon_i \ ,$$

where r is the total return for the day (from the close of after-hours trading on the previous day to the close of after-hours trading on the current day) and r_{ci} the return from the close of after-hours trading on the previous day to the end of period i on the current day. For each asset, the lower panels report the difference between the regression R^2 for period i and the share of overall daily return variance that accrues up to the end of period i,

$$\psi_i = R_i^2 - \frac{\text{var}(r_{ci})}{\text{var}(r)} \ .$$

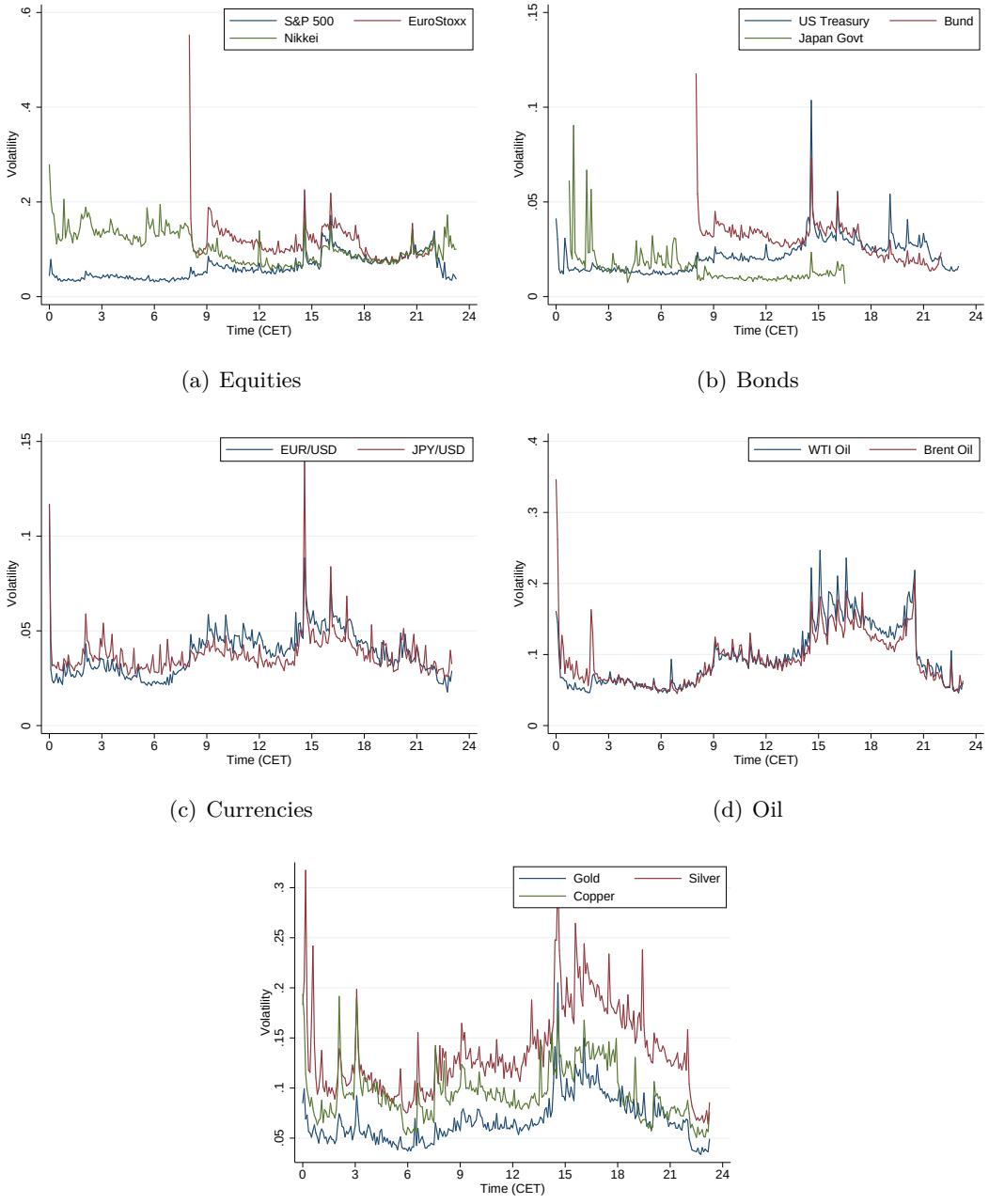

(a) Equities

(b) Bonds

(c) Currencies

(d) Oil

(e) Metals

FIGURE 2.4. VOLATILITY DURING THE TRADING DAY.

This figure shows the average return volatility of the different instruments for each five-minute interval during the trading day. Volatility is computed as the square root of the average squared return during each interval.

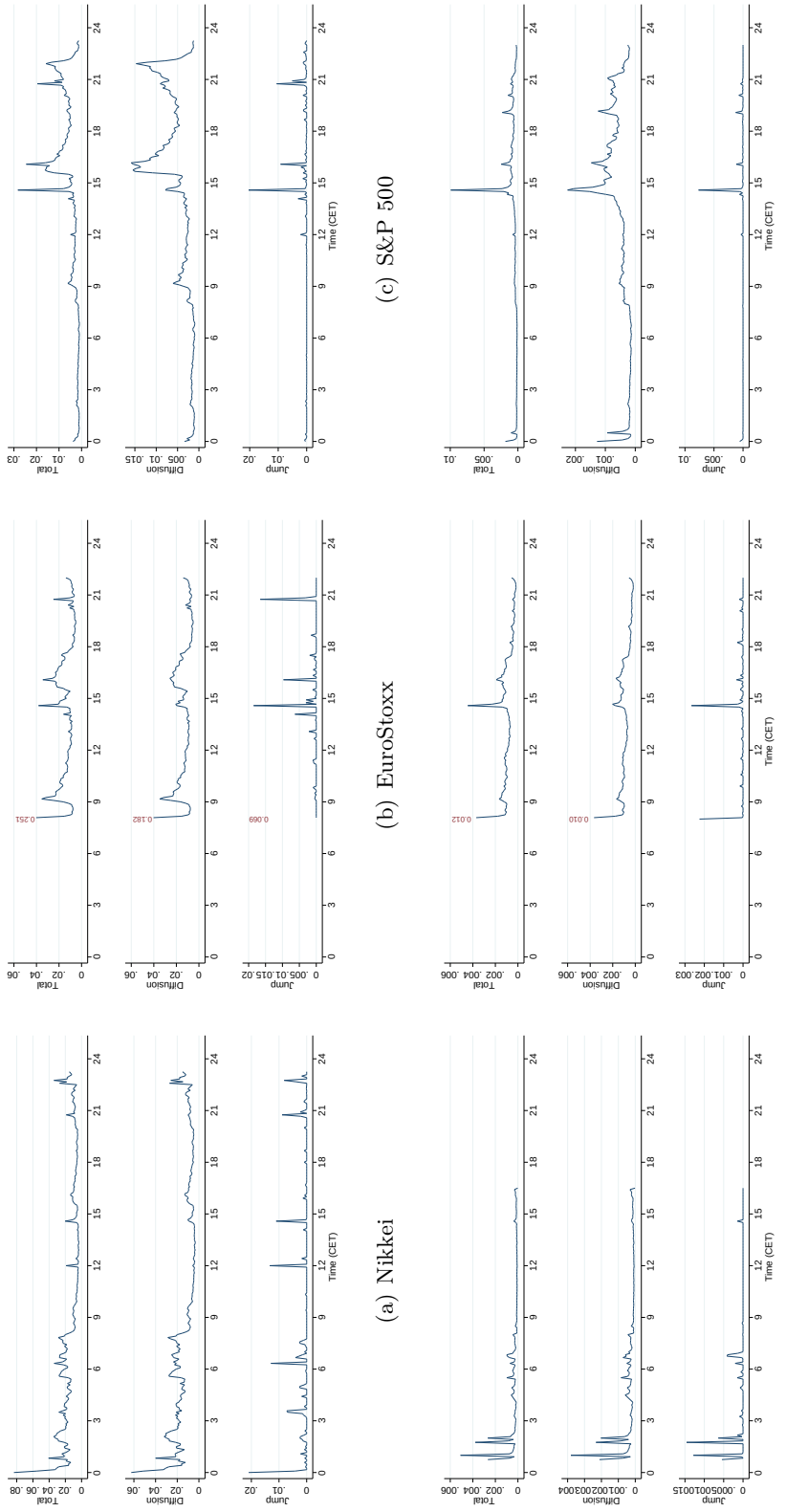

(a) Nikkei (b) EuroStoxx (c) S&P 500

(d) Japan Govt (e) Bund (f) US Treasury

(g) JPY/USD (h) EUR/USD

FIGURE 2.5

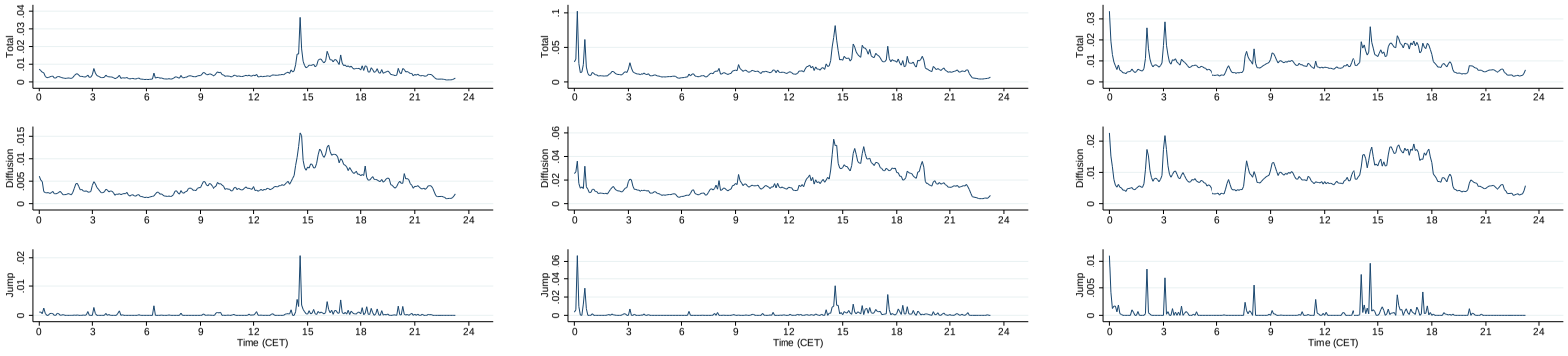

(i) Gold (j) Silver (k) Copper

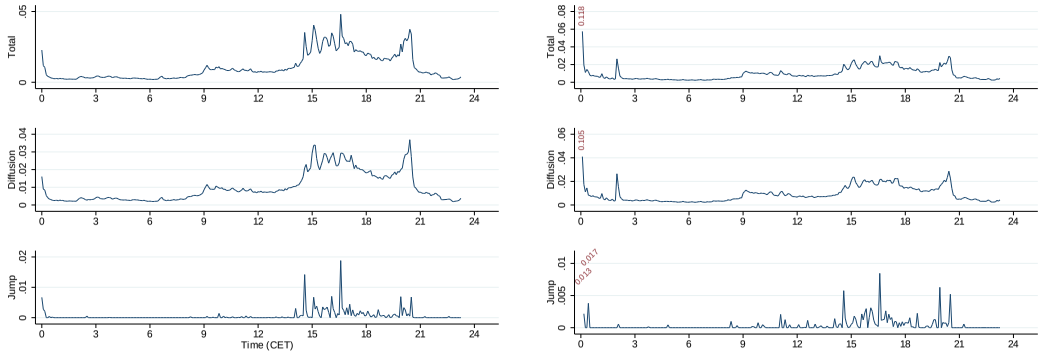

(l) WTI Oil (m) Brent Oil

FIGURE 2.5. DIFFUSION AND JUMP RISK DURING THE TRADING DAY.

For each asset, the upper panel reports the average total return variance for each five-minute interval during the trading day. The middle panel shows average diffusion variance, the bottom panel average jump variance. Each trading day, for each five-minute interval i, diffusion variance DV_i is estimated using the jump-robust integrated variance estimator $MedRV$ proposed by Andersen et al. (2012):

$$DV_i = \frac{\pi}{6 - 4\sqrt{3} + \pi} \text{ med } \left(|r_{i-1}|, |r_i|, |r_{i+1}| \right)^2 ,$$

where r_i denotes the return in interval i and "med" the median. The Lee and Mykland (2008) centered test statistic $\frac{|\mathcal{L}_i| - C_n}{S_n}$ with a confidence level of 99.9% and a window size $K = 288$ is then used in order to determine whether a jump has occurred during each interval i. If no jump has occurred during interval i, then jump variance is set to zero and total variance equals diffusion variance. If a jump has occurred during interval i, then jump variance is computed as $JV_i = \max\{r_i^2 - DV_i, 0\}$ and total variance is $TV_i = DV_i + JV_i$. The figure reports the average of TV_i, DV_i and JV_i across days.

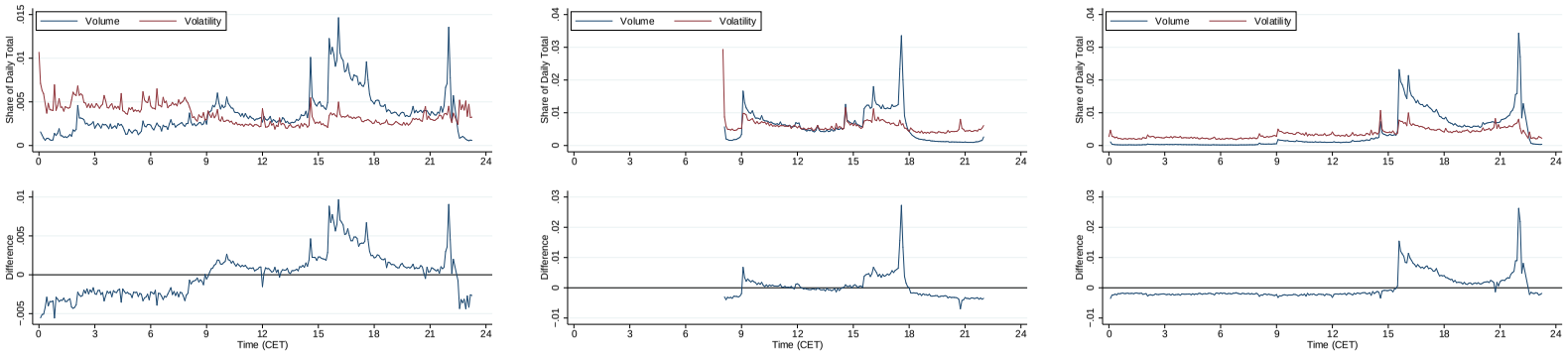

(a) Nikkei (b) EuroStoxx (c) S&P 500

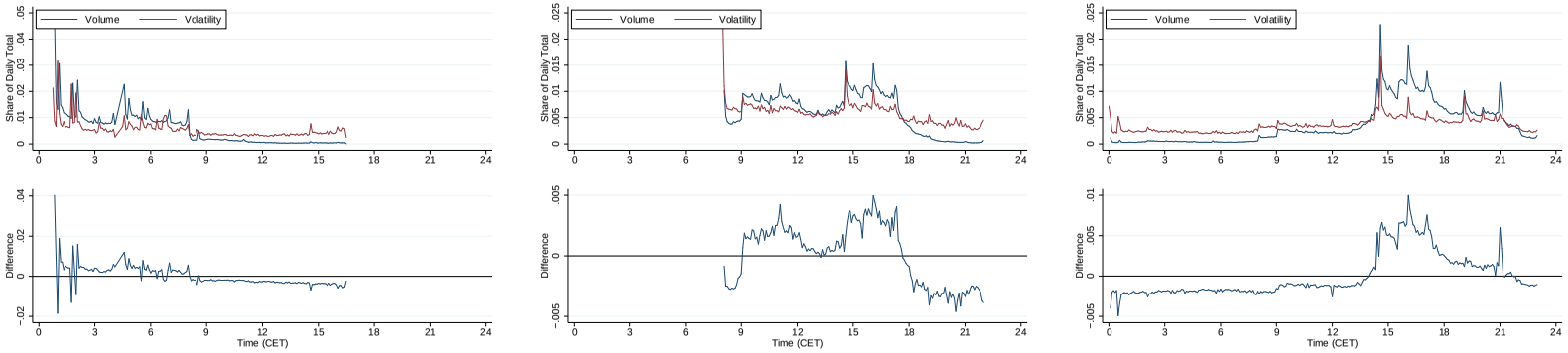

(d) Japan Govt (e) Bund (f) US Treasury

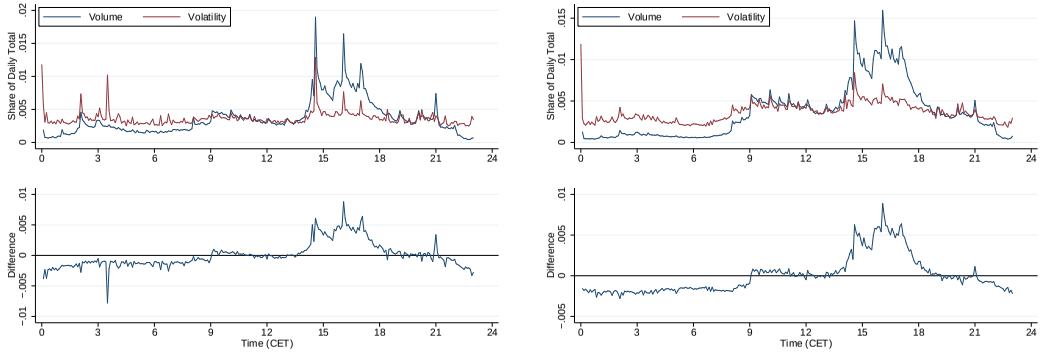

(g) JPY/USD (h) EUR/USD

FIGURE 2.6

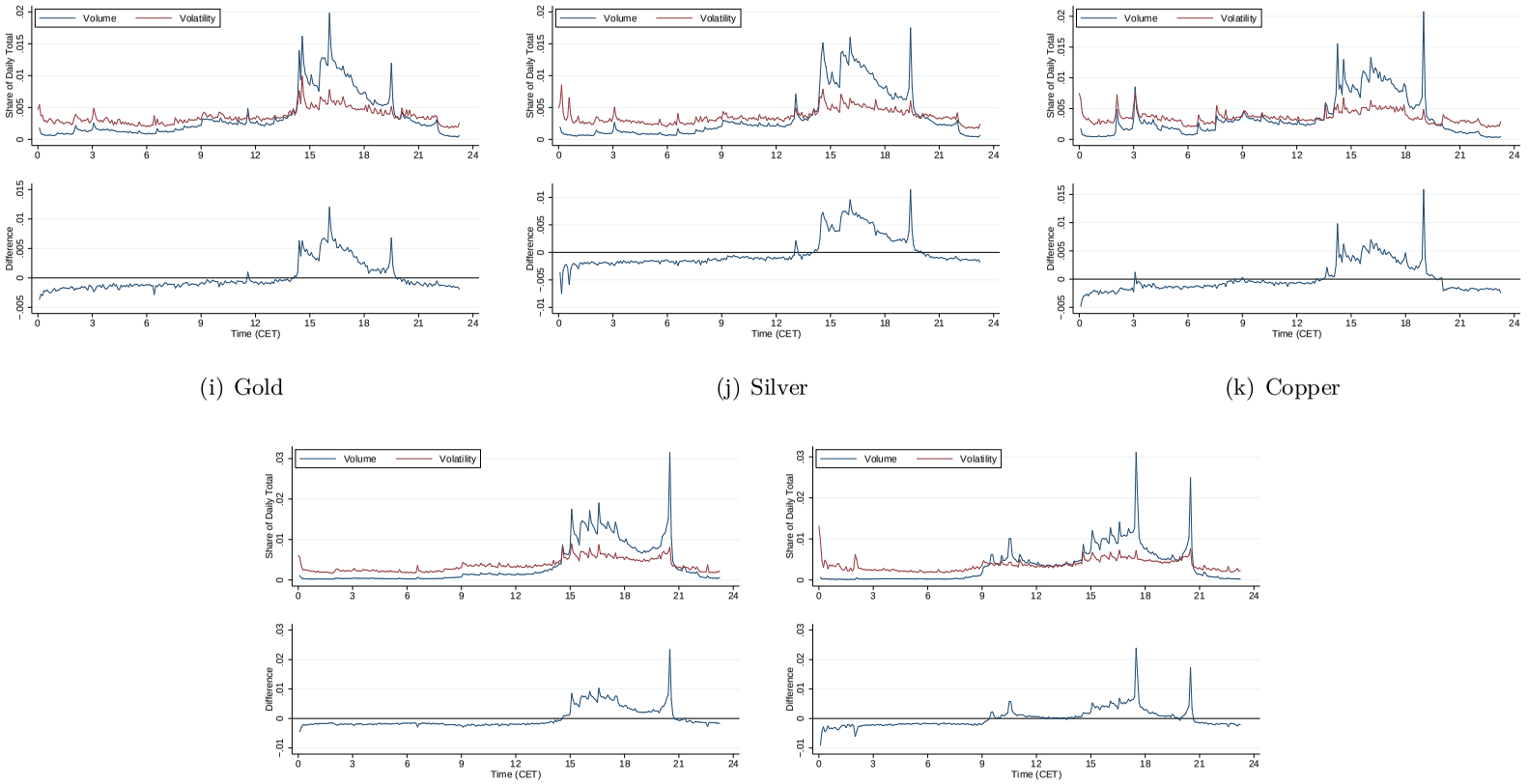

(i) Gold (j) Silver (k) Copper

(l) WTI Oil (m) Brent Oil

FIGURE 2.6. VOLUME AND VOLATILITY DURING THE TRADING DAY, AND THE DIFFERENCE BETWEEN THE TWO.

For each asset, the upper panel reports the share of total daily trading volume and return volatility arising during each five-minute interval during the trading day. The bottom panel reports the difference between the volume share and the volatility share.

3 Multimarket Informed Trading and Risk Aversion

This paper investigates the triangular trade-off between leverage, market depth, and risk in informed traders' choice of their preferred trading venue upon a private signal with a potentially big price impact (jump). Within a sequential trading model involving a stock and an options market, I study the utility maximizing trading strategy of heterogeneously risk-averse and imperfectly informed traders. I find a semi-separating equilibrium that separates more risk-averse traders into the stock and less risk-averse traders into the options market to be a robust outcome of the model. Relative to the risk-neutral benchmark, the proportion of conditional informed stock trading is always higher under a semi-separating equilibrium. Furthermore, the model predicts that conditional informed stock trading is increasing in market makers' assessment of the cross-market adverse selection risk, but with decreasing sensitivity as the latter increases. An analysis of trading data prior to US M&A announcements provides empirical evidence for the equilibrium characteristics postulated by the model.

3.1 Introduction

Where do informed traders trade? The answer to this question is crucial in understanding how decentralized asymmetric information about joint underlying risks manifests itself in asset prices that are traded on different venues. Economically, a keen knowledge of this process is of fundamental importance as information revealing prices are indispensable for achieving efficient resource allocations within any market economy.

Given the past decades' dramatically growing derivative markets, one important setting in which multimarket informed trading has been studied extensively is that of a stock and coexisting options market. Option contracts, as first pointed out by Black (1975), offer a considerable leverage advantage compared to the underlying stock and therefore represent a natural habitat for informed traders. However, the existing literature is inconclusive regarding the informational content of option trades with respect to future stock price movements (see below).

In this paper, I reflect upon two elements that are usually not jointly accounted for in the literature and combine them within a framework of sequential multimarket trading à la Glosten and Milgrom (1985). First, I model underlying stock dynamics to be driven by (i) 'regular' and relatively small value changes, represented by a binomial lattice, and (ii) an uncertain jump component which follows an asymmetric exponential distribution. Such stock dynamics constitute a reasonable trade-off between real-world return statistics and analytical tractability,

I am indebted to my advisor Marc Chesney for his support and guidance. I thank Jerôme Detemple, René Stulz, Yuan Zhang, Alexandre Ziegler, and participants at the University of Zurich PhD seminar and the SFI Research Days 2014 for helpful comments.

as they allow for benchmark option prices in semi-closed form. Second, I assume informed traders to be only imperfectly informed about the sign of a future jump when choosing to trade in either the stock or the options market. Importantly, I allow for heterogeneity among their distaste towards the risk from trading upon their private but imperfect signal.[1]

I find that, in general, an informed trading equilibrium is semi-separating in the sense that more risk-averse traders prefer to trade in the stock market, whereas less risk-averse traders choose to trade options. Furthermore, such a semi-separating equilibrium exhibits two distinct features. First, the higher market makers' perceived risk of asymmetric information θ, the bigger the proportion of informed stock relative to informed options trading and vice versa. This result could explain why in some empirical studies informed option trading is less likely discernible than its initial comparative leverage advantage would suggest.

Second, *conditional* informed *stock* trading is strongly concave in market makers' perceived risk of informed trading. Specifically, for low values of θ, the proportion of informed traders who choose the stock over the options market increases rapidly in the latter, but becomes less and less sensitive as θ increases further. The intuition behind both features requires some elaboration and is provided in the subsequent paragraphs. By jointly analyzing pre-M&A announcement abnormal trading volume of target firms' stocks and call options, I provide empirical evidence for both patterns of multimarket informed trading.

Most existing models of multimarket informed trading that involve both stocks and equity options (see literature review below) point to the two securities' implicit leverage and relative market liquidity as main forces behind informed traders' choice of their preferred trading venue. I argue that accounting for option contracts' higher inherent risk in combination with informed traders' risk aversion provides an intuitive explanation for the above described characteristics of a semi-separating equilibrium.

Equity options' comparative leverage advantage is a direct consequence of their asymmetric payoff profile. Given informed traders' imperfect information regarding the final stock value, they face the risk of big adverse price movements such that previously purchased options end up being out-of-the-money (OTM) ex post, i.e., expiring worthless at maturity.[2] Moreover, this risk is particularly pronounced for options that are already OTM when acquired, which in turn, however, provide the highest possible leverage ex ante. Thus, the more risk-averse a given informed trader is, the more likely she is willing to trade-off options' leverage advantage in return for the stock's linear and therefore less risky payoff structure. Irrespectively of the security's type, a deeper market with more liquidity trading always makes it easier for the informed traders to trade without being detected by market makers, thereby avoiding higher spreads. Figure 3.1 summarizes the three cornerstones of my model.

Now, based on the above argument, it is possible to provide the intuition of *how* informed

[1] More specifically, I consider a continuum of informed traders, all having a CRRA utility function, but with varying risk aversion parameter γ.

[2] For simplicity, I only consider European options. However, a similar argument is also valid for American options' nonlinear payoff structure.

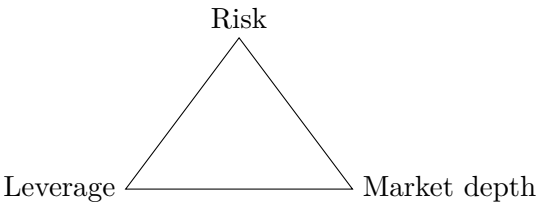

FIGURE 3.1. TRIANGLE OF MULTIMARKET INFORMED TRADING

traders' varying risk aversion explains (i) why a semi-separating equilibrium occurs even when market makers' perceived risk of informed trading θ is low, and (ii) why the conditional proportion of informed stock trading is an increasing and concave function in θ. If θ is low and the corresponding spreads in market makers' price quotes are small, the very risk-averse traders still prefer to forgo the options' big leverage advantage and trade in the less risky stock market instead. This explains (i) for low values of θ.

Regarding (ii), as θ increases, market makers revise their respective price quotes to account for the increased risk of engaging with superior informed traders. By doing so, they reduce option's initial leverage advantage relative to the stock, which again causes more and more risk-averse traders to switch from trading options to trading the stock. However, as this is anticipated by rational market makers, stock quotes are adjusted more strongly than options quotes. Eventually, i.e., as θ becomes high enough, the initially lower stock spread starts to catch up, which then makes it relatively more attractive for the less risk-averse traders to continue trading in the options market. Thus, this explains both (ii) as well as (i) for high values of θ.

In summary, the narrative that motivates my model's sequential trading setup is the following. At the beginning of any given trading day, an unobserved fraction of traders may receive a private signal about the stock's future value. Based on the above introduced stock dynamics, this piece of private information is assumed to have a specific but realistic structure. In particular, I assume that informed traders learn about the certain occurrence of an upcoming jump in the stock value, however, they only know its sign and distribution but have no further information about its exact size and timing. Moreover, their private signal neither rules out the possibility of additional jumps, nor does it affect 'regular' stock value movements.

In order to rule out no-trading equilibria due to fully revealing prices (see Grossman (1981) and Milgrom and Stokey (1982)), I adopt the literature's common assumption of exogenously given liquidity traders. As in Glosten and Milgrom (1985), the presence of such liquidity traders provides competitive market makers with the possibility to protect themselves against the risk of adverse selection by charging bid-ask spreads in return for market clearing. I assume trading is carried out sequentially, i.e., traders willing to buy or sell at current market quotes are randomly selected and provided with the opportunity to trade. Hence, market makers generally do not know ex-ante, whether an arriving trader is informed or is solely trading for exogenous liquidity reasons. Throughout the sequential trading process, market makers continuously update their ex-ante beliefs about the potential presence of informed traders and adjust their bid and ask quotes accordingly. In the rational expectation equilibrium, informed traders maximize expected

utility and market makers set price quotes to break even in expectation. The so achieved separation of potentially informed traders between the stock and the options market thus needs to be as conjectured by market makers when setting their quotes.

I test the model's equilibrium prediction by looking at both stock and options trading data of US target firms prior to their respective M&A announcements. There are two reasons why this data is particularly well suited for an empirical test of my model. On the one hand, post-M&A announcement returns of US target firms are generally huge (on average around 20% per day when conditioning on nonnegative returns (see below)) and nicely fit an exponential jump distribution. On the other hand, there exists strong empirical evidence (see below) for both informed stock *and* informed options trading involving a target firm's stock prior to the announcement. Consistent with the theory, I find that the higher the overall proportion of abnormal trading volume, the greater the relative amount of abnormal *stock* trading. Furthermore, as predicted by the theory, the sensitivity of this positive relation becomes weaker as the overall level of abnormal trading increases.

My paper relates to the rich and steadily growing literature on lead-lag relationships between the options and the underlying stock market. As mentioned above however, its findings are somewhat inconclusive. Depending on the analyzed explanatory variable(s) and the considered time horizon, certain contributions do whereas others do not find any empirical evidence for nonredundant information in option trading data. For instance, in a recent paper An et al. (2014) show that past call implied volatilities predict underlying stock returns over a window of up to six months. In contrast, based on tick-by-tick quote data, Muravyev et al. (2013) reject the notion that equity option quotes comprise any economically significant information regarding future stock price changes. Both papers provide a comprehensive review of the respective empirical literature. Chesney et al. (2015) propose an econometric approach to identify abnormal option trades that are unlikely to have been initiated by liquidity traders.

Moreover, this paper is closely related to previous theoretical investigations of informed trading strategies in the joint presence of stock and options markets. Biais and Hillion (1994) analyze informed and liquidity trading in a complete market setting including a risk free bond, a stock, and a European option. Assuming a perfectly informed and risk-neutral insider, they determine equilibrium informed (and liquidity) trading patterns for all three asset classes. Furthermore, they show that options can have both a positive (by avoiding market breakdowns) as well as a negative (by enlarging the set of trading activities) effect on markets' informational efficiency. Easley et al. (1998) derive a profit condition such that informed traders' expected gains from trading options exceed those from trading the stock. The authors consider this condition necessary for the existence of a pooling equilibrium, in which both *homogeneous* informed traders and liquidity traders are pooled together in the options market.[3] Similarly to Biais and Hillion (1994), Easley et al. (1998) assume informed traders to be perfectly informed about next period's stock value.

In line with my model's stock value dynamics, Johnson and So (2013) assume that informed

[3]Note that due to the heterogeneity of informed traders' degree of risk aversion, a semi-separating equilibrium in my model refers to the separation of a continuum of *informed* traders into two markets.

traders receive a signal about an 'information arrival shock' but none regarding the stock's regular 'diffusive shock' component. Like Easley et al. (1998), they do not specify informed traders' utility function. According to their model, homogeneous informed traders almost surely prefer one market over the other. In the model by An et al. (2014), informed traders, uninformed traders, and one market dealer are all risk-averse with CARA utility and an identical risk aversion coefficient. Based on a simplified option value that is linear in the stock price, they show how changes in the option price are endogenously correlated with next period's stock return and realized volatility. However, neither do An et al. (2014) introduce a sequential trading process that allows market makers' beliefs about the prevailing risk of asymmetric information to change, nor do they discuss the role of risk aversion in informed agents' trading decisions.

The remainder of the paper is organized as follows. Section 3.2 introduces the model and reviews its assumptions. Section 3.3 derives the condition for a semi-separating equilibrium of multimarket informed trading. Section 3.4 presents numerically obtained equilibria and discusses their comparative statics. Based on trading data prior to M&A announcements, Section 3.5 provides an empirical test of the model's main predictions. Section 3.6 concludes.

3.2 Model

Following Easley et al. (1998), I introduce a sequential trading model à la Glosten and Milgrom (1985) to a setting with two markets and three risky assets: (i) an equity market that trades shares in a risky stock and (ii) an options market simultaneously trading a European call and put option on one share of the stock. In the presence of *imperfectly* informed and exogenous liquidity traders, each market is made by a competitive market maker observing the complete order flow in both the equity and the derivatives market. In contrast to Kyle's (1985) gradual trading model, Glosten and Milgrom (1985) assume informed traders to behave competitively, i.e., to fully exploit their informational advantage as soon as being offered the opportunity to trade. In equilibrium, both market makers apply rational expectations in order to quote bid and ask prices such as to break even in expectation.

3.2.1 Stock Value Dynamics

In this simple trading economy, risky assets are exchanged against a risk-free security earning a constant rate r (continuously compounded) per unit of time. The stock's value process is composed of two independent components: (i) a binomial lattice, representing regular, i.e., relatively small value changes, and (ii) a jump component that incorporates sudden and potentially big value shifts implied by the rare arrival of extreme information shocks.

Formally, under the physical probability measure $\mathbb{P}$, the commonly observable stock value between t and $t + \Delta t$ evolves as follows

$$S_{t+\Delta t} = S_t \times X \times V^{N_{t+\Delta t} - N_t}, \tag{3.1}$$

where X is a discrete random variable taking values u with probability p and d with probability $1-p$, $0 < d < 1 < u$, N_t is a Poisson counting process with intensity λ and $Y := \log V$ has an asymmetric double exponential distribution with density

$$f_Y = \tilde{p} \times \eta_1 e^{-\eta_1 y} 1_{\{y \geq 0\}} + (1-\tilde{p}) \times \eta_2 e^{\eta_2 y} 1_{\{y<0\}}, \tag{3.2}$$

where $\eta_1 > 1$, $\eta_2 > 0$, and $0 < \tilde{p} < 1$.[4] The parameter $\tilde{p}$ in Eq. (3.2) can be interpreted as the probability of a positive jump, i.e., $1-\tilde{p}$ corresponds to the probability of a negative jump. Based on Eq. (3.1), one can write the stock value at T, where $T := t + n\Delta t$ and $n \in \mathbb{N}$, as

$$S_T = S_t \times \underbrace{\prod_{t=1}^{n} X_i}_{\substack{\text{lattice} \\ \text{component}}} \times \underbrace{\prod_{j=1}^{N_T - N_t} V_j}_{\substack{\text{jump} \\ \text{component}}}, \tag{3.3}$$

where I assume both sequences $\{X_i\}$ and $\{V_j\}$ to be i.i.d.[5] Additionally, all three sources of randomness, the Xs, Vs, and N_t are assumed to be mutually independent. Note that, in the presence of asymmetric information about future jumps, i.e., about future realizations of N_T, the actual trading price will likely deviate from the value process in Eq. (3.1).

Given its obvious discontinuous structure, the specification of the stock value dynamics in Eq. (3.3) requires some further elaboration on its jump component. Recalling that V is a globally differentiable transformation of Y, one easily computes $E^{\mathbb{P}}[V|Y \geq 0] = \frac{\eta_1}{\eta_1 - 1}$ and $E^{\mathbb{P}}[V|Y < 0] = \frac{\eta_2}{\eta_2 + 1}$, respectively.[6] Note that, if $Y \geq 0$, than $V \in [1, \infty)$ and, if $Y < 0$, than $V \in (0, 1)$. Hence, $\tilde{p}$ and $1-\tilde{p}$ in Eq. (3.2) can be interpreted as the probabilities of a positive and negative jump with expected values equal to $\frac{\eta_1}{\eta_1 - 1} > 1$ and $\frac{\eta_2}{\eta_2 + 1} < 1$, respectively. Therefore, the values u and d of the Xs in Eq. (3.3)'s lattice component are chosen subject to

$$u \ll E^{\mathbb{P}}[V|Y \geq 0] = \frac{\eta_1}{\eta_1 - 1}, \qquad \text{and} \qquad d \gg E^{\mathbb{P}}[V|Y < 0] = \frac{\eta_2}{\eta_2 + 1}, \tag{3.4}$$

i.e., such that the absolute value shift caused by an average positive or negative jump is substantially greater than the respective value changes due to regular up and down movements.

In particular, if one sets $u = e^{\sigma\sqrt{\Delta t}}$ and $d = \frac{1}{u}$ as proposed by Cox et al. (1979) (for any $\sigma > 0$ satisfying the inequalities in Eq. (3.4)) and $p = \frac{1}{2}(1 + \frac{\mu}{\sigma}\sqrt{\Delta t})$, the lattice part of Eq. (3.3) converges, as $n \to \infty$ for a fixed T (i.e., as $\Delta t \to 0$), to a geometric Brownian motion with

---

[4] See, e.g., Kou (2002) for a detailed discussion on the asymmetric double exponential jump distribution.

[5] For the stock dynamics in Eq. (3.1), I implicitly assume $\mathbb{P}(N_{t+\Delta t} - N_t > 1) = 0$ a.s.

[6] Since V is a globally differentiable, strictly monotone transformation of Y, it holds that

$$E^{\mathbb{P}}[V|Y \geq 0] = \int_{e^0}^{e^\infty} v \cdot \eta_1 \exp(-\eta_1 \log(v)) \frac{1}{v} \, \mathrm{d}v = \frac{\eta_1}{\eta_1 - 1},$$

and analogously

$$E^{\mathbb{P}}[V|Y < 0] = \int_{e^{-\infty}}^{e^0} v \cdot \eta_2 \exp(\eta_2 \log(v)) \frac{1}{v} \, \mathrm{d}v = \frac{\eta_2}{\eta_2 + 1}.$$

TABLE 3.1. PARAMETERS FOR PATH SIMULATIONS

S_t	100	λ	1
u	1.01	η_1	8
d	$1/u$	η_2	8
p	0.51	$\tilde{p}$	0.5
T	1	Δt	1/250

Notes: This table provides the parameter values of Eq. (3.3) as used for the path simulations displayed in Figure 3.2.

drift μ and volatility σ. In contrast to these specifications of u and d, the distribution of the Vs does not depend on n. Hence, in the limit as $n \to \infty$, the only part responsible for potential discontinuities in the stock value is its jump component.

As illustration, Figure 3.2 shows four stock value realizations generated by simulating Eq. (3.3) with parameter choices as in Table 3.1. The base scenario of the numerical analysis in Section 3.4 relies on the same parameter values. Given the specifications in Table 3.1, the holding period return equals 8.1% in expectation with a standard deviation of 26.8%.[7] On average, the stock value jumps once every 250 time steps ($\lambda = 1$), with positive and negative jumps occurring with equal probability ($\tilde{p} = 0.5$). The expected jump size is substantial, i.e., 14.3% for positive and -11.1% for negative jumps, respectively.

Additionally, there exist a call option c and a put option p, each controlling one share of the stock described in Eq. (3.3). Both contracts are of the European type, i.e., they can be exercised at maturity T only. Their respective payoffs Π^c and Π^p at T are given by

$$\Pi_T^c = \max(S_T - K^c, 0), \quad \text{and} \quad \Pi_T^p = \max(K^p - S_T, 0),$$

where K^c and K^p denote the strike price of the call and the put, respectively.

3.2.2 Informed and Liquidity Traders

Trading occurs sequentially between stock value realizations and is initiated by two types of agents: informed and uninformed traders arriving one by one. Whereas the former only trade upon their private information, the latter are assumed to solely trade for liquidity purposes that are exogenous to the model. As noted by Easley et al. (1998), liquidity trading is a natural feature of derivatives markets, which frequently witness purely hedging motivated trades.

Exogenous liquidity trading is realistically assumed to be evenly distributed across all possible trades within each asset class. More specifically, for both the stock and the call (put) option, buyer and seller initiated transactions occur with equal probability. Additionally, retaining the

[7] The second moment of S_T can easily be calculated given

$$Var(V) = \tilde{p}\eta_1 \left(\frac{1}{\eta_1 - 2} - \frac{2E^{\mathbb{P}}[V]}{\eta_1 - 1} + \frac{E^{\mathbb{P}}[V]^2}{\eta_1} \right) + (1 - \tilde{p})\eta_2 \left(\frac{1}{\eta_2 + 2} - \frac{2E^{\mathbb{P}}[V]}{\eta_2 + 1} + \frac{E^{\mathbb{P}}[V]^2}{\eta_2} \right)$$

for all $\eta_1 > 2$, where $E^{\mathbb{P}}[V] = \tilde{p}\frac{\eta_1}{\eta_1 - 1} + (1 - \tilde{p})\frac{\eta_2}{\eta_2 + 1}$.

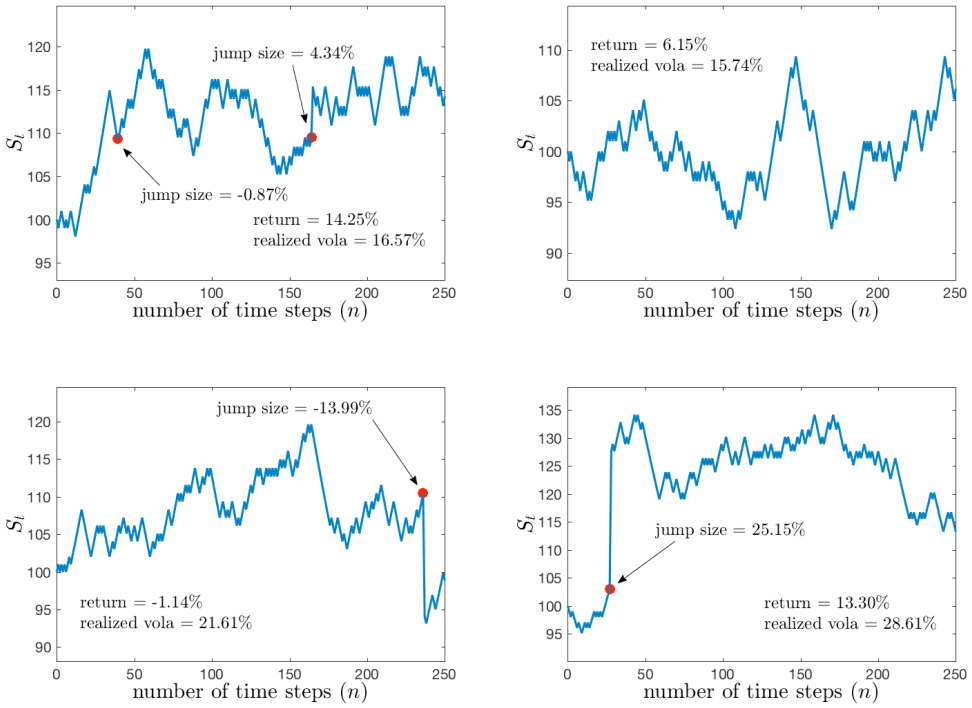

FIGURE 3.2. SIMULATIONS OF THE STOCK VALUE PROCESS

Notes: This figure shows four simulations of the stock value process as defined in Eq. (3.3) with parameter value choices as in Table 3.1. For every sample path, the respective return and realized volatility are computed.

symmetry between both option contracts, liquidity traders are assumed to engage in as many call as put trades. By α I denote liquidity traders' proportion of stock to total (stock and option) orders. Thus, on average, $\frac{\alpha}{2}$ of all liquidity orders are placed to buy (sell) shares in the stock, while $\frac{1-\alpha}{4}$ are liquidity-based buy (sell) call (put) orders.

Informed traders are wealth constrained, i.e., they are endowed with initial capital W_{t_0}. Moreover, they are homogeneous with respect to (i) their investment opportunity set, and (ii) the functional form of their utility $U(\cdot)$ in terminal wealth W_T. Importantly, by imposing power utility, i.e., $U(W_T) = W_T^\gamma/\gamma$, informed traders are assumed to be risk-averse. However, they are heterogeneous with regard to their respective degree of risk aversion. In particular, I assume a continuum of competitive informed traders uniformly distributed over $\gamma \in (0, 1)$.[8]

This specification has two main advantages. First, it is well documented in the experimental literature that the majority of individuals' estimated coefficient of relative risk aversion $1 - \gamma$ lies between 0 and 1 (see, e.g., Holt and Laury (2002), Goeree et al. (2002), Goeree et al. (2003), Goeree and Holt (2004), Biais et al. (2017), and Fattinger (2017)). Second, the average risk aversion parameter measured in the lab lies close to $\gamma = 1/2$, i.e., reasonably approximates the 'median informed trader' in my model.

At any stock value realization prior to the options' expiration T, an unknown proportion of

[8] As pointed out by Easley and O'Hara (1987), the factor that affects equilibrium asset prices is not the number of informed traders per se, but rather the ratio of informed to uninformed trades.

informed traders may receive a private signal regarding the occurrence *and* the sign of a future stock value jump to take place with certainty until T. Denoting such an information event by $t^\star \in \{t_0, t_0 + \Delta t, ..., T - \Delta t\}$, the informed traders thus know that there will be at least one positive (negative) jump with distribution $f_Y = \eta_1 e^{-\eta_1 y} 1_{\{y \geq 0\}}$ ($f_Y = \eta_2 e^{\eta_2 y} 1_{\{y<0\}}$) between $t^\star + \Delta t$ and T.[9]

I assume informed traders' signal to be independent of the stock value process in Eq. (3.3). Hence, at $t^\star$, the actual value process—only known to informed traders—then reads (for $t = t^\star$)

$$S_T = \begin{cases} \overline{S}_T := S_{t^\star} \times \prod_{i=1}^{n} X_i \times \prod_{j=1}^{N_T - N_{t^\star}} V_j \times \overline{V}, & \text{if signal is positive,} \\ \underline{S}_T := S_{t^\star} \times \prod_{i=1}^{n} X_i \times \prod_{j=1}^{N_T - N_{t^\star}} V_j \times \underline{V}, & \text{if signal is negative,} \end{cases} \tag{3.5}$$

where $\overline{Y} := \log \overline{V}$ and $\underline{Y} := \log \underline{V}$ follow an exponential distribution with densities $f_{\overline{Y}} = \eta_1 e^{-\eta_1 \overline{y}} 1_{\{\overline{y} \geq 0\}}$ and $f_{\underline{Y}} = \eta_2 e^{\eta_2 \underline{y}} 1_{\{\underline{y}<0\}}$, respectively. In other words, at $t^\star$, informed traders know with certainty that there either will be one positive or one negative jump until T, independently of the realizations of the Xs, Vs, and N_t.

In line with Glosten and Milgrom (1985), I assume informed traders to enter expected utility maximizing trades, as soon as given the chance to profit from their informational advantage. Thus, whenever they are randomly offered the opportunity to trade, they do trade as much as possible. Put differently, informed traders are not behaving strategically when timing their market transactions. Note that this is not only consistent with their competitive nature, but also with the fact that their private signal carries no information regarding the exact jump time, which itself is an element of $\{t^\star + \Delta t, t^\star + 2\Delta t, ..., T\}$. Hence, by trading as soon as possible, they are minimizing the risk of missing out on their private information.

Following Easley et al. (1998), I assume that informed traders only trade in *either* the stock *or* the options market.[10] Comparing these two alternatives, Black (1975) was the first to point to options' inherent leverage advantage that is particularly attractive to informed traders. Pan and Poteshman (2006) find deep out-of-the-money (OTM) option transactions to exhibit strong predictability regarding future underlying stock returns, whereas less leveraged contracts contain very little, if any, predictive power.

Ensuring options' inherent leverage advantage, I assume both the call and the put option to be OTM, i.e., $K^c > S_{t^\star}$ and $K^p < S_{t^\star}$, respectively. Finally, motivated by the options' moneyness, I assume that informed traders either trade (buy or short sell) the stock or *buy* options instead. If recipients of a negative signal decide to short sell the stock, they are required to deposit their short sale proceeds together with their initial wealth as collateral with the stock

[9] For simplicity, I assume that potential private signals simultaneously occur with stock value realizations, i.e., informed traders know that the stock value may jump at $t^\star + \Delta t$ the earliest.

[10] An alternative assumption yielding similar equilibrium implications would be to consider a large number of identically risk-averse (same γ) informed traders who can simultaneously trade in both markets. Depending on their risk aversion, they then either invest a higher proportion of their wealth in the less risky stock or the more levered options.

market maker.[11] Due to their relatively low price, selling an OTM put (call) upon a positive (negative) signal would be comparably unattractive. In reality, OTM options are generally more frequently traded than their in-the-money (ITM) counterparts, thereby giving the former a comparative liquidity advantage over the latter. Moreover, investors intending to write options are usually subject to substantial margin requirements, which leaves the selling of options even less compelling. In line with my model's private nature of the received signal, Cremers et al. (2015) find that option *purchases* but not sales predict stock returns ahead of *unscheduled* news events.

3.2.3 Market Makers

There are two market makers, one that sets buy (ask) and sell (bid) prices for the stock and one that sets buy and sell prices for both option contracts. I follow the literature's common assumption that market making is a perfectly competitive business. Thus, each market maker sets bid and ask prices to break even in expectation.

As in Easley et al. (1998), I assume that both market makers observe all incoming orders in either market. Hence, their bid and ask prices always equal the respective conditional expected asset values implied by the complete order history. More specifically, at any time t_i' during trading period i, i.e., $\forall t_i' \in [t_i, t_i + \Delta t)$, both market makers compute conditional expectations based on the same set of beliefs: (i) the likelihood of a previous information event $\theta_{t_i'}$ and (ii) the conditional probability that a potentially informed trader decides to trade in the stock (options) market $\theta_{S,t_i'}$ $(1 - \theta_{S,t_i'})$.

For simplification, I assume both market makers to be risk-neutral. This considerably simplifies the computation of their asset evaluations in both cases, i.e., with or without conditioning on asymmetric information. Importantly, since informed traders are risk-averse, risk-neutral pricing induces trading incentives driven by differing risk preferences. Specifically, due to their asymmetric payoff profile, options become relatively more expensive for risk-averse traders than the stock when priced by risk-neutral market makers. Hence, this might bias multimarket trading equilibria towards informed stock trading.

In order to control for such an effect, I repeat the numerical analysis presented in Section 3.4 for risk-adjusted asset prices. However, due to the model's incomplete market, the therefore applied risk-neutral pricing measure derived in Appendix A3 is not unique. Hence, to avoid further assumptions regarding informed traders' preferences towards the model's different risk sources, I henceforth focus on risk-neutral market makers. Most importantly, the qualitative results are the same for both approaches and the respective small differences are pointed out throughout the various parts of Section 3.4.[12]

Following Easley and O'Hara (1987) and Easley et al. (1998), I assume sequential trading, i.e., after every stock value realization, *sequentially* and randomly selected traders have the

[11] In order to retain the symmetry between informed stock purchases and informed stock sales, I assume that neither the stock market maker nor the informed traders earn any interests on such deposits.

[12] Detailed results are available on request.

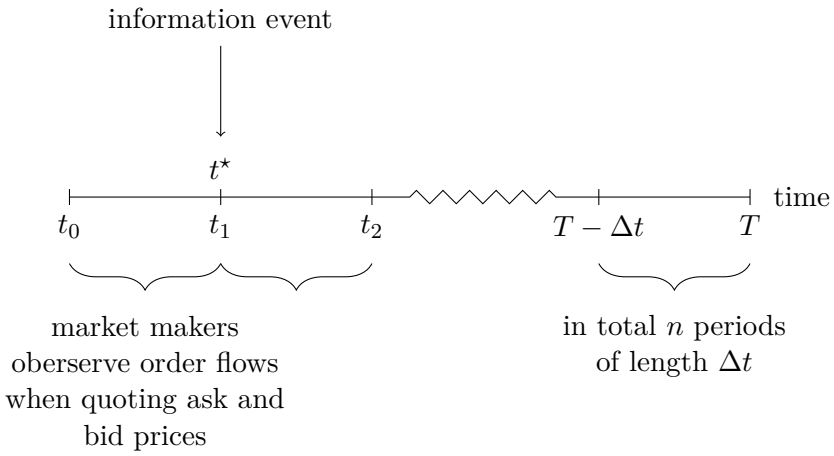

FIGURE 3.3. ILLUSTRATION OF SEQUENTIAL TRADING BETWEEN STOCK VALUE REALIZATIONS.

opportunity to trade in either the stock or the options market. Subsequently to any given value realization, each market maker continuously updates her beliefs regarding the probability of being matched with an informed trader. This sequential trading process thus allows for additional stock price fluctuations between two value realizations. For the purpose of this study, I focus on trading periods starting after value realizations for which prior accumulating trading patterns have led market makers to correctly rule out the occurrence of any preceding information events. Hence, while providing bid and ask prices, market makers are aware that maximum one price signal has occurred so far.[13] Figure 3.3 illustrates the sequence of value realizations at $t_0, t_1, ..., T$ and the market makers' sequential trading with anonymous traders in between.

3.3 Equilibrium Informed Trading

In equilibrium, all agents take optimal actions given their rational expectations. I impose the following two equilibrium conditions (*ECs*):

1. By simultaneously observing stock price realizations and the complete history of order flows, the market makers set price quotes to earn zero expected profits. (*EC1*)

2. Based on market makers' updated price quotes, the informed traders' expected utility maximizing trades are as conjectured by the former. (*EC2*)

Clearly, any potential equilibrium has to satisfy both conditions simultaneously.

3.3.1 Market Prices in the Presence of Asymmetric Information

In order to compute expected break-even market prices (as imposed by *EC1*), two cases have to be distinguished. On the one hand, there is the benchmark case in which both market makers

[13] In case of several information events, the same logic regarding market makers' continuous updating process applies. However, the corresponding spread calculations (see below) become more involved since they not only have to account for multiple stock value jumps, but, given the random jump size, also continually evaluate whether these jumps have already been part of the gradually observable stock value realizations.

assign a zero probability to the risk of trading with an informed trader. On the other hand, there is the complementary case in which either one considers it possible that certain stock or option orders have been placed by informed traders. Hence, assuming the latter, each market maker believes the probability θ to be nonzero and therefore adds (subtracts) a probability-weighted information premium (haircut) to the benchmark asset value. I henceforth refer to such deviations from benchmark values as 'information spreads'.[14]

3.3.1.1 Benchmark Asset Values

I start by deriving risk-neutral asset values for the benchmark case, i.e., in the absence of asymmetric information. If market makers can rule out the presence of informed traders with certainty, information spreads for all risky assets equal zero. The stock value at t, $t \in \{t_0, t_1, ..., T\}$, is then simply given by the observable value process S_t. For the analysis of informed trading in the remainder of the paper, the focus lies on short-lived private signals, e.g., referring to one trading week or one month. Hence, for the computations of the options' benchmark values, I assume, without severely restricting the original model setup, that the probability of more than one unanticipated jump between t and T is close to zero, i.e., $\mathbb{P}(N_T - N_t > 1) \approx 0$. Thus, the possibility of several unanticipated jumps can be neglected.[15] However, the initial modelling intention of confronting potentially informed traders with the risk of unknown positive or negative jumps until T is preserved.

Based on this assumption, I can compute the benchmark European call value as its expected discounted payoff under $\mathbb{P}$, i.e.,

$$c_t = E_t^{\mathbb{P}}[e^{-r(T-t)}\Pi_T^c],$$

where the discount rate r is justified by the option market maker's risk neutrality. Appendix B3 summarizes the derivation of the time-t call value given in semi-closed form by

$$\begin{aligned} c_t = e^{-r(T-t)}\Bigg[& e^{-\bar{\lambda}}\left(\sum_{i=l^*}^{\bar{n}} \phi[i,\bar{n};p](S_t u^i d^{\bar{n}-i} - K^c)\right) + \\ & \bar{\lambda}e^{-\bar{\lambda}}\Bigg\{\sum_{i=0}^{\bar{n}} \phi[i,\bar{n};p]\Bigg\{(1-\tilde{p})\eta_2\left(S_t u^i d^{\bar{n}-i}\frac{1-(b_l^i \wedge 1)^{\eta_2+1}}{\eta_2+1} - K^c\frac{1-(b_l^i \wedge 1)^{\eta_2}}{\eta_2}\right) \\ & + \tilde{p}\eta_1\left(S_t u^i d^{\bar{n}-i}\frac{(b_l^i \vee 1)^{-\eta_1+1}}{\eta_1-1} - K^c\frac{(b_l^i \vee 1)^{-\eta_1}}{\eta_1}\right)\Bigg\}\Bigg\}\Bigg], \end{aligned} \tag{3.6}$$

where $\phi[i,\bar{n};p] \equiv \frac{\bar{n}!}{i!(\bar{n}-i)!}p^i(1-p)^{\bar{n}-i}$, $\bar{n} := n - \frac{t-t_0}{\Delta t}$, $\bar{\lambda} := \lambda(T-t)$, $b_l^i = \frac{K^c}{u^i d^{n-i} S_t}$ denotes the necessary jump size such that the call option ends up in the money at maturity, and l^* is the smallest nonnegative integer such that the same holds true in the case of no jumps. The first

[14] In the market microstructure literature these deviations are often referred to as adverse selection spreads.

[15] This assumption is mathematically justified whenever the intensity parameter λ of the counting process N_t and the length of the considered time period $(T-t)$ are small enough such that $\mathbb{P}(N_T - N_t = 2) = \frac{\lambda(T-t)^2}{2!}e^{-\lambda(T-t)} \approx 0$. This is ensured throughout the numerical analysis in Section 3.4.

term in Eq. (3.6) refers to the case where there is no stock value jump between t and the call's maturity T, whereas the second term corresponds to the case where one jump occurs until T.

Analogously, one can show that the benchmark European put value

$$p_t = E_t^{\mathbb{P}}[e^{-r(T-t)}\Pi_T^p]$$

is given by

$$\begin{aligned} p_t = e^{-r(T-t)}\Bigg[e^{-\bar{\lambda}}\left(\sum_{i=0}^{u^*\wedge\bar{n}}\phi[i,\bar{n};p](K^p - S_t u^i d^{\bar{n}-i})\right) + \\ \bar{\lambda}e^{-\bar{\lambda}}\Bigg\{\sum_{i=0}^{\bar{n}}\phi[i,\bar{n};p]\Bigg\{(1-\tilde{p})\eta_2\left(K^p\frac{(b_u^i\wedge 1)^{\eta_2}}{\eta_2} - S_t u^i d^{\bar{n}-i}\frac{(b_u^i\wedge 1)^{\eta_2+1}}{\eta_2+1}\right) \\ + \tilde{p}\eta_1\left(K^p\frac{(b_u^i\wedge 1)^{-\eta_1} - (b_u^i)^{-\eta_1}}{\eta_1}\right. \\ \left. - S_t u^i d^{\bar{n}-i}\frac{(b_u^i)^{1-\eta_1} - (b_u^i\wedge 1)^{1-\eta_1}}{1-\eta_1}\right)\Bigg\}\Bigg\}\Bigg], \quad (3.7) \end{aligned}$$

where $b_u^i = \frac{K^p}{u^i d^{\bar{n}-i} S_t}$ denotes the necessary jump size such that the put option ends up in the money at maturity and u^* is the largest nonnegative integer such that the same holds true in the case of no jumps.

3.3.1.2 Information Spreads

Based on informed traders' set of possible trades, it is evident that market makers might consider any stock and call buy order to stem from a potentially informed trader who has received a positive jump signal. Equivalently, any stock sell and put buy order could be submitted by an informed trader whose signal has been negative. I denote market makers' perceived risk regarding the presence of 'positively' ('negatively') informed traders by θ^+ (θ^-) and the corresponding conditional probability of an informed *stock* trade by θ_S, respectively. Note that θ_S may be different for positive and negative signals.

In the case of abnormally high levels of stock and/or call buy orders during trading period i, both market makers sequentially update their estimates of θ^+ and θ_S. By $\{\text{informed}, \text{uninformed}\}$ and $\{\text{shares}, \text{options}\}$ I denote the two possible event space partitions of any randomly arriving trader. Bayes' rule then implies that at t_i', $t_i' \in [t_i, t_i + \Delta t)$, the probability of a newly arriving *informed* stock buyer equals (henceforth neglecting subscript i)

$$\begin{aligned} \mathbb{P}(\text{informed}|\text{shares}) &= \frac{\mathbb{P}(\text{informed})\mathbb{P}(\text{shares}|\text{informed})}{\mathbb{P}(\text{informed})\mathbb{P}(\text{shares}|\text{informed}) + \mathbb{P}(\text{uninformed})\mathbb{P}(\text{shares}|\text{uninformed})} \\ &= \frac{\theta_{t'}^+\theta_{S,t'}}{\theta_{t'}^+\theta_{S,t'} + (1-\theta_{t'}^+)\frac{\alpha}{2}}, \end{aligned}$$

where $\alpha/2$ represents the proportion of stock buys among all liquidity trades. By condition *EC1*,

the equilibrium stock ask price set by the stock market maker at t' needs to satisfy

$$a_{S_{t'}} = S_t + \underbrace{\overbrace{(\overline{S}_t - S_t)}^{\text{value of pos. jump}} \frac{\theta^+_{t'}\theta_{S,t'}}{\theta^+_{t'}\theta_{S,t'} + (1-\theta^+_{t'})\frac{\alpha}{2}}}_{\text{information spread stock}}, \tag{3.8}$$

where $\overline{S}_t$ denotes the market maker's time-t stock value in the certain case of a future positive jump and is given below.

Accordingly, the time-t' probability with which the options market maker sells a call to a newly arriving *informed* trader equals

$$\mathbb{P}(\text{informed}|\text{options}) \quad = \quad \frac{\theta^+_{t'}(1-\theta_{S,t'})}{\theta^+_{t'}(1-\theta_{S,t'}) + (1-\theta^+_{t'})\frac{1-\alpha}{4}},$$

where $(1-\alpha)/4$ represents the proportion of call buys among all liquidity trades. Thus, the time-t' equilibrium call ask price set by the options market maker has to satisfy

$$a_{c_{t'}} = c_t + \underbrace{\overbrace{(\overline{c}_t - c_t)}^{\text{value of pos. jump}} \frac{\theta^+_{t'}(1-\theta_{S,t'})}{\theta^+_{t'}(1-\theta_{S,t'}) + (1-\theta^+_{t'})\frac{1-\alpha}{4}}}_{\text{information spread call option}}, \tag{3.9}$$

where $\overline{c}_t$ denotes her time-t call value in the case of a positive signal and is derived below.

The information spreads in Eq. (3.8) and Eq. (3.9) correspond to the assets' excess values due to a priced in future jump times the respective probability of informed trading. Since the excess values only depend on the last realization of the observable stock value, they remain constant between t and $t+\Delta t$. In contrast, the conditional probabilities of informed trading are likely to fluctuate between value realizations, thereby reflecting market makers' updated beliefs regarding the presence of informed traders.

Recalling market makers' risk neutrality, $\overline{S}_t$ in Eq. (3.8) is given by the product of the current stock value realization S_t and the expected positive jump size, i.e.,

$$\overline{S}_t = S_t E^{\mathbb{P}}\left[\overline{V}\right] = S_t \frac{\eta_1}{\eta_1 - 1}.$$

Accounting for the future positive jump, $\overline{c}_t$ in Eq. (3.9) is given by

$$\begin{aligned}
\overline{c}_t &= E^{\mathbb{P}}_t[e^{-r(T-t)}\max(\overline{S}_T - K^c, 0)] \\
&= e^{-r(T-t)}e^{-\bar{\lambda}}\sum_{i=0}^{\bar{n}}\phi[i,\bar{n};p]\Bigg\{\int_{b^i_l\vee 1}^{\infty}(S_t u^i d^{\bar{n}-i}\overline{v} - K^c)\eta_1\overline{v}^{(-\eta_1-1)}\mathrm{d}\overline{v} \\
&\qquad + \bar{\lambda}\int_0^{\infty}\int_1^{\infty}\max(S_t u^i d^{\bar{n}-i}v\overline{v} - K^c, 0)\eta_1\overline{v}^{(-\eta_1-1)}\mathrm{d}\overline{v}\,\mathrm{d}F_V\Bigg\}.
\end{aligned}$$

Solving the first integral yields

$$\overline{c}_t = e^{-r(T-t)}e^{-\bar{\lambda}}\sum_{i=0}^{\bar{n}}\phi[i,\bar{n};p]\Bigg\{\eta_1\left(S_t u^i d^{\bar{n}-i}\frac{(b_l^i \vee 1)^{-\eta_1+1}}{\eta_1-1} - K^c\frac{(b_l^i \vee 1)^{-\eta_1}}{\eta_1}\right) + \bar{\lambda}\int_0^\infty\int_1^\infty \max(S_t u^i d^{\bar{n}-i}v\overline{v} - K^c, 0)\eta_1\overline{v}^{(-\eta_1-1)}\mathrm{d}\overline{v}\,\mathrm{d}F_V\Bigg\}.$$

In the case of abnormally high levels of arriving stock sell and/or put buy orders, market makers sequentially adjust their estimates of θ^- and θ_S. Thus, again implied by Bayes' rule and condition *EC1*, the time-t' equilibrium stock bid price set by the stock market maker has to satisfy

$$b_{S_{t'}} = S_t + \underbrace{\overbrace{(\underline{S}_t - S_t)}^{\text{value of neg. jump}}\frac{\theta_{t'}^+\theta_{S,t'}}{\theta_{t'}^-\theta_{S,t'} + (1-\theta_{t'}^-)\frac{\alpha}{2}}}_{\text{information spread stock}}, \tag{3.10}$$

where $\underline{S}_t$ denotes the market maker's time-t' stock value in the sure case of dealing with a negatively informed stock buyer. Analogously, the time-t' equilibrium put ask price set by the options market maker needs to satisfy

$$a_{p_{t'}} = p_t + \underbrace{\overbrace{(\underline{p}_t - p_t)}^{\text{value of neg. jump}}\frac{\theta_{t'}^-(1-\theta_{S,t'})}{\theta_{t'}^-(1-\theta_{S,t'}) + (1-\theta_{t'}^-)\frac{1-\alpha}{4}}}_{\text{information spread put option}}, \tag{3.11}$$

where $\underline{p}_t$ denotes her time-t put value in the case of a negative signal.

Note that in Eq. (3.10), the information spread is actually negative since $\underline{S}_t - S_t < 0$. It indeed makes sense that the stock market maker is only willing to pay less than S_t per share, if she assigns a nonzero probability to the risk of being matched with a negatively informed trader. $\underline{S}_t$ in Eq. (3.10) and $\underline{p}_t$ in Eq. (3.11) are given by

$$\underline{S}_t = S_t E_t^{\mathbb{P}}[\underline{V}] = S_t\frac{\eta_2}{\eta_2+1},$$

and

$$\underline{p}_t = e^{-r(T-t)}e^{-\bar{\lambda}}\sum_{i=0}^{\bar{n}}\phi[i,\bar{n};p]\Bigg\{\eta_2\left(K^p\frac{(b_u^i \wedge 1)^{\eta_2+1}}{\eta_2+1} - S_t u^i d^{\bar{n}-i}\frac{(b_u^i \wedge 1)^{\eta_2}}{\eta_2}\right) + \bar{\lambda}\int_0^\infty\int_0^1 \max(K^p - S_t u^i d^{\bar{n}-i}v\underline{v}, 0)\eta_2\underline{v}^{(\eta_2-1)}\mathrm{d}\underline{v}\,\mathrm{d}F_V\Bigg\},$$

respectively.

As in Easley et al. (1998), both market makers protect themselves against the adverse selection risk from privately informed traders by quoting divergent bid and ask prices. However, given my assumption that informed traders only *buy* options, the bid-ask spreads in the options

market are solely driven by increasing ask prices. Options' bid prices are therefore always equal to their respective benchmark values. Via the sequential trading process market makers learn about potential preceding signals. Hence, in the limit, bid and ask prices converge to the asset values that fully reveal any price relevant information. After having determined market makers' bid and ask prices that yield zero expected profits conditional on *EC2*, I now turn to the derivation of the equilibrium probability of informed stock trading $\theta_S^\star$.

3.3.2 Equilibrium Informed Stock and Options Trading

Informed traders maximize their expected utility of terminal wealth W_T by trading in *either* the stock *or* the options market. Therefore, there exist three fundamentally different types of informed trading equilibria: (i) all informed traders only trade in the stock market, i.e., $\theta_S^\star = 1$, (ii) some trade in the stock and others in the options market, i.e., $\theta_S^\star \in (0,1)$, and (iii) they exclusively trade in the options market, i.e., $\theta_S^\star = 0$. I refer to $\theta_S^\star \in (0,1)$ as a 'semi-separating equilibrium of informed trading' in which heterogeneously risk-averse informed traders are separated between the stock and the options market. Due to the exogenous liquidity trading of the uninformed, the bid and ask prices in Eq. (3.8) – Eq. (3.11) are sufficient to determine the equilibrium proportion $\theta_S^\star$ satisfying *EC1* and *EC2*.

As it turns out, a given informed trader's risk-aversion is the key variable which determines whether she prefers to trade shares or to buy OTM options. This is intuitive, given the stock's and the options' different risk-return profiles: Whereas the latter's leverage potential is much higher, the former thus is clearly less risky. To see this, one recalls that informed traders' private signal is imperfect. Hence, it is possible that the post-trading stock value realizations until T are to the disadvantage of the informed traders. If they have bought (sold) shares, their final wealth nevertheless is almost surely strictly positive. In contrast, if they have decided to buy OTM options, these derivative contracts are then likely to expire worthless, thereby completely eliminating informed traders' wealth.

The following proposition establishes the condition for a semi-separating equilibrium in both cases, i.e., for a positive and negative signal.

Proposition (Semi-separating equilibrium)**.** *In the case of a positive signal at t and given market makers' time-t' beliefs regarding θ^+, $t' \in [t, t+\Delta t)$, $\theta_{S,t'}^\star$ corresponds to a time-t' semi-separating equilibrium satisfying EC1 and EC2 iff*

$$E_{t'}^{\mathbb{P}}\left[U\left(\frac{W_{t_0}}{a_S(\boldsymbol{\theta}_{\boldsymbol{S},\boldsymbol{t'}}^\star|\theta_{t'}^+)}\overline{S}_T\right)\Big|_{\gamma=\boldsymbol{\theta}_{\boldsymbol{S},\boldsymbol{t'}}^\star}\right] \overset{!}{=} E_{t'}^{\mathbb{P}}\left[U\left(\frac{W_{t_0}}{a_c(\boldsymbol{\theta}_{\boldsymbol{S},\boldsymbol{t'}}^\star|\theta_{t'}^+)}\overline{c}_T\right)\Big|_{\gamma=\boldsymbol{\theta}_{\boldsymbol{S},\boldsymbol{t'}}^\star}\right], \tag{3.12}$$

such that $\theta_{S,t'}^\star \in (0,1)$. In the case of a negative signal at t, assuming short selling requires an interest-free deposit of all time-t' proceeds, $\theta_{S,t'}^\star$ corresponds to a time-t' semi-separating

equilibrium iff

$$E^{\mathbb{P}}_{t'}\left[U\left(W_{t_0}\left(1+\frac{b_S(\boldsymbol{\theta^\star_{S,t'}}|\theta^-_{t'})-\underline{S}_T}{b_S(\boldsymbol{\theta^\star_{S,t'}}|\theta^-_{t'})}\right)\right)\Big|_{\gamma=\boldsymbol{\theta^\star_{S,t'}}}\right] \overset{!}{=} E^{\mathbb{P}}_{t'}\left[U\left(\frac{W_{t_0}}{a_p(\boldsymbol{\theta^\star_{S,t'}}|\theta^-_{t'})}\underline{p}_T\right)\Big|_{\gamma=\boldsymbol{\theta^\star_{S,t'}}}\right], \quad (3.13)$$

such that $\theta^\star_{S,t'} \in (0,1)$.

Proof. Recall that informed traders are uniformly distributed over $\gamma \in (0,1)$. In the case of a positive signal, the LHS of Eq. (3.12) equals the $\theta^\star_{S,t'}$-th informed trader's expected utility from buying $\frac{W_{t_0}}{a_S(\theta^\star_{S,t'}|\theta^+_{t'})}$ shares of the stock at t', whereas the RHS corresponds to her expected utility from buying $\frac{W_{t_0}}{a_c(\theta^\star_{S,t'}|\theta^+_{t'})}$ units of the call option (in both cases the initial endowment is fully invested). If Eq. (3.12) holds, she is *indifferent* between the two trades. Moreover, the relative attractiveness (in expected utility terms) of buying shares is strictly decreasing in γ, i.e., strictly increasing in her risk aversion $1-\gamma$ (see proof of Result 3.2 in Appendix D3). Therefore, if Eq. (3.12) holds, exactly $\theta^\star_{S,t'}$ percent of informed traders buy shares and $1-\theta^\star_{S,t'}$ percent buy calls, which again corresponds to the market makers' beliefs underlying their respective ask prices in Eq. (3.8) and Eq. (3.9).

In the case of a negative signal, the LHS of Eq. (3.13) equals the $\theta^\star_{S,t'}$-th informed trader's expected utility from short selling $\frac{W_{t_0}}{b_S(\theta^\star_{S,t'}|\theta^-_{t'})}$ shares of the stock, whereas the RHS corresponds to her expected utility from buying $\frac{W_{t_0}}{a_p(\theta^\star_{S,t'}|\theta^-_{t'})}$ units of the put option. The relative attractiveness of short selling shares is strictly decreasing in γ (see proof of Result 3.2 in Appendix D3). Hence, the exact analogue argument as in the case of a positive signal applies. This completes the proof. □

The intuition behind a semi-separating equilibrium is simple. Based on market makers' price quotes, informed traders choose the trading venue that allows them to maximize their expected utility. Relatively more risk-averse traders will prefer to trade shares, whereas relatively less risk-averse traders will decide to buy options. In equilibrium, these two proportions must exactly equal market makers' anticipations thereof, i.e., $\theta^\star_S$ percent of informed traders have to choose the stock over the options market. Because informed traders are uniformly distributed over $\gamma \in (0,1)$, this indeed is the case if the informed trader with $\gamma = \theta^\star_S$ is indifferent between trading shares or options. Furthermore, since ask and bid prices are functions of θ^+ (θ^-), it follows that $\theta^\star_S$ also depends on market makers' beliefs regarding the aggregated presence of informed traders across markets.

The condition for a semi-separating equilibrium in Eq. (3.12) is equivalent to

$$\textit{Eq. (3.12)} \quad \Leftrightarrow \quad \frac{E^{\mathbb{P}}_{t'}\left[\overline{S}^\gamma_T\right]}{a_S(\theta^\star_{S,t'}|\theta^+_{t'})^\gamma}\Bigg|_{\gamma=\theta^\star_{S,t'}} \overset{!}{=} \frac{E^{\mathbb{P}}_{t'}\left[\overline{c}^\gamma_T\right]}{a_c(\theta^\star_{S,t'}|\theta^+_{t'})^\gamma}\Bigg|_{\gamma=\theta^\star_{S,t'}}, \quad (3.14)$$

and Eq. (3.13) is equivalent to

$$\text{Eq. (3.13)} \quad \Leftrightarrow \quad E_{t'}^{\mathbb{P}}\left[\left(1+\frac{b_S(\theta^{\star}_{S,t'}|\theta^{-}_{t'})-\underline{S}_T}{b_S(\theta^{\star}_{S,t'}|\theta^{-}_{t'})}\right)^{\gamma}\Bigg|_{\gamma=\theta^{\star}_{S,t'}}\right] \overset{!}{=} \frac{E_{t'}^{\mathbb{P}}\left[\underline{p}_T^{\gamma}\right]}{a_p(\theta^{\star}_{S,t'}|\theta^{-}_{t'})^{\gamma}}\Bigg|_{\gamma=\theta^{\star}_{S,t'}}. \tag{3.15}$$

Hence, $\theta^{\star}_S$ does not depend on informed traders' initial capital endowment. In order to solve for $\theta^{\star}_S$, one has to separately compute the two expectations in Eq. (3.14) and Eq. (3.15), respectively, whose explicit forms are provided in Appendix C3.

Given the explicit expressions of Eq. (3.14) and Eq. (3.15), it is possible to iteratively solve for a semi-separating equilibrium. Before turning to the numerical analysis of the model, I briefly discuss the existence and uniqueness of such an equilibrium.

Result 3.1 (Existence)**.** *If, for $\epsilon, \delta > 0$, there exists a $\theta^{\epsilon}_S \in (\epsilon, 1]$ and a $\theta^{\delta}_S \in [0, 1-\delta)$ both satisfying the equality in Eq. (3.12) (Eq. (3.13)) but with $\gamma^{\epsilon} = \epsilon$ and $\gamma^{\delta} = 1-\delta$, respectively, then there also exists a semi-separating equilibrium $\theta^{\star}_S \in (0, 1)$.*

Proof. See Appendix D3. □

Thus, if there exists (i) a relatively more risk-averse informed trader who is indifferent between trading in the two markets at the maximum stock and minimum option spread *and* (ii) a relatively less risk-averse informed trader who is indifferent between the two markets at the minimum stock and maximum option spread, then there also exists a semi-separating equilibrium. For a high n, i.e., for many remaining stock value movements until T, the above result allows for a simple check regarding the existence of a semi-separating equilibrium. The subsequent numerical analysis in Section 3.4 asserts that, for a wide range of parameter values, such an equilibrium indeed exists.

Result 3.2 (Uniqueness)**.** *If there exists a semi-separating equilibrium $\theta^{\star}_S$ satisfying Eq. (3.12) (Eq. (3.13)), then it is unique.*

Proof. See Appendix D3. □

Hence, it is known ex-ante that any interior solution $\theta^{\star}_S$ to Eq. (3.12) (Eq. (3.13)) found by numerical iteration corresponds to the only existing equilibrium. Furthermore, in the special case of a positive signal, the following statement regarding the functional form of $\theta^{\star}_S$ can be made.

Result 3.3 (Equilibrium trading upon positive signal)**.** *In the case of a positive signal, the semi-separating equilibrium $\theta^{\star}_S$ is given by a fixed point of the solution to a quadratic equation.*

Proof. See Appendix D3. □

Relying on the above result significantly simplifies (and speeds-up) the numerical computation of $\theta^{\star}_S$.

TABLE 3.2. PARAMETERS FOR NUMERICAL ANALYSIS

		Base Case			
S_{t_0}	100	K^c	105	r	0.02
d	$1/u$	K^p	95	n	$\{5, 25\}$
p	0.51	Δt	1/250	α	0.9
		Jump Scenario 1			
η_1	8	$\tilde{p}$	0.5	u	1.01
η_2	8	λ	1		
		Jump Scenario 2			
η_1	10	$\tilde{p}$	0.4	u	1.02
η_2	5	λ	1		

Notes: This table provides the parameter values for the numerical analysis. The parameters in the top panel are thereby combined with those of either jump scenario. r denotes the risk-free interest rate (continuously compounded) and K^c (K^p) the call (put) option's strike price. $\lambda^{\mathbb{P}}$ is the jump frequency under the risk-neutral measure. All remaining parameters specify the stock value process as given in Eq. (3.3).

3.4 Numerical Analysis

Based on the above derived sufficient conditions for a semi-separating equilibrium, $\theta_S^\star$ can be obtained numerically given market makers' beliefs about θ^+ or θ^-, respectively. However, it proves helpful to first disentangle θ_S from the indifferent trader's risk aversion and separately analyze the equalities in Eq. (3.12) and Eq. (3.13) with respect to ceteris paribus changes in θ^+ (θ^-) and γ.

Throughout the following numerical analysis, all results are based on the parameters given in Table 3.2. For ease of notation, all calculations are carried out for $t_i = t_i' = t_0$, i.e., focusing on the very beginning of the first trading period, while the time subscript is omitted. However, since I consider the whole range of market makers' beliefs, this can be done without loss of generality. If one thinks of years as the respective time unit, $n \in \{5, 25\}$ in combination with a duration Δt of 1/250 between stock value realizations implies a remaining number of five or 25 trading days until T, respectively. This is consistent with a rather short-lived private signal. As postulated above, strike prices are set such that both options are OTM at t_0. On average, there is one jump per time unit unrelated to private information. If not otherwise specified, liquidity traders' proportion of stock to total orders α is set to 0.9. This is closely in line with the empirically observed proportions in Section 3.5.[16]

The parameters of the first jump scenario are those of Table 3.1 that underlie the path simulations in Figure 3.2. The parameters of the second scenario correspond to the one of the numerical option pricing example in Kou (2002). The second scenario complements the first one

[16]Based on the respective measures in Section 3.5, 47.5% of pre-M&A announcement liquidity-based trading volume correspond to stock buys, whereas 2.6% are call purchases.

by allowing for a higher asymmetry between positive and negative jumps.[17] Under scenario 2, the average size of positive jumps equals 11.1% and -16.7% for negative jumps. Moreover, the latter are somewhat more likely (with a probability $\tilde{p}$ of 60%) than the former.

Finally, the up movement parameter u in scenario 2 (1.02) is set slightly higher than in scenario 1 (1.01). This is because I aim for reasonable first and second moments of unconditional holding period returns. Overall, the parameter values in scenario 1 imply an expected return over one time unit of 8.1% with a standard deviation equal to 26.8%, whereas under scenario 2 the corresponding values are 9.7% and 42.1%, respectively. This is approximately in line with an average realized volatility of single-name S&P 100 constituents of around 32% per annum (see, e.g., Buraschi et al. (2009)).

3.4.1 The Indifference Surface

A semi-separating equilibrium $\theta_S^\star(\theta^{+/-})$ is reached if the $\theta_S^\star$-th informed trader is indifferent between trading shares or buying options. By construction, the $\theta_S^\star$-th informed trader's coefficient of relative risk aversion γ equals $\theta_S^\star$. Hence, both market makers' beliefs regarding the potential presence of informed traders $\theta^{+/-}$ as well as their respective risk aversion $1-\gamma$ are crucial for determining $\theta_S^\star$.

The analysis of what henceforth shall be referred to as 'indifference surfaces' lends itself for a better understanding of the structure behind any semi-separating equilibrium. If an informed trader with risk aversion $1-\gamma$ could *split* her orders between shares and options, then, for any given pair $(\gamma, \theta^{+/-})$, the indifference surface indicates her proportion of stock to total orders that *equalizes* her expected utility across trading venues. Naturally, if there exists no such proportion $\theta_S \in (0,1)$ the surface is bounded between zero and one. Formally speaking, all points on the indifference surface which are strictly positive but smaller than one do satisfy the same condition as in Eq. (3.12) or Eq. (3.13), respectively, but with differing values for θ_S and γ.

Distinguishing between positive and negative private signals, Figure 3.4 shows the indifference surfaces for both jump scenarios in Table 3.2 with $n = 25$. The first dimension of each indifference surface corresponds to the risk aversion parameter γ, where $1-\gamma$ measures relative risk aversion. The conditional proportion of stock orders is decreasing in γ, i.e., $\theta_S(\gamma, \theta^{+/-})$ is larger for informed traders who are more risk-averse. This result is not surprising, considering the options' asymmetric and hence more risky payoff profile. Due to their nonzero probability of expiring OTM, i.e., to be completely worthless at T, any sufficiently risk-averse trader prefers to exclusively invest in shares, which almost surely yield a strictly positive payoff.

The second dimension of the indifference surfaces in Figure 3.4 corresponds to the market makers' beliefs regarding the potential presence of informed traders $\theta^{+/-}$. My numerical analysis shows that the proportion of stock orders is increasing in $\theta^{+/-}$. Again, this is very intuitive. The call's (put's) comparative leverage advantage over the stock is decreasing in θ^+ (θ^-), as the market makers' quote adjustments as given in Eq. (3.8) – Eq. (3.11) are relatively larger

[17] This corresponds to the empirical fact that stock price time series usually exhibit greater negative than positive jumps (in absolute values).

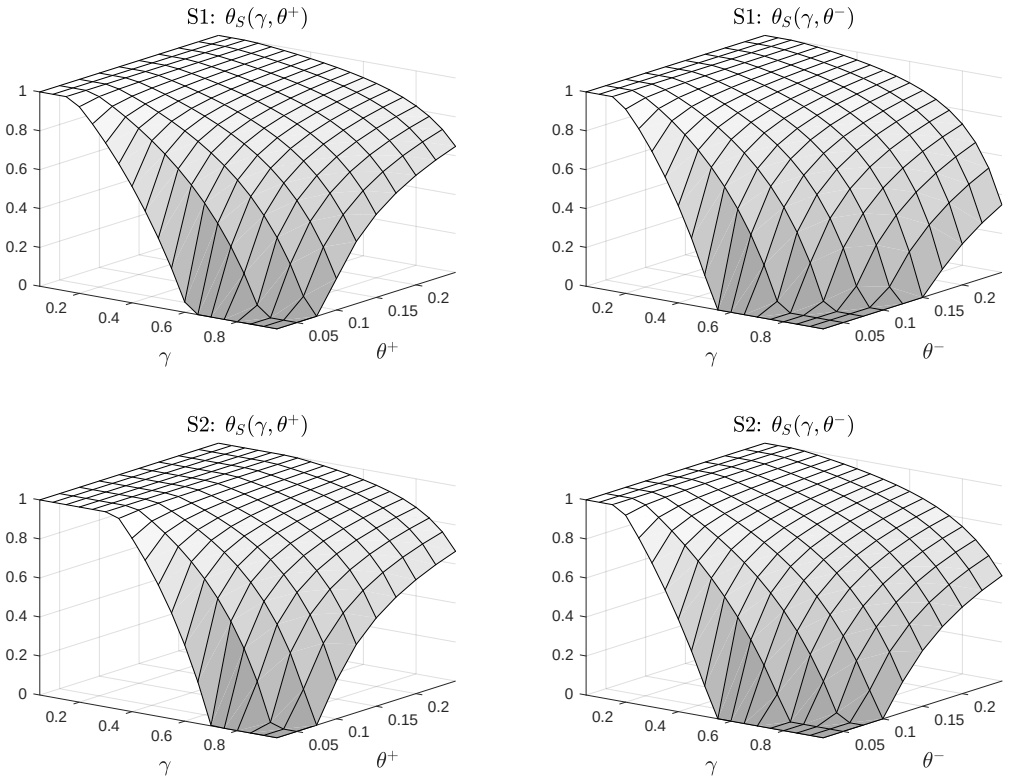

FIGURE 3.4. INDIFFERENCE SURFACES

Notes: This figure plots the indifference surfaces for scenario 1 (S1) and scenario 2 (S2) as specified in Table 3.2 with $n = 25$ stock value realizations. Given market makers' beliefs regarding the likelihood of informed trading θ^+ (θ^-), each surface corresponds to the anticipated proportion θ_S of informed stock trading for which the γ-informed trader is indifferent between trading in the stock or the options market.

for options than for the stock. Hence, the corresponding spreads effectively lessen the options' leverage advantage. Therefore, the higher $\theta^{+/-}$, the smaller this leverage advantage and the larger θ_S in Figure 3.4. The sensitivity of θ_S with respect to $\theta^{+/-}$ moreover negatively depends on a given informed trader's risk aversion $1 - \gamma$. As soon as her risk aversion exceeds a certain threshold, she prefers to only trade shares, independently of the level of $\theta^{+/-}$.[18]

Overall, the four surfaces in Figure 3.4 look quite similar. In order to better visualize the differences in $\theta_S(\gamma, \theta^{+/-})$ across the four different cases, Figure 3.5 shows the respective difference plots. The top two plots depict positive differences $\theta_S^+ - \theta_S^-$ for most $(\gamma, \theta^{+/-})$-values, indicating a higher proportion of informed *stock* trading for a positive signal. Equivalently, over the same neighborhood of the $(\gamma, \theta^{+/-})$-plane, informed traders buy more puts than calls. For both jump scenarios, these differences are increasing in γ and decreasing in $\theta^{+/-}$. This higher attractiveness of the put relative to the call is clearly most pronounced for high values of γ in scenario 1 and small values of $\theta^{+/-}$ in scenario 2.

[18]The general validity of this behavior of $\theta_S(\gamma, \theta^{+/-})$ is verified by the proof of Result 3.2 in Appendix D3.

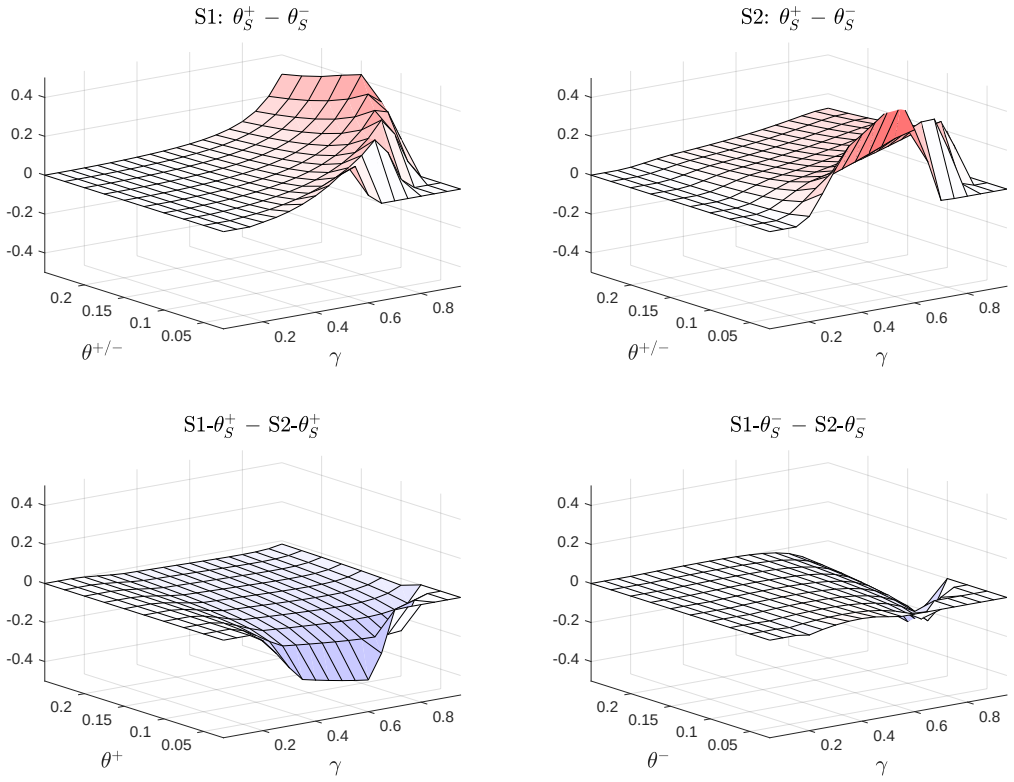

FIGURE 3.5. DIFFERENCES BETWEEN INDIFFERENCE SURFACES

Notes: This figure plots the differences between the indifferent surfaces in Figure 3.4. The top two plots show the differences between the likelihood of a positive signal θ^+ and the likelihood of a negative signal θ^-. The bottom two plots show the differences between scenarios 1 (S1) and scenario 2 (S2) as specified in Table 3.2.

First, due to the stock value process' positive drift, the call is more expensive than the put in scenario 1. For any given level of $\theta^{+/-}$, the put therefore provides a higher leverage compared to the call. At the same time, the former's risk of expiring OTM is also higher. Thus, the less risk-averse a given informed trader is, the more options she buys in the case of a negative relative to a positive signal. Second, in scenario 2, this effect is mitigated by a higher probability of a strongly negative jump. Furthermore, due to the larger negative than positive price shock (in expectation), the put's leverage advantage for informed traders still outweighs the one by the call, as long as information spreads are low.

The bottom two plots in Figure 3.5 show the differences in relative informed stock trading across the two jump scenarios in Table 3.2. Independently of the signal's sign, for most values of $(\gamma, \theta^{+/-})$, informed traders are willing to buy more options in the case of bigger positive and smaller negative jumps (scenario 1). As shown in the lower left plot, below a certain level of risk aversion, informed traders buy more calls under scenario 1 when θ^+ is low. The reason is that the higher volatility from regular stock value movements (larger u) increases the call's ask price under scenario 2. This in turn decreases the call's leverage for an informed trader, especially

when information spreads are low.

However, referring to the case of a negative signal shown in the lower right plot, this same effect is dominated by the put's higher potential leverage when trading against the *unconditional* expected jump size.[19] More specifically, the unconditional expected jump multiplier is 1.016 in scenario 1 and 0.944 in scenario 2. Hence, solely the put under scenario 2 can be pushed into the money by an average jump only.[20] In other words, buying puts upon a negative signal may provide a higher leverage under scenario 1, even though the *conditional* expected impact of a negative jump is bigger under scenario 2. As shown in Figure 3.5, this is exactly the case for the here considered parameters: The less risk-averse a given informed trader is, the more puts she is willing to buy under scenario 1, despite having to bear the risk of another jump whose mean is positive.

In case both market makers are risk-averse and thus rely on the risk-neutral probability measure in Appendix A3 when quoting their break-even ask and bid prices, the call becomes somewhat less and the put somewhat more expensive.[21] This lowers the differences between relative informed call and put purchases in the top row of Figure 3.5, as the stock value process' drift is reduced to the risk-free rate r.

3.4.2 Multimarket Equilibrium

The above indifference analysis demonstrates the driving forces behind a potential semi-separating equilibrium for which market makers' price quotes must leave the $\theta_S^\star$-th informed trader indifferent between trading either in the stock or the options market. Applying the above proposition, I numerically solve for $\theta_S^\star$ considering both jump scenarios in Table 3.2. Figure 3.6 presents multimarket informed trading equilibria for each combination of jump scenarios and number of stock value realizations. Every depicted $\theta_S^\star \in (0,1)$ corresponds to a semi-separating equilibrium, where $\theta_S^\star$ percent of either positively (circles) or negatively (squares) informed traders choose to trade in the stock market.

Overall, Figure 3.6 reveals two striking characteristics of multimarket informed trading equilibria. First, the existence of a semi-separating equilibrium is very robust with respect to market makers' estimate of the overall probability of informed trading. Across the whole range of $\theta^{+/-}$, the corresponding proportion of conditional informed stock trading $\theta_S^\star(\theta^{+/-})$ is strictly bigger than zero but smaller than one, i.e., there are always some informed traders who prefer to trade in the stock rather than in the options market. Given the parameter choices of Table 3.2, this proportion is consistently above 20%, but as $\theta^{+/-}$ converges to one, so does the fraction of informed stock trading.

---

[19] I verify this by an additional ceteris paribus analysis keeping u fixed across jump scenarios.

[20] Recall that the unconditional expected jump size equals $E^{\mathbb{P}}[V] = \tilde{p}\frac{\eta_1}{\eta_1 - 1} + (1-\tilde{p})\frac{\eta_2}{\eta_2+1}$. Given the put's strike price K^p of 95, it follows that $S_{t_0} \times 0.944 < K^p$.

[21] This is due to the risk-neutral measure's lower likelihood of an up movement u, which is again implied by the usual martingale condition with respect to the stock value process.

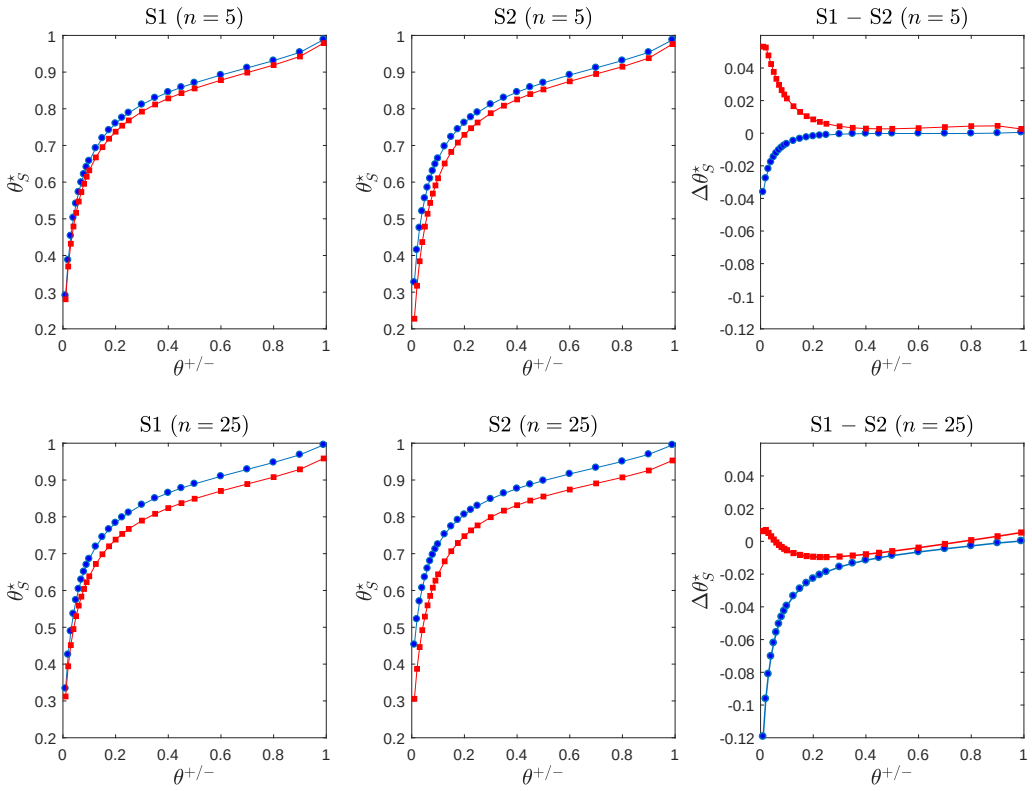

FIGURE 3.6. MULTIMARKET INFORMED TRADING IN EQUILIBRIUM

Notes: This figure shows proportional informed stock trading $\theta_S^\star$ in equilibrium as a function of market makers' perceived likelihood of positively (circles) (negatively (squares)) informed trading θ^+ (θ^-). The left and middle columns plot trading equilibria based on scenario 1 (S1) and scenario 2 (S2) as specified in Table 3.2, respectively. The right column presents the respective differences between the two. In the top (bottom) row, the number of stock value realizations is set to $n = 5$ ($n = 25$).

Second, the dependence of $\theta_S^\star$ on $\theta^{+/-}$ has a very distinctive form: (i) the higher the probability of informed trading, the bigger is the proportion of informed traders who choose the stock over the options market in order to benefit from their private information. (ii) up until very high levels of $\theta^{+/-}$, this relation is clearly concave, i.e., the additional fraction of informed traders opting for the stock market increases very fast for low values of $\theta^{+/-}$, but less and less so as $\theta^{+/-}$ becomes larger.

The intuition for this specific functional form is simple. If the probability of informed trading rises, market makers adjust their respective quotes to account for the risk of trading with an informed trader. By doing so, the options' initial leverage advantage decreases, leaving the relatively more risk-averse informed traders to switch from buying options to trading shares. However, since these more risk-averse traders react very sensitively to a reduction of options' comparative leverage advantage, the stock's information spread starts to catch up quickly due to the fast growing $\theta_S^\star$. Yet, from the perspective of the less risk-averse traders, a high fraction of informed stock trading diminishes the attractiveness of switching from the stock to the options

market. Therefore, almost risk-neutral traders, i.e., those whose γ is close to one, keep on buying options even for very high levels of $\theta^{+/-}$.

More specifically, when comparing informed call to informed put trading, Figure 3.6 unveils that, given the stock value's positive drift, the cheaper put is relatively more attractive to the informed traders than is the call ($\theta_S^\star$-squares below $\theta_S^\star$-circles). This effect becomes more pronounced under a negatively skewed jump distribution (scenario 2) and as the option's time to maturity $n \times \Delta t$ increases.

Furthermore, referring to Figure 3.6's right column, informed call trading is higher under scenario 1 ($\Delta\theta_S^\star < 0$), where the expected size of a positive jump is larger than under scenario 2. Accordingly, at least for low n, informed put trading is more attractive under scenario 2, in which negative jumps exhibit a larger average price impact. However, as the number of stock value realizations increases, this clear-cut pattern disappears in the case of the put. The reason thereof again lies in the put's higher leverage potential under scenario 1, given that scenario 2's unconditional expected jump size is sufficient to push the stock value below the put's strike price, which itself becomes more likely as n increases.

Finally, informed option trading decreases faster in the probability of informed trading $\theta^{+/-}$ if options' time to maturity is shorter (not explicitly shown). This is intuitive, given that for a lower n the private signal's information precision is greater, which in turn implies higher information spreads. Consistently, for low values of $\theta^{+/-}$, i.e., when information spreads are small, informed option trading is higher for $n = 5$ than for $n = 25$. Since informed traders are risk-averse, they ceteris paribus prefer to buy options when the risk of adverse stock value movements is smaller.

Assuming market makers to be risk-averse only marginally affects mulitmarket trading equilibria. The stock value's lower drift under the risk-neutral measure generally reduces the proportional differences between informed call and put trading across all cases considered in Figure 3.6. More importantly, however, both the robust existence of a semi-separating equilibrium as well as the distinct functional form of $\theta_S^\star(\theta^{+/-})$ prevail.

3.4.3 Risk Aversion, Equilibrium Spreads, and Market Depth

So far, the implication of the model's key element, i.e., informed traders' risk aversion, has not been discussed in isolation. For one exemplary case, the left plot of Figure 3.7 shows the difference between equilibrium informed stock trading $\theta_S^\star$ and the proportion of stock trades θ_S^{RN} for which a risk-neutral ($\gamma = 1$) informed trader is indifferent between the two markets. This simple exercise uncovers two important effects of risk aversion on multimarket informed trading.

First, the difference between risk-averse and risk-neutral informed stock trading starts around one third and quickly rises to reach a value close to 70%. Overall, for *relatively* low probabilities of informed trading, i.e., up to 20%, the proportion of informed stock trading under a semi-separating equilibrium is approximately 50% higher (in absolute differences) than under the risk-neutral benchmark.

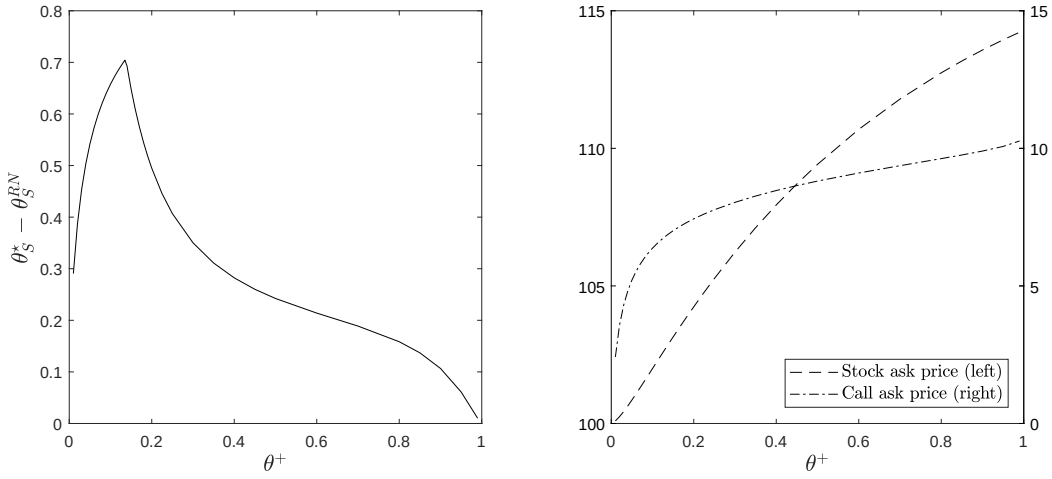

FIGURE 3.7. IMPACT OF RISK AVERSION & SPREAD COMPARISON

Notes: This figure illustrates the impact of informed traders' risk aversion on equilibrium informed trading (left plot) and compares the equilibrium information spreads between the stock and the call in the case of a positive signal (right plot). Both plots are based on scenario 1 as given in Table 3.2 and $n = 5$ value realizations. The left plot shows the difference between equilibrium informed stock trading $\theta_S^\star$, as shown in top left plot of Figure 3.6, and the proportion of stock trades θ_S^{RN} for which a risk-neutral ($\gamma = 1$) informed trader is indifferent between the two markets. Based on $\theta_S^\star$ in the left plot, the right plot shows the ask prices for the stock and the call as given in Eq. (3.8) and Eq. (3.9), respectively.

Second, as the probability of informed trading further increases, the distance between the two proportions starts to decrease and eventually approaches zero as the occurrence of a private signal becomes common knowledge. Formally speaking, the hump shape in the left plot of Figure 3.7 is a direct consequence of a semi-separating equilibrium's strongly concave dependence on the probability of informed trading. As $\theta_S^{RN}(\theta^{+/-})$ increases less strongly at the beginning but more so for higher values of $\theta^{+/-}$, the above pattern arises.

In summary, imperfectly informed traders' risk aversion offers an intuitive explanation why, for realistic levels of $\theta^{+/-}$, informed option trading could indeed be lower than relative market depth and Black's (1975) leverage argument suggest. Generally, the above described pattern is robust to the considered sign of the private signal as well as across jump scenarios.

The right plot of Figure 3.7 illustrates why simply testing the predicted equilibrium properties via empirically observed stock and option bid-ask spreads might be difficult. Based on the corresponding semi-separating equilibrium for a positive signal, it depicts the stock and the call ask price as given in Eq. (3.8) and Eq. (3.9), respectively, for different values of θ^+. One notes that the former's information spread is first smaller than the latter's but then becomes larger as θ^+ increases, again a direct implication of the semi-separating equilibrium's concavity. Moreover, around the median value of my empirical measure for θ, i.e., 8.5% (see below), the slopes of the two curves more or less coincide.

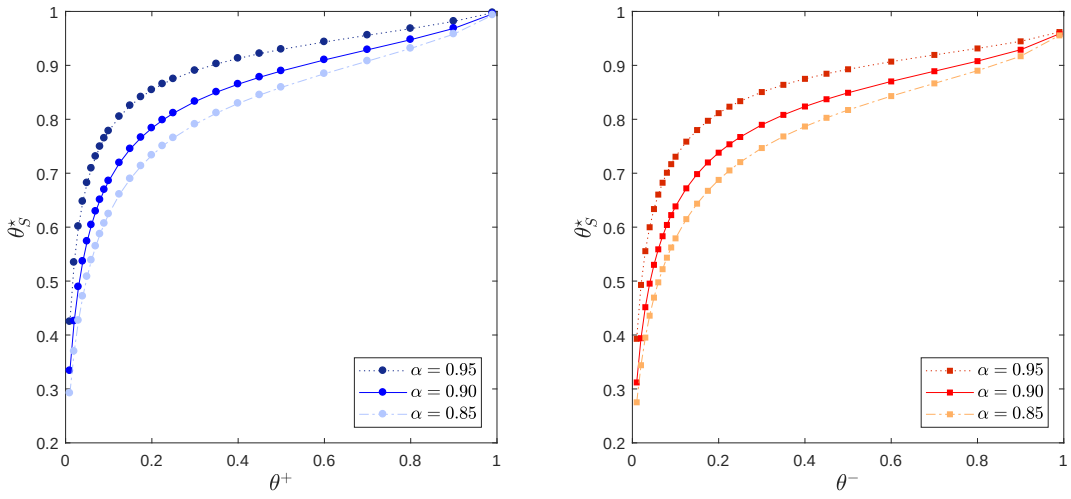

FIGURE 3.8. IMPACT OF RELATIVE MARKET DEPTH

Notes: This figure shows equilibrium informed stock trading upon a positive (left plot) and negative (right plot) signal for varying levels of relative stock market depth. α denotes the proportion of liquidity stock trades (relative to total liquidity trades) which are evenly distributed among stock buys and sells. Both plots are based on scenario 1 as given in Table 3.2 and $n = 25$ value realizations.

Another interesting question is how equilibrium informed stock trading reacts in response to exogenous changes in stock market depth. Intuitively, one expects an increase in the proportion of liquidity-based stock orders α to diminish options' inherent leverage advantage, as informed option trading becomes more easily detectable by market makers. Formally, this can be verified by recalling Eq. (3.9) and Eq. (3.11), where options' information spreads react more sensitive to $\theta^{+/-}$ as α becomes larger and vice versa.

Figure 3.8 shows the relationship between $\theta_S^\star$ and $\theta^{+/-}$ for varying values of α. As expected, a higher α, i.e., a relative increase in stock market depth, ceteris paribus leads to a larger proportion of conditional informed stock trading. Furthermore, in line with the concavity of a semi-separating equilibrium, an increased sensitivity of conditional informed stock trading for lower probabilities of multimarket informed trading is observed.

3.5 Empirical Evidence

My numerical analysis has unveiled two main implications of informed traders' risk aversion on equilibrium multimarket trading: On the one hand, the existence of a semi-separating equilibrium appears to be a robust phenomenon with regard to varying market makers' beliefs about the overall likelihood of informed trading $\theta^{+/-}$. On the other hand, equilibrium informed *stock* trading $\theta_S^\star$ features a positive and strongly concave relationship with respect to the joint probability of informed trading $\theta^{+/-}$.

One way of testing these two findings empirically is by simultaneously looking at stock and options trading activities prior to merger and acquisitions (M&A) announcements. M&A an-

nouncements are often followed by a substantial jump in the target company's stock price (see, e.g., Schwert (1996)). Furthermore, in contrast to, e.g., periodically scheduled earning announcements or other anticipated corporate media releases, pre-M&A announcement periods are less likely to experience purely speculative trading. Therefore, I consider such pre-announcement periods as an ideal case study for testing my model's predictions regarding multimarket informed trading patterns in the presence of an imminent and extreme informational event.

Unsurprisingly, this paper is not the first to investigate pre-announcement trading volume in the target's underlying stock and options contracts. For instance, Cao et al. (2005) find that both buyer-seller initiated stock volume imbalances as well as call volume imbalances predict post-announcement returns. In particular, Cao et al. (2005) document that takeover targets with the highest call-imbalance build-ups exhibit the largest stock returns on the announcement day. Similarly, by looking at more recent data, Augustin et al. (2015) provide evidence of informed traders engaging in directional option strategies on the target's stock before the announcement.[22]

Since post-announcement jumps in the targets' stock value are generally positive, the following analysis applies to the case of informed stock and option trading upon a *positive* signal, i.e., it focuses on the function $\theta_S^\star(\theta^+)$. To ease readability, I henceforth omit the superscripts '*' and '$^+$'.

3.5.1 Data Selection and Sample Description

My empirical analysis relies on data from four different sources: Thomson Reuters SDC Platinum database, OptionMetrics, Center for Research in Securities Prices (CRSP), and the NYSE Trade and Quote (TAQ) database. The sample period spans from 2005 up to and including 2012, covering a steady increase of the US stock market (until the end of 2007), the following financial crisis and its aftermath, as well as the subsequent recovery of US equity prices.

I search for all M&A deals with a US target firm in the SCD Platinum database. By relying on the targets' CUSIPs, I then check each deal for the availability of options trading data in OptionMetrics. Out of 83'945 transactions in the SDC Platinum database, I find options trading data on a total of 815 target firms. However, in 499 cases the acquirer's and the targets CUSIP are identical. Since my main focus lies on transactions where the target is acquired by or merged with an independent acquirer, these 499 deals are eliminated from the sample. This leaves me with a final sample of 316 M&A transactions with a median percentage of shares acquired equal to 100% (mean of 78.9% and standard deviation of 36.2%).

All 316 identified targets with actively traded options are matched with stock and options trading variables from CRSP and OptionMetrics. Relying on the algorithm proposed by Lee and Ready (1991), the daily stock trading volume is further divided into buyer and seller initiated trades. Specifically, trades with transaction prices above (below) the prevailing quote midpoint are classified as buyer (seller) initiated; trades with transaction prices *at* the midpoint are classified as buyer (seller) initiated if the quote midpoint is higher (lower) relative to the preceding trade. All remaining trades are regarded as cross-trades and excluded. I match trades

[22] For further references, see the literature review in Augustin et al. (2015).

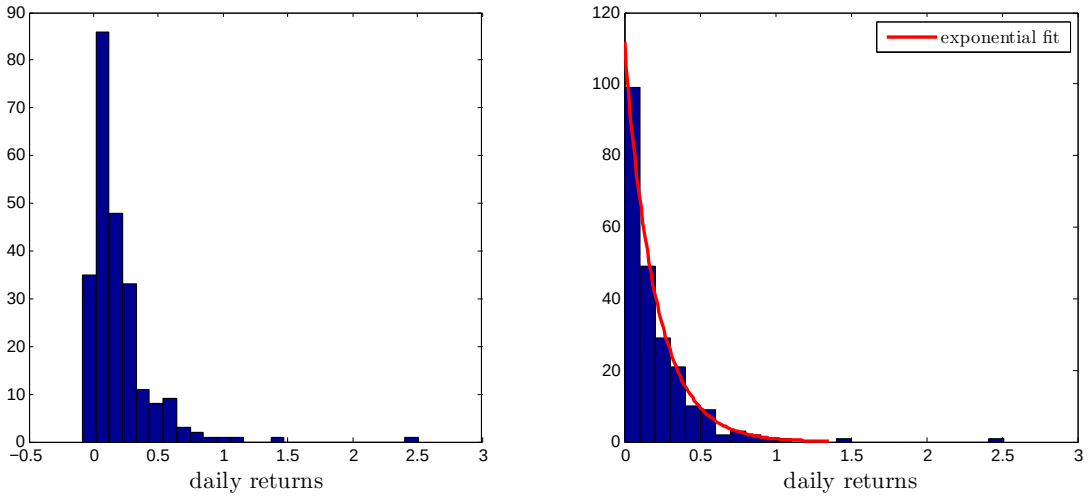

FIGURE 3.9. DAILY STOCK RETURNS ON THE POST-EVENT DATE

Notes: This figure plots the (conditional) distributions of M&A targets' daily stock returns on the post-event date. Returns are measured in decimal numbers, e.g., 0.2 corresponds to a daily return of 20%. The left plot contains all daily returns, whereas the right plot only contains nonnegative returns and additionally depicts the density of the fitted exponential distribution.

to National Best Bid and Offer (NBBO) quotes with a lag of one second (instead of five seconds as in Lee and Ready (1991)).[23] The therefore required intraday transaction data (ticks and NBBO quotes) are taken from the NYSE TAQ database.

To ensure that the selected post-event date indeed corresponds to the trading day at which the stock price is adjusted for the newly revealed information, I move the former to either the previous or subsequent trading day of the announcement, if its return exceeds the one realized on the actual announcement date.[24] Figure 3.9 shows the distribution of the daily stock returns on the post-event date. Out of the 316 daily returns (left histogram), 228 are nonnegative (right histogram). Note that the distribution of the nonnegative returns lies close to its exponential fit, with an average implied jump size of 0.205, i.e., 20.5%. Consequently, the (positive part) of our model's asymmetric double exponential jump distribution seems to describe post-M&A announcement target returns reasonably well.

Based on this sample, appropriate measures for both θ, the overall likelihood of informed trading, as well as for θ_S, the conditional proportion of informed *stock* trading, have to be constructed. However, this task is not straightforward. For the former, one could aim for some kind of measure based on Easley et al. (1996), i.e., developing a likelihood function of a multimarket version of their well-known PIN measure. Due to the unavailability of the required

[23] I apply this shorter time lag because of the higher speed with which my sample's market transactions were executed compared to the early nineties.

[24] In case that both the stock return on the previous *and* the subsequent trading day are higher than the respective return on the announcement date, the trading day with the highest return is chosen as post-event date.

options trading data, the construction of such a measure is unfeasible. Moreover, given the short-lived nature of the considered private signal, the validity and the stability of PIN-based measures are at least questionable. Instead, as it is usually done, I base my measures of θ and θ_S on abnormal stock and options trading volume.

3.5.2 Measures of Multimarket Informed Trading

Basically, I measure the likelihood of informed trading as the proportion of *abnormal* to *total* stock and options trading volume. Equivalently, I measure conditional informed stock trading as the proportion of *abnormal stock* relative to *total abnormal* stock and options trading volume. In particular, I try to adopt a *one-to-one* translation of the model's inherent structure to the *simultaneous* measurement of both θ and θ_S.

Given the models' assumption of liquidity trades' (locally) time invariant distribution, both within and across markets, I estimate multimarket informed trading up to and including the pre-announcement date t by

$$\theta_t := \frac{1}{5}\sum_{i=0}^{4}\theta_{t-i} \quad \& \quad \theta_{S,t} := \frac{1}{5}\sum_{i=0}^{4}\theta_{S,t-i}, \tag{3.16}$$

where each pair $(\theta_{t-i}, \theta_{S,t-i}) \in [0,1] \times [0,1]$ minimizes the sum of squared deviations from the following simple equation system

$$\begin{aligned} \underbrace{\theta_{t-i}\theta_{S,t-i}}_{\substack{\text{informed}\\ \text{stock trading}}} \; + \; (1-\theta_{t-i})\left(\frac{1}{50}\sum_{j=11}^{60}\frac{B_{t-i-j}}{V_{t-i-j}}\right) &= \frac{B_{t-i}}{V_{t-i}} \\ \underbrace{\theta_{t-i}\,(1-\theta_{S,t-i})}_{\substack{\text{informed call}\\ \text{options trading}}} \; + \; (1-\theta_{t-i})\left(\frac{1}{50}\sum_{j=11}^{60}\frac{V^{c,otm}_{t-i-j}}{V_{t-i-j}}\right) &= \frac{V^{c,otm}_{t-i}}{V_{t-i}}, \end{aligned} \tag{3.17}$$

where $V := B + S + V^{c,otm} + V^{p,otm}$ is defined as the sum of total stock buys B, total stock sells S, total OTM call volume $V^{c,otm}$, and total OTM put volume $V^{p,otm}$.

Since I am presuming the occurrence of a positive signal, informed stock trading is reflected in abnormal buyer initiated stock volume. Due to the unavailability of intraday option data, as well as the limited applicability of a Lee & Ready-like algorithm for infrequently traded stock options, I do not distinguish between buyer and seller initiated options volume. Hence, I rely on fluctuations of total call volume as an indicator of informed option trading. Again, sticking as closely to my model as possible, I only consider short dated OTM options. Specifically, a call (put) is classified as being OTM, if its ratio of current stock to strike price is smaller (greater) or equal than 0.95 (1.05). Short dated options are required to have a remaining time to maturity of no more than 30 days.[25] Finally, both stock buys and sells are divided by 100 in order to

[25]The equity options in OptionMetrics are generally American-style options, i.e., they can be exercised anytime up to maturity. However, given the considered timing, it would be irrational for informed traders to exercise their calls *before* the realization of the informational event that initiated their option trades in the first place.

make them directly comparable to the observed option volume, where each derivative contract is written on 100 shares of the stock.

In the literature, it is well documented that potentially informed trading prior to M&A announcements is in no way limited to the pre-announcement day only. For example, Augustin et al. (2015) find that abnormal option trading volume is most pronounced during the four days prior to the announcement. Hence, my measures of informed trading rely on average trading patterns over the last trading week before the announcement day, henceforth referred to as event window. Liquidity traders' proportions of stock buys and total call volume are estimated over the 50 trading days preceding the last ten days prior to the respective event date and, as pointed out above, align reasonably well with $\alpha = 0.9$.

The intuition behind the system in Eq. (3.17) is straight forward. The equations simply state that the proportion of total stock buys (total call volume) at day t equals the weighted sum of liquidity traders' proportional stock buys (call volume) and informed traders' proportional stock (call) trading, where the weights correspond to the probabilities of the partition $\{\text{informed}, \text{uninformed}\}$ of traders' information set. The measured degree of informed trading thus depends on the differences between these weighted values and the system's RHS, i.e., the proportions of total stock buys and total call volume relative to total trading volume, averaged over the pre-announcement trading week.

3.5.3 Summary Statistics and Regression Analysis

The above analysis has shown that an increasing probability of engaging in informed trades causes market makers to adjust their price quotes in such a way that leads to a higher proportion of informed stock trading. I test this relation by estimating the following two regressions:

$$\theta_{S,nt} = const + \beta_1 \theta_{nt} + \mathbf{bc}_{nt} + \epsilon_{nt} \tag{3.18}$$

$$\theta_{S,nt} = const + \beta_1 \theta_{nt} + \beta_2 \left(\theta_{nt}\right)^2 + \mathbf{bc}_{nt} + \epsilon_{nt}, \tag{3.19}$$

where nt refers to the target n at event date t and $\mathbf{c}$ is a vector of control variables. My main explanatory variables of interest in Eq. (3.18) and Eq. (3.19) are θ_{nt} and $(\theta_{nt})^2$, respectively. First, I expect the coefficient β_1 to be positive in both regressions, capturing the positive effect of total informed trading on informed stock trading. Second, I expect β_2 to be negative, accounting for the concave relation between θ and θ_S implied by the model. Third, in accordance with this postulated concavity of conditional informed stock trading, my expectation is that the explanatory power of Eq. (3.19) should be considerably higher compared to the one of Eq. (3.18).

Table 3.3 presents the summary statistics of the regression variables. Starting from my original data set, I find 239 estimates of $(\theta, \theta_S) \in [0,1] \times [0,1]$.[26] For 236 event dates, there exist observations of both (θ, θ_S) as well as of the controls in $\mathbf{c}$. I consider four additional covariates: relative abnormal stock volume ASV, average relative bid-ask spreads for the stock BAS and the

[26] For the remaining 77 announcements there is either one of the variables in Eq. (3.17) missing for every event date $t-4, ..., t$, or there exists no option data for the event date t.

TABLE 3.3. SUMMARY STATISTICS OF REGRESSION VARIABLES

Variable	Mean	Std	Q25	Median	Q75
θ_S	0.5423	0.2499	0.3754	0.5626	0.7700
θ	0.0992	0.0710	0.0497	0.0845	0.1264
θ *squared*	0.0149	0.0283	0.0025	0.0071	0.0160
ASV	0.9912	0.8548	0.9308	0.9961	1.0020
BAS	0.0023	0.0025	0.0008	0.0014	0.0026
MOM	0.0011	0.0044	-0.0011	0.0010	0.0037
$BAS^{c,otm}$	0.5624	0.1982	0.4214	0.5393	0.6723

Notes: This table provides the summary statistics for the full sample period from January 2005 to December 2012. The mean, standard deviation (std), the 25th (Q25), 50th (median), and 75th (Q75) quantiles are reported. The measures of informed trading θ_S and θ are defined in Eq. (3.16). ASV is the average relative abnormal stock volume. BAS and $BAS^{c,otm}$ denote the average relative bid-ask spreads for the stock and the OTM calls, respectively. MOM is a momentum measure based on averaged daily stock returns. The last four are control variables and lagged relatively to θ_S and θ (see Section 3.5.3 for details). The total number of observations equals 236.

OTM calls $BAS^{c,otm}$, and a momentum factor MOM. ASV accounts for the average abnormal stock volume between six and ten days prior to the announcement and is defined as

$$ASV_t := \frac{1}{5}\sum_{i=5}^{9} \frac{V^S_{t-i} - \overline{V}^S_{t-i}}{\left(V^S_{t-i} - \overline{V}^S_{t-i}\right) + \left(V^{otm}_{t-i} - \overline{V}^{otm}_{t-i}\right)},$$

where $V^S := B + S$, $V^{otm} := V^{c,otm} + V^{p,otm}$, $\overline{V}_t := \text{median}\left(\{V_{t-60}, V_{t-59}, ..., V_{t-11}\}\right)$, and all variables are computed as described above. BAS, $BAS^{c,otm}$, and MOM are calculated over the past 60 trading days up to and including $t-5$. The latter thereby simply corresponds to the average daily return.

According to Table 3.3, the median proportion of informed trading is around 8.5%. The median proportion of informed stock trading equals 56.3%. Hence, on average, a little more than half of the abnormal trading volume is observed in the stock market. Almost all of the abnormal trading volume during the week prior to the event window stems from stock trading, where the values of ASV can become greater than one because also negative abnormal (options) volume is considered. Average relative bid-ask spreads are substantially bigger for OTM calls than for stocks. The median value of averaged daily stock returns prior to the event window is slightly positive (0.1%).

The results from running the regressions specified in Eq. (3.18) and Eq. (3.19) are reported in Table 3.4. In the odd columns, the estimation results for Eq. (3.18) are presented, where more and more covariates are added when moving from (I) to (V). In all three columns, the estimated coefficient $\hat{\beta}_1$ is positive, providing empirical evidence for a *positive* dependence between total informed trading and conditional informed stock trading. The even columns report the estimation results for Eq. (3.19), which additionally account for the effect of the squared term $(\theta)^2$ on θ_S. All three columns (II), (IV), and (VI) present strong empirical evidence for

TABLE 3.4. REGRESSION RESULTS

Inf. stock trading	(I)	(II)	(III)	(IV)	(V)	(VI)
const	0.4821^{a}	0.3529^{a}	0.4866^{a}	0.3965^{a}	0.3777^{a}	0.3226^{a}
	(9.85)	(9.51)	(7.76)	(6.47)	(5.80)	(4.98)
θ	0.7385^{b}	3.0703^{a}	0.7290^{b}	3.0208^{a}	1.0171^{a}	2.9800^{a}
	(1.72)	(8.24)	(1.76)	(7.58)	(2.91)	(7.67)
θ *squared*		-6.6212^{a}		-6.5186^{a}		-5.8353^{a}
		(-7.13)		(-6.58)		(-5.92)
ASV			-0.0110	-0.0156	-0.0147	-0.0179
			(-0.45)	(-0.62)	(-0.60)	(-0.73)
BAS			-15.6897^{b}	-12.0139^{b}	-8.9688	-7.6783
			(-1.99)	(-1.73)	(-1.06)	(-1.02)
MOM			-2.7973	-2.1986	-1.5405	-1.3496
			(-0.77)	(-0.66)	(-0.45)	(-0.42)
$BAS^{c,otm}$			0.0614	-0.0064	0.0431	-0.0113
			(0.52)	(-0.06)	(0.38)	(-0.10)
θ_S *lagged*					0.2441^{a}	0.1826^{a}
					(3.56)	(2.80)
θ *lagged*					-0.6880^{a}	-0.4696^{b}
					(-2.68)	(-1.88)
Year FE	yes	yes	yes	yes	yes	yes
R^2	0.0726	0.1888	0.0810	0.1942	0.1359	0.2226
N	239	239	236	236	236	236
F-statistic		32.7896		31.1878		24.5413
p-value		3.21×10^{-8}		6.81×10^{-8}		1.45×10^{-6}

Notes: This table reports the estimates of the two regression models (with and without controls) defined in Eq. (3.18) and Eq. (3.19), respectively. The aim of these estimations is to investigate the influence of the explanatory variables θ and $(\theta)^2$ on relative informed stock trading θ_S. Both measures are defined in Eq. (3.16). The remaining covariates are control variables and lagged relatively to θ and θ_S. *ASV* is the average relative abnormal stock volume. *BAS* and $BAS^{c,otm}$ denote the average relative bid-ask spreads for the stock and the OTM calls, respectively. *MOM* is a momentum measure based on averaged daily stock returns (see Section 3.5.3 for details). In the last two columns, these control variables are complemented by θ *lagged* and θ_S *lagged* which are also computed by relying on Eq. (3.16) but over the preceding trading week. Each column shows the estimated coefficients and heteroscedasticity robust t-statistics in parentheses. Year fixed effects are added to each regression (where the last year is omitted in order to overcome the dummy variable trap). Superscripts ^{a} and ^{b} indicate statistical significance at the 1% and 5%-level, respectively. To test for the non-linear behavior of conditional informed stock trading, an F-test between each respective pair of regressions is conducted.

a *concave* relation between θ and θ_S, where the estimate $\hat{\beta}_1$ from Eq. (3.19) is always positive and the estimate $\hat{\beta}_2$ always negative.[27] In general, across both the odd and even columns, the estimated coefficients $\hat{\beta}_1$ and $\hat{\beta}_2$ remain quite stable.

[27] I check for potential endogeneity issues by computing the correlation between the main explanatory variables, i.e., θ and $(\theta)^2$, and the residuals of the respective regressions. In all cases, these correlations never exceed the value of 10^{-6}.

Of all the control variables in Table 3.3, only the coefficient for the stocks' average bid-ask spreads is statistically significant, indicating that decreasing stock market liquidity also reduces, ceteris paribus, the proportion of informed stock trading. However, if one additionally includes both lagged values of θ_S and θ, this effect disappears.[28] Furthermore, the results in columns (V) and (VI) indicate that there exists a certain degree of autocorrelation in the case of θ_S. Interestingly, θ *lagged* appears to have a negative influence on subsequent informed stock trading. However, compared to θ the coefficients in both columns are considerably smaller and less significant. Finally, I conduct an F-test between each pair of regressions, i.e., between (I) and (II) etc., in order to test the statistical significance of the non-linear behavior of conditional informed stock trading. The results strongly reject a linear relation in favor of a concave effect of θ on θ_S. In summary, there exists empirical support for both the postulated sign as well as for the functional form of $\theta_S(\theta)$.

3.6 Conclusion

I have presented a model of multimarket informed trading that identifies the preferred trading venue of heterogeneously risk-averse and imperfectly informed agents who can either trade in the stock or in the corresponding options market. My focus lies on private signals which, once revealed, exhibit the potential of causing significant shocks in the underlying asset value. I model these shocks as jumps following an asymmetric double exponential distribution, where informed traders' informational advantage consists of two components: (i) they know that a jump will occur, and (ii) they are aware of its sign, i.e., from which side of the exponential distribution it will be drawn.

Throughout a random sequential trading process, competitive market makers continuously update their beliefs regarding the risk of meeting a superior informed trader. Given their updated beliefs, they adjust their respective price quotes to break even in expectation. In order to avoid no-trading equilibria, I posit the presence of exogenously arriving liquidity traders. In the rational expectation equilibrium, any resulting separation of informed traders between venues must be as conjectured by market makers, i.e., such that the former thereby maximize their expected utility from trading.

I show that a multimarket informed trading equilibrium can only be semi-separating, i.e., separating heterogeneously risk-averse informed traders *across* the two markets, if, given market makers' price quotes, all informed traders who opt for the options market are less risk-averse than those opting for the stock market. My numerical analysis provides two striking characteristics of such a semi-separating equilibrium. First, its existence is robust with respect to market makers' beliefs regarding the overall probability of informed trading. Second, the higher this probability, the larger the conditional probability of informed stock trading, where the sensitivity of this relation decreases as the former increases.

[28] θ *lagged* and θ_S *lagged* are computed according to Eq. (3.16) but over the preceding trading week, i.e., letting i run from five to nine.

Relative to the risk-neutral benchmark, the proportion of conditional informed stock trading is always higher under a semi-separating equilibrium. This difference is particularly pronounced, if market makers' perceive the risk of adverse selection to be relatively low. Hence, accounting for informed traders' risk aversion could explain why it is less likely to observe informed option trading in real-world data than one would expect when solely considering options' comparative leverage advantage and relative market depth.

Given that the post-announcement returns of firms targeted by M&A transactions closely follow an exponential jump distribution, I test my model's prediction by looking at those firms' pre-announcement stock and options trading data. I find the relative amount of abnormal stock trading to be increasing in the overall proportion of abnormal trading volume. As predicted by the model, the sensitivity of this positive relationship declines for higher levels of aggregated abnormal trading volume.

A3 Examplary Risk-Neutral Pricing Measure

In order to mitigate trading incentives induced by different risk preferences, I alternatively assume both market makers to be risk-averse in the sense that they rely on a risk-neutral pricing measure when computing the discounted conditional expectation(s) of their traded asset payoff(s).

Due to the three different sources of risk, i.e., X_i, V_i, and N_t, the market of the considered economy is incomplete (see, e.g., Kou (2002)). As a consequence, the benchmark risk-neutral pricing measure is not unique. In order to derive such an equivalent probability measure $\mathbb{Q}$, I follow Merton (1976) by assuming that V_i and N_t have the same distribution under $\mathbb{Q}$ as under $\mathbb{P}$.[29] Since the market prices for different risks are not the subject of this paper, I consider this simplifying assumption acceptable.[30]

Based on this assumption, the $\mathbb{Q}$-likelihood of more than one jump between t and T is also negligible, i.e., it holds that $\mathbb{Q}(N_T - N_t > 1) \approx 0$. Thus, one can solve for the risk-neutral probability $\mathbb{Q}(X = u) \equiv q$ of an up movement of the stock value between t and $t+\Delta t$ by imposing the following martingale condition on S_t under $\mathbb{Q}$

$$\begin{aligned} E_t^{\mathbb{Q}}[e^{-r\Delta t} S_{t+\Delta t}] &= e^{-r\Delta t}\Big\{\mathbb{Q}(N_{t+\Delta t} - N_t = 0) \times (qS_t u + (1-q)S_t d) + \\ &\qquad \mathbb{Q}(N_{t+\Delta t} - N_t = 1) \times (qS_t u + (1-q)S_t d) \times E^{\mathbb{Q}}[V]\Big\} \\ &\stackrel{!}{=} S_t \\ \Leftrightarrow \quad q &= \frac{e^{r\Delta t} - de^{-\lambda\Delta t}(1 + \lambda\Delta t E^{\mathbb{P}}[V])}{(u-d)e^{-\lambda\Delta t}(1 + \lambda\Delta t E^{\mathbb{P}}[V])}. \end{aligned} \tag{A3.1}$$

Relying on Eq. (A3.1), the risk-adjusted call and put values are given by their expected discounted payoffs under $\mathbb{Q}$, i.e.,

$$c_t = E_t^{\mathbb{Q}}[e^{-r(T-t)}\Pi_T^c] \quad \text{and} \quad p_t = E_t^{\mathbb{Q}}[e^{-r(T-t)}\Pi_T^p],$$

respectively.

Moreover, in the absence of a jump size risk premium, a risk-averse market maker's evaluation of the stock under asymmetric information remains the same as in Subsection 3.3.1.2. Hence, Eq. (A3.1) can also be applied for computing risk-adjusted conditional option values.

[29] Merton's (1976) underlying assumption is that jump risk is purely idiosyncratic and therefore can be eliminated completely by diversification.

[30] Here, I moreover refer to liquidity traders' unspecified risk preferences and consumption distributions as sufficient degrees of freedom in order to equilibrate presumed stock value dynamics.

B3 Derivation of Benchmark Call Price

Due to independence and the law of total probability the benchmark price of the European call option at time t (under risk neutrality) is

$$\begin{aligned}
c_t &= E_t^{\mathbb{P}}[e^{-r(T-t)}\Pi_T^c] \\
&= e^{-r(T-t)}\mathbb{P}(N_T - N_t = 0)\left(\sum_{i=0}^{\bar{n}}\mathbb{P}\left(\prod_{i=1}^{\bar{n}} X_i = u^i d^{\bar{n}-i}\right)\max(S_t u^i d^{\bar{n}-i} - K^c, 0)\right) + \\
&\quad e^{-r(T-t)}\mathbb{P}(N_T - N_t = 1)\left(\sum_{i=0}^{\bar{n}}\mathbb{P}\left(\prod_{i=1}^{\bar{n}} X_i = u^i d^{\bar{n}-i}\right)E^{\mathbb{P}}[\max(S_t u^i d^{\bar{n}-i}V - K^c, 0)]\right) \\
&= e^{-r(T-t)}e^{-\bar{\lambda}}\left(\sum_{i=l^*}^{\bar{n}}\frac{\bar{n}!}{i!(\bar{n}-i)!}p^i(1-p)^{\bar{n}-i}(S_t u^i d^{\bar{n}-i} - K^c)\right) + \\
&\quad e^{-r(T-t)}\bar{\lambda}e^{-\bar{\lambda}}\left\{\left(\sum_{i=0}^{\bar{n}}\frac{\bar{n}!}{i!(\bar{n}-i)!}p^i(1-p)^{\bar{n}-i}\int_{b_l^i\wedge 1}^{1}(S_t u^i d^{\bar{n}-i}v - K^c)(1-\tilde{p})\eta_2 v^{\eta_2-1}\mathrm{d}v\right) + \right. \\
&\qquad \left.\left(\sum_{i=0}^{\bar{n}}\frac{\bar{n}!}{i!(\bar{n}-i)!}p^i(1-p)^{\bar{n}-i}\int_{b_l^i\vee 1}^{\infty}(S_t u^i d^{\bar{n}-i}v - K^c)\tilde{p}\eta_1 v^{-(\eta_1+1)}\mathrm{d}v\right)\right\},
\end{aligned}$$

where $\bar{n} := n - \frac{t-t_0}{\Delta t}$, $\bar{\lambda} := \lambda(T-t)$, $b_l^i = \frac{K^c}{u^i d^{n-i} S_t}$ denotes the necessary jump size such that the call option ends up in the money at maturity, and l^* is the smallest nonnegative integer such that the same holds true in the case of no jumps. The integrals in the above equation can easily be solved yielding the following call price

$$\begin{aligned}
c_t = e^{-r(T-t)}\Bigg[&e^{-\bar{\lambda}}\left(\sum_{i=l^*}^{\bar{n}}\phi[i,\bar{n};p](S_t u^i d^{\bar{n}-i} - K^c)\right) + \\
&\bar{\lambda}e^{-\bar{\lambda}}\Bigg\{\sum_{i=0}^{\bar{n}}\phi[i,\bar{n};p]\Bigg\{(1-\tilde{p})\eta_2\left(S_t u^i d^{\bar{n}-i}\frac{1-(b_l^i\wedge 1)^{\eta_2+1}}{\eta_2+1} - K^c\frac{1-(b_l^i\wedge 1)^{\eta_2}}{\eta_2}\right) \\
&\qquad + \tilde{p}\eta_1\left(S_t u^i d^{\bar{n}-i}\frac{(b_l^i\vee 1)^{-\eta_1+1}}{\eta_1-1} - K^c\frac{(b_l^i\vee 1)^{-\eta_1}}{\eta_1}\right)\Bigg\}\Bigg\}\Bigg],
\end{aligned} \tag{B3.1}$$

where $\phi[i,\bar{n};p] \equiv \frac{\bar{n}!}{i!(\bar{n}-i)!}p^i(1-p)^{\bar{n}-i}$.

C3 Derivation of Expectations in Eq. (3.14) and Eq. (3.15)

The first expectation $E_t^{\mathbb{P}}\left[\overline{S}_T^{\gamma}\right]$ in Eq. (3.14) can be written as a sum of weighted stock value up and down movements

$$\begin{aligned} E_t^{\mathbb{P}}\left[\overline{S}_T^{\gamma}\right] &= e^{-\bar{\lambda}}\sum_{i=0}^{\bar{n}}\phi[i,\bar{n};p]\left\{\int_1^{\infty}(S_t u^i d^{\bar{n}-i}\overline{v})^{\gamma}\eta_1\overline{v}^{(-\eta_1-1)}\mathrm{d}\overline{v}\right. \\ &\qquad \left. +\bar{\lambda}\int_0^{\infty}\int_1^{\infty}(S_t u^i d^{\bar{n}-i}v\overline{v})^{\gamma}\eta_1\overline{v}^{(-\eta_1-1)}\mathrm{d}\overline{v}\,\mathrm{d}F_V\right\} \\ &= e^{-\bar{\lambda}}\sum_{i=0}^{\bar{n}}\phi[i,\bar{n};p]\left\{(S_t u^i d^{\bar{n}-i})^{\gamma}\frac{\eta_1}{\eta_1-\gamma}\right. \\ &\qquad \left. +\bar{\lambda}(S_t u^i d^{\bar{n}-i})^{\gamma}\left(\frac{(1-\tilde{p})\eta_1\eta_2}{(\gamma+\eta_2)(\eta_1-\gamma)}+\frac{\tilde{p}\eta_1^2}{(\eta_1-\gamma)^2}\right)\right\}, \end{aligned}$$

where $\bar{\lambda} := \lambda(T-t)$. The first term in curly brackets corresponds to the case of one positive jump only, while the second term contains two jumps, of which one is surly positive. The remaining expectation terms are, however, less straight forward to compute. The RHS in Eq. (3.14) is given by

$$\begin{aligned} E_t^{\mathbb{P}}\left[\,\overline{c}_T^{\gamma}\,\right] = e^{-\bar{\lambda}}\sum_{i=0}^{\bar{n}}\phi[i,\bar{n};p]&\left\{\int_{b_l^i\vee 1}^{\infty}(S_t u^i d^{\bar{n}-i}\overline{v}-K^c)^{\gamma}\eta_1\overline{v}^{(-\eta_1-1)}\mathrm{d}\overline{v}\right. \\ &\left. +\bar{\lambda}\int_0^{\infty}\int_1^{\infty}\max(S_t u^i d^{\bar{n}-i}v\overline{v}-K^c,0)^{\gamma}\eta_1\overline{v}^{(-\eta_1-1)}\mathrm{d}\overline{v}\,\mathrm{d}F_V\right\}. \end{aligned}$$

Due to the more complicated structure of the integrand, it is not possible to solve the above double integral in closed form.

Similarly, for the case of a negative signal, the respective terms in Eq. (3.15) are given by

$$\begin{aligned} E_t^{\mathbb{P}}\left[\left(1+\frac{b_{S_t}-\underline{S}_T}{b_{S_t}}\right)^{\gamma}\right] = e^{-\bar{\lambda}}\sum_{i=0}^{\bar{n}}\phi[i,\bar{n};p]&\left\{\int_0^1\left(1+\frac{b_{S_t}-S_t u^i d^{\bar{n}-i}\underline{v}}{b_{S_t}}\right)^{\gamma}\eta_2\underline{v}^{\eta_2-1}\mathrm{d}\underline{v}\right. \\ &\left. +\bar{\lambda}\int_0^{\infty}\int_0^1\left(1+\frac{b_{S_t}-S_t u^i d^{\bar{n}-i}v\underline{v}}{b_{S_t}}\right)^{\gamma}\eta_2\underline{v}^{\eta_2-1}\mathrm{d}\underline{v}\,\mathrm{d}F_V\right\}, \end{aligned}$$

and

$$\begin{aligned} E_t^{\mathbb{P}}\left[\underline{p}_T^{\gamma}\right] = e^{-\bar{\lambda}}\sum_{i=0}^{\bar{n}}\phi[i,\bar{n};p]&\left\{\int_0^{b_u^i\wedge 1}(K^p-S_t u^i d^{\bar{n}-i}\underline{v})^{\gamma}\eta_2\underline{v}^{\eta_2-1}\mathrm{d}\underline{v}\right. \\ &\left. +\bar{\lambda}\int_0^{\infty}\int_0^1\max(K^p-S_t u^i d^{\bar{n}-i}v\underline{v},0)^{\gamma}\eta_2\underline{v}^{\eta_2-1}\mathrm{d}\underline{v}\,\mathrm{d}F_V\right\}, \end{aligned}$$

respectively.

D3 Additional Proofs

Proof of Result 3.1. Both the LHS and the RHS of Eq. (3.14) as well as of Eq. (3.15) are continuous in $\gamma \in (0,1)$. Hence, given the conditions of Result 3.1, it directly follows from the proof of Result 3.2 below that $\bar{\theta}_S(\bar{\gamma})$ as a function of $\bar{\gamma}$ has to cross the bisector of $\mathbb{R}^2_+$ somewhere over $(0,1)$. This completes the proof. □

Proof of Result 3.2. The proof's structure identically applies to both a positive and a negative signal and shall here be demonstrated for the latter case. For a fixed $\bar{\gamma}$, the partial derivative of the utility term on the LHS of Eq. (3.13) with respect to θ_S equals

$$\frac{\partial}{\partial \theta_{S,t}} U\left(W_{t_0}\left(1+\frac{b_S(\theta_{S,t}|\theta_t^-)-\underline{S}_T}{b_S(\theta_{S,t}|\theta_t^-)}\right)\right) = \underbrace{U'(\cdot)}_{>0}\underbrace{\left(W_{t_0}\frac{\underline{S}_T}{b_S(\theta_{S,t}|\theta_t^-)^2}\right)}_{>0}\frac{\partial b_S(\theta_{S,t}|\theta_t^-)}{\partial \theta_{S,t}},$$

where

$$\frac{\partial b_S(\theta_{S,t}|\theta_t^-)}{\partial \theta_{S,t}} = \underbrace{(\underline{S}_t - S_t)}_{<0}\underbrace{\frac{(1-\theta_t^-)^{\frac{\alpha}{2}}}{\left(\theta_t^-\theta_{S,t}+(1-\theta_t^-)^{\frac{\alpha}{2}}\right)^2}}_{>0} < 0,$$

and thus $\frac{\partial}{\partial \theta_{S,t}} U_{LHS}(\cdot)$ is strictly negative.

Analogously, the partial derivative of the utility term on the RHS of Eq. (3.13) is given by

$$\frac{\partial}{\partial \theta_{S,t}} U\left(\frac{W_{t_0}}{a_p(\theta_{S,t}|\theta_t^-)}\underline{p}_T\right) = \underbrace{U'(\cdot)}_{>0}\underbrace{\left(\frac{-W_{t_0}}{a_p(\theta_{S,t}|\theta_t^-)^2}\underline{p}_T\right)}_{<0}\frac{\partial a_p(\theta_{S,t}|\theta_t^-)}{\partial \theta_{S,t}},$$

where

$$\frac{\partial a_p(\theta_{S,t}|\theta_t^-)}{\partial \theta_{S,t}} = \underbrace{(\underline{p}_t - p_t)}_{>0}\underbrace{\frac{-(1-\theta_t^-)^{\frac{1-\alpha}{4}}}{\left(\theta_t^-(1-\theta_{S,t})+(1-\theta_t^-)^{\frac{1-\alpha}{4}}\right)^2}}_{<0} < 0,$$

hence, $\frac{\partial}{\partial \theta_{S,t}} U_{RHS}(\cdot)$ is strictly positive. This implies that for a fixed $\bar{\gamma}$, there can be only *one* corresponding $\theta_{S,t}(\bar{\gamma}) \in (0,1)$, hereafter denoted by $\bar{\theta}_S$, that satisfies the equality in Eq. (3.13), but *not* necessarily equals $\bar{\gamma}$.

Let $\bar{U}$ denote the utility level in Eq. (3.13) corresponding to $\bar{\theta}_S$. Due to its asymmetric payoff profile, the 'normalized' put option value on the RHS of Eq. (3.15) exhibits a less centered probability mass over $(0,\infty)$ than the 'normalized' payoff from short selling on the LHS of Eq. (3.15). Given the strict concavity of informed traders' utility function, it thus directly follows that

$$E_t^{\mathbb{P}}\left[\left(1+\frac{b_S(\bar{\theta}_{S,t}|\theta_t^-)-\underline{S}_T}{b_S(\bar{\theta}_{S,t}|\theta_t^-)}\right)^{\gamma}\right] > \bar{U} \quad \forall \gamma < \bar{\gamma},$$

and

$$\frac{E_t^{\mathbb{P}}\left[\underline{p}_T^{\gamma}\right]}{a_p(\bar{\theta}_{S,t}|\theta_t^-)^{\gamma}} > \bar{U} \quad \forall \gamma > \bar{\gamma},$$

i.e., all informed traders who are less (more) risk-averse than their $\bar{\gamma}$-th counterpart will prefer to buy (short sell) put options (shares). Hence, in order to preserve the validity of Eq. (3.13), a strictly increasing $\bar{\gamma}$ therefore requires a strictly decreasing $\bar{\theta}_S$ and vice versa, i.e., $\bar{\theta}_S$ is strictly decreasing in $\bar{\gamma}$. This completes the proof. □

Proof of Result 3.3. Assuming Eq. (3.14) to hold for any fixed $\bar{\gamma}$ not necessarily equal to $\theta_{S,t}$, it follows that

$$\begin{aligned}
&\underbrace{E^{\mathbb{P}}_{t'}\left[\overline{c}_T^{\bar{\gamma}}\right]^{1/\bar{\gamma}}}_{=:A}\left(S_t+\underbrace{(\overline{S}_t-S_t)}_{=:S^+}\frac{\theta^+_{t'}\theta_{S,t'}(\bar{\gamma})}{\theta^+_{t'}\theta_{S,t'}(\bar{\gamma})+(1-\theta^+_{t'})\frac{\alpha}{2}}\right)= \\
&\underbrace{E^{\mathbb{P}}_{t'}\left[\overline{S}_T^{\bar{\gamma}}\right]^{1/\bar{\gamma}}}_{=:B}\left(c_t+\underbrace{(\overline{c}_t-c_t)}_{=:c^+}\frac{\theta^+_{t'}(1-\theta_{S,t'}(\bar{\gamma}))}{\theta^+_{t'}(1-\theta_{S,t'}(\bar{\gamma}))+(1-\theta^+_{t'})\frac{1-\alpha}{4}}\right),
\end{aligned} \tag{D3.1}$$

for $t' \in [t, t+\Delta t)$. In the following, in order to ease notation, I again omit the time subscripts in Eq. (D3.1) and simply write θ_S instead of $\theta_S(\bar{\gamma})$.

Rearranging terms in Eq. (D3.1) yields

$$ASD + AS^+\theta\theta_S\left[\theta(1-\theta_S)+(1-\theta)\frac{1-\alpha}{4}\right] = BcD + Bc^+\theta(1-\theta_S)\left[\theta\theta_S+(1-\theta)\frac{\alpha}{2}\right], \tag{D3.2}$$

where

$$\begin{aligned}
D &:= \left[\theta(1-\theta_S)+(1-\theta)\frac{1-\alpha}{4}\right]\left[\theta\theta_S+(1-\theta)\frac{\alpha}{2}\right] \\
&= \theta_S\left[\theta^2+\theta(1-\theta)\frac{1-3\alpha}{4}\right]+\theta(1-\theta)\frac{\alpha}{2}+(1-\theta)^2\frac{\alpha(1-\alpha)}{8}-\theta^2\theta_S^2.
\end{aligned}$$

Solving for θ_S in Eq. (D3.2), one gets the following quadratic equation

$$\begin{aligned}
&\theta_S^2\underbrace{\left[\theta(B(c+c^+)-A(S+S^+))\right]}_{=:a}+ \\
&\theta_S\underbrace{\left[(AS-Bc)\left(\theta+(1-\theta)\frac{1-3\alpha}{4}\right)+AS^+\left(\theta+\frac{1-\alpha}{4}(1-\theta)\right)-Bc^+\left(\theta+\frac{\alpha}{2}(\theta-1)\right)\right]}_{=:b}+ \\
&\underbrace{\left[(AS-Bc)(1-\theta)\frac{\alpha}{2}\left(1+\frac{1-\theta}{\theta}\frac{\alpha(1-\alpha)}{8}\right)-Bc^+(1-\theta)\frac{\alpha}{2}\right]}_{=:d}=0.
\end{aligned} \tag{D3.3}$$

The solution to Eq. (D3.3) is of course given by

$$\theta_S(\bar{\gamma}) = \frac{-b \pm \sqrt{b^2-4ad}}{2a}. \tag{D3.4}$$

Recalling Eq. (3.14), it thus follows that $\theta^\star_S(\theta^+)$ is a fixed point of Eq. (D3.4). Moreover, recalling Result 3.2, there can maximally exist one such fixed point in $(0,1)$ corresponding to

an interior solution. Therefore, it can always be determined which sign in Eq. (D3.4) yields the semi-separating equilibrium. This completes the proof. □

4 Indebtedness, Interests, and Incentives: State-contingent Sovereign Debt Revisited

Joint with Andrin Bögli

This paper studies state-contingent debt as an alternative refinancing instrument for advanced economies. In times of high sovereign indebtedness, increasing yields impose eminent debt roll-over risks. We analyze the welfare implications of two state-contingent debt instruments: puttable and GDP-to-debt-indexed bonds, both temporary in nature and intended to improve deleveraging feasibility. In return for an insurance premium, puttable bonds offer protection against sovereign default, thereby internalizing the implicit risk-sharing mechanism inherited by the ECB's 'Outright Monetary Transactions' program. Similar to GDP-linked debt, bonds indexed to a country's GDP-to-debt ratio, henceforth 'GDR bonds', allow for consumption smoothing via state-contingent interest payments. In contrast to GDP-linked debt, GDR bonds permit competitive risk-return profiles even in the face of pessimistic growth outlooks. We find that, in the presence of default costs, state-contingent bonds allow for substantial welfare improvements relative to standard sovereign debt. For risk-averse consumers, the counter-cyclical fiscal leeway created by GDR bonds dominates the interest savings provided by puttable bonds. We verify this preference order by calibrating our model to the five Eurozone countries most heavily affected by the debt crisis: Portugal, Ireland, Italy, Greece, and Spain. We discuss implied deleveraging incentives, limited commitment, and practical implementation issues for GDR bonds.

4.1 Introduction

Even though the most acute symptoms of the Eurozone's sovereign debt crisis have abated, the necessary precondition for its recrudescence still persists to date: massive debt-to-GDP levels in many European countries. Surging public debt burdens arguably pose substantial refinancing risks, if perceived default probabilities should shift upwards again (Calvo (1988)). This has led both the press as well as renowned macroeconomists to recently rediscover the benefits of state-

We would like to thank Konrad Adler, Markus Brunnermeier, Marc Chesney, Sebastian Dörr, Lucas Fuhrer, Seraina Grünewald, Michel Habib, David Hémous, Andreas Müller, Steven Ongena, Jean-Charles Rochet, Alexander Wagner, Jiri Woschitz, Alexandre Ziegler, Fabrizio Zilibotti, and participants at the UZH Finance Poster Workshop 2015, the Zurich Workshop on Economics 2015, the MFA 2016, the Spring Meeting of Young Economists 2016, and the URPP Financial Market Regulation doctoral colloquium at the University of Zurich for very helpful comments and suggestions.

contingent bonds as an alternative refinancing instrument,[1] but this time for the pre-restructured debt of advanced economies.[2]

This paper investigates the welfare implications of state-contingent debt as a temporary device against swelling refinancing costs of highly indebted sovereigns. Our focus lies on governments whose economically required deleveraging efforts under standard sovereign debt are so immense that they have to be considered politically infeasible. We demonstrate state-contingent debt's virtue of providing more space for mitigating sovereign default risk. If sovereign borrowing is contractible—a requirement whose practicability is discussed—this even holds true in the presence of low growth expectations, i.e., when the issuance of standard GDP-indexed bonds is particularly difficult.

In light of the European Central Bank (ECB)'s most effective crisis response, i.e., its 'Outright Monetary Transactions' program (OMT), we consider two types of state-contingent debt instruments: (i) puttable debt and (ii) GDP-to-debt-linked bonds, henceforth simply GDR (GDP-to-debt ratio) bonds. Investors in puttable debt receive the right to put their claims with a third party in return for a fixed payment and are thus insured against sovereign default. GDR bonds offer state-contingent interests that are *inversely* related to sovereign indebtedness. Hence, conditionally on sufficient deleveraging, their interest payments can still be positive under zero or even negative growth.

We find that, in the presence of non-negligible default costs, state-contingent bonds generally lead to substantial welfare gains. In terms of relative welfare improvements for risk-averse consumers, the *counter-cyclical* fiscal spending allowed for by GDR bonds' *cyclical* interest charges (as a function of GDP) proves superior to puttable bonds' simple insurance mechanism. For both instruments, governments deleveraging incentives as well as practical implementation issues are discussed.

The ECB's crisis mitigation efforts covered a wide range of non-standard monetary policy measures: from expanding volume and maturities of lending operations to adjusting collateral requirements for repo transactions, followed by direct interventions in securities markets. Whereas the effects of the first such direct intervention, i.e., the 'Securities Markets Program' (SMP), remained limited, the sole announcement of its successor OMT in July 2012 significantly calmed sovereign bond markets. In essence, OMT allows the ECB to buy unlimited amounts of distressed government bonds (with maturities up to three years) on the secondary market, as long as the issuing government agrees to comply with certain coercive measures.[3]

---

[1]For example, 'The Economist' referred to suggestions from Morgan Stanley to allow governments to issue GDP-linked bonds (source: A chronic problem, *The Economist*, May 14, 2016, http://www.economist.com/node/21698669). Blanchard et al. (2016) argue for a large scale issuance of growth-indexed bonds in advanced economies during normal times. They show for several Eurozone countries how GDP-indexed bonds could significantly reduce the upper-tail risk of excessive sovereign indebtedness, thereby attenuating implied default probabilities.

[2]Historically, securities linked to national growth have only been issued during the process of debt restructuring. More recently, Argentina (2005), Greece (2012), and Ukraine (2015) issued warrant-like instruments, where payments are conditional on realized growth rates.

[3]For an overview of the ECB's non-standard measures up to and including OMT see, e.g., the speech by Peter Praet, member of the executive board of the ECB, on April 17, 2013 (source: https://www.ecb.europa.eu/press/key/date/2013/html/sp130417.en.html).

Following Merton (1977), OMT's conditional guarantee to buy traded sovereign bonds to reduce distressed yields can be interpreted as a written put option: The issuing government has the right to initiate purchases of its own bonds, once their price has fallen below a certain threshold. Since its first announcement, this ex-ante free option indirectly offered to OMT eligible countries received considerable opposition among Eurozone countries, particularly from Germany.[4] Concerns were raised that OMT's free option results in substantial risk redistribution among member countries and fails to sufficiently reinforce fiscal discipline of candidate governments.

In the context of OMT, state-contingency is achieved through lower interest rates during times of high perceived default probabilities. The closest *incentive-compatible* alternative to OMT are puttable bonds, where an intergovernmental organization insures investors against default, thereby substantially lowering interest payable by the issuing government. Importantly, contrary to OMT, the issuing government has to *ex-ante* compensate the insurance provider by paying the insurance premium in return.[5] Thus, puttable bonds internalize the risk-sharing costs which remain non-remunerated under OMT.

First, motivated by OMT's inherent insurance mechanism, we start our analysis with puttable debt in the absence of default costs other than investors' foregone repayments, and relate our results to the seminal corporate debt valuation model by Merton (1974). The rationale underlying puttable sovereign debt is simple. Newly issued puttable bonds contain an embedded put option which serves as default protection for investors. If the sovereign is unable to refinance its liabilities at maturity, i.e., whenever the government defaults on its puttable debt, the writer of the embedded put option repays investors in full (principal and accrued interests) and acquires the initial claim against the issuing sovereign.

Abstracting from any credit risk on the insurance guarantor's side, puttable bonds correspond to a risk-free investment and therefore only pay the risk-free rate. In the context of OMT, default protection is provided by the ECB, i.e., more precisely by its stakeholders. In sharp contrast to OMT, in order to issue puttable debt, the sovereign would have to ex-ante compensate the ECB or another sufficiently capitalized intergovernmental agency for writing the embedded option.

Merton (1974) shows that the spread between risky debt and otherwise similar but credit risk-free debt can be interpreted as the value of a put option on total assets. In the absence of default costs, we demonstrate the validity of Merton's (1974) equivalence result within the sustainable sovereign debt model of Collard et al. (2015). They model sovereign borrowing to be solely constrained by credit markets' willingness to lend. Relying on uniformly distributed GDP growth rates, which allow for closed-form solutions, we show that a risk-neutral government is exactly indifferent between paying for protection against increased refinancing pressure today

[4]The Federal Constitutional Court of Germany questioned OMT's compliance with EU law. It was finally declared to be in line with the ECB's official mandate of price stability and thus considered legal by the European Court of Justice on June 16, 2015 (source: judgment of the court in case C-62/14, June 16, 2015, http://curia.europa.eu/jcms/jcms/j_6/).

[5]In contrast to credit default swaps (CDS) on sovereign debt, the embedded default insurance of puttable bonds can not be disentangled from the underlying default exposure. Moreover, the insurance premium is paid in full at issuance, rather then periodically over the bonds' lifetime.

versus accepting lower publicly financed consumption or even the risk of default tomorrow. However, as soon as default imposes additional costs on the defaulting government, the lower default probability under puttable debt's reduced financing costs becomes be welfare improving.

Second, we introduce costs incurred in case of sovereign default. As soon as default imposes significant disutility on the defaulting government,[6] it has incentives not to overborrow. Based on actual country-specific yield spreads, we calibrate these costs such that the implied default probabilities are consistent with Merton's (1974) equivalence result. Hence, in the presence of non-negligible default costs, instead of following Collard et al. (2015), we adopt a one-shot perspective, where a risk-neutral government trades off publicly financed private consumption against expected default costs when choosing its optimal borrowing rate. In particular, our starting point is an already highly indebted government whose outstanding debt contains considerable default risk and therefore imposes high refinancing costs.[7]

Within this new setting, we compare utilities between alternative state-contingent refinancing instruments. In the spirit of Blanchard et al.'s (2016) current analysis for various Eurozone countries, we additionally consider GDP-linked debt. To allow state-contingent debt instruments to be welfare improving, we introduce a risk-averse consumer, who optimizes her utility from publicly financed consumption conditional on the government's borrowing policy. In order to account for the different frequencies between private consumption decisions and the passage of public budgets, the former is modeled in continuous time, whereas public borrowing remains constant over the considered period.

In contrast to standard GDP-linked debt, GDR bonds' interest payments *inversely* depend on a government's *relative indebtedness*, i.e., whenever its GDP-to-debt ratio rises, the payable interests increase. In addition to imposing state-contingent financing costs, GDR bonds provide a new signaling device for the issuing government. Even if credit markets have very pessimistic growth projections, GDR bonds can still offer competitive risk-return profiles to reluctant investors, *given* that the issuing government can credibly commit itself to a sustainable deleveraging. In case of insurmountable limited commitment concerns by potential investors, equipping GDR bonds with an embedded put option written by a third counterparty, i.e., similar to puttable bonds, could foster the enforceability of previous deleveraging commitments. The assertiveness of the former European Troika in the Eurozone's recent debt renegotiations provides some evidence for such a supranational party's potential enforcement power (see discussion in Section 4.5).

---

[6] Examples comprise trade disruption or reputational costs for the defaulting government (see Section 4.3).

[7] In contrast to the analysis of puttable debt within the model of Collard et al. (2015), increased refinancing pressure here occurs due to high perceived default probabilities, instead of tighter credit market conditions. Lane (2012) provides an intuitive explanation, how—in the presence of high indebtedness—sudden shifts in sentiments can cause a multicountry currency union to jump from a sustainable equilibrium to one with highly increased yields and unsustainable debt levels. In the context of the Eurozone, such effects were likely amplified by internal flights-to-safety. Indeed, the empirical evidence of De Grauwe and Ji (2012) suggests a significant effect of negative market sentiments on the spreads of Greece, Ireland, Portugal, and Spain between 2010 and 2011. Up to the introduction of OMT, the severe effects of market sentiments were also pointed out by both the International Monetary Fund (IMF) (source: IMF Global Financial Stability Report, April 2012, `http://www.imf.org/external/pubs/ft/gfsr/2012/01/`) and the ECB (source: Draghi, M., ECB press conference, September 6, 2012, `http://www.ecb.europa.eu/press/pressconf/2012/html/is120906.en.html`).

We conduct a sensitivity analysis of optimal government borrowing under (i) standard sovereign debt, (ii) puttable debt, and (iii) GDR bonds. In the context of all three instruments, we confirm the model's capability to deliver intuitive results with respect to its parameters. For instance, we find the government's optimal borrowing rate to be increasing in GDP growth, U-shaped in growth volatility (manageable versus unmanageably high growth risk), and to decrease in consumer risk aversion and default costs. Moreover, GDR bonds' state-contingency reduces the interest burden during times of low growth. This allows the issuing government to deleverage less dramatically than under standard or puttable debt, while keeping its default probability constant.

Third, in order to evaluate the welfare implications of state-contingent debt in the presence of default costs, we run a case study calibrating our model to the five Eurozone countries whose bond yields were most heavily affected by the debt crisis: Portugal, Ireland, Italy, Greece, and Spain. We calibrate country-specific default costs to match historical default probabilities implied by sovereign credit ratings prior to the ECB's OMT announcement. We find that, across growth scenarios, switching from standard to puttable debt leads to welfare improvements.

In comparison to puttable debt, GDR bonds consistently yield superior utility levels. Contrary to former's simple insurance mechanism, GDR bonds' state-contingent interest charges allow the risk-averse representative agent to considerably smooth her within-period consumption path. Hence, in our calibration, GDR bonds' consumption smoothing effect outweighs puttable debt's more substantial reduction in expected default costs. Moreover, we show that even for very pessimistic growth projections (i.e., the fifth percentile of historical growth rates), GDR bonds' expected Sharpe ratios are around unity (or even higher) for all five countries.

Our paper relates to the literature on state-contingent sovereign bonds. Emerging economies regularly face the risk of exogenous and undiversifiable income shocks that may cause capital flow reversals and potentially lead to severe contractions. In order to provide developing countries the possibility to hedge themselves against non-contractible shocks, Caballero (2003) proposes the International Monetary Fund (IMF) to supply a market for state-contingent bonds. Such bonds would reduce refinancing pressure in case of a severe income shock by, e.g., relating interest payments to income flows or by offering state-contingent insurance payments.[8] Caballero's (2003) proposal can be viewed as an alternative to the IMF's already existing contingent credit lines for emerging economies. The potentially stabilizing properties of puttable sovereign bonds for emerging countries without access to interest rate derivative markets are pointed out by Neftci and Santos (2003).

GDP-linked securities represent the most prominent example of state-contingent sovereign debt discussed in the literature. Shiller (1994, 2003) argues for macro markets to trade GDP-linked perpetual claims on fractions of countries' respective GDP. Borensztein et al. (2004) identify four major benefits of GDP-linked bonds over standard sovereign bonds: (i) lower like-

[8] As an example for the latter, Caballero (2003) argues that "Chile could eliminate most, if not all, of its deep recessions by embedding into its external bonds a long-term put option, yielding US$ 6-8 billions when the price of copper [its main export commodity] falls by more than two standard deviations" (Caballero, 2003, p. 34). In the context of private corporations, Chidambaran et al. (2001) discuss how the gold-mining company Freeport McMoRan's usage of gold-linked depository shares helped to reduce its financing costs.

lihood of sovereign defaults, (ii) fewer damaging pro-cyclical fiscal policy implementations, (iii) the opportunity for a smoother intertemporal tax path, and (iv) lower likelihood of government overspending during booms.[9] In the context of the Eurozone's recent debt crisis, the stabilizing effects of GDP-linked bonds on the public finances of advanced economies have repeatedly been emphasized by Barr et al. (2014) and Blanchard et al. (2016), among others.

Naturally, our paper also relates to the numerous alternative proposals brought forward in response to the currency union's vulnerability to surging public debt levels. The so-called 'Eurobonds', probably the most prominently discussed of all suggestions, refer to government bonds jointly issued by all Eurozone member countries. Since their credit risk relies on the solvency of the Eurozone as a whole, the associated reduction in the risk of destabilizing attacks on national government bond markets would be substantial (Favero and Missale (2012)).

The general concern among fiscally stronger member states (Germany in particular) has been that Eurobonds could incentivize less disciplined member states to overborrow. Henderson and Pearson (2011) share this concern and consequently propose the introduction of common senior debt with maturity of less than one year called 'Eurobills' aiming at easening debt rollover for Eurozone countries. Eurobills would be introduced permanently and participation in the market tied to compliance with certain governance criteria. Brunnermeier et al. (2011) suggest the creation of a 'European Debt Agency' that would buy national sovereign bonds up to 60% of GDP for each member country. By securitization and the re-issuance of different tranches of bonds, it could satisfy the demand for a safe asset which should also be used as main collateral in central bank liquidity operations.

The remainder of the paper is organized as follows. Section 4.2 analyzes the effects of puttable debt for a shortsighted risk-neutral government in the absence of default costs. While allowing for default costs, Section 4.3 additionally introduces GDR bonds in the context of a continuously consuming risk-averse agent. In Section 4.4, relative welfare effects of both puttable and GDR bonds relative to standard sovereign debt are estimated based on an empirical case study. Section 4.5 discusses potential implementation issues of GDR bonds and presents our concluding remarks.

4.2 Puttable Debt in the Absence of Default Costs

Motivated by OMT's implicitly written put option, we begin our analysis of state-contingent debt by introducing puttable bonds into a stylized model of sovereign borrowing, where default does not cause any costs to the defaulting government. We deliberately choose this starting point, as the absence of default costs allows for a useful benchmark assessment of puttable bonds' potential welfare effects.

In summary, if costs of default are negligible, Merton's (1974) reinterpretation of risk-adjusted spreads as put options can be explicitly verified within Collard et al.'s (2015) closed model of endogenous government borrowing. This insight proves valuable when evaluating put-

[9] For a detailed literature overview on GDP-linked bonds see, e.g., Barr et al. (2014).

table debt's welfare enhancing reduction in default risk in the presence of nonzero default costs as introduced in Section 4.3.

Abstracting from any kind of default costs is similar to the assumption of a shortsighted government discussed in Rochet (2006) and Collard et al. (2015).[10] Shortsighted governments always borrow as much as possible, since they do not take future repayments into account. Under this extreme assumption, sovereign debt levels are capped *only* by credit markets' willingness to lend.

Furthermore, we start by assuming lenders to be shortsighted as well, i.e., in the sense that interest spikes from the distant past do not make them anticipate any potential tightening of credit availability in the future. In other words, until confronted by a credit shock, they regard the risk-free interest rate as constant. This assumption is not crucial, but considerably simplifies the model's introduction, and is subsequently relaxed when we analyze puttable debt as response to increasing refinancing costs.

4.2.1 Government Borrowing

Relying on Collard et al.'s (2015) notation, we denote by Y_t the country's GDP at period t, by b_t the incumbent government's date-t proceeds from issuing zero-coupon debt with face value d_t maturing at $t+1$, both expressed as fractions (denoted in lowercase) of Y_t, and by α the government's primary surplus, also expressed as a fraction of Y_t and assumed to be constant over time. At any given date t, publicly financed consumption c_t is given by

$$c_t = ((1-\alpha) + b_t)Y_t - d_{t-1}Y_{t-1}, \tag{4.1}$$

i.e., private consumers receive the sum of their income net of the government's surplus and new borrowing proceeds net of expenses from repaying maturing government debt. Intuitively, sovereign default then occurs at $t+1$ if

$$(\alpha + b_{t+1})Y_{t+1} < d_t Y_t, \tag{4.2}$$

i.e., if the sum of primary surplus and proceeds from newly issued debt are insufficient to repay its current creditors.[11] We assume that even in case of default, publicly financed consumption is never negative, i.e., $c_t \geq 0$.

[10] Collard et al. (2016) argue that the therefrom deduced concept of 'excusable default'—governments only default on maturing debt if their budget constraint does not allow them to repay—better explains empirically observed sovereign debt levels than the more familiar concept of 'strategic default'.

[11] This condition of sovereign default is different from Eaton and Gersovitz' (1981) concept of strategic default. Collard et al. (2015) refer to mounting empricial evidence that most sovereigns do not default voluntarily. Moreover, Collard et al. (2016) show that calibrated 'excusable' default models, i.e., in the spirit of Cond. (4.2), yield much more realistic debt-levels than models of strategic default.

Collard et al. (2015) assume zero recovery in default.[12] Given its shortsightedness, the government aims to maximize the proceeds from borrowing at every date t. Hence, its t-proceeds from borrowing are then given by

$$b_t = \max_{d_t} \frac{d_t}{1+R_t} \mathbb{P}((\alpha + b_{t+1})Y_{t+1} \geq d_t Y_t), \tag{4.3}$$

where R_t denotes the market-implied risk-adjusted discount rate prevailing at t. Eq. (4.3) simply states that investors are only willing to lend the discounted expected repayment value of the newly issued zero-coupon bond. Assuming risk-neutral and shortsighted credit markets, Eq. (4.3) can be written as

$$b_t = \max_{d_t} \frac{d_t}{1+r} \mathbb{P}((\alpha + b_{t+1})Y_{t+1} \geq d_t Y_t), \tag{4.4}$$

where r refers to the risk-free interest rate, initially regarded as time-invariant by lenders.

The right-hand side of Eq. (4.4) exhibits a 'Laffer curve property'. At the maximum, the effects of increasing debt levels and default probabilities offset each other. Cond. (4.2) is equivalent to

$$(\alpha + b_{t+1})g_{t+1} < d_t,$$

where $g_{t+1} \equiv Y_{t+1}/Y_t$ denotes the continuous growth rate between date t and $t+1$ assumed to be i.i.d. with cdf $F(\cdot)$. Thus, relying on future borrowing proceeds b_{t+1}, the government avoids default at $t+1$ with probability

$$\mathbb{P}((\alpha + b_{t+1})g_{t+1} \geq d_t) = \mathbb{P}\left(g_{t+1} \geq \frac{d_t}{\alpha + b_{t+1}}\right) \equiv 1 - F\left(\frac{d_t}{\alpha + b_{t+1}}\right).$$

Collard et al. (2015) define maximum sustainable borrowing b_M as the fixed point

$$b_M = \frac{\alpha + b_M}{1+r} g_M (1 - F(g_M)), \tag{4.5}$$

where

$$(\alpha + b_M)g_M \equiv d_M$$

identifies maximum sustainable debt d_M and g_M satisfies

$$g_M = \arg\max_g g(1 - F(g)). \tag{4.6}$$

We now introduce a credit shock scenario as presented in Figure 4.1. After many consecutive periods with low risk-free rates r_L, an unanticipated shock at t tightens credit availability. This has two immediate effects: First, the risk-free rate rises from r_L to r_H. Second, shortsighted lenders are reminded of interests' time variability, which directly affects their willingness to lend,

[12] Alternatively, one could assume that creditors can (partially) claim the government's primary surplus upon default. However, even if creditors receive the entire primary surplus, the maximum sustainable debt in Collard et al. (2015) only increases slightly, due to its very low associated default probability.

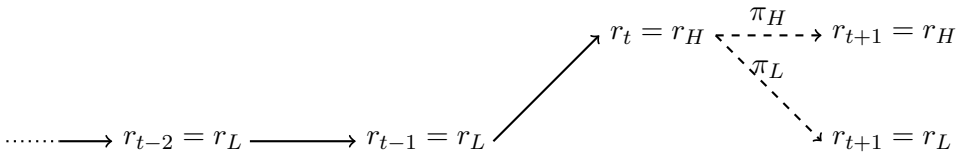

FIGURE 4.1. UNEXPECTED RISE IN RISK-FREE INTEREST RATES

Notes: This figure illustrates a rare and unanticipated tightening of credit market conditions at t, modeled by an increase in the risk-free interest rate r_t from r_L to r_H. Thereafter, credit markets become aware of interest rates' stochastic nature and form beliefs about future risk-free rates at $t+1$: either r_{t+1} stays at r_H with probability π_H, or it decreases to r_L with probability $\pi_L = 1 - \pi_H$.

i.e., Eq. (4.4) becomes

$$b_t = \max_{d_t} \frac{d_t}{1+r_H} \mathbb{P}((\alpha + b_{t+1})Y_{t+1} \geq d_t Y_t), \tag{4.7}$$

i.e., the discount rate increases to r_H.

Given the present interest rate shock, lenders *now* consider interest rates to be random but stationary, i.e.,

$$r_s \overset{\text{i.i.d.}}{\sim} r \sim r_L + B(1, \pi_H)(r_H - r_L) \;\; \forall s \geq t+1, \tag{4.8}$$

where $B(1, \pi_H)$ denotes a Bernoulli distribution with 'success' probability π_H. Defining $\beta_t \equiv (1+r_t)b_t$ and recalling the stationarity of the country's growth rate, i.e., $g_s \overset{\text{i.i.d.}}{\sim} g \;\; \forall s \geq t+1$, we can rewrite Eq. (4.7) as

$$\beta_t = \max_{d_t} d_t \mathbb{P}\left(\left(\alpha + \frac{\beta_{t+1}}{1+r}\right) g \geq d_t\right).$$

With stochastic interest rates as defined in Eq. (4.8), maximum sustainable debt d_M becomes a function of β_M given by

$$d_M(\beta_M) = \arg\max_d d\left(1 - \pi_L \underbrace{F\left(\frac{d}{\alpha + \frac{\beta_M}{1+r_L}}\right)}_{\substack{\text{default probability} \\ \text{given } d \text{ if } r = r_L}} - \pi_H \underbrace{F\left(\frac{d}{\alpha + \frac{\beta_M}{1+r_H}}\right)}_{\substack{\text{default probability} \\ \text{given } d \text{ if } r = r_H}}\right), \tag{4.9}$$

where maximum sustainable borrowing $b_M(t) = \beta_M/(1+r_t)$ is state-dependent and β_M is the corresponding fixed point, i.e.,

$$\beta_M = d_M(\beta_M)\left(1 - \pi_L F\left(\frac{d_M(\beta_M)}{\alpha + \frac{\beta_M}{1+r_L}}\right) - \pi_H F\left(\frac{d_M(\beta_M)}{\alpha + \frac{\beta_M}{1+r_H}}\right)\right). \tag{4.10}$$

Due to the uncertainty about future interest rates, maximum sustainable debt in Eq. (4.9) is no longer indirectly implied by g_M in Eq. (4.6), but instead needs to take into account r's binomial distribution and the state-dependent default thresholds.

As demonstrated by Rochet (2006), assuming g to be uniformly distributed on $[1 + \mu_g -$

$\sigma_g, 1+\mu_g+\sigma_g]$, Eq. (4.9) and Eq. (4.10) then imply

$$d_M = \frac{1+\mu_g+\sigma_g}{2\left(\frac{\pi_L}{\alpha+\frac{\beta_M}{1+r_L}}+\frac{\pi_H}{\alpha+\frac{\beta_M}{1+r_H}}\right)} \tag{4.11}$$

$$\beta_M = \frac{(1+\mu_g+\sigma_g)^2}{8\sigma\left(\frac{\pi_L}{\alpha+\frac{\beta_M}{1+r_L}}+\frac{\pi_H}{\alpha+\frac{\beta_M}{1+r_H}}\right)}. \tag{4.12}$$

The following lemma gives the closed form solution to Eq. (4.12), on which we rely for our analysis of puttable debt below.

Lemma 4.1. *If* $(r_L, r_H) \in [0,1)\times[0,1)$, $g \sim U[1+\mu_g-\sigma_g, 1+\mu_g+\sigma_g]$, *and* $(1+\mu_g+\sigma_g)^2(8\sigma)^{-1} < \mathbb{E}[1+r]$, *then the fixed point in Eq. (4.12) is given by*

$$\beta_M = \frac{-B-\sqrt{B^2-4AC}}{2A} > 0,$$

where

$$A := \frac{(1+\mu_g+\sigma_g)^2}{8\sigma} - \mathbb{E}[1+r]$$

$$B := \alpha\left(\frac{(1+\mu_g+\sigma_g)^2}{8\sigma}(2+r_L+r_H) - (1+r_L)(1+r_H)\right)$$

$$C := \alpha^2\frac{(1+\mu_g+\sigma_g)^2}{8\sigma}(1+r_L)(1+r_H).$$

Proof. For proof see Appendix A4. □

4.2.2 Refinancing Costs During Credit Shock: Standard versus Puttable Debt

Suppose now that the government is given the possibility to buy protection against increased refinancing costs at t by issuing puttable instead of standard debt. The main difference between puttable and standard debt is that the former insures investors against sovereign default, i.e., in case of default at $t+1$, a third party guarantees to repay them in full. From investors' perspective, assuming the insurance writer to be sufficiently solvent, such puttable bonds correspond to a risk-free investment. We impose the following conditions for issuing puttable debt at t:

C1. The government's date-t proceeds may not surpass $b_M(t)$, i.e., they may not be higher than in the absence of puttable bonds.

C2. The government is required to ex-ante compensate the guarantor for the *initial* default risk taken over, i.e., for the default risk in absence of puttable bonds.

C3. The government is only allowed to issue puttable bonds, if the payment of the ex-ante insurance premium does not cause it to already default at t.

TABLE 4.1. STANDARD VS. PUTTABLE DEBT

	Standard debt	Puttable debt
Type	zero-coupon	zero-coupon
Insurance	no	yes
Ex-ante premium	none	put price p_t
Spread	$R_t \equiv \frac{d_M}{b_M(t)} - 1$	risk-free rate r_t

Notes: This table compares standard and puttable debt available to the government to refinance its debt at t. R_t denotes the spread on date-t borrowing proceeds $b_M(t)$ to be paid to investors at $t+1$, if the government chooses standard debt. In case it chooses to issue puttable debt, p_t denotes the ex-ante premium to be paid by the issuing government to the insurance provider at t.

Condition C1 is intuitive given the intended risk managing character of puttable debt. Hence, it would be counterproductive, if sovereigns would be allowed to borrow more in the presence of high interest rates than available under low refinancing costs. In fact, C1 prevents higher borrowing due to a risk-shifting effect. C2 directly manifests itself in the ex-ante payable insurance premium (see below). Finally, C3 is simply imposed by the government's budget constraint which does not allow for negative consumption *after* borrowing proceeds.

Table 4.1 contrasts the government's two refinancing options at date t in more detail. For the issuing government, the refinancing costs of standard and puttable debt differ in two dimensions: on the one hand, the issuance of puttable bonds requires an ex-ante payment to the insurance guarantor at t. This premium compensates the third party for providing investors with insurance against sovereign default. The date-t value of the insurance p_t corresponds to the price of an European put option on sovereign debt with maturity $t+1$ and a strike price equal to the debt's face value plus accrued interests. On the other hand, the issuing government is in return protected against higher interests on its date-t borrowing proceeds due at $t+1$. Since investors are insured against default risk, the payable interests on $b_M(t)Y_t$ are reduced from the default-adjusted spread R_H to the current risk-free rate r_H, where

$$R_H \equiv \frac{d_M}{b_M|R_H} - 1,$$

and $b_M|R_H$ denotes maximum sustainable borrowing under high (default adjusted) interest rates.

Moving to an *intertemporal* perspective, the discounted expected sum of current and future publicly financed consumption equals

$$\mathbb{E}\left[\sum_{s\geq t} \delta^{s-t} c_s\right], \tag{4.13}$$

where δ is the discount factor and c_s is given by Eq. (4.1). Note that, for $\delta < 1$, the borrowing policy in Eq. (4.10) is consistent with the maximization of Eq. (4.13) by a risk-neutral govern-

TABLE 4.2. CONSUMPTION UNDER STANDARD VS. PUTTABLE DEBT (NO DEFAULT COSTS)

	Standard debt (1)	Puttable debt (2)	Δ (1)−(2)
Consumption at t	c_t	$c_t - p_t$	p_t
Discounted expected consumption at $t+1$	$\delta\mathbb{E}[c_{t+1}\|R_H]$	$\delta\mathbb{E}[c_{t+1}\|r_H]$	$\delta b_M(t)\,(r_H - R_H)\,Y_t$

Notes: This table compares current and future publicly financed consumption levels under the issuance of standard and puttable debt, given an increase in the risk-free rate from r_L to r_H at t. The third column lists the differences at t and $t+1$ from the perspective of a risk-neutral government. p_t denotes the date-t put price, δ the government's discount factor, $b_M(t)$ date-t maximum borrowing under stochastic interest rates, and R_H the default-adjusted spread based on r_H.

ment who is indifferent towards variations in private consumption. A risk-averse government, in contrast, might have an incentive to smooth private consumption across time by borrowing less if production is very high in order to avoid future default. In Section 4.3, we account for such consumption smoothing benefits by introducing a risk-averse consumer.

Consistent with the above analysis, we can rewrite date-t private consumption as

$$c_t = ((1-\alpha) + b_M(t))Y_t - d_{t-1}Y_{t-1},$$

and at $t+1$, given a preceding refinancing with standard debt, as

$$c_{t+1}|R_H = ((1-\alpha) + b_M(t+1))Y_{t+1} - b_M(t)(1+R_H)Y_t,$$

where we rely on the identity $b_t(1+R_t) \equiv d_t$ with $R \in \{R_L, R_H\}$ denoting the state-dependent spread to be paid by the government on its borrowing proceeds.

In the presence of puttable debt, refinancing public debt with puttable bonds reduces date-t private consumption by the put option premium, i.e.,

$$c_t - p_t,$$

where at $t+1$ the put option either pays $b_M(t)(1+R_H)Y_t$ in case of default (zero recovery) or nothing otherwise. Note that the put option's strike price is set equal to the borrowing proceeds' face value plus accrued interests in absence of puttable debt (see C2 above). At $t+1$, due to the lower spread charged by insured investors, private consumption increases to

$$c_{t+1}|r_H = ((1-\alpha) + b_M(t+1))Y_{t+1} - b_M(t)(1+r_H)Y_t,$$

where it holds that $c_{t+1}|r_H \geq c_{t+1}|R_H$. The (discounted) differences in (expected) private consumption from issuing either standard or puttable debt are summarized in Table 4.2.

Lemma 4.2. *If $g \sim U[1+\mu_g-\sigma_g, 1+\mu_g+\sigma_g]$, then a risk-neutral government facing no default*

costs is indifferent between issuing standard or puttable debt in response to a credit shock.

Proof. For proof see Appendix A4. □

Lemma 4.2 is in line with Merton (1974), implying that the put option price p_t is equal to the discounted spread $\delta(R_H - r_H)$ to be paid on the borrowing proceeds $b_M(t)Y_t$ financed by puttable bonds. In other words, a risk-neutral government's disutility from having to pay the insurance premium at t is exactly offset by higher private consumption due to lower interest payments at $t+1$. Hence, as long as there are no default costs, a risk-neutral government is indifferent between issuing standard or puttable debt in response to an increase in interest rates.

Proposition 4.1. *If $R_H > r_H$ and the probability of default under standard debt with spread R_H is nonzero, then the issuance of puttable debt always decreases the risk of sovereign default. In particular, if $g \sim U[1+\mu_g-\sigma_g, 1+\mu_g+\sigma_g]$ and $b_M(t)(1+R_H)/(\alpha+b_M(t+1)) > 1+\mu_g-\sigma_g$, then moving from standard to puttable debt decreases the government's default probability by*

$$\min\left(\frac{b_M(t)(R_H-r_H)}{2\sigma_g\left(\alpha+b_M(t+1)\right)}, \frac{\frac{b_M(t)(1+R_H)}{\alpha+b_M(t+1)}-(1+\mu_g-\sigma_g)}{2\sigma_g}\right),$$

where the first (second) term applies in case of a nonzero (zero) default probability under r_H.

Proof. For proof see Appendix A4. □

So far we have been abstracting from any costs to be borne by a defaulting sovereign. However, as soon as we introduce such sovereign default costs, Proposition 4.1 has important implications: reducing a government's default probability attenuates expected disutilities from default and, therefore, enhances social welfare. Hence, facing non-negligible default costs, even a risk-neutral government may be better off provided access to puttable bonds when facing increasing refinancing costs.

Furthermore, in the presence of a risk-averse consumer, a comparison to the consumption-smoothing benefits from GDP-linked bonds springs to mind. How puttable debt's reduction in expected default costs compares to GDP-linked debt's decrease in consumption variability is the focus of the following two sections.

4.3 State-contingent Borrowing in the Presence of Default Costs

Our previous working assumption of zero default costs incurred by a defaulting sovereign is arguably unrealistic. Borensztein and Panizza (2009) distinguish among four different types of sovereign default costs: (i) reputational costs, (ii) international trade exclusion costs, (iii) costs due to negative shocks on the domestic banking system, and (iv) political costs borne by the incumbent government. They find that the economic costs are generally significant, but short-lived. However, sovereign defaults often bring far-reaching consequences for elected officials. The authors document that in 18 out of 19 cases studied, the ruling coalition lost votes following the default and their electoral support declined on average by 16%.

Probably more meaningful to our case is the indirect measure of default costs given by the sheer amount of fiscal tightening that has been accepted by the Hellenic government during its ongoing debt negotiations in return for numerous bailout packages. In March 2012, the Greek government and its counter parties, i.e., the European Commission, Eurogroup, ECB, and IMF, signed the 'Second Economic Adjustment Programme for Greece'.[13] The austerity measures imposed by this second bailout package revised the total amount of fiscal cost reductions to approximately 65 billion Euros between 2010 and 2014, which corresponded to more than 30% of Greece's then GDP.[14]

As soon as default imposes significant disutility on the defaulting government, the latter has incentives not to overborrow. Based on actual country-specific yield spreads, we calibrate these costs such that the implied default probabilities are in line with Merton's (1974) equivalence result. Instead of following Collard et al. (2015), we adopt a simpler one-shot perspective, where a risk-neutral government trades off publicly financed private consumption against expected default costs when choosing its optimal borrowing rate. Given the intended temporary nature of the hereafter considered refinancing instruments, we deem such a one-period view appropriate.[15] In particular, our starting point is an already highly indebted government whose bonds contain a considerable default risk and therefore impose high refinancing costs. In contrast to the analysis of puttable debt within the model of Collard et al. (2015), increased refinancing pressure here occurs due to high perceived default probabilities, instead of tighter credit market conditions.

Within this new setting, we compare utility gains from state-contingent refinancing instruments. In particular, similar to Blanchard et al. (2016), we now also consider GDP-linked debt. To allow such debt instruments to be welfare improving, we introduce a risk-averse consumer who optimizes her utility from publicly financed consumption conditional on the government's borrowing policy. In order to account for the time discrepancy between private consumption decisions and changes to public budget plans, the former are modeled continuously. Solving for private consumption in continuous time also allows us to consider the imperfect foreseeability of future debt levels due to deviations of private consumption from expectations, while fully accounting for GDP-linked debt's intertemporal consumption smoothing effect.

In contrast to standard GDP-linked bonds, we introduce bonds linked to a country's GDP-to-debt ratio, referred to as GDR bonds, where interest payments *inversely* depend on a government's *relative indebtedness*, i.e., implying counter-cyclical interest rate dynamics with respect to relative indebtedness. If a country's relative indebtedness increases, interest payments on GDR bonds decrease and vice versa. Thanks to GDR bonds' variable interest rates, negative shocks in GDP lead to a lower interest burden, relaxing the sovereign's refinancing pressure. In addition to imposing state-contingent financing costs, GDR bonds provide a new signaling device for the issuing government. Even if credit markets have very pessimistic growth projec-

[13]The second package was followed by a third bailout package signed in 2015.

[14]Source: Excessive austerity killing Greece, *Kathimerini (English edition)*, September 30, 2012, http://www.ekathimerini.com/145032/article/ekathimerini/business/excessive-austerity-killing-greece.

[15]In addition, it allows us to calibrate the model to data from highly indebted Eurozone countries in Section 4.4. A model based on Collard et al. (2015) could not account for realistic default probabilities given the historically low GDP growth volatilities.

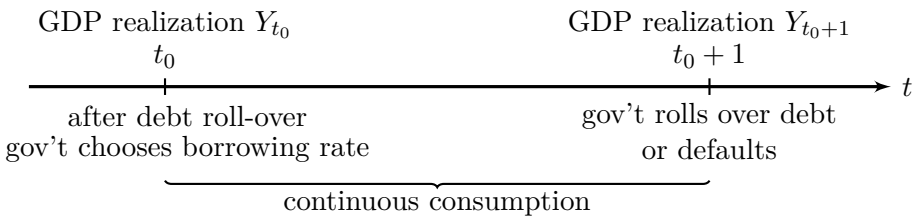

FIGURE 4.2. TIMING OF DEBT REFINANCING WITH CONTINUOUS CONSUMPTION

tions, GDR bonds can still offer competitive risk-return profiles to reluctant investors, assuming that the issuing government can credibly commit itself to a sufficient deleveraging.[16]

Figure 4.2 summarizes the timing of our model where the government chooses its borrowing rate at t_0 which then remains fixed until $t_0 + 1$. During the period, a risk-averse consumer continuously maximizes her utility from publicly financed consumption, conditional on the government's fixed borrowing policy. At $t_0 + 1$, the government either refinances its debt (and sets a new borrowing rate) or defaults.

4.3.1 Dynamics - Indebtedness and GDP

The state variable of interest is a sovereign's annual GDP in relation to its accumulated public debt.[17] More specifically, we assume the following dynamics

$$dY_t = Y_t \left(\mu_Y dt + \sigma_Y dB_t\right), \tag{4.14}$$

where Y_t denotes the country's rolling annual GDP and B_t a standard Brownian motion. In addition, we model the dynamics of sovereign debt as

$$dD_t = D_t \mu_D dt, \tag{4.15}$$

where D_t corresponds to government date-t debt. Since we are considering a short-term decision problem (one-period borrowing under the risk of default), we consider it sensible to model the sovereign's real GDP growth rate μ_Y and GDP volatility σ_Y to be exogenous and constant over the considered time period. The proposed dynamics are consistent with Collard et al. (2015), who assume log-normally distributed growth rates. At the beginning of the period, i.e., at t_0, a country's government chooses its borrowing rate μ_D subject to its budget constraint.

We assume a country's short-term wealth W_t disposable for consumption to be additive in

[16] In case of irreconcilable limited commitment concerns of potential investors, equipping the GDR bonds with a puttable component could foster the enforceability of initial deleveraging commitments. See also Section 4.5.

[17] This is in analogy to the third criterion of the euro convergence criteria (also known as the Maastricht criteria) which were established in 1992.

Y_t and D_t,[18] i.e.,

$$dW_t := (1-\alpha)\, dY_t + (\mu_D - R)\, D_t dt - c_t dt, \quad W_{t_0} := (1-\alpha) Y_{t_0} + D_{t_0}. \tag{4.16}$$

Here, c_t denotes the risk-averse consumer's continuous consumption and, as in Section 4.2, α indicates the country's primary surplus. Interest payments on government debt are given by RD_t, where R denotes the risk-adjusted interest rate, which is assumed constant over one period. Note that, in contrast to Section 4.2, R is now exogenous.

Under puttable government debt as described in Section 4.2, investors possess the option to put their bonds in case the country's debt-to-GDP level exceeds a certain threshold, i.e., if the country defaults. This credit insurance is provided by an intergovernmental agency which, in return, is compensated with the corresponding insurance premium (payable ex-ante). As a result, the issuing government only pays the risk-free interest on its debt but has to pay a fixed fee to the insurance guarantor at issuance. The budget constraint then reads

$$dW_t := (1-\alpha)\, dY_t + (\mu_D - r)\, D_t dt - c_t dt, \quad W_{t_0} := (1-\alpha) Y_{t_0} + D_{t_0} - p_{t_0}, \tag{4.17}$$

where r denotes the constant risk-free interest rate and p_{t_0} corresponds to the put price at t_0, i.e., the ex-ante payable insurance premium, which lowers the initial wealth available for consumption.

The put price corresponds to the discounted value of the issued government debt multiplied by the probability of default. Assuming the insurance guarantor to be risk-neutral, the corresponding discount rate equals the risk-free rate.[19] The put price is then given by

$$p_{t_0} = e^{-r} D_{t_0} \mathbb{P}\left(\frac{D_{t_0+1} - (W_{t_0+1} - W_{t_0})}{Y_{t_0+1}} - \frac{D_{t_0}}{Y_{t_0}} > 0 \right), \tag{4.18}$$

where we impose, consistent with Section 4.2, zero recovery in default. For simplification, we assume that the country defaults whenever sovereign debt minus the change in disposable wealth relative to GDP is larger than the initial debt-to-GDP ratio. However, this somewhat strict default condition only has a small level effect and does not change our qualitative results. Moreover, in Section 4.4, we calibrate default costs such that the thereby induced default probability *under* the optimal borrowing rate is consistent with credit-rating-implied default risk. Since the debt-to-GDP ratio itself neglects changes in W_t between t_0 and $t_0 + 1$, we have to account for potential differences in disposable wealth due to the consumer's actual consumption. If she overconsumes, i.e., if she consumes more than production growth and public borrowing allows for, disposable wealth is reduced, which in turn increases the probability of sovereign default. We

[18] As in Section 4.2, we deliberately abstract from consumption financed by issuing private debt.

[19] Note that, in order to compute the put price, we consider that the government needs to pay the ex-ante risk-adjusted interest rate on its debt and neglect a lower interest rate's decreasing effect on the ex-post default probability. This is consistent with condition C2 in Section 4.2. Consequently, our estimated put price reflects a conservatively high estimate, as issuing puttable debt arguably reduces the chance that the put is exercised. Hence, a lower put price could possibly be negotiated, unless the intergovernmental agency has full bargaining power.

implicitly assume that all produced goods need to be consumed within one period and cannot be stored for later times.[20]

4.3.2 Government Borrowing with GDR Bonds and Default Costs

The government chooses its optimal borrowing rate subject to maximizing expected utility from consumption of its risk-averse consumer, while simultaneously accounting for default risk. We solve the government's optimization problem by backward induction. First, following Merton's (1969) lifetime portfolio allocation approach, we determine the consumer's optimal consumption over time for a given constant borrowing rate μ_D set by the government. We model the risk-averse consumer as a representative agent with CRRA-utility. Given the borrowing rate μ_D, our representative agent chooses her optimal consumption plan $c_t^\star$ over a finite horizon, i.e., $\forall t \in (t_0, t_0+1)$, subject to her budget constraint. While doing so, she may consume more or less aggressively, depending on her time preference as well as the relative value she assigns to her end of period wealth. In addition, we assume that the representative agent, in contrast to the government, does not incorporate any default costs into her consumption decisions.

Let the dynamics of short-term wealth W_t disposable for consumption under GDR bonds be

$$dW_t := (1-\alpha)\, dY_t + \left(\mu_D dt - \frac{d\left(Y_t/D_t\right)}{Y_t/D_t}\right) D_t - c_t dt, \quad W_{t_0} := (1-\alpha)Y_{t_0} + D_{t_0}, \tag{4.19}$$

where $d\left(Y_t/D_t\right)/\left(Y_t/D_t\right)$ reflects the interest payments on GDR bonds, indicating the link between interest rates and relative indebtedness. The interest payments are increasing in changes in Y_t and decreasing in D_t. Note that our approach connects interest payments to the inverse of relative indebtedness, whereas only the borrowing rate can be set by the government.

We require the representative agent's budget constraint to be of multiplicative form of disposable wealth in order to ensure a closed-form solution to her optimal consumption problem. Therefore, we rewrite the budget constraint by substituting Eq. (4.14) and Eq. (4.15) in Eq. (4.19) as

$$dW_t = \left((1-\alpha)Y_t - D_t\right)\left(\mu_Y dt + \sigma_Y dB_t\right) + 2\mu_D D_t dt - c_t dt,$$

and restate

$$d\widetilde{W}_t = \widetilde{W}_t\left(\mu_Y dt + \sigma_Y dB_t\right) - \widetilde{c}_t dt, \quad \widetilde{W}_{t_0} := (1-\alpha)\, Y_{t_0} - D_{t_0}, \tag{4.20}$$

where $\widetilde{W}_t$ denotes the adjusted disposable wealth and $\widetilde{c}_t := c_t - 2\mu_D D_t$ adjusted consumption.[21]

We apply dynamic programming (see, e.g., Merton (1969)) to solve for the CRRA-representative agent's optimal consumption path

$$\widetilde{c}_t^\star = \arg\max_{\widetilde{c}_t} \mathbb{E}\left[\int_{t_0}^{t_0+1} u(\widetilde{c}_s, s)\mathrm{ds} + \bar{u}(\widetilde{W}_{t_0+1}, t_0+1)\right], \tag{4.21}$$

[20] In addition, we neglect investments which Gali et al. (2007) have shown to remain unaffected by a shock in government spending.

[21] Under standard as well as puttable debt, the necessary restatement of the corresponding budget constraints in Eq. (4.16) and Eq. (4.17) is achieved by setting $\widetilde{W}_{t_0} := (1-\alpha)Y_{t_0}$ and $\widetilde{c}_t := c_t - (\mu_D - R)D_t$. The resulting (restated) budget constraint is equal to Eq. (4.20).

subject to the budget constraint in Eq. (4.20). It follows from CRRA-preferences that

$$u(\widetilde{c}_t, \widetilde{W}_t) = e^{-\rho t} \frac{\widetilde{c}_t^{1-\gamma}}{1-\gamma},$$

and utility of bequest

$$\bar{u}(\widetilde{W}_{t_0+1}, t_0+1) = e^{-\rho(t+1)} I(t_0+1) \frac{\widetilde{W}_{t_0+1}^{1-\gamma}}{1-\gamma},$$

for time preference $\rho \geq 0$ and risk aversion $\gamma > 0$, where $I(t_0+1)$ denotes the relative weight the consumer assigns to her end of period wealth.

Lemma 4.3. *The solution to the dynamic programming problem in Eq. (4.21) subject to the budget constraint in Eq. (4.20) is given by the optimal consumption plan*

$$\widetilde{c}_t^{\star} = \frac{\widetilde{W}_t}{\frac{1}{\phi} + e^{-\phi(t_0+1-t)} \left(I(t_0+1)^{\frac{1}{\gamma}} - \frac{1}{\phi} \right)}, \tag{4.22}$$

where

$$\phi = \frac{1}{\gamma} \left(\rho - (1-\gamma) \left(\mu_Y - \frac{\gamma \sigma_Y^2}{2} \right) \right).$$

Proof. For proof see Appendix A4. □

Finally, substituting $\widetilde{c}_t := c_t - 2\mu_D D_t$ into Eq. (4.22) yields the consumer's effective optimal consumption plan

$$c_t^{\star} = \frac{\widetilde{W}_t}{\frac{1}{\phi} + e^{-\phi(t_0+1-t)} \left(I(t_0+1)^{\frac{1}{\gamma}} - \frac{1}{\phi} \right)} + 2D_t \mu_D.$$

The variable c_t reflects the consumer's excess consumption and might take on negative values. In order to derive the utility of consumption, we add a base consumption level $\bar{c}$, assumed to be fixed in the short term (over one period). Adding $\bar{c}$ ensures that utility is derived from total consumption which itself is positive.

Second, having computed the optimal consumption path of the representative agent, we solve the government's optimization problem in terms of its optimal borrowing decision. The government aims to pick the optimal borrowing rate $\mu_D^{\star}$ that maximizes the expected utility of its risk-averse consumer while accounting for possible default costs.[22]

Once the government has chosen the optimal borrowing rate at t_0, the same cannot be changed until t_0+1. Hence, the government chooses $\mu_D^{\star}$ such that

$$\begin{aligned} \mu_D^{\star} &= \arg\max_{\mu_D} U_t(\mu_D) \\ &= \arg\max_{\mu_D} \mathbb{E}\Bigg[\underbrace{\int_{t_0}^{t_0+1} u(c_s^{\star} + \bar{c}, s)\mathrm{d}s + \bar{u}(W_{t_0+1}, t_0+1)}_{\text{utility of consumption and bequest}} - \underbrace{e^{-\rho}\Psi \mathbf{1}_{\{\eta > D_{t_0}/Y_{t_0}\}}}_{\text{discounted costs of default}} \Bigg], \end{aligned} \tag{4.23}$$

[22] Similar to Müller et al. (2016), we also model welfare to be additively separable in the utility of consumption and a linear default costs component.

where

$$\eta = \frac{D_{t_0+1} - (W_{t_0+1} - W_{t_0})}{Y_{t_0+1}}.$$

In Eq. (4.23), $c_s^\star$ denotes the representative agent's optimal time-dependent excess consumption at time s. W_{t_0+1} reflects the wealth at the end of the period as computed by $W_{t_0+1} = W_{t_0} + \int_{t_0}^{t_0+1} \mathrm{d}\widetilde{W}_s$. The last term in Eq. (4.23) corresponds to a risk-neutral government's expected default costs discounted to time t_0, imposing equal time preferences as for the representative consumer.

Proposition 4.2. *If expected default costs under GDR bonds are sufficiently high to incentivize the government to choose a bounded $\mu_D^\star$, then this $\mu_D^\star$ is unique.*

Proof. For proof see Appendix A4. □

In summary, when choosing its optimal borrowing rate, a heavily indebted government needs to optimally trade off higher accumulated consumption versus an increasing probability of default. GDR bonds might provide more space to reduce sovereign borrowing, while not too severely limiting consumption. Therefore, GDR bonds could potentially allow for more sustainable deleveraging policies.

4.3.3 Comparative Statics

The comparative statics analysis of the above refinancing instruments requires an analogous result as in Proposition 4.2 but for standard and puttable debt.

Corollary 4.1. *If expected default costs under standard debt and puttable debt are sufficiently high to incentivize the government to choose a bounded $\mu_D^\star$, then this $\mu_D^\star$ is unique.*

Proof. For proof see Appendix A4. □

Figure 4.3 presents the comparative statics of a government's optimal borrowing rate $\mu_D^\star$ under standard sovereign debt, puttable debt, and GDR bonds.[23] Similarly, Figure 4.4 displays the comparative statics of the corresponding default probabilities given the government's optimal borrowing rate $\mu_D^\star$. By referring to the various plots in Figure 4.3 and Figure 4.4, we are able to make several interesting statements regarding the sensitivity of $\mu_D^\star$ and the implied default probability with respect to changes of model parameters:

[23] Theoretically, by applying the implicit function theorem, one can derive the sensitivity of the optimal borrowing rate with respect to model parameters. However, since the optimal borrowing rate depends on intertemporal utility of consumption, we cannot compute closed-form solutions as, to the best of our knowledge, its integral over time can only be solved numerically. This prevents us from applying the implicit function theorem with respect to most parameters. There is one important exception: We can compute the sensitivity of the optimal borrowing rate with respect to default costs under all three refinancing instruments, as they only influence the expected default costs but not intertemporal consumption. We find that $\partial \mu_D^\star / \partial \psi < 0 \ \forall \psi \in \mathbb{R}^+$. Derivations are available on request.

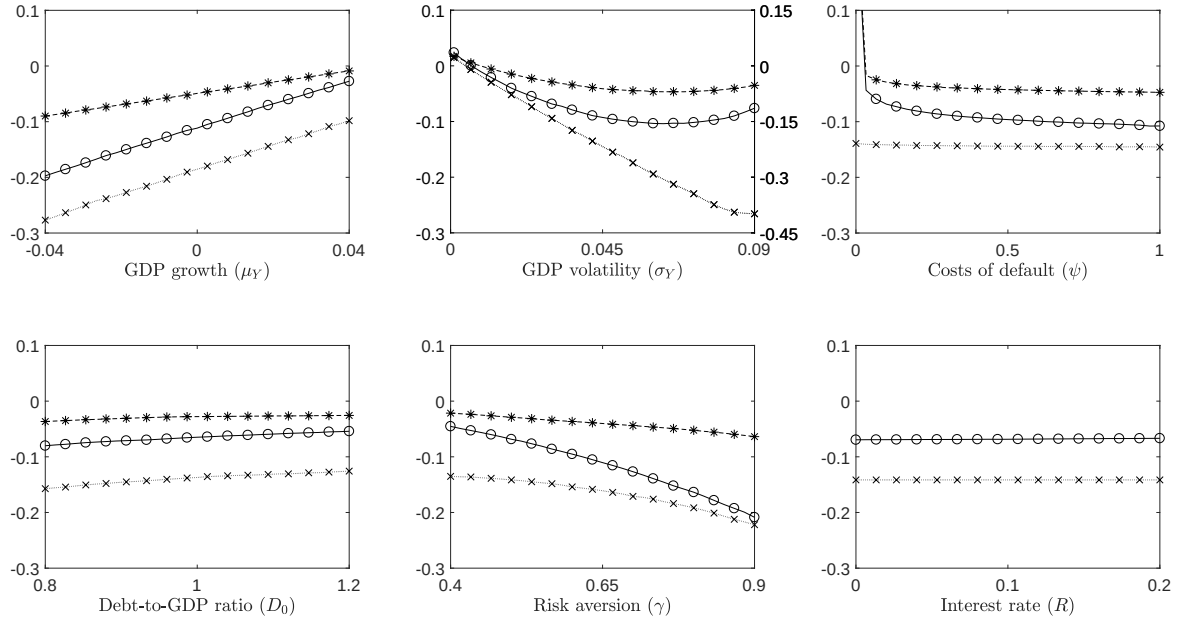

FIGURE 4.3. COMPARATIVE STATICS OF THE OPTIMAL BORROWING RATE

Notes: This figure shows the government's optimal borrowing rate $\mu_D^\star$ under the three refinancing instruments, i.e., standard sovereign debt (solid, circles), puttable debt (dotted, crosses), and GDR bonds (dashed, asterisks), with respect to model parameters. Initial values: $\mu_Y = 0.02$, $\sigma_Y = 0.03$, $Y_0 = 1$, $D_0 = 0.95$, $\alpha = 0.03$, $\rho = 0.03$, $\gamma = 0.5$, $I(t_0 + 1) = 10$, $\Psi = 0.1$. Note that, for GDP volatility, $\mu_D^\star$ under puttable bonds is depicted on the right axis.

1. Unsurprisingly, the optimal borrowing rate is increasing in GDP growth. This is intuitive since a higher GDP growth rate allows to accelerate debt-financed consumption without increasing relative indebtedness. Thanks to lower interest expenses under low growth, relying on GDR bonds enables the government to borrow more than under standard or puttable debt without increasing the implied default probability. Regardless of the level of μ_Y, the probability of default remains very low under standard debt and GDR bonds, and close to zero under puttable debt. A change in the GDP growth rate has a negligible impact on the default probability under all three refinancing instruments.

2. The uncertainty of future GDP growth and the optimal borrowing rate under standard and GDR bonds feature a U-shaped relationship. For very low levels of σ_Y, i.e., in an almost deterministic model, we observe an optimal borrowing rate that induces the debt-to-GDP ratio to approach but not to cross the default threshold. However, once the growth shocks become non-negligible, the government's optimal borrowing rate decreases significantly. In order to prevent the risk of large enough negative shocks that could trigger default, it is optimal to preemptively smooth out the potential destabilizing effects on relative indebtedness by borrowing less. However, GDR bonds' variable interest rates alleviate the risk of such shocks, thereby lowering the government's need to further reduce borrowing.

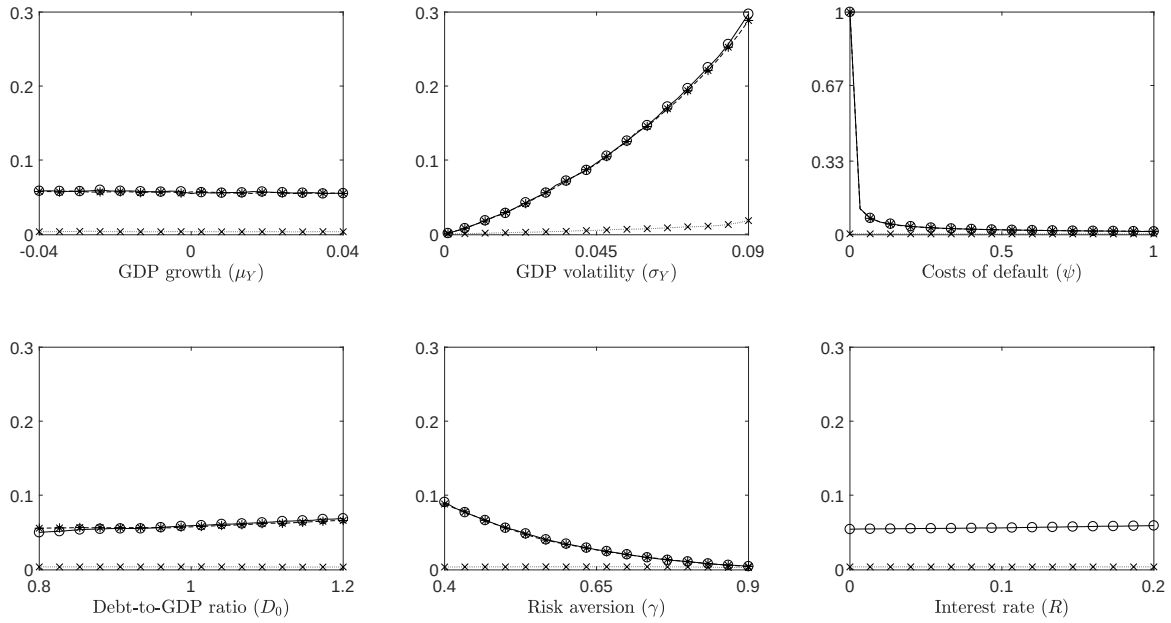

FIGURE 4.4. COMPARATIVE STATICS OF THE PROBABILITY OF DEFAULT GIVEN OPTIMAL BORROWING

Notes: This figure shows the government's probability of default given given the optimal borrowing rate $\mu_D^\star$ under the three refinancing instruments, i.e., standard sovereign debt (solid, circles), puttable debt (dotted, crosses), and GDR bonds (dashed, asterisks), with respect to model parameters. Initial values: $\mu_Y = 0.02$, $\sigma_Y = 0.03$, $Y_0 = 1$, $D_0 = 0.95$, $\alpha = 0.03$, $\rho = 0.03$, $\gamma = 0.5$, $I(t_0 + 1) = 10$, $\Psi = 0.1$.

Once GDP volatility exceeds a certain level, the risk that the country ends up in default starts to increase significantly. If the government wanted to further limit the probability of default, massive and costly (in terms of foregone consumption) cuts in the optimal borrowing rate were needed. As a result, the government's optimal borrowing level starts increasing again when the chance to enter default becomes substantial (i.e., more than $> 20\%$ for the given parameters). Under puttable debt, the optimal borrowing rate is decreasing in growth volatility since higher uncertainty leads to a higher payable put price. As a result, the government chooses a very low borrowing rate in order to sustain a tiny default probability, thereby minimizing its insurance costs.

3. Regardless of the refinancing instrument, the implied optimal borrowing rate is decreasing in the imposed default costs. The higher these costs, the higher are the incentives not to enter default. As a consequence, the government borrows less if the costs of default are high. Similarly, the probability of default is decreasing in the associated costs, hence the country minimizes its default risk once the corresponding costs are substantial enough.

4. The initial debt-to-GDP ratio's effect on optimal borrowing is slightly positive. The higher this ratio, the smaller is the impact of a negative growth shock. As a consequence, the government can marginally increase borrowing as the default risk becomes less sensitive

to growth uncertainty. In addition, the marginal return on borrowing is increasing in the initial debt level, which motivates, ceteris paribus, higher borrowing costs. Both effects seem counterproductive, as countries with higher indebtedness borrow more. However, the first effect is only due to our simplified definition of sovereign default. Moreover, the optimal borrowing rate is negative for all levels of the initial debt-to-GDP ratio. The relative indebtedness is hence even decreasing for high levels of debt, just at a slower pace. The effect of the initial debt-to-GDP ratio on the probability of default is tiny.

5. The consumer's risk aversion inversely affects the optimal borrowing rate. If less risk averse, she prefers higher (debt-financed) consumption today at the cost of a higher default probability tomorrow. For a strongly risk-averse consumer, by contrast, the government decreases its borrowing rate in order to reduce the implied default risk. Puttable debt's inherent insurance mechanism as well as GDR bonds' interst rate structure both alleviate the optimal borrowing rate's sensitivity to the consumer's risk aversion.

6. Under standard sovereign debt, the optimal borrowing rate is slightly increasing in the interest rate. The higher the interest payments, the more does the government need to borrow in order to maintain consumption. Under puttable debt, the government pays the risk-free rate on its bonds. Hence, R only affects the value of the put as we assume that the government has to compensate the insurance guarantor for its initial default risk (see Section 4.2), thereby conservatively neglecting a lower interest rate's decreasing effect on the ex-post default probability. However, the effect of the interest rate on the government's optimal borrowing rate under puttable debt is negligible.[24]

In summary, we find two persistent patterns across all parameter variations. First, optimal borrowing is highest under GDR and lowest under puttable bonds. GDR bonds allow the government to borrow more without substantially increasing its default probability compared to standard debt, thereby making the deleveraging committment more feasible. Under puttable debt, by contrast, the government extends its deleveraging effort in order to reduce the imposed insurance costs. Second, we observe the default probability to be almost equal for standard and GDR bonds but substantially lower for puttable bonds. This indicates that the latter's ex-ante payable insurance premium incentivizes the government to choose very low borrowing rates which in turn almost completely eliminate its default risk. Specifically, the reduction in borrowing further amplifies the default probability decreasing effect of puttable bonds' per se lower interest rates.

4.4 Case Study: Portugal, Ireland, Italy, Greece, and Spain

We now investigate GDR bonds' potential virtue of mitigating the risk of swelling refinancing costs in the presence of high indebtedness by analyzing the cases of Portugal, Ireland, Italy,

[24] Similarly, the effect of the consumer's time-preference is rather weak and only plays a minor role in determining $\mu_D^\star$ and the corresponding default probability. Marginally, the lower the consumer's patience, i.e., the higher ρ, the more she wants to consume today, leaving the government to prefer a higher optimal borrowing rate.

Greece and Spain at the time of the OMT announcement on July 26, 2012. We base our analysis on a comparison of the model predicted effectiveness of the following three refinancing instruments: (i) the status quo with standard debt, (ii) puttable (risk-free) debt in return for an ex-ante insurance premium in the spirit of Section 4.2, and (iii) GDR bonds as introduced in Section 4.3. Like in Section 4.3, we analyze those three refinancing instruments in an environment with continuous consumption and existing default costs.

In 2010, under the status quo, highly indebted Eurozone countries raised concerns regarding sovereign default after having reportedly been targeted by speculative attacks on their bond yields.[25] Such attacks, that ultimately resulted in an upwards shift of the country's perceived default risk, lead to higher demanded yields, which ultimately increase—likely amplified by the currency union's internal flight-to-safety—its actual default probability. Indeed, the empirical evidence of De Grauwe and Ji (2012) suggests a significant effect of negative market sentiments on the spreads of Greece, Ireland, Portugal, and Spain. In particular, the sovereign bond yields of Portugal, Ireland, and Greece soared to unprecedented levels due to fears of imminent sovereign default. By the end of 2011, as shown in Figure 4.5, long-term bond yields had climbed to 13.08% for Portugal, 8.70% for Ireland, and even 21.14% for Greece, respectively.[26] At these levels, refinancing became very expensive, which finally led the ECB to announce its OMT program in the summer of 2012.

Table 4.3 provides an overview of the calibrated parameters for the five countries.[27] Since there is a monotone one-to-one relation between a country's optimal borrowing rate and its default costs (see Footnote 23), we calibrate the latter such that its respective default probability under the status quo is equal to one implied by its actual sovereign credit rating prior to the OMT announcement. We therefore borrow Moody's historical default probabilities, implying a default probability of 1.9% for a Baa rating (Italy and Spain), 6.3% for a Ba rating (Portugal and Ireland), and 33.3% for a C rating (Greece), respectively.[28] Unfortunately, historical default probabilities are not available for subgroups. For instance, we cannot distinguish between the default probabilities of Portugal (Ba3) and Ireland (Ba1). Clearly, Portugal's higher interest rate (10.2% versus 5.2%) indicates a higher default probability.[29] Except for Greece, we use 4-year generic government bond yields in order to be in line with Collard et al. (2015), who rely on an average duration of sovereign debt equal to four years. For Greece, due to limited data

[25] As highlighted by both the IMF (source: IMF Global Financial Stability Report, April 2012, http://www.imf.org/external/pubs/ft/gfsr/2012/01/) and the ECB (source: Draghi, M., ECB press conference, September 6, 2012, http://www.ecb.europa.eu/press/pressconf/2012/html/is120906.en.html).

[26] Despite the rise in yields, the governments of Portugal, Ireland, Italy, Greece, and Spain increased sovereign borrowing over the same time period, indicating that higher refinancing costs force countries to borrow more in order to finance consumption (source: Eurostat, http://ec.europa.eu/eurostat/en/web/government-finance-statistics/statistics-illustrated).

[27] Our results are robust to changes in the standard values of parameters ρ, γ, and $I(t_0+1)$.

[28] Source: Moody's, Sovereign Default and Recovery Rates, 1983-2008, March 2009, https://www.moodys.com/sites/products/DefaultResearch/2007400000587968.pdf.

[29] We additionally analyze the three refinancing instruments' effectiveness for probabilities of default as implied by traded CDS-spreads and find similar results.

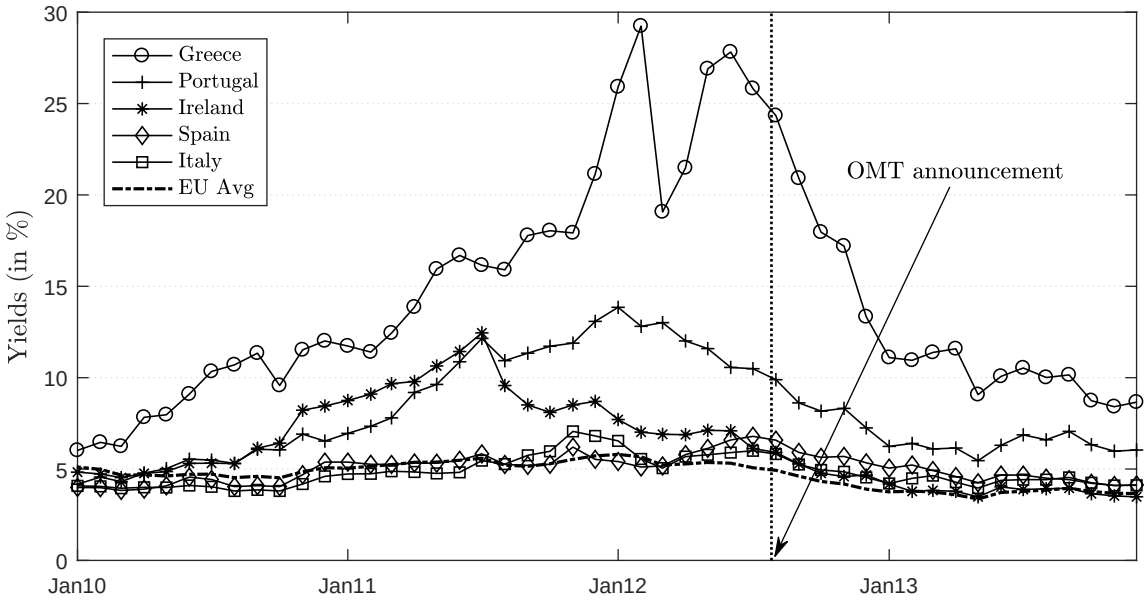

FIGURE 4.5. 10-YEAR YIELDS ON SELECTED GOVERNMENT BONDS.

Notes: This figure shows 10-year yields on government bonds for Portugal, Ireland, Italy, Greece, and Spain based on ECB data.

availability, we rely on its 10-year government bond yield.

We set $I(t_0+1) = 7$, as we find this level to provide sufficient incentives to save a significant part of disposable wealth for future periods. Given this weight on the consumer's end of period wealth, the expected disposable wealth is slightly increasing (on average 0.04% under the status quo). In addition, a comparative statics analysis with respect to $I(t_0 + 1)$ reveals that the sensitivity of the optimal borrowing rate to changes in the former is very small and negligible for levels of $I(t_0 + 1)$ around seven. This is desirable as we do not want this parameter choice to influence our results with respect to the optimal borrowing policies.

In addition, under (iii) GDR bonds, we need to ensure that the initial value $\widetilde{W}_{t_0}$ is non-negative. A negative initial value of the process $\widetilde{W}_t$ would imply that higher GDP growth and more borrowing decrease disposable wealth for consumption. As a consequence, we limit GDR debt issuance to the maximum value such that $\widetilde{W}_{t_0}$ is nonnegative.

In order to test the three different sovereign borrowing policies for different GDP growth realizations, we introduce a scenario analysis with respect to the realizations of μ_Y. We consider three realizations of the GDP growth rate: (i) the best out of the 5% worst realizations of μ_Y, i.e., the fifth historical percentile,[30] (ii) zero-growth, and (iii) the historical average growth rate. We then compare overall utility of the three refinancing instruments under these three scenarios.

[30]We again assume a normally distributed growth rate, implying the fifth percentile to equal $\mu_Y - 1.645\sigma_Y$, where μ_Y and σ_Y denote the historical average GDP growth rate and volatility based on yearly OECD data (http://stats.oecd.org).

TABLE 4.3. PARAMETERS

Parameter	Variable	Portugal	Ireland	Italy	Greece	Spain
GDP growth	μ_Y	2.29%	3.35%	1.68%	1.57%	2.01%
GDP volatility	σ_Y	3.46%	3.50%	2.31%	3.68%	2.23%
Debt-to-GDP ratio	D_0/Y_0	102.41%	110.55%	108.35%	111.11%	61.83%
Interest rate	R	10.22%	5.19%	5.85%	27.82%	6.95%
MPS	α	0.23%	6.74%	6.51%	4.37%	4.01%
Consumption	$\bar{c}$	65.82%	45.57%	61.51%	69.88%	57.82%
Risk aversion	γ	0.5	0.5	0.5	0.5	0.5
Time preference	ρ	5.00%	5.00%	5.00%	5.00%	5.00%
Default costs	Ψ	0.13	0.21	0.42	0.02	0.28
Risk free rate	r	1.30%	1.30%	1.30%	1.30%	1.30%

Notes: This table presents the calibrated parameters for Portugal, Ireland, Italy, Greece, and Spain. We use yearly OECD (http://stats.oecd.org) GDP data for the years 1970-2011 to compute μ_Y and σ_Y. D_0/Y_0 corresponds to relative indebtedness as of the end of 2011 and is based on World Bank data (http://data.worldbank.org). We use yield data of 4-year generic government bonds per July 26, 2012 from Bloomberg for all countries except Greece. As there is no data on traded government bonds with maturity less than ten years for Greece at that time, we use 10-year government bond yields provided by the Bank of Greece (http://www.bankofgreece.gr). MPS corresponds to the maximum primary surplus based on OECD data. Consumption denotes national consumption in the year 2011 based on World Bank data. Standard values are assumed for γ and ρ. Default costs are set such that the default probability under the status quo and historical GDP growth matches the sovereign default probability according to Moody's credit rating at the time of OMT announcement. The continuously compounded yield on a German 4-year government bond as of July 26, 2012 serves as a proxy for the risk-free interest rate r.

Figure 4.6 displays the resulting differences in utility for Portugal, Ireland, Italy, Greece, and Spain.

We find that, across growth scenarios, switching from standard to puttable debt leads to welfare improvements. The savings from lower interest payments more than compensate the government for its ex-ante insurance payment. Due to countries' low borrowing rates, the value of the put option is relatively low considering prevailing interest rate levels, ranging from 0.18% (Spain) to 0.76% (Ireland) of GDP. The effect of the three different GDP growth scenarios on the insurance premium is small. In addition, default probabilities under puttable debt (0.48% on average) are substantially lower than under the status quo (11.05%). This finding is consistent with the result from Section 4.2, i.e., that, under the presence of default costs, puttable debt's default risk mitigation is welfare improving. Only Ireland, due to its comparably low interest rate, does not experience a substantial utility increase when issuing puttable bonds.

Moreover, Figure 4.6 highlights that GDR bonds consistently outperform puttable bonds. The welfare improvements induced by the former are especially pronounced for the case of zero or negative GDP growth, where GDR bonds imply significantly lower interest payments. Thus, contrary to puttable debt's simple insurance mechanism, GDR bonds' state-contingent interest charges allow the risk-averse consumer to considerably smooth her within-period consumption

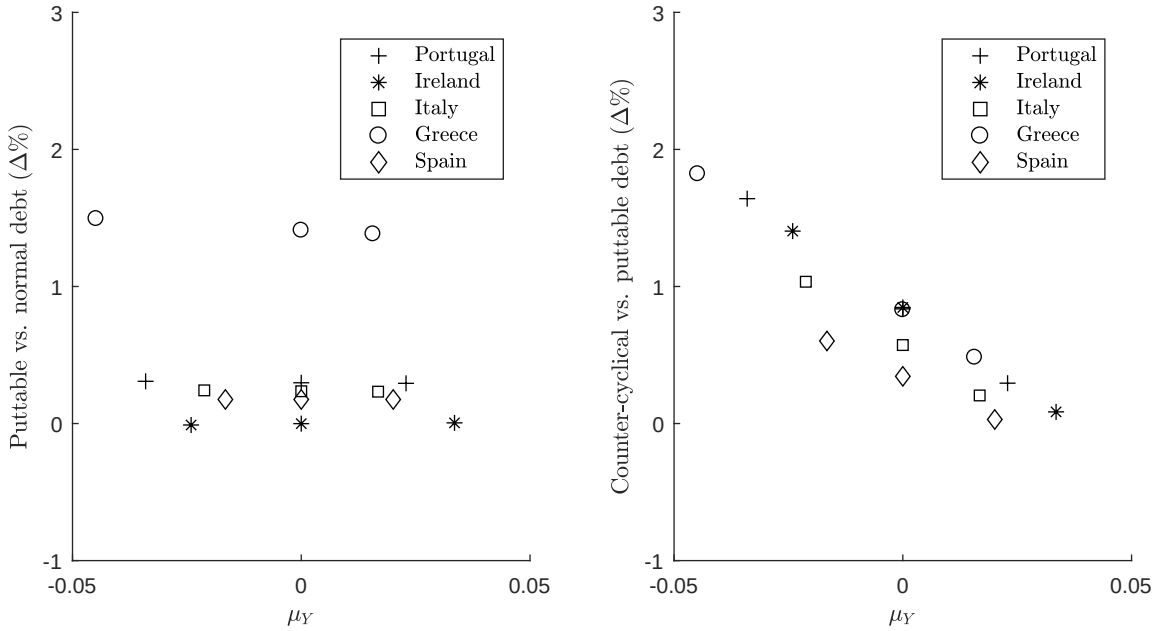

FIGURE 4.6. UTILITY COMPARISON BETWEEN PUTTABLE AND NORMAL BONDS (LEFT) AS WELL AS GDR AND PUTTABLE BONDS (RIGHT)

Notes: The left-hand side plot provides the relative utility differences between puttable and standard debt. The right-hand side plot displays relative utility differences between GDR bonds and puttable debt.

path, without increasing associated default risks too heavily. On average, optimal borrowing rates are approximately twice as low under standard debt than under GDR bonds, and even two times lower for puttable relative to standard debt. In summary, the data-implied default costs are not high enough such that puttable debt's reduction in default risk would keep up with GDR bonds' capability to smooth consumption.

If one instead considers more pessimistic (risk-neutral) default probabilities implied by historical CDS spreads, the price of puttable debt's embedded put option becomes larger. This can change the relation between puttable and standard debt: As the ex-ante payable insurance premium increases, wealth disposable for consumption is reduced, making standard debt relatively more attractive. However, GDR bonds are still outperforming both normal and puttable bonds, leaving the above results robust to changes in the calibration of default probabilities.[31]

To sum up, it hardly depends on the realization of the GDP growth rates which instrument is most beneficial. We find the status quo with standard debt to be inferior to puttable debt. Furthermore, GDR bonds which are inversely linked to relative indebtedness, provide even higher

[31]On average, imposing CDS-implied default probabilities, i.e., lowering Ψ, increases utility under normal and GDR bonds by 0.13% and under puttable bonds by 0.01%. As a consequence, puttable bonds are relatively less attractive under CDS-implied default probabilities. This discrepancy to Section 4.2 arises due to the significantly lower default costs and the high weight on the consumer's reduced utility of bequest, which is absent in Section 4.2's analysis of puttable debt. More importantly, under lower values of Ψ, GDR bonds still allow for higher utility levels relative to normal and puttable debt.

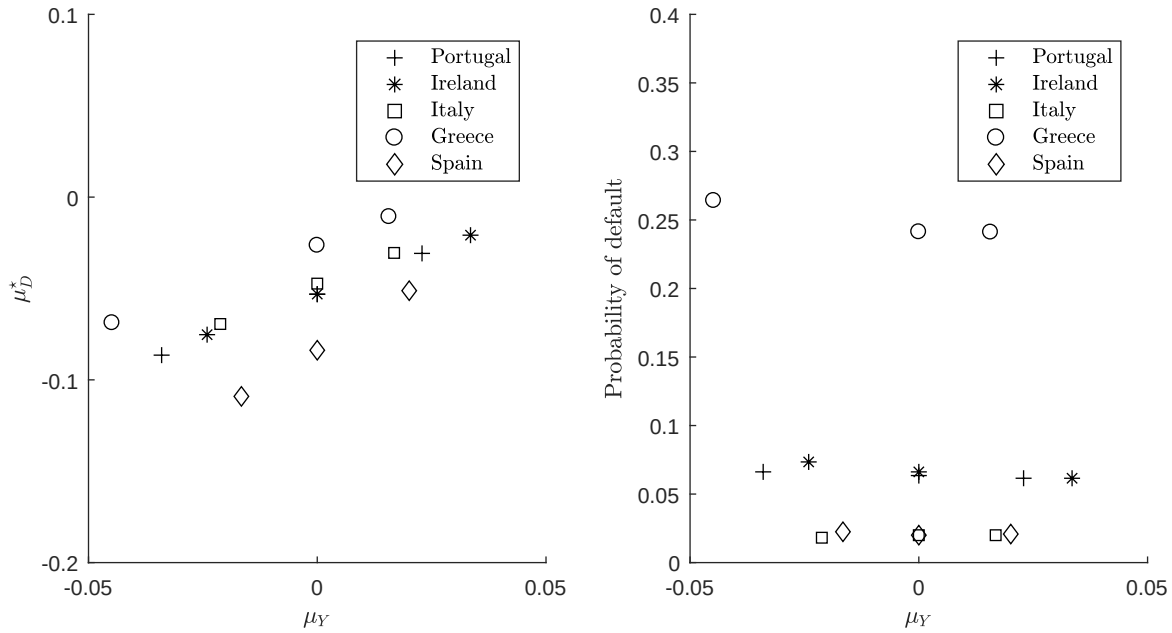

FIGURE 4.7. OPTIMAL BORROWING RATE (LEFT) AND DEFAULT PROBABILITY (RIGHT) UNDER GDR BONDS

Notes: The left-hand side plot shows the optimal borrowing rate of Portugal, Ireland, Italy, Greece, and Spain under GDR bonds. The right-hand side plot displays the respective probabilities of sovereign default.

utility than the issuance of puttable debt. Retrospectively, issuing GDR bonds might have been an expedient refinancing alternative for the herein considered countries.

Having selected our preferred refinancing instrument, we plot the optimal borrowing rates under GDR bonds as well as the corresponding default probabilities for the three GDP growth scenarios in Figure 4.7. We find the optimal borrowing rates to lie between -10.90% (Spain with $\mu_Y = -1.66\%$) and -1.07% (Greece with $\mu_Y = 1.57\%$). Hence, GDR bonds' incentive structure appears sufficient in inducing the issuing government to choose a deleveraging borrowing rate. Figure 4.7 shows that neither the absolute level of the probability of default nor the order of the five countries depend on the GDP growth rate.

Finally, we compute the Sharpe ratio of GDR bonds in order to evaluate their potential attractiveness to risk-averse investors. The respective Sharpe ratios equal $(\mu_Y - \mu_D^\star - r_f)/\sigma_Y$, where $\mu_Y - \mu_D^\star$ reflects GDR bonds' expected interest rate. If the Sharpe ratio of such an investment instrument was below a minimum threshold, investors would not be willing to provide funds, as their expected compensation would be too small given the associated risk level. Table 4.4 presents the computed Sharpe ratios for the three growth scenarios considered above.

Overall, the Sharpe ratios are high, i.e., between 0.61 and 4.09. Regardless of the realization of the GDP growth rate, GDR bonds appear to be an attractive investment instrument, since the optimal borrowing rates are always negative. In sharp contrast to standard GDP-indexed bonds, GDR bonds' Sharpe ratios remain competitive even for negative growth rates.

Table 4.4. Sharpe ratios under GDR bonds: Scenario analysis

	Negative GDP growth	Zero GDP growth	Positive GDP growth
Portugal	1.48	1.50	1.51
Ireland	1.42	1.48	1.51
Italy	2.03	1.99	1.99
Greece	0.61	0.68	0.68
Spain	4.09	3.70	3.14

Notes: This table displays the Sharpe ratios of GDR bonds as computed by $SR = (\mu_Y - \mu_D^\star - r_f)/\sigma_Y$, where $\mu_D^\star$ reflects the optimal borrowing rate of the government. The negative GDP growth scenario features the best out of the 5% worst historical realizations of μ_Y, i.e., the fifth historical percentile, zero GDP growth implies $\mu_Y = 0$, and positive GDP growth corresponds to the historical average growth rate. We use yearly GDP growth and volatility data from the OECD (http://stats.oecd.org).

However, if governments possibly deviated from their initial optimal borrowing rate *after* having issued GDR bonds, their actual risk-return profile could deteriorate.[32] If markets deem this risk unacceptable, establishing an intergovernmental agency as counterparty (writer) of GDR embedded put options could foster the credibility of initially proclaimed deleveraging intentions. Buying such a put option would give hesitant investors the right to hand over their GDR bonds to the option writer for a fixed amount, in case prices fell sharply due to a too high μ_D. Hence, the put option would insure investors against overborrowing by the GDR bonds issuing government.

In addition, the put premium would fairly compensate the option writing counterparty for guaranteeing credit insurance. Importantly, the latter nevertheless had to maintain the enforceability of Ψ upon option exercise. The case of Greece provides indicative evidence that such intergovernmental institutions, i.e., the European Commission, Eurogroup, ECB, and IMF, indeed possess enough power to conditionally force Eurozone debtor countries to massive cuts in fiscal spending. In Section 4.5 below, potential risks associated with the implementation of GDR bonds are addressed more generally.

4.5 Discussion and Concluding Remarks

In summary, our analysis indicates considerable virtues of GDR over puttable bonds in terms of welfare improvements. Naturally, the introduction of a novel financial contract such as GDR bonds brings about many new factors, which all need to be considered in detail. In this final section, we address the most apparent points. We argue that—albeit justified—they can be dealt with in reasonable manner.

[32] This, in fact, could happen if Ψ decreases or if default costs are not enforceable (see discussion in Section 4.5).

Risk of Limited Commitment

Given the inverse relation between interests paid on GDR bonds and a country's current GDP-to-debt ratio, a natural concern is that issuing governments simply keep on increasing their debt to lower payable interests on outstanding GDRs. From an ex-ante perspective, this is no problem since investors are only willing to purchase GDRs, if the government can credibly commit itself to a deleveraging borrowing rate. Ex-post, however, a limited commitment problem due to a lack of enforceability may arise.

The enforceability of non-positive borrowing rates could, e.g., be achieved by contractually forbidding the issuing government to auction any non-authorized debt during the GDRs' lifetime. For this purpose, an intergovernmental organization would have to be established, similar to, e.g., the former European Troika (recently renamed as 'European Quadriga'), who enforces compliance with such contractual agreements. To be itself credible, it needs to be empowered to impose sanctions, e.g., predefined coercive measures, in case of contravention.

Alternatively, similar to puttable debt, GDR bonds could be complemented by an embedded put option. Whenever the government's GDP-to-debt ratio at GDRs' maturity falls below a certain threshold, investors could put their bonds with the above mentioned organization and receive a fixed payment in return. In case their GDR bonds get put, sanctions are imposed on the issuing government. Note that, contrary to puttable debt discussed above, the writer of the embedded put option would be compensated with the insurance premium paid by investors instead of the issuing government.

Growth Risk

By construction, returns to GDR bonds are pro-cyclical, i.e., if growth rates are positive (negative), interests increase (decrease). Hence, similar to GDP-linked bonds (see Blanchard et al. (2016)), GDRs represent so-called 'high beta' instruments, for which investors demand higher expected returns per unit of risk.

In light of the above calibrated Sharpe ratios, we argue that GDRs easily exceed the necessary return-for-risk profile usually demanded by investors for 'high beta' securities. Particularly, GDRs' Sharpe ratios are generally high due to the relatively low levels of growth volatility. Moreover, growth rates are only imperfectly correlated across countries. Hence, making GDRs available to a widely dispersed foreign investor base further reduces country-specific growth risks borne by investors.

Novelty and Liquidity Risk

Newly introduced GDR bonds would entail substantial novelty and liquidity risks. Historically, GDP-linked bonds have been mainly issued by developing countries, often during debt restructuring. In the context of the potential isssuers we have in mind, Blanchard et al. (2016) conclude: "With relatively strong institutions and an independent statistical agency, advanced economies are in a better position to give confidence to investors that data on economic growth will remain untampered and reliable." (Blanchard et al., 2016, p.3)

The absence of a reasonably liquid secondary market usually complicates the introduction of novel financial securities, such as GDP-linked bonds (Barr et al. (2014)). A minimum scale and sufficient standardization would therefore facilitate the successful implementation of GDRs. The Sharpe ratios calibrated for Portugal, Ireland, Italy, Greece, and Spain firmly appear high enough to compensate for GDRs' potential novelty and liquidity risks. In case of unexpectedly high initial liquidity concerns and novelty aversion, making GDRs puttable, as discussed above, jointly decreases both types of risks.

In conclusion, we believe GDP-to-debt-index bonds to constitute a promising alternative for managing the risk of future spikes in government yields for highly indebted Eurozone countries, of whom there still are many. If implemented appropriately, they could be an effective state-contingent debt instrument, temporary mitigating refinancing pressure and smoothing private consumption, thereby creating space and time for a less painful, but more sustainable sovereign deleveraging.

A4 Proofs

Proof of Lemma 4.1. We start from Eq. (4.12), rearranging yields

$$\beta_M \left(\frac{\pi_L}{\alpha + \frac{\beta_M}{1+rL}} + \frac{\pi_H}{\alpha + \frac{\beta_M}{1+rH}} \right) = \frac{(1+\mu_g+\sigma_g)^2}{8\sigma_g} \quad \Leftrightarrow$$
$$\frac{\beta_M^2(\mathbb{E}[1+r]) + \beta_M(\alpha(1+r_L)(1+r_H))}{\beta_M^2 + \beta_M\alpha(2+r_L+r_H) + \alpha^2(1+r_L)(1+r_H)} = \frac{(1+\mu_g+\sigma_g)^2}{8\sigma_g},$$

which leads us to the following quadratic equation

$$\beta_M^2 \underbrace{\left(\frac{(1+\mu_g+\sigma_g)^2}{8\sigma_g} - \mathbb{E}[1+r] \right)}_{=:A} + \beta_M \underbrace{\left(\frac{(1+\mu_g+\sigma_g)^2}{8\sigma_g} \alpha(2+r_L+r_H) - \alpha(1+r_L)(1+r_H) \right)}_{=:B}$$
$$+ \underbrace{\frac{(1+\mu_g+\sigma_g)^2}{8\sigma_g} \alpha^2(1+r_L)(1+r_H)}_{=:C} = 0. \tag{A4.1}$$

Whenever $A \geq 0$, it must be that

$$\frac{(1+\mu_g+\sigma_g)^2}{8\sigma_g} \geq \mathbb{E}[1+r] \geq 1,$$

where the second inequality holds since $0 \leq r < 1$. Hence, $A \geq 0$ directly implies $B > 0$. However, if both A and B are nonnegative, there exists no nonnegative solution β_M to Eq. (A4.1). A nonnegative β_M therefore requires that $A < 0$, i.e.,

$$\mathbb{E}[1+r] > \frac{(1+\mu_g+\sigma_g)^2}{8\sigma_g},$$

and because $C \geq 0$, the maximum β_M is given by

$$\beta_M = \frac{-B - \sqrt{B^2 - 4AC}}{2A} > 0.$$

This completes the proof. □

Proof of Lemma 4.2. We prove Lemma 4.2 in two steps. First, we compute the date-t put option value. A standard European put option with strike price x, underlying S, and maturity $t+1$ yields the following payoff at expiration

$$\max(x - S_{t+1}, 0).$$

In the context of puttable bonds, this payoff can be written as

$$\max\left(b_M(t)(1+R_H)Y_t - \alpha Y_{t+1}, 0\right).$$

In the following, we denote by $\underline{g}$ the growth-rate threshold below which the put option yields a positive payoff at maturity, i.e., the minimum growth rate necessary to prevent government default:

$$b_M(t)(1+R_H)Y_t = (\alpha + b_M(t+1))Y_t\underline{g} \quad \Leftrightarrow \quad \frac{b_M(t)(1+R_H)}{\alpha + b_M(t+1)} = \underline{g}(r_{t+1}).$$

Since $\underline{g}$ is state-dependent, we write it as a function of r_{t+1}. Given risk-neutrality and that $r_t = r_H$, the date-t put price then equals

$$\begin{aligned}
&\delta\left(\mathbb{P}\left(g < \underline{g}(r_{t+1})\right) \times E_t\left[b_M(t)(1+R_H)Y_t - \alpha Y_{t+1} | g < \underline{g}(r_{t+1})\right]\right) = \\
&\frac{1}{1+r_H}\left(\pi_L \frac{\underline{g}(r_L) - 1 - \mu_g + \sigma_g}{2\sigma_g} \times \left(b_M(t)(1+R_H) - \alpha\frac{1+\mu_g-\sigma_g+\underline{g}(r_L)}{2}\right)Y_t + \right. \\
&\left. \pi_H \frac{\underline{g}(r_H) - 1 - \mu_g + \sigma_g}{2\sigma_g} \times \left(b_M(t)(1+R_H) - \alpha\frac{1+\mu_g-\sigma_g+\underline{g}(r_H)}{2}\right)Y_t\right),
\end{aligned} \tag{A4.2}$$

where the conditional expectation can be calculated in closed form by relying on the uniform distribution of g. Recalling the assumption of zero recovery in default from Section 4.2, Eq. (A4.2) finally implies

$$p_t = \frac{1}{1+r_H}\left(\pi_L \frac{\underline{g}(r_L) - 1 - \mu_g + \sigma_g}{2\sigma_g} + \pi_H \frac{\underline{g}(r_H) - 1 - \mu_g + \sigma_g}{2\sigma_g}\right) \times b_M(t)(1+R_H)Y_t. \tag{A4.3}$$

Second, we show that the government is indeed indifferent between issuing normal and puttable debt, i.e., that the following equation holds:

$$p_t = \underbrace{\delta}_{=\frac{1}{1+r_H}} b_M(t)(R_H - r_H)Y_t. \tag{A4.4}$$

Plugging Eq. (A4.3) into Eq. (A4.4) and after some tedious but simple algebra wet get

$$\underbrace{b(t)(1+r_H)}_{\equiv\beta_M} = \left(8\sigma\left(\frac{\pi_L}{\alpha + \frac{\beta_M}{1+r_L}} + \frac{\pi_H}{\alpha + \frac{\beta_M}{1+r_H}}\right)\right)^{-1} \frac{1+r_H}{1+R_H}\left(\frac{2\sigma(R_H - r_h)}{1+R_H} + 1 + \mu_g - \sigma_g\right). \tag{A4.5}$$

Now, Eq. (4.12) implies

$$R_H := \frac{d_M}{b_M(t)} - 1 = \frac{d_M}{\beta_M/(1+r_H)} - 1 = \frac{4\sigma_g(1+r_H)}{1+\mu_g+\sigma_g} - 1. \tag{A4.6}$$

Plugging Eq. (A4.6) into Eq. (A4.5) and simplifying finally yields

$$\beta_M = \frac{(1+\mu_g+\sigma_g)^2}{8\sigma\left(\frac{\pi_L}{\alpha + \frac{\beta_M}{1+r_L}} + \frac{\pi_H}{\alpha + \frac{\beta_M}{1+r_H}}\right)}.$$

This completes the proof. □

Proof of Proposition 4.1. In the absence of puttable bonds, if $r_t = r_H$, the government defaults at $t+1$ whenever

$$b_M(t)(1+R_H)Y_t > (\alpha + b_M(t+1))Y_t g_{t+1} \quad \Leftrightarrow \quad \frac{b_M(t)(1+R_H)}{\alpha + b_M(t+1)} > g_{t+1},$$

i.e., the probability of default is given by

$$\mathbb{P}|R_H := \mathbb{P}\left(g < \frac{b_M(t)(1+R_H)}{\alpha + b_M(t+1)}\right).$$

Given the uniform distribution of g, we get

$$\mathbb{P}|R_H = \frac{\frac{b_M(t)(1+R_H)}{\alpha+b_M(t+1)} - (1+\mu_g-\sigma_g)}{2\sigma_g}. \tag{A4.7}$$

We have to distinguish between two cases: First, if $b_M(t)(1+r_H)/(\alpha+b_M(t+1)) > 1+\mu_g-\sigma_g$, Eq. (A4.7) implies that issuing puttable instead of standard debt reduces the default probability by

$$\mathbb{P}|R_H - \mathbb{P}|r_H = \frac{b_M(t)(R_H - r_H)}{2\sigma_g\left(\alpha + b_M(t+1)\right)}.$$

Second, in the complementary case, i.e., if $\mathbb{P}|r_H = 0$, puttable bonds eliminate the whole default risk imposed by standard bonds. This completes the proof. □

Proof of Lemma 4.3. In order to solve for optimal consumption, we apply standard dynamic programing techniques as described in, e.g., Merton (1969). We want to solve for

$$\widetilde{c}_t^{\star} = \arg\max_{\widetilde{c}_t} U(\widetilde{c}_t, \widetilde{W}_{t_0+1}) = \arg\max_{\widetilde{c}_t} \mathbb{E}\left[\int_{t_0}^{t_0+1} u(\widetilde{c}_t, t)\mathrm{d}t + \bar{u}(\widetilde{W}_{t_0+1}, t_0+1)\right]$$

subject to the budget constraint

$$d\widetilde{W}_t = \widetilde{W}_t\left(\mu_Y dt + \sigma_Y dB_t\right) - \widetilde{c}_t dt,$$

where $u(\widetilde{c}_t, \widetilde{W}_t) = e^{-\rho t}\widetilde{c}_t^{1-\gamma}(1-\gamma)^{-1}$ and $\bar{u}(\widetilde{W}_{t_0+1}, t_0+1) = e^{-\rho(t_0+1)}I(t_0+1)\widetilde{W}_{t_0+1}^{1-\gamma}(1-\gamma)^{-1}$ for $\rho \geq 0$ and $\gamma > 0$.

The conjectured solution is of the form

$$J(\widetilde{W}_t, t) = e^{-\rho t}I(t)\frac{\widetilde{W}_t^{1-\gamma}}{1-\gamma},$$

yielding the following Bellman equation

$$\max_{c_t} J_{\widetilde{W}}\left(\widetilde{W}_t\mu_Y - \widetilde{c}_t\right) + J_t + \frac{1}{2}J_{\widetilde{W}\widetilde{W}}\widetilde{W}_t^2\sigma_Y^2 + e^{-\rho t}\frac{\widetilde{c}_t^{1-\gamma}}{1-\gamma} = 0 \tag{A4.8}$$

subject to the following boundary condition

$$J(\widetilde{W}_{t_0+1}, t_0+1) = e^{-\rho(t_0+1)} I(t_0+1) \frac{\widetilde{W}_{t_0+1}^{1-\gamma}}{1-\gamma}.$$

Eq. (A4.8) yields the following first order condition for $\widetilde{c}_t^\star$, i.e.,

$$-J_{\widetilde{W}} + e^{-\rho t}(\widetilde{c}_t^\star)^{-\gamma} = 0 \Leftrightarrow \widetilde{c}_t^\star = I(t)^{-\frac{1}{\gamma}} \widetilde{W}_t. \tag{A4.9}$$

Plugging the value function's partial derivatives together with Eq. (A4.9) into Eq. (A4.8) gives

$$e^{-\rho t} I(t) \widetilde{W}_t^{-\gamma} \left(\widetilde{W} \mu_Y - I(t)^{-\frac{1}{\gamma}} \widetilde{W}_t \right) + e^{-\rho t} \frac{\widetilde{W}_t^{1-\gamma}}{1-\gamma} (I'(t) - \rho I(t)) +$$
$$\frac{1}{2}(-\gamma) e^{-\rho t} I(t) \widetilde{W}_t^{1-\gamma} \sigma_Y^2 + e^{-\rho t} \frac{1}{1-\gamma} \left(I(t)^{-\frac{1}{\gamma}} \right)^{1-\gamma} \widetilde{W}_t^{1-\gamma} = 0,$$

which can be simplified to the following ODE

$$I(t) \underbrace{\left(\rho - (1-\gamma) \left(\mu_Y - \frac{\sigma_Y^2 \gamma)}{2} \right) \right)}_{=:\xi} - \gamma I(t)^{\frac{\gamma-1}{\gamma}} = I'(t),$$

or equivalently

$$I(t)^{\frac{1-\gamma}{\gamma}} I'(t) = I(t)^{\frac{1}{\gamma}} \xi - \gamma.$$

If we set $Z(t) := I(t)^{\frac{1}{\gamma}}$, i.e., $Z'(t) = \frac{1}{\gamma} I(t)^{\frac{1-\gamma}{\gamma}} I'(t)$, hence we get the following ODE

$$\gamma Z'(t) = Z(t)\xi - \gamma \Leftrightarrow Z'(t) = Z(t) \underbrace{\frac{\xi}{\gamma}}_{=:\phi} - 1 \tag{A4.10}$$

with boundary condition $Z(t_0+1) = I(t_0+1)^{\frac{1}{\gamma}}$. The corresponding homogenous ODE is

$$Z'(t) = Z(t)\phi \Rightarrow Z(t) = e^{\phi t} C,$$

where $C \in \mathbb{R}$ is some integration constant.

We can solve the non-homogenous equation in Eq. (A4.10) by applying the variation of constants, i.e.,

$$Z'(t) = \phi e^{\phi t} C(t) + e^{\phi t} C'(t). \tag{A4.11}$$

Plugging Eq. (A4.11) into Eq. (A4.10) yields

$$\phi e^{\phi t} C(t) + e^{\phi t} C'(t) = e^{\phi t} C(t) \phi - 1 \Leftrightarrow C'(t) = -e^{-\phi t},$$

which has the solution $C(t) = \frac{1}{\phi} e^{-\phi t} + \widetilde{C}$, i.e., we get $Z(t) = \frac{1}{\phi} + e^{\phi t} \widetilde{C}$ and recalling the respective

boundary condition yields

$$Z(t_0+1) = \frac{1}{\phi} + e^{\phi(t_0+1)}\widetilde{C} = I(t_0+1)^{\frac{1}{\gamma}} \Leftrightarrow \widetilde{C} = \left(I(t_0+1)^{\frac{1}{\gamma}} - \frac{1}{\phi}\right) e^{-\phi(t_0+1)}.$$

Hence, we have found $Z(t) = \frac{1}{\phi} + e^{\phi(t-(t_0+1))}\left(I(t_0+1)^{\frac{1}{\gamma}} - \frac{1}{\phi}\right)$, which by the above definition of $Z(t)$ gives us

$$I(t) = \left(\frac{1}{\phi} + e^{\phi(t-(t_0+1))}\left(I(t_0+1)^{\frac{1}{\gamma}} - \frac{1}{\phi}\right)\right)^{\gamma},$$

and by Eq. (A4.9) we thus finally get

$$\widetilde{c}_t^{\star} = \frac{\widetilde{W}_t}{\frac{1}{\phi} + e^{-\phi(t_0+1-t)}\left(I(t_0+1)^{\frac{1}{\gamma}} - \frac{1}{\phi}\right)},$$

where

$$\phi = \frac{1}{\gamma}\left(\rho - (1-\gamma)\left(\mu_Y - \frac{\gamma\sigma_Y^2}{2}\right)\right).$$

This completes the proof. □

Proof of Proposition 4.2. We first note that due to the definition of $\tilde{c}_t$ in Eq. (4.20), W_{t_0+1} does not depend on μ_D since additional borrowings are immediately consumed by the representative agent.

For $u(\cdot)$ in Eq. (4.23), we get

$$\frac{\partial}{\partial \mu_D} u(c_s^{\star}, s) = u(c_s^{\star} + \bar{c}, s) = e^{-\rho s}\frac{2D_s}{(c_s^{\star} + \bar{c})^{\gamma}} > 0. \tag{A4.12}$$

The discounted expected default costs in Eq. (4.20) equal

$$\mathbb{E}\left[e^{-\rho}\Psi \mathbf{1}_{\left\{\frac{D_{t_0+1}-\Delta W}{Y_{t_0+1}} > \frac{D_{t_0}}{Y_{t_0}}\right\}}\right] = e^{-\rho}\Psi\mathbb{P}\left(\frac{D_{t_0+1}-\Delta W}{Y_{t_0+1}} > \frac{D_{t_0}}{Y_{t_0}}\right), \tag{A4.13}$$

where $\Delta W := W_{t_0+1} - W_{t_0}$. Rewriting the probability of default and taking the first partial derivative with respect to μ_D yields

$$\begin{aligned}\frac{\partial}{\partial \mu_D}\mathbb{P}\left(\frac{D_{t_0+1}-\Delta W}{Y_{t_0+1}} > \frac{D_{t_0}}{Y_{t_0}}\right) &= \frac{\partial}{\partial \mu_D}\mathbb{P}\left(Y_{t_0+1}\frac{Y_{t_0}}{D_{t_0}} + \Delta W < D_{t_0}e^{\mu_D}\right) \\ &= \frac{\partial}{\partial \mu_D} G\left(D_{t_0}e^{\mu_D}\right) \\ &= g\left(D_{t_0}e^{\mu_D}\right) D_{t_0}e^{\mu_D} \geq 0, \end{aligned} \tag{A4.14}$$

where $G(\cdot)$ denotes the cdf of $Y_{t_0+1}\frac{Y_{t_0}}{D_{t_0}} + \Delta W$, and we have relied on $\mu_D \perp\!\!\!\perp \Delta W$.

Let $\mu_D^{\star}$ denote a bounded solution to Eq. (4.20). At $\mu_D^{\star}$ it then has to hold that Eq. (A4.14) is strictly positive. Thus, for a bounded solution to Eq. (4.20), the strictly positive marginal utility from higher consumption between t_0 and t_0+1 needs to be offset by the effect of a

strictly increasing default probability. In addition, we have to ensure that the derivative of the power utility in Eq. (A4.12) and the part in Eq. (A4.14) can maximally interesect twice (at the maximum and (local) minimum). For this to hold, Eq. (A4.14) needs to converge faster to zero than Eq. (A4.12) which is true as Eq. (A4.14) converges exponentially. Hence, there can be only one interior $\mu_D^\star$. This completes the proof. □

Proof of Corollary 4.1. Analogous to the proof of Proposition 4.2, we note that due to the definition of $\tilde{c}_t$ in the restatement of Eq. (4.16) under standard debt, i.e., $c_t = \tilde{c}_t - (\mu_D - R)$, and Eq. (4.17) under puttable debt, i.e., $c_t = \tilde{c}_t - (\mu_D - r)$, W_{t_0+1} does not depend on μ_D since additional borrowings are immediately consumed by the representative agent.

For $u(\cdot)$ in Eq. (4.23), we get

$$\frac{\partial}{\partial \mu_D} u(c_s^\star + \bar{c}, s) = e^{-\rho s} \frac{D_s}{(c_s^\star + \bar{c})^\gamma} > 0. \tag{A4.15}$$

The discounted expected default costs in Eq. (4.20) are given in Eq. (A4.13) and the first partial derivative with respect to μ_D is positive as shown in Eq. (A4.14).

Let $\mu_D^\star$ denote a bounded solution to Eq. (4.20). At $\mu_D^\star$ it then has to hold that Eq. (A4.14) is strictly positive. Thus, for a bounded solution to Eq. (4.20), the strictly positive marginal utility from higher consumption between t_0 and $t_0 + 1$ needs to be offset by the effect of a strictly increasing default probability. In addition, we have to ensure that the derivative of the power utility in Eq. (A4.15) and the part in Eq. (A4.14) can maximally interesect twice (at the maximum and (local) minimum). For this to hold, Eq. (A4.14) needs to converge faster to zero than Eq. (A4.15) which is true as Eq. (A4.14) converges exponentially. Hence, there can be only one interior $\mu_D^\star$. This completes the proof. □

Part III

Bibliography

Bibliography

Abdellaoui, M., A. Baillon, L. Placido, and P. Wakker (2011). The Rich Domain of Uncertainty: Source Functions and Their Experimental Implementation. *American Economic Review 101*, 695–723.

Admati, A. R. and P. Pfleiderer (1988). A Theory of Intraday Patterns: Volume and Price Variability. *Review of Financial Studies 1*(1), 3–40.

Aït-Sahalia, Y. and J. Jacod (2009). Estimating the Degree of Activity of Jumps in High Frequency Data. *Annals of Statistics 37*, 2202–2244.

Almeida, A., C. Goodhart, and R. Payne (1998). The Effects of Macroeconomic News on High Frequency Exchange Rate Behavior. *Journal of Financial and Quantitative Analysis 33*(3), 383–408.

Amromin, G., J. Huang, C. Sialm, and E. Zhong (2011). Complex Mortgages. *NBER Working Paper (17315)*.

An, B.-J., A. Ang, T. G. Bali, and N. Cakici (2014). The Joint Cross Section of Stocks and Options. *Journal of Finance 69*(5), 2279–2337.

Andersen, T. G. and T. Bollerslev (1998). Deutsche Mark–Dollar Volatility: Intraday Activity Patterns, Macroeconomic Announcements, and Longer Run Dependencies. *Journal of Finance 53*(1), 219–265.

Andersen, T. G., T. Bollerslev, F. X. Diebold, and C. Vega (2007). Real-time Price Discovery in Global Stock, Bond and Foreign Exchange Markets. *Journal of International Economics 73*(2), 251–277.

Andersen, T. G., D. Dobrev, and E. Schaumburg (2012). Jump-Robust Volatility Estimation using Nearest Neighbor Truncation. *Journal of Econometrics 169*(1), 75–93.

Armantier, O. and N. Treich (2016). The Rich Domain of Risk. *Management Science 62*(7), 1954–1969.

Arora, S., B. Barak, M. Brunnermeier, and R. Ge (2011). Computational Complexity and Information Asymmetry in Financial Products. *Communications of the ACM 54*(5), 101–107.

Arrow, K. J. (1964). The Role of Securities in the Optimal Allocation of Risk-bearing. *Review of Economic Studies 31*(2), 91–96.

Asparouhove, E., P. Bossaerts, J. Eguia, and W. R. Zame (2015). Asset Pricing and Asymmetric Reasoning. *Journal of Political Economy 123*, 66–122.

Asparouhove, E., P. Bossaerts, R. Nilanjan, and W. R. Zame (2016). "Lucas" in the Laboratory. *Journal of Finance 71*(6), 2727–2780.

Augustin, P., M. Brenner, and M. Subrahmanyam (2015). Informed Options Trading prior to M&A Announcements: Insider Trading? *Working Paper*.

Barclay, M. J. and T. Hendershott (2003). Price Discovery and Trading after Hours. *Review of Financial Studies 16*(4), 1041–1073.

Barr, D., O. Bush, and A. Pienkowski (2014). GDP-linked Bonds and Sovereign Default. In *Life After Debt*, pp. 246–275. Springer.

Batten, J. A. and B. M. Lucey (2010). Volatility in the Gold Futures Market. *Applied Economics Letters 17*(2), 187–190.

Becker, K. G., J. E. Finnerty, and J. Friedman (1995). Economic News and Equity Market Linkages between the U.S. and U.K. *Journal of Banking & Finance 19*(7), 1191–1210.

Biais, B. and P. Hillion (1994). Insider and Liquidity Trading in Stock and Options Markets. *Review of Financial Studies 7*, 734–780.

Biais, B., P. Hillion, and C. Spatt (1999). Price Discovery and Learning during the Preopening Period in the Paris Bourse. *Journal of Political Economy 107*(6), 1218–1248.

Biais, B., T. Mariotti, S. Moinas, and S. Pouget (2017). Asset Pricing and Risk Sharing in a Complete Market: An experimental Investigation. *Working Paper*.

Black, F. (1975). Facts and Fantasy in the Use of Options and Corporate Liabilities. *Financial Analysis Journal 31*, 36–41, 61–72.

Blanchard, O., P. Mauro, and J. Acalin (2016). The Case for Growth-Indexed Bonds in Advanced Economies Today. *Policy Brief Peterson Institute for International Economics*.

Booth, G. G., M. Chowdhury, T. Martikainen, and Y. Tse (1997). Intraday Volatility in International Stock Index Futures Markets: Meteor Showers or Heat Waves? *Management Science 43*(11), 1564–1576.

Booth, G. G. and R. W. So (2003). Intraday Volatility Spillovers in the German Equity Index Derivatives Markets. *Applied Financial Economics 13*(7), 487–494.

Borensztein, E., P. Mauro, M. Ottaviani, and S. Claessens (2004). The Case for GDP-Indexed Bonds. *Economic Policy 19 (38)*, 165–216.

Borensztein, E. and U. Panizza (2009). The Costs of Sovereign Default. *IMF Economic Review 56 (4)*, 683–741.

Borghans, L., J. J. Heckman, B. H. Golsteyn, and H. Meijers (2009). Gender Differences in Risk Aversion and Ambiguity Aversion. *Journal of the European Economic Association 7*(2-3), 649–658.

Bossaerts, P., P. Ghirardato, S. Guarnaschelli, and W. R. Zame (2010). Ambiguity in Asset Markets: Theory and Experiment. *Review of Financial Studies 23*, 1325–1359.

Bossaerts, P. and C. Murawski (2016). How Humans Solve Complex Problems: The Case of the Knapsack Problem. *Scientific Reports 6*, 34851.

Breedon, F. and A. Ranaldo (2013). Intraday Patterns in FX Returns and Order Flow. *Journal of Money, Credit and Banking 45*(5), 953–965.

Broadie, M., M. Chernov, and M. Johannes (2007). Model Specification and Risk Premia: Evidence from Futures Options. *Journal of Finance 62*(3), 1453–1490.

Brock, W. A. and A. W. Kleidon (1992). Periodic Market Closure and Trading Volume: A Model of Intraday Bids and Asks. *Journal of Economic Dynamics and Control 16*(3), 451–489.

Brunnermeier, K. and M. Oehmke (2009). Complexity in Financial Markets. *Working paper*.

Brunnermeier, M., L. Garicano, P. R. Lane, M. Pagano, R. Reis, T. Santos, D. Thesmar, S. V. Neiuwerburgh, and D. Vayanos (2011). ESBies: A realistic reform of Europe's financial architecture. *VoxEU.org 25. October*.

Buraschi, A., F. Trojani, and A. Vedolin (2009). Equilibrium Index and Single-Stock Volatility Risk Premia. *Working Paper*.

Caballero, R. J. (2003). The Future of the IMF. *American Economic Review 93 (2)*, 31–38.

Calvo, G. (1988). Servicing the Public Debt: The Role of Expectations. *American Economic Review 78 (4)*, 647–661.

Cao, C., Z. Chen, and J. M. Griffin (2005). Informational Content of Option Volume Prior to Takeovers. *Journal of Business 78*(3), 1073–1109.

Carlin, B. (2009). Strategic Price Complexity in Retail Financial Markets. *Journal of Financial Economics 91*, 278–287.

Carlin, B., S. Kogan, and R. Lowery (2013). Trading Complex Assets. *Journal of Finance 68*, 1937–1960.

Carlin, B. and G. Manso (2011). Obfuscation, Learning, and the Evolution of Investor Sophistication. *Review of Financial Studies 24*, 755–785.

Célérier, C. and B. Vallée (2017). Catering to Investors Through Security Design: Headline Rate and Complexity. *Quarterly Journal of Economics (forthcoming)*.

Chateauneuf, A., J. Eichberger, and S. Grant (2007). Choice under Uncertainty with the Best and Worst in Mind: Neo-additive Capacities. *Journal of Economic Theory 137*(1), 538–567.

Chernov, M., A. R. Gallant, E. Ghysels, and G. Tauchen (2003). Alternative Models for Stock Price Dynamics. *Journal of Econometrics 116*(1), 225–257.

Chesney, M., R. Crameri, and L. Mancini (2015). Detecting Abnormal Trading Activities in Option Markets. *Journal of Empirical Finance 33*, 263–275.

Chidambaran, N., C. S. Fernando, and P. A. Spindt (2001). Credit Enhancement through Financial Engineering: Freeport McMoRan's Gold-Denominated Depositary Shares. *Journal of Financial Economics 60*(2), 487–528.

Christie-David, R., M. Chaudhry, and T. W. Koch (2000). Do Macroeconomics News Releases Affect Gold and Silver Prices? *Journal of Economics and Business 52*(5), 405–421.

Collard, F., M. Habib, and J.-C. Rochet (2015). Sovereign Debt Sustainability in Advanced Economies. *Journal of the European Economic Association 13*, 381–420.

Collard, F., M. Habib, and J.-C. Rochet (2016). The Reluctant Defaulter: A Tale of High Government Debt. *Working Paper*.

Constantinides, G. (1982). Intertemporal Asset Pricing with Heterogeneous Consumers, and Without Demand Aggregation. *Journal of Business 55*, 253–267.

Cox, J. C., S. A. Ross, and M. Rubinstein (1979). Option Pricing: A Simplified Approach. *Journal of Financial Economics 7*, 229–263.

Craig, A., A. Dravid, and M. Richardson (1995). Market Efficiency around the Clock: Some Supporting Evidence Using Foreign-based Derivatives. *Journal of Financial Economics 39*(2), 161–180.

Cremers, M., A. Fodor, and D. Weinbaum (2015). Where Do Informed Traders Trade First? Option Trading Activity, News Releases, and Stock Return Predictability. *Working Paper*.

Cyree, K. B. and D. B. Winters (2001). An Intraday Examination of the Federal Funds Market: Implications for the Theories of the Reverse-J Pattern. *Journal of Business 74*(4), 535–556.

Daigler, R. T. (1997). Intraday Futures Volatility and Theories of Market Behavior. *Journal of Futures Markets 17*(1), 45–74.

De Grauwe, P. and Y. Ji (2012). Mispricing of Sovereign Risk and Multiple Equilibria in the Eurozone. *CEPS Working Paper*.

Debreu, G. (1959). *Theory of Value: An Axiomatic Analysis of Economic Equilibrium*. Number 17. Yale University Press.

Dimmock, S. G., R. Kouwenberg, O. S. Mitchell, and K. Peijnenburg (2016). Ambiguity Aversion and Household Portfolio Choice Puzzles: Empirical Evidence. *Journal of Financial Economics 119*(3), 559–577.

Dow, J. and S. R. da Costa Werlang (1992). Uncertainty Aversion, Risk Aversion, and the Optimal Choice of Portfolio. *Econometrica*, 197–204.

Duffie, D. and C.-F. Huang (1985). Implementing Arrow-Debreu Equilibria by Continuous Trading of Few Long-lived Securities. *Econometrica*, 1337–1356.

Easley, D., N. Kiefer, M. O'Hara, and J. Paperman (1996). Liquidity, Information, and Infrequently Traded Stocks. *Journal of Finance 51*, 1405–1436.

Easley, D. and M. O'Hara (1987). Price, Trade Size, and Information in Securities Markets. *Journal of Financial Economics 19*, 69–90.

Easley, D., M. O'Hara, and P. S. Srinivas (1998). Option Volume and Stock Prices: Evidence Where Informed Traders Trade. *Journal of Finance 53 (2)*, 431–465.

Eaton, J. and M. Gersovitz (1981). Debt with Potential Repudiation: Theoretical and Empirical Analysis. *Review of Economic Studies 48 (2)*, 289–309.

Ederington, L. H. and J. H. Lee (1993). How Markets Process Information: News Releases and Volatility. *Journal of Finance 48*(4), 1161–1191.

Ekman, P. D. (1992). Intraday Patterns in the S&P 500 Index Futures Market. *Journal of Futures Markets 12*(4), 365–381.

Ellison, G. (2005). A Model of Add-On Pricing. *Quarterly Journal of Economics 120*, 585–637.

Ellison, G. and S. Ellison (2009). Search, Obfuscation, and Price Elasticities on the Internet. *Econometrica 77*, 427–452.

Ellsberg, D. (1961). Risk, Ambiguity, and the Savage Axioms. *Quarterly Journal of Economics 75*, 643–669.

Engle, R. F., T. Ito, and W.-L. Lin (1990). Meteor Showers or Heat Waves? Heteroskedastic Intra-daily Volatility in the Foreign Exchange Market. *Econometrica 58*, 525–542.

Epstein, L. G. and M. Schneider (2010). Ambiguity and Asset Markets. *Annual Review of Financial Economics 2*(1), 315–346.

Eraker, B. (2004). Do Stock Prices and Volatility Jump? Reconciling Evidence from Spot and Option Prices. *Journal of Finance 59*(3), 1367–1403.

Evans, M. D. and R. K. Lyons (2008). How is Macro News Transmitted to Exchange Rates? *Journal of Financial Economics 88*(1), 26–50.

Fattinger, F. (2017). Trading Complex Risks. *Working Paper*.

Favero, C. and A. Missale (2012). Sovereign Spreads in the Euro Area: Which Prospects for a Eurobond? *Economic Policy 27 (70)*, 231–273.

Fleming, J., C. Kirby, and B. Ostdiek (1998). Information and Volatility Linkages in the Stock, Bond, and Money Markets. *Journal of Financial Economics 49*(1), 111–137.

Fox, C. R. and A. Tversky (1995). Ambiguity Aversion and Comparative Ignorance. *Quarterly Journal of Economics 110*(3), 585–603.

Gabaix, X. and D. Laibson (2006). Shrouded Attributes, Consumer Myopia, and Information Suppression in Competitive Markets. *Quarterly Journal of Economics 121*, 505–540.

Gali, J., J. D. Lopez-Salido, and J. Vallés (2007). Understanding The Effects of Government Spending on Consumption. *Journal of the European Economic Association 5(1)*, 227–270.

Ghent, A., W. Tourous, and R. Valkanov (2014). Complexity in Structured Finance: Financial Wizardry or Smoke and Mirrors? *Working Paper*.

Ghirardato, P., F. Maccheroni, and M. Marinacci (2004). Differentiating Ambiguity and Attitude. *Journal of Economic Theory 118*, 133–173.

Gilboa, I. and D. Schmeidler (1989). Maxmin Expected Utility with a Non-unique Prior. *Journal of Mathematical Economics 18*, 141–153.

Glosten, L. R. and P. R. Milgrom (1985). Bid, Ask and Transaction Prices in a Specialist Market with Heterogeneously Informed Traders. *Journal of Financial Economics 14*(1), 71–100.

Goeree, J. K. and C. A. Holt (2004). A Model of Noisy Introspection. *Games and Economic Behavior 46*(2), 365–382.

Goeree, J. K., C. A. Holt, and T. R. Palfrey (2002). Quantal Response Equilibrium and Overbidding in Private-Value Auctions. *Journal of Economic Theory 104*(1), 247–272.

Goeree, J. K., C. A. Holt, and T. R. Palfrey (2003). Risk Averse Behavior in Generalized Matching Pennies Games. *Games and Economic Behavior 45*(1), 97–113.

Greenwald, B. C. and J. E. Stiglitz (1986). Externalities in Economies with Imperfect Information and Incomplete Markets. *Quarterly Journal of Economics 101*(2), 229–264.

Griffin, J., R. Lowery, and A. Saretto (2013). Complex Securities and Underwriter Reputation: Do Reputable Underwriters Produce Better Securities? *Working Paper*.

Grossman, S. J. (1981). An Introduction to the Theory of Rational Expectations Under Asymmetric Information. *Review of Economic Studies 48*, 541–559.

Grossman, S. J. and J. E. Stiglitz (1980). On the Impossibility of Informationally Efficient Markets. *American Economic Review 70*(3), 393–408.

Halevy, Y. (2007). Ellsberg Revisited: An Experimental Study. *Econometrica 75*(2), 503–536.

Harvey, C. R. and R. D. Huang (1991). Volatility in the Foreign Currency Futures Market. *Review of Financial Studies 4*(3), 543–569.

Henderson, B. and N. Pearson (2011). The Dark Side of Financial Innovation: A Case Study of the Pricing of a Retail Financial Product. *Journal of Financial Economics 100*, 227–247.

Hens, T. and M. Rieger (2008). The Dark Side of the Moon: Structured Products from the Customer's Perspective. *Working Paper*.

Holt, C. A. and S. K. Laury (2002). Risk Aversion and Incentive Effects. *American Economic Review 92*(5), 1644–1655.

Huberman, G. and W. Stanzl (2004). Price Manipulation and Quasi-Arbitrage. *Econometrica 72*(4), 1247–1275.

Jiang, G. J., E. Konstantinidi, and G. Skiadopoulos (2012). Volatility Spillovers and the Effect of News Announcements. *Journal of Banking & Finance 36*(8), 2260–2273.

Johnson, T. L. and E. C. So (2013). A Simple Multimarket Measure of Information Asymmetry. *Working Paper*.

Jordan, J. V., W. E. Seale, S. J. Dinehart, and D. E. Kenyon (1988). The Intraday Variability of Soybean Futures Prices: Information and Trading Effects. *Review of Futures Markets 7*, 96–109.

Kahneman, D., J. L. Knetsch, and R. H. Thaler (1991). Anomalies: The Endowment Effect, Loss Aversion, and Status Quo Bias. *Journal of Economic Perspectives 5*(1), 193–206.

Klibanoff, P., M. Marinacci, and S. Mukerji (2005). A Smooth Model of Decision Making under Ambiguity. *Econometrica 73*(6), 1849–1892.

Knight, F. H. (1921). *Risk, Uncertainty and Profit.* Boston, New York, Houghton Mifflin Company.

Kou, S. G. (2002). A Jump-Diffusion Model for Option Pricing. *Management Science 48 (2)*, 1086–1101.

Kreps, D. M. (1982). Multiperiod Securities and the Efficient Allocation of Risk: A Comment on the Black-Scholes Option Pricing Model. In *The Economics of Information and Uncertainty*, pp. 203–232. University of Chicago Press.

Kyle, A. S. (1985). Continuous Auctions and Insider Trading. *Econometrica 15*, 1315–1335.

Lahaye, J., S. Laurent, and C. J. Neely (2011). Jumps, Cojumps and Macro Announcements. *Journal of Applied Econometrics 26*(6), 893–921.

Lane, P. R. (2012). The European Sovereign Debt Crisis. *Journal of Economic Perspectives 26 (3)*, 49–68.

Lee, C. and M. Ready (1991). Inferring Trade Direction from Intraday Data. *Journal of Finance 46*, 733–746.

Lee, J. H. and S. C. Linn (1994). Intraday and Overnight Volatility of Stock Index and Stock Index Futures Returns. *Review of Futures Markets 13*, 1–29.

Lee, S. S. and P. A. Mykland (2008). Jumps in Financial Markets: A New Nonparametric Test and Jump Dynamics. *Review of Financial Studies 21*(6), 2535–2563.

Lin, W.-L., R. F. Engle, and T. Ito (1994). Do Bulls and Bears Move across Borders? International Transmission of Stock Returns and Volatility. *Review of Financial Studies 7*(3), 507–538.

Lucas, R. E. (1987). *Models of Business Cycles*, Volume 26. Basil Blackwell Oxford.

Luce, R. D. (1959). *Individual Choice Behavior: A Theoretical Analysis*. John Wiley and sons.

McKelvey, R. D. and T. R. Palfrey (1995). Quantal Response Equilibria for Normal Form Games. *Games and Economic Behavior 10*(1), 6–38.

McKelvey, R. D. and T. R. Palfrey (1998). Quantal Response Equilibria for Extensive Form Games. *Experimental Economics 1*(1), 9–41.

Merton, R. C. (1969). Lifetime Portfolio Selection under Uncertainty: The Continuous-Time Case. *Review of Economics and Statistics 51*, 247–257.

Merton, R. C. (1974). On the Pricing of Corporate Debt: The Risk Structure of Interest Rates. *Journal of Finance 29*(2), 449–470.

Merton, R. C. (1976). Option Pricing when Underlying Stock Returns are Discontinuous. *Journal of Financial Economics 3*(1-2), 125–144.

Merton, R. C. (1977). An Analytic Derivation of the Cost of Deposit Insurance and Loan Guarantees. *Journal of Banking & Finance 1*, 3–11.

Milgrom, P. and N. Stokey (1982). Information, Trade and Common Knowledge. *Journal of Economic Theory 26*, 17–27.

Müller, A., K. Storesletten, and F. Zilibotti (2016). Sovereign Debt and Structural Reforms. *Working Paper*.

Muravyev, D., N. D. Pearson, and J. P. Broussard (2013). Is there Price Discovery in Equity Options? *Journal of Financial Economics 107*(2), 259–283.

Neftci, S. N. and A. O. Santos (2003). Puttable and Extendible Bonds: Developing Interest Rate Derivatives for Emerging Markets. *IMF Working Paper*.

Neumark, D., P. A. Tinsley, and S. Tosini (1991). After-hours Stock Prices and Post-crash Hangovers. *Journal of Finance 46*(1), 159–178.

Pan, J. and A. M. Poteshman (2006). The Information in Option Volume for Future Stock Prices. *Review of Financial Studies 19*(3), 871–908.

Radner, R. (1972). Existence of Equilibrium of Plans, Prices, and Price Expectations in a Sequence of Markets. *Econometrica 40*(2), 289–303.

Rochet, J.-C. (2006). Why do Countries Default? *Working Paper*.

Sato, Y. (2014). Opacity in Financial Markets. *Review of Financial Studies 27*, 3502–3546.

Schwert, G. (1996). Markup Pricing in Mergers and Acquisitions. *Journal of Financial Economics 41*, 153–192.

Shiller, R. J. (1994). *Macro Markets: Creating Institutions for Managing Society's Largest Economic Risks*. Oxford University Press.

Shiller, R. J. (2003). *The New Financial Order: Risk in the 21st Century*. Princeton University Press.

Tversky, A. and D. Kahneman (1992). Advances in Prospect Theory: Cumulative Representation of Uncertainty. *Journal of Risk and Uncertainty 5*(4), 297–323.

Werner, I. M. and A. W. Kleidon (1996). U.K. and U.S. Trading of British Cross-listed Stocks: An Intraday Analysis of Market Integration. *Review of Financial Studies 9*(2), 619–664.

Wood, R. A., T. H. McInish, and J. K. Ord (1985). An Investigation of Transactions Data for NYSE Stocks. *Journal of Finance 40*(3), 723–739.

Yates, F. (1934). Contingency Tables Involving Small Numbers and the χ^2 Test. *Supplement to the Journal of the Royal Statistical Society 1*(2), 217–235.

Zwergel, B. and S. Heiden (2012). Intraday Futures Patterns and Volume–Volatility Relationships: The German Evidence. *Review of Management Science 40*, 723–739.

Part IV

Curriculum Vitae

Curriculum Vitae

Personal details

Name:	Felix Fattinger
Date of Birth:	June 17, 1984
Place of Birth:	Zurich, Switzerland
Nationality:	Swiss

Education

09/2011 – 10/2017	**PhD program at the Department of Banking and Finance** University of Zurich, Switzerland Supervisor: Prof. Dr. Marc Chesney 01/2016 – 12/2016: Visiting PhD student Toulouse School of Economics, France
09/2009 – 04/2012	**Master of Science in Quantitative Finance** University of Zurich and Swiss Federal Institute of Technology, Switzerland
10/2006 – 04/2010	**Bachelor of Arts in Banking and Finance** University of Zurich, Switzerland 09/2008 – 01/2009: Exchange student HEC, University of Lausanne, Switzerland

Professional experience

10/2012 – 10/2017	Research and teaching assistant at University of Zurich Chair of Quantitative Finance, Prof. Dr. Marc Chesney Zurich, Switzerland
10/2008 – 08/2011	Junior research and teaching assistant at University of Zurich Department of Banking and Finance Zurich, Switzerland
06/2008 – 09/2008	Internship at UBS Investment Bank, FX Cash Distribution & Trading Opfikon, Switzerland
07/2007 – 09/2007	Internship, Union Bancaire Privée, Emerging Markets Fixed Income Zurich, Switzerland